

THE ANALYSIS OF STRUCTURAL FATIGUE

by

DAVID GRAEME FORD, B.E.(Aero.), B.A.

A Thesis submitted for the degree of
Doctor of Philosophy of the University of London
and for the Diploma of Membership of
Imperial College in Aeronautical Engineering

1967

SUMMARY

Structural fatigue is considered as the interaction between the processes of cumulative damage and crack propagation. A general fatigue problem is defined in which the scatter arises from the variability of initial failures and equations are found for the growth of average crack lengths and the moments of their probability distribution.

In order to set up the crack-damage equations the Bastenaire theory of damage was used which makes direct use of the initial life distribution. Some aspects of this were generalised and the effect of endurance limits was considered in the light of the two-distribution theory of Swanson.

Crack propagation is described in terms of fracture mechanics and a new non-dimensional presentation is used which explains most of the effect of mean loads. This also allows some uniformity in the discussion of brittle fracture and fatigue cracking and an extension for random loads is suggested which allows for the additional rates observed by Paris.

The crack-damage equations are essentially a system of differential equations and there is a discussion of some features of their solutions. After this the application of matrix force methods is considered as an illustration of the general theory. This is essentially a finite element extension of fracture mechanics, in which a moving element replaces the crack tips familiar in continua. The stress intensity thus calculated is then usable to predict rates of crack growth for the general fatigue problem.

ACKNOWLEDGEMENTS

The author is indebted to Professor J.H. Argyris for his original encouragement of this project and also to Mr. S. Kelsey and Dr. K. Thomas for many helpful discussions. He must also thank Dr. D.J. Burns of the Department of Mechanical Engineering for discussions and many useful references.

Special thanks are also due to Miss M. Hudgell for her patient typing, Miss J. Bruntnell for most of the figures and to my wife for proof reading and collation. The author must also thank the Commonwealth Department of Supply for a scholarship and for help during its tenure.

CONTENTS

ACKNOWLEDGEMENTS	iii
NOTATION	viii
INTRODUCTION	1
I DAMAGE THEORY	7
1.1 Bastenaire Damage-Equivalence	7
2.0 Growth of Damage	10
2.1 Effect of Load Order	11
2.2 Relation to Life Distribution	12
2.3 Miner-Palmgren Damage	13
2.4 Damage for Log-normal Lives	15
2.5 Effect of Endurance Limits	19
3.0 Correlation Effects	23
4.0 Corrosion Fatigue	24
5.0 Two Parameter Damage	26
5.1 Generalised Corrosion Fatigue	27
5.2 Canonical Form of Multidimensional Damage	30
5.3 Variance under Programme Loading	31
5.4 Log-normal Damage with Several Parameters	35
6.0 Final Note on Applicability	38
II FINAL FAILURE, HAZARDS AND RELIABILITY	39
1.0 Failure Rate and Hazards	39
2.0 Effect of Inspection and Repairs	41
2.1 Several Initial Failures	47
3.0 Hazards from Several Cracks	48
3.1 Exponential Distributions	50
3.2 Two-Sided Exponential Distribution	54
3.2.1 Several Cracks	57
III CRACK PROPAGATION AND FAILURE	59
1.0 Introduction	59
2.0 Elastic Stresses	59
2.1 Tip Stresses and Intensities	61
2.2 Special Cases	63

3.0	General Solutions	63
3.1	Two-Dimensional Case	65
3.2	Lyell-Sanders' Method	66
3.3	Experimental Methods	67
4.0*	Other Modes of Fracture	68
4.1*	Edge Sliding	68
4.2*	Screw Sliding	69
4.3	Effects of Other Modes	70
4.4	Additivity of Driving Forces	71
5.0	Effect of Non-linearities and Local Geometric Changes	72
5.1	Cracks in Cylinders	74
6.0	Plastic Stress Systems	75
6.1	Work Done during Extension	78
6.2	Correction to γ	82
7.0	Griffith-Irwin Theory	83
7.1	Static Fracture	85
7.2	Multiply Cracked Structures	88
8.0	Fatigue Cracks	89
8.1	Non-Dimensional Variables	89
8.2	Experimental Results	92
8.21	Discussion	92
8.3	The Role of Grain Boundaries	97
8.4	Statistical Analysis of Results	98
8.5	Work Hardening	99
9.0	Crack Growth under Random Loads	99
9.1	Some Feasible Residual Stresses	102
9.2	Effect of Load Sequence	104
9.3	Form of Preload Delay	106
9.4	A Fourth Power Model of Random Growth	106
9.5	Generalisation	109
9.6	Behaviour of Work Function	110
9.7	Very Small Driving Forces	112
9.8	Possible Form of W	113
9.9	Some Possible Experiments	114
IV	THE CRACK-DAMAGE EQUATIONS	116
1.0	Direct Solution	118
2.0	The Initial Crack	119
3.0	The Role of Damage Equations	121
3.1	Monte-Carlo Solution	122

4.0	Independence of Initial Failure Times	124
4.1	Improvement of Monte-Carlo Method	126
4.2	An Identity	128
5.0	The Development of Cracks	129
5.1	One Crack Illustration	131
5.2	Several Cracks	135
5.3	Moment Generating Function for Several Cracks	138
6.0	Complete Equations	142
6.1	General and Multiparametric Damage	144
6.2	Nature of Cracks	145
6.3	Initial Densities of Crack Lengths	146
7.0	Variance and Covariance	152
8.0	Estimation of Initial Failures and Initial Crack Lengths	157
V	NUMERICAL SOLUTION	160
1.0	A Class of Empirical Distributions	161
1.1	Behaviour of $M_T(-a)$	165
2.1	Summarising Rates and Damages	170
2.2	Expectation Integrals	174
VI	MATRIX FORCE METHODS	175
1.0	General Modification Method	176
1.1	Use of Transformed Loads	178
2.0	Inverse of Modification Matrix	183
2.1	Solution by Elimination	186
2.2	Discussion	188
3.0	The Representation of Cracking	189
3.1	The Use of Moving Elements	191
3.2	Fitting Generalised Stresses to Arbitrary Stress Systems	193
3.3	Modified Flexibilities	196
VII	CRACKS IN RECTANGULAR PANELS	200
1.0	Generalised Stresses	200
1.1	Flexibility	204

2.1	Crack Conditions	206
2.2	Cut Corners and Averaged Conditions	208
2.3	Choice of Deleted Loads	210
3.0	Self-Equilibrating Systems	210
4.0	Natural Loads for Moving Element	212
4.1	Form of M	212
4.2	Strain Energy of Cracked Panel	213
4.3	Computation of Generalised Stresses	215
4.4	Optimum Tip Position	216
4.41	Results	218
4.5	Maximum Strain Energies	222
VIII INTERPOLATIONS AND PROGRAMME STRATEGY		226
1.0	Main Programme	229
2.1	General Crack Step	229
2.2*	Quadrature with Mixed Quantities	230
3.1	Interpolation of Loads	231
3.2	Imbedding of Moving Element	233
3.21	Local Lattice Coordinates	236
3.22	Edges	236
3.23*	Note	237
4.1*	Changes of Flexibility	237
4.2*	Computer Storage of Matrices	240
4.3*	Matrix Operations	241
CONCLUSIONS		244
Appendix A		
JOINT DENSITY $f(\mathbf{a} n)$ AND NUMERICAL EXPECTATIONS		248
Appendix B		
CALCULATION OF SUBTENDED ANGLES AT CRACK TIP		253
REFERENCES		256

Notation

This will be described as it arises. However some of the more common symbols are listed below. It is impossible to avoid clashes overall but an attempt has been made to avoid them in any one chapter and to show some uniformity among quantities of the same physical nature which in different contexts may appear as vectors, general scalars or subscripted quantities.

Functional Notation

As far as possible this is based on the physical nature of the function. Thus $F(x)$ and $F(y)$ are not the same function with different arguments but two generally different distributions of x and y respectively. If we want the same function with different arguments it is often written as

$$F(x) \text{ or } F_x(x) \text{ or } F_x(y) \text{ for example.}$$

This is also true for the matrix functions such as $A(a, F)$ which represents a set of damage rates each of which, in general, depends on all the elements of a and F .

Matrix Notation

I_r	Unit matrix, r -th order
O	Matrix of zeros
B	Usually a rectangular matrix but often a vector.
x	Usually a column vector.
F_i	Diagonal matrix with elements F_i .
K^{-t}	Inverse of the transposed matrix K^t . These indices are not commutative in the addition laws.
$[x_i]$	The matrix consisting of the columns x_i .

[BC]	Partitioned matrix.
e_N	N-th order column vector with unit elements.
$[x_{ij}]$	Matrix with elements x_{ij} in i-th row and j-th column.
$\{x_i\}$	Column vector with elements x_i .
$\{x_i\}$	Column vector with submatrices x_i .

Statistical Notation

Pr(A) Probability of the event A.

Pr(A|B) Probability of A given B, a conditional probability.
The vertical stroke always implies a condition and is used in other contexts as below.

F(x) Probability distribution or distribution function of x defined as $\text{Pr}(x' \leq x)$. Also called the cumulative distribution or merely distribution.

F(x|n) Conditional distribution of x given n.

f(x) Probability density (density or distribution) of x.
= $dF(x)/dx$ if F(x) is differentiable,
= Pr(Obtaining x) for discrete events.

$\mathcal{E}[\phi(x)] = \int \phi(x) dF(x)$ Expectation of $\phi(x)$. This is sometimes called an average and the integral itself is the Lebesgue-Stieltje type.

dF(x) Element in Stieltje integral = $f(x)dx$ for the differentiable parts of F(x). An analogous usage is the shear force formula.

Shear force = $\int dW(x)$ where

dW(x) = Load density, including concentrated loads.

M(t) = $\int \exp(xt) dF(x)$ Moment generating function of x.

$\phi(t)$ = $\int \exp(ixt) dF(x)$ Characteristic function of x.
(Fourier transform).

$\Psi(t)$ = $\log M(t)$ Cumulant generating function of x.

All the arguments here have vector equivalents. In the generating functions xt is replaced by the scalar product $x^t t$.

μ_r r-th moment = $\int x^r dF(x)$.

$\mu \equiv \mu_1$ Mean
 $\sigma^2 = \mu_2 - \mu^2$ Variance or second cumulant = $\int (x-\mu)^2 dF(x)$
 $\sigma_{i,j}$ Covariance or one of the second order multi-variate cumulants.
 $x:f(x)$ x has the density function (is distributed as) $f(x)$.
 \hat{K} Estimate of K .

Common Notation

$\mathbf{a}, \mathbf{a} = \mathbf{a}(n|t) = \{a_1, \dots, a_N\}$ Crack lengths.
 $\mathbf{A}, \mathbf{A}(F,S), \mathbf{A}(D,S), \mathbf{A}(F,S), \mathbf{A}(F,\mathbf{a})$ Damage rates or rate vectors.
 $\mathbf{A}^{-1}, \mathbf{A}_1^{-1}$ Covariance matrices
 $\mathbf{A} = [\mathbf{A}_j] = [\boldsymbol{\tau}_i]^{-t}$ Non-singular transformation Ch.II.
 a_0 Initial crack length.
 r Non-zero crack lengths.
 a, b Sides of panel.
 \mathbf{b} Stress response matrix for structure.
 \mathbf{b} Means of two-sided exponential distribution.
 $\mathbf{BS} = \mathbf{0}$ Crack conditions.
 $\mathbf{B}_* = \begin{bmatrix} \mathbf{IO} \\ \mathbf{B} \end{bmatrix}$ Load transformation matrix.
 $\mathbf{b}_0, \mathbf{b}_1$ Statically determinate and self-equilibrating systems.
 $\mathbf{b}_m, \mathbf{b}_c, \mathbf{b}_{1m}, \mathbf{b}_{1c}$ Submatrices of \mathbf{b} etc. corresponding to modifications or cutouts.
 \mathbf{C} Corrosion damage
 $c(S)$ Rate of corrosion.
 $\mathbf{c}_0, \mathbf{c}_1$ Corresponding to $\mathbf{b}_0, \mathbf{b}_1$ with transformed loads.
 $c a_0^\alpha$ Minimum crack rate.
 $\mathbf{D} \equiv \mathbf{b}_1^t \mathbf{f} \mathbf{b}_1$
 \mathbf{D}, \mathbf{D} Damage or damage vector.

- e Error vector.
- E Upper endurance limit or Young's modulus.
- $e_N = \{1 \dots 1\}$, n-th order.
- f Element flexibility matrix.
- $F, \mathbf{F} = F_i$ Canonical damage(s).
- $[f_i]$ Canonical damage rates.
- $f_o = f(a|n)$, $a=a_o$ Initial density of crack lengths.
- $F_c = P_r$ (Corrosion failure|n cycles).
- $F_d = P_r$ (Fatigue failure|n cycles).
- $F_E(n)$ Empirical, stepped, distribution function.
- F_{N-r} Relevant canonical damages.
- f_r Initial density of crack rate.
- f_Δ Change of element flexibilities.
- $f(\theta) = r/\rho$ Boundary of plastic zone.
- $f_{vr} = P_r$ (final f. in (T_{v-1}, T_v) | Repair time T_r)
- g, g_Δ Element flexibility and alteration for transformed loads.
- $G = E/2(1+\nu)$ Shear modulus.
- g Energy release rate or driving force.
- g_I Critical driving force for plane strain fracture.
- g_a, g_m Driving forces based on alternating and mean loads respectively.
- H Generalised initial strains.
- H_{c*}, H_m Submatrices of H corresponding to (transformed) cutouts and modifications.
- $h(n) = P_r$ (Failure at n | No previous failure) Risk or hazard.
- $H(n) = \int_0^n h(t) dt$
- h_s Hazard for static failure (no fatigue cracks).
- $H(F, S)$ Hazard in reliability form of damage.
- $k = \bar{R}(n-n')/\Delta a$ Reduced time, Chapter IV, Sec.6.3.
- K Stress intensity factor, eq. (3.5).

- $K, \mathbf{K} = \{k_i\}$ Crack rate factors, Chapter IV.
 K_{h^*}, K_{c^*} Uncoupled coefficient of modification matrix.
 $K_c, K_{cm} (= K_{mc}^t), K_m$ Submatrices of modification matrix (6.13).
 K_T, K_{Ti} Theoretical stress concentration factors.
 ℓ^2 Area of moving element.

 m Number of simulated tests, Chapter IV.
 \mathbf{m} Component of constant crack rate.
 \mathbf{M} Interpolation matrix.
 M, M_i Moving element and its size.
 M_T General MGF of $T(x)$.
 $M_T(-a) = M_T(m, n)$ (Generally $a \neq$ average crack length).
 m, n Parameters of transition beta distribution (5.4).

 n Number of cycles of applied load.
 N Number of cracks in structure, Chapter IV.
 n_f Average number of cycles for crack tip to cross a given maximum plastic zone.
 $N(S)$ Average S-N curve (log-lives).
 $N(\mu, \sigma^2)$ Normally distributed, mean μ , variance σ^2 .

 $p = E / 2\pi\sigma_y^2$ Nominal plastic zone based on maximum load.
 P Maximum load in corrosion example.
 P Panel with altered flexibility.
 P Arbitrary set of generalised stresses.
 $\mathbf{P}_N = [P_{Ni}]$ Set of natural loads.
 $p_a = E g_a / 2\pi\sigma_y^2$ Plastic region based on alternating load.
 $p_m = E g_m / 2\pi\sigma_y^2$ Plastic region based on mean load.
 $p_f = n_f^{-1}$ -th fractile of $f(p_a)$, (3.33).
 $p(S) = R_r$ (Eventual failure | constant load S).
 $P(S)$ Generating function.
 $p_v = P_r$ (Initial crack during (T_{v-1}, T_v)).

$Q(s)$	Generating function.
r	Subscript referring to r -th initial failure, at a particular place, among m simulated tests.
R	Vector of external loads.
\bar{R}	Average initial crack rate.
R_0	Random initial crack rate.
$R(\mathbf{a} n) \equiv R(\mathbf{a}) = \{R_i(\mathbf{a} n)\}$	General crack rates, Chapter IV.
$\bar{R}(\mathbf{a} n) = \{\bar{R}_i(\mathbf{a} n)\} = \int R(\mathbf{a})dF(\mathbf{a} n)$	Average crack rates.
s^2	Sample variance.
S	Fatigue load on simple specimen.
S, T	Generalised stresses.
S_a	Submatrix of S for finite contributions to interpolation MS_a .
$s_i(S)$	Secondary damage parameters, (1.42).
S_m	Submatrix of load in modified members.
t	Thickness.
$t, \mathbf{t} = \{t_i\}$	Initial failure times in cycles.
t_{ir}	r -th initial failure for crack i out of m simulated tests.
$T(R_0), T(x)$	Transition curves from distribution functions.
T_v	Time of v -th inspection ($T_0=0$).
$u = (x-\mu)/\sigma$	Standardised variate.
u, \mathbf{u}	Transformed variable in MGFs or CGFs.
U	Virtual work or sometimes strain energy.
U_{12}, w_p etc.	Strain energies of triangular sectors.
U_a, U_m	Typical integrals for flexibility, Chapter VI, Sec.3.1.
u, v	Displacements.
$\mathbf{v},$	Generalised strains
$W, W(a, \beta), W(x), W_p$	Work function or resistance to crack extension.

x	Crack extension.
\mathbf{x}, \mathbf{y}	Random vectors
(x, y, φ)	Tip position and crack direction.
α, β	Number of bays along each side of panel structure.
$\beta, \hat{\beta}$	Parameters and estimates in general linear regression.
$\gamma = g_m/g_a$	Mean load parameter.
$\epsilon_1 - \epsilon_2$	Difference between principal strains.
θ	Angular argument for $M_T(-a)$, Chapter V.
μ	Strain energy of standardised moving element.
$\boldsymbol{\mu}$	Vector of mean value.
ν	Poisson's ratio.
$\boldsymbol{\xi} = \boldsymbol{\xi}(\mathbf{x})$	
ξ, η	Non-dimensional panel co-ordinates ($ \xi , \eta \leq 1$).
$\xi_i(S)$	Load dependence of damage parameter, (1.42).
$\rho = \rho_o/p$	Coarseness, used as a load measure.
ρ	Arbitrary set of deformation modes.
ρ_o	Average grain size.
$\rho_N = \{\rho_{N_i}(\mathbf{r})\}$	Natural modes of deformation.
σ^2	Variance.
Σ	Standard generalised stresses on moving element.
$\Sigma = [\sigma_{.j}] = [\sigma_{ij}]$	Covariance matrix of crack lengths.
$\sigma_1, \dots, \sigma_4$	Sequence of residual stress systems.
σ_m	Stress pattern in moving element.
$\sigma_N = [\sigma_{N_i}(\mathbf{r})]$	Stress patterns for natural loads.
Σ_x, Σ_y	Covariance matrices.
$\sigma_{xx}, \sigma_{yy}, \tau_{xy}$	Stress components.
σ_y	Yield stress.
$\tau_G = t/p$	Relative thickness, (3.28)
$[\tau_i] = \mathbf{A}^{-t}$	

- φ Flexibility of element $dx dy$.
- ψ Crack direction.
- $\Psi(\psi) = \{\Psi_1 \Psi_c\} = \{\Psi_1 \Psi_2 \Psi_3\}$ Equations (7.4), (7.7).
- ω Frequency.

INTRODUCTION

The efficient use of structural material and the higher stresses thereby entailed have made fatigue a paramount concern in the design of aircraft.

Nowadays fatigue resistance is ensured first at the stage of static stress analysis and secondly by full or large scale testing. The latter is extremely expensive but, like the corresponding tests to static failure, large scale fatigue tests are likely to stay.

The first process is essentially a comparison between stresses in the structure and those of a simpler specimen, similar in such respect as material and stress concentration factor, whose behaviour is already known. From this viewpoint cumulative damage theories (here abbreviated as "damage") are simply a means of making this comparison in similar circumstances.

Because the stresses are those of the undisturbed structure this approach at best can only predict initial failures although it has also been applied to final collapse. In actual fact there are three main stages in any fatigue failure, namely:

(a) Damage, where molecular changes occur but the material is still coherent in the engineering sense.

(b) Crack growth which begins at initial fracture. For our purposes this may continue indefinitely or at least until the structure falls apart. In practice this stage is interrupted by (c).

(c) Static fracture, in which the applied load exceeds the current ultimate strength which is obviously reduced by previous cracking.

All these processes are random and in any particular case (b) will affect (a) and (c). When average crack rates are considered it will be shown that in addition, damage affects the rate.

The final failure (c) is most prominently displayed by the fail-safe philosophy where the designer's aim is to minimise the probability of static failure over short periods of time by reducing growth rates and repairing those cracks which become too long.

As implied by fail-safe theory, final failure is closely connected with the conditional probability of failure during a fatigue cycle, given that there is no previous failure. In the literature on reliability this probability is often termed the hazard or risk and by a standard argument it leads directly to the fatigue life distribution for the complete structure so that stage (c) is most directly related to the accepted sense of fatigue failure.

It is now time to define the general fatigue problem in the sense of this thesis and this will also clarify the meaning of its solution.

We first suppose that we have absolute knowledge, of a simple specimen (whose existence is doubtful), which has been distilled into laws of damage and of crack propagation. Since this data concerns random variables we assume precision in the statistical sense that all probability distributions have been perfectly estimated.

Having set up laws for simple specimens we next imagine a structure with a fixed number of possible crack sites (possibly infinite for the moment). Then the general fatigue problem will be solved when the probability distributions of all crack lengths and initial failure times are known as functions or functionals depending

on the number of cycles. When these are known it is possible to apply a theory of strength for the crack distribution at any stage and calculate the hazard in (c), thereby obtaining the life distribution. Thus the basic problem is to predict the interaction of cracking and damage over a number of cycles.

To set up the general problem we finally need to relate conditions on various parts of the structure to those of simple specimens as indeed one relates static stresses to the yield point of an ordinary tensile specimen. This is obviously some kind of structural analysis and, within the definition, a complete solution of the general fatigue problem need not bear any relation to reality when the associated stressing is inappropriate.

On the other hand "stress analysis" refers here to any means of transforming external loads into stresses whether good or bad. It includes topics such as vibration analysis, gust response or the response to random noise. Included equally is the use of average stress or the continual use of stresses from the virgin structure.

The second method is the basis of much present practice so that when there are several cracks one cannot guess at the interaction with the damage. The first procedure has the merit that progressive changes are allowed for and we could distinguish such cases as true fatigue problems.

As the following example shows this degree of generality is still enough to encompass problems quite unrelated to structural fatigue. Suppose we have a capacitor in some electric circuit subject to random voltages. Before it fails completely its performance may deteriorate affecting the applied voltages by way of the circuit.

Then if the period before deterioration is regarded as a pre-crack or damage stage and the amount of deterioration treated as a crack length the problem is exactly analogous to the general fatigue problem.

We now summarise the contents of each chapter. In Chapter 1 some aspects of damage are discussed and there is a brief description of Bastenaire's theory of damages. This seems to be the most comprehensive and satisfying and also the least known of current theories. It leads quite simply to differential equations for probability distributions which later combine neatly with those for crack growth. Multidimensional damage is mentioned and as an example a rough theory of corrosion fatigue is presented.

In Chapter II various aspects of reliability theory are discussed. They are mostly well known and we refer to their applications in fatigue. As we stated, this is most relevant to hazards, final failure and the overall life distribution.

Chapter III discusses crack propagation from the viewpoint of fracture mechanics, a study pioneered by Paris. A new non-dimensional presentation of test results is suggested and there is a parallel resume of standard Griffith-Irwin fracture theory also in a non-dimensional form. Based on this representation there is also a tentative theory of crack growth under random loads but several shortcomings become evident in present-day experimental results on crack growth.

In Chapter IV we finally treat the crack-damage equations which describe the general fatigue problem with a finite number of cracks and with Bastenaire damage. The problem is first approached as one involving Monte-

Carlo or model sampling. This leads to an important theorem that initial lives are independent. After this we develop differential equations for average crack lengths and the moment generating function of random crack lengths (in effect the Laplace transform of the joint length distribution). For n cracks and r -dimensional damage it transpires that $(1+r)2^n$ differential equations can be found whose solutions are effectively that of the general fatigue problem. Chapter V describes a numerical solution of the differential equations with approximate evaluation of the expectation integrals which form the forcing functions.

The final chapters are related to structural aspects. In general the progress of a crack is regarded as an imposition of zero load conditions together with changes of flexibility. This is equivalent to a cutout in a transformed set of loads. The main interest lies in the calculation of flexibility changes and the cutout conditions and also in an efficient organisation of cutout computations. There is also some discussion of changes in self-equilibrating systems appropriate to cutouts.

A new procedure for computing modifications has been developed which is based on standard triangularisation methods. To simulate cracks it is necessary to have a sufficiently refined idealisation. We have considered a rectangular sheet stringer grid in which the skin elements have nine generalised stresses which may be roughly described as two loads on each corner and an overall shear.

To find the flexibility changes associated with small crack extensions the concept of a moving element has been introduced. This is a finite element analogue of the crack tip and within it one assumes the stress pattern to be appropriate to a crack rather than the idealisation

used elsewhere. Using standardised data which has been calculated it is possible by numerical integration to find the modified flexibilities of elements near the crack, using interpolated stresses. These can then be used in the standard modification technique.

The chapters may be divided into four groups the first of which, Chapters I, IV and V, is concerned with cumulative damage theory and its application in the crack-damage equations. Chapters II and III are each self-contained and the last three chapters VI, VII and VIII concern the structural and computational aspects above. Equations are freshly numbered in each chapter and for referring to those elsewhere the chapter number is prefixed to the equation number, e.g. Eq. (2.20).

Chapter I

DAMAGE THEORY

The term damage is used here to describe any fatigue process not causing the immediate growth of a crack in the engineering sense of material becoming incapable of transmitting stress. The transition from damage to the cracked state we define as initial failure and the essential task of damage theory is to predict the probability distribution of initial lives for a given distribution of applied stress at the point in question. Although cracks elsewhere may influence the stresses and we later consider the probability of a local crack, these stresses are taken to be acting on uncracked material. This follows from our definition of damage. It will be noted that none of the well known damage theories satisfy this definition since they ignore statistical aspects. There is an extension of Miner damage which remedies this lack but the approach differs from that here and whether the result is a true damage is not certain.

1.1 Bastenaire Damage - Equivalence

The type of damage above is the one we use throughout, generally abbreviated to "damage". It is a general abstract form of damage evolved by Bastenaire¹ from an examination of the meaning to be attributed to the statement that two pieces of material are equally damaged. In this chapter the theory will be briefly sketched together with some consequences and generalisations.

We start with the axiom that v_0 cycles of some constant reference stress S_0 , or in Bastenaire's notation

$$(S(n)v_1) \rightarrow (S_0 v_0).$$

This means that if both tests are continued further at another, possibly different, constant load the residual life to initial failure has the same probability distribution in each case. In his paper Bastenaire does not specify whether initial or final failure but initial failure is consistent with our approach here.

If the state of the material changes continuously with the programmes then it is possible for two or more programmes to be equivalent to $(S_o v_o)$ i.e.,

$$(S_1(n)v_1) \rightarrow (S_o v_o)$$

$$(S_2(n)v_2) \rightarrow (S_o v_o) .$$

For convenience we suppose throughout that number of load cycles are continuous quantities.

If $S_1(n) \equiv S_1$ and the load in question is constant it is possible to speak of a reverse equivalence not implied above. In particular the reciprocal equivalence

$$(S_o v_o) \rightleftharpoons (S_1 v_1)$$

implies the following requirements for residual lives $N_1 - v_1$ and $N_o - v_o$ and their distribution functions $F(N_1 - v_1)$ and $F(N_o - v_o)$,

$$(S_1 v_1) \Rightarrow F(N_o - v_o) \quad , \quad (S_o v_o) \Rightarrow F(N_1 - v_1) \quad \dots \quad (1)$$

We shall say that there exists a damage if the relative values of a single quantity, the damage, are enough to determine whether the average residual life of one specimen is less than that of another. Since only relative values are important various measures of damage remain equivalent under any monotone transformation. We

also suppose that damage is differentiable.

Suppose we have a damage D and consider the equivalent constant loads above. Then trivially

$$(S_o v_o) = F(N_o - v_o)$$

and by equivalence

$$(S_1 v_1) = F(N_o - v_o) .$$

Because D exists

$$(S_o v_o) = F(N_1 - v_1)$$

so that $D = (S_o v_o) = (S_1 v_1)$ or $(S_1 v_1) = (S_o v_o)$ for $S \in \{S\}$.

This reasoning also applies to programmes since either $(S_o v_o)$ or $(S_1 v_1)$ are equivalent to a set of programmes. To show this one can start with an arbitrary programme $(S(n)v)$ and adjust it until the damage for a set number of cycles coincides with D . This is possible because all quantities are continuous. The existence of damage thus implies the existence of a set of programmes completely equivalent to one another.

Conversely if a set of programmes contains complete equivalence then they are all equivalent to some particular constant load test, $(S_o v_i)$ say, except that different numbers of applied loads in these programmes will alter $N_o - v_i$ the mean residual life at S_o .

If it is assumed that residual life is always reduced by further testing at any load then $1/(N_o - v_i)$ is monotone increasing with n and therefore a damage so that in this case a set of equivalent programmes implies the existence of damage and conversely. (The inversion is simply so that damage

will increase with time and is not strictly necessary.)

No mention has yet been made of all possible loads or programmes so that it is possible to visualise a set of loads or programmes to which a damage is applicable while there is another set where it is not.

The well known relief due to high loads is such a case where one-parameter damage is invalidated by yielding. On a macroscopic scale damage will seem reduced (from favourable residual stresses) with respect to low loads but not with respect to high so that the damage of the material cannot be transferred as the programme alters. This situation is easily corrected by allowing for residual stresses and it is also true that all known improvements of this kind can be explained by stress relief. If programmes are also allowed to produce an indirectly estimated residual stress as well as effect the damage then the number of possibilities can be considerably increased and indeed such a theory may cover all possible cases. However such a residual stress is a second parameter so that by definition no stress relief is allowable through one dimensional damage except by accurate stress analysis.

2.0 Growth of Damage

By definition the damage D summarises the whole past history of a specimen. Therefore its rate of increase depends on only D and the current stress, i.e.,

$$dD = A(D,S)dn + B(D,S)dS \quad \dots \quad (2)$$

The second term here is the effect of the rate of load change in the programme and may also be regarded as a predictor of loads in the immediate future. Since only the past can affect D this term must vanish leaving

$$\frac{dD}{dn} = A(D,S) \quad \dots \quad (3)$$

When averaged this will later become one of the crack-damage equations. It generalises an equation of Torbe's² which, in contrast to the above, he used for "historical" damage.

2.1 Effect of Load Order

Because different loading histories can lead to the same damage, D also includes some load sequence effects. As an example consider the two sequences

$$(S_1 v_1) + (S_2 v_2) = A \quad (= \text{defined as } \vec{a})$$

and $(S_2 v_2) + (S_1 v_1) = B$

differing only in order. Now let

$$(S_1 v_1) = (S_o n_1)$$

$$(S_2 v_2) = (S_o n_2)$$

so that

$$A = (S_o n_1) + (S_2 v_2) \quad \dots \quad (4)$$

$$B = (S_o n_2) + (S_1 v_1) .$$

To be definite put $n_1 < n_2$ and make the reference stress $S_o = S_2$. On substituting for S_o

$$A = (S_2 n_1 + n_2)$$

$$B = (S_2 n_2) + (S_1 v_1) .$$

There is no reason why A and B should be equal and this becomes most obvious if $v_1 = n_1$ in which case

$$\begin{aligned}
 n_2 &= v_2 \neq n_1 \\
 \text{and} \quad A &= (S_2 n_1 + n_2) \\
 B &= (S_2 v_2) + (S_1 v_1) \\
 &\neq A \quad \dots \quad (5)
 \end{aligned}$$

2.2 Relation to Life Distribution

The existence of reciprocal and transverse equivalence has been shown to imply a monotonically increasing damage D . For any programme $S(n)$ we also have, by definition,

$$\begin{aligned}
 &\text{Prob (Failure before } n \text{ cycles | for given programme } S(n)) = \\
 &= F(n|S(n)) \text{ where } 0 < F < 1, 0 < n < \infty.
 \end{aligned}$$

Thus F and D are corresponding damages. For many purposes the arbitrary damage is best taken as the life distribution and this life distribution is sufficient to evaluate the effect of one dimensional damage for any programme.

This simple outcome is complicated by the existence of endurance limits. For use later we remark that Swanson³ has shown that near the endurance limit the life distribution is bimodal and well approximated by the form

$$f(n) = p f_1(n) + (1-p) f_2(n) \quad \dots \quad (6)$$

where

$$p = \text{Pr ("short" life)}.$$

If there is a true endurance limit

$$\bar{n}(2) = \int_0^{\infty} n dF_2(n) \rightarrow \infty$$

and $1-p$ becomes the probability that the specimen never fails. This is indicated by some unpublished test results of Mann⁴ on steel. If damage is transformed to life distribution then (3) becomes

$$\frac{dF}{dn} = f(n) = A(F, S(n)) = (1-F) \cdot H(F, S(n)) \dots (7)$$

say, where the last formula will be called the reliability form and H the hazard. If the damage is F it will be called canonical. For a restricted range of stress $\{S\}$ the canonical damage becomes

$$\frac{dD}{dn} = f(n|\{S\}) \dots (8)$$

and if $S : f(S)$ then the expected canonical damage is

$$f(n|F) = \int f(n|S, F) dF(S) \dots (9)$$

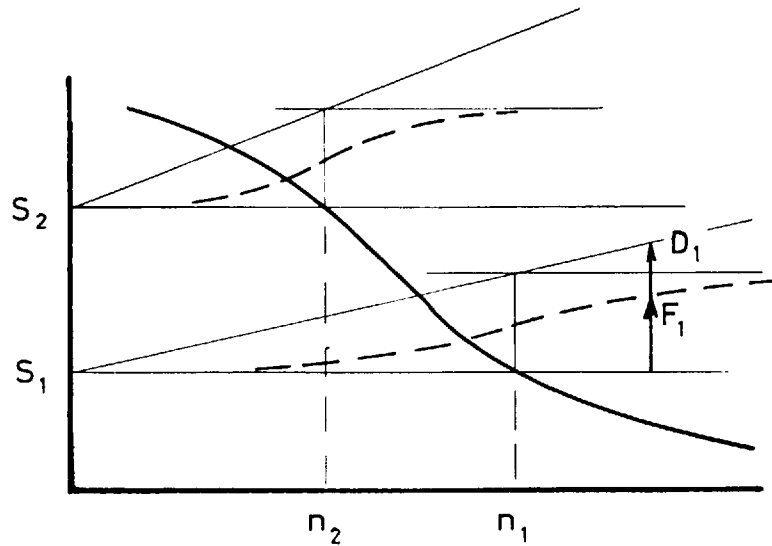
which agrees with dF/dn as a standard result in probability theory. In a later section complications related to the equivalence of damage rate and density will be considered.

2.3 Miner⁵-Palmgren⁶ Damage

Before proceeding further the theory above will be illustrated by the two cases of so-called linear damage and the theory to be used later. To be definite let unit damage occur when n reaches the mean life (constant load). In this formulation it is possible that $D > 1$ and this change from the normal theory reflects the inconsistency of most damage theories when statistical questions arise. In the figure

$$dD/dn = 1/n(S)$$

which is constant.



Let the loads $S : f(S)$. Then at any time n

$$\begin{aligned} \frac{dD}{dn} &= \int \frac{dD}{dn} \Big|_S dF(S) \\ &= \int \frac{dF(S)}{N(S)} = d_0 \text{ say} \quad \dots \quad (10) \end{aligned}$$

which is equivalent to the usual result.

Having found D the distribution of initial failures is immediate. We choose the life distribution for any particular constant load S_1 , F_1 in the figure say. For this load then

$$F_1 = F_1(D_1) \quad \dots \quad (11)$$

and if $D(n)$ is the solution in (10) then the corresponding value of the life distribution function is

$$F = F(n) = F_1(D(n)) \quad \dots \quad (12)$$

For Miner damage $D = nd_0$ so that if the programme has passed through D_1/d_0 cycles the damage will be D_1 and the life distribution as in (11). Since they are linear the damage curves shown must be affine and therefore any associated damages are also affine. The converse proposition that any affine damages must be Miner-Palmgren

damage was first established by B.F. Langer.⁷ In particular the standard deviation of the lives at any load must be proportional to the mean and by (10) this holds for random loads also so that all life distributions are similar except for a change of scale. This is obviously too restrictive for practical use.

2.4 Damage for log-normal Lives

The inherent restriction of Miner-Palmgren damage arises from the limited use made of the S-N information. If we use all the constant-load information in the form of canonical damage then a perfect one-parameter theory will follow. Any divergence from reality must then arise from the neglect of other damage parameters. For Miner damage mean lives were sufficient; below we use the variance also and approximate the canonical damage as log-normal distribution thereby following a long tradition in the treatment of fatigue results.

Let

$x : N(\mu, \sigma^2)$ indicate that x is normally distributed with mean μ and variance σ^2 . Equivalently,

$$f(x) = n(\mu, \sigma^2) = \frac{1}{\sqrt{2\pi}\sigma} e^{-\frac{1}{2\sigma^2}(x-\mu)^2} \dots \quad (13)$$

and if $u = (x-\mu)/\sigma$ we can define

$$\varphi(u) = f(u), \quad F(u) = \Phi(u) = \frac{1}{\sqrt{2\pi}} \int_{-\infty}^u e^{-\frac{1}{2}x^2} dx. \dots \quad (13A)$$

Since $F(n) = F(u) = \Phi(u)$

u is a suitable measure of damage.

At any stress S

$$u = (N - N(S)) / \sigma(S) \quad \dots \quad (14)$$

and $N = \log n$.

By the usual transformation formula

$$\begin{aligned} f(n|S) &= \varphi(u) \left| \frac{du}{dn} \right| \\ &= \frac{\varphi(u)}{\sigma(S)} \exp \{-u\sigma(S) - N(S)\}, \end{aligned}$$

and when this is averaged over the load density $f(S)$

$$f(n) = \varphi(u) \int_0^1 \frac{e^{-u\sigma(S)}}{\sigma(S)n(S)} dF(S)$$

and since $F(n) = \Phi(u)$ this is in the form (3) (here independent of S). In practice cracks elsewhere may affect the local stresses and $F(S)$ will depend on n . This change will be slow enough to allow $F(S)$ to be replaced by a short term distribution $F(S|n)$ say.

Now consider the moments of the initial life distribution $f(n)$ ($=dD/dn$). The r -th moment is

$$\begin{aligned} \mu_r &= \int_0^\infty n^r dF(n) \\ &= \int_0^\infty n^r \varphi(u) \int_0^1 \frac{e^{-u\sigma(S)} dF(S)}{\sigma(S)n(S)} \cdot dn \end{aligned}$$

If $f(S)$ is independent of n as the notation implies we can change the order of integration. If we also change the variable n to u then by (14)

$$\mu_r = \int_0^1 e^{rN(S)} dF(S) \int_{-\infty}^{\infty} \exp\{r u \sigma(S)\} d\Phi(u).$$

$$= \int_0^1 e^{r N(S)} dF(S) \int_{-\infty}^{\infty} e^{r u \sigma(S)} e^{-\frac{1}{2}u^2} \frac{du}{\sqrt{2\pi}}$$

The second integral is now obtainable by completing the square in the exponent whereupon the factor left after a linear change of variable is

$$\exp\left(\frac{1}{2}r^2 \sigma^2(S)\right)$$

and

$$\mu_r = \int_0^1 \exp\left\{r N(S) + \frac{1}{2}r^2 \sigma^2(S)\right\} dF(S) \quad \dots \quad (16)$$

The integrand here is the r -th moment of the constant load life at S which suggests that the distribution itself may also be a similar averaging over the S - n data. Let us form the characteristic function

$$\varphi_n(t) = \int_{-\infty}^{\infty} e^{int} dF(n)$$

which by the same procedure becomes

$$\int_0^1 \int_{-\infty}^{\infty} \exp\{it \cdot e^{u\sigma(S)+N(S)}\} \varphi(u) du dF(S) \quad \dots \quad (15)$$

representing the expectation over $F(S)$ of the characteristic functions of the constant load life distributions which are here log-normal. The random load life distribution can now be found as a Fourier inversion integral and when this is commuted with the outside integral in (15) we know that the overall density is in fact an average as envisaged. This is only true if the stress distribution is constant over the life or in other words the local stresses are not affected by cracks elsewhere.

Now suppose that cracks have affected the stress by a factor $k(n)$ and let $F_0(S)$ be the initial stress distribution so that

$$F(S|n) = F_0(S/k(n)).$$

As in (15) then

$$\begin{aligned} \frac{dD}{dn} &= \varphi(u) \int_0^1 \left| \frac{du}{dn} \right|_S \text{const} dF(S|n) \\ &= \varphi(u) \int_0^1 \left| \frac{du}{dn} \right|_S \frac{dF_0(S/k)}{k(n)} \end{aligned}$$

which again has the form (3) since $u \Leftrightarrow D$ and within a scale factor $k \Leftrightarrow S$. This is still a density and the corresponding moments are

$$\begin{aligned} u_r &= \int_{-\infty}^{\infty} \frac{n^r \varphi(u)}{k(n)} dn \int \frac{e^{-u\sigma(S)}}{\sigma(S)N_0(S)} dF_0(S/k(n)) \\ &= \int_{-\infty}^{\infty} \int_0^1 \frac{\exp\{-\frac{1}{2}u^2 + ru(S) + rN(S)\}}{\sqrt{2\pi}k(\exp(u\sigma(S) + N(S)))} dF_0(S/K) du \end{aligned}$$

after the integrand is expanded. Substituting the initial stresses,

$$u_r = \int_{-\infty}^{\infty} d\phi(u) \int_0^k \exp\{ru\sigma(kS) + rN(kS)\} dF_0(S) du \quad \dots (17)$$

If the contribution of high stresses to the inside integral is small the upper limit may be taken as a constant and we can change the order of integration. The integral over life then becomes

$$\begin{aligned} \int e^{ru\sigma(kS) + rn(kS)} d\phi(u) &= \int e^{ru\bar{\sigma}(S) + r\bar{N}(S)} \cdot e^{r(u(\sigma - \bar{\sigma}) + (N - \bar{N}))} d\phi(u) \\ &= \exp\{r\bar{N}(S) + \frac{1}{2}r^2\bar{\sigma}^2(S)\} \cdot \{\text{mean value of } \int e^{r(u(\sigma - \bar{\sigma}) + (N - \bar{N}))} du\} \end{aligned}$$

by the mean value theorem. The second factor reverts to

$$\int_0^{\infty} \exp\{r-1[u\sigma(kS) + N(kS)] - r[u\bar{\sigma}(S) + \bar{N}(S)]\} dn \quad \dots (18)$$

on changing the variable back to n .

If the mean value of this integral is set to unity for $r=1,2$ then this fixes $\sigma(S)$ and $N(S)$ as functions of S . We have thus defined a fictitious S - n curve for which (16) remains true when $r=1,2$ but not for higher values. This is similar to the fictitious S - n curve introduced by Freudenthal⁸ to allow for "stress interaction". Since Freudenthal's damage is related to final failure the physical basis of the effect here is similar except that in his case there is a self-interaction because of the local crack. As a method of computation, the form of (18) would indicate that it is best avoided in favour of (17) where a 4-point Gaussian formula should give good results quickly.

2.5 Effect of Endurance Limits

If we draw contours of canonical damage (constant load) on an S - n diagram these define equal probabilities of prior failure and we have a surface $F(N|S)$ on the S - n plane. This has zero height along $n=0$ and in general is asymptotically 1 as $n \rightarrow \infty$.

In the diagram cross sections at two loads are shown, appropriate to the simple programme on the left. Since damage is effectively $F(n)$ the path followed by the material during the programme is that shown, with damage transference along the contours, and the total number of cycles is the sum of segments such as a and b . This geometric interpretation of (3) is easily generalised to any programme or type of one-parameter damage and in particular (9) may be interpreted as the averaging of slopes along contours such as AB in the figure.

When some of the loads are below the endurance limit there is a finite probability of infinite life which may

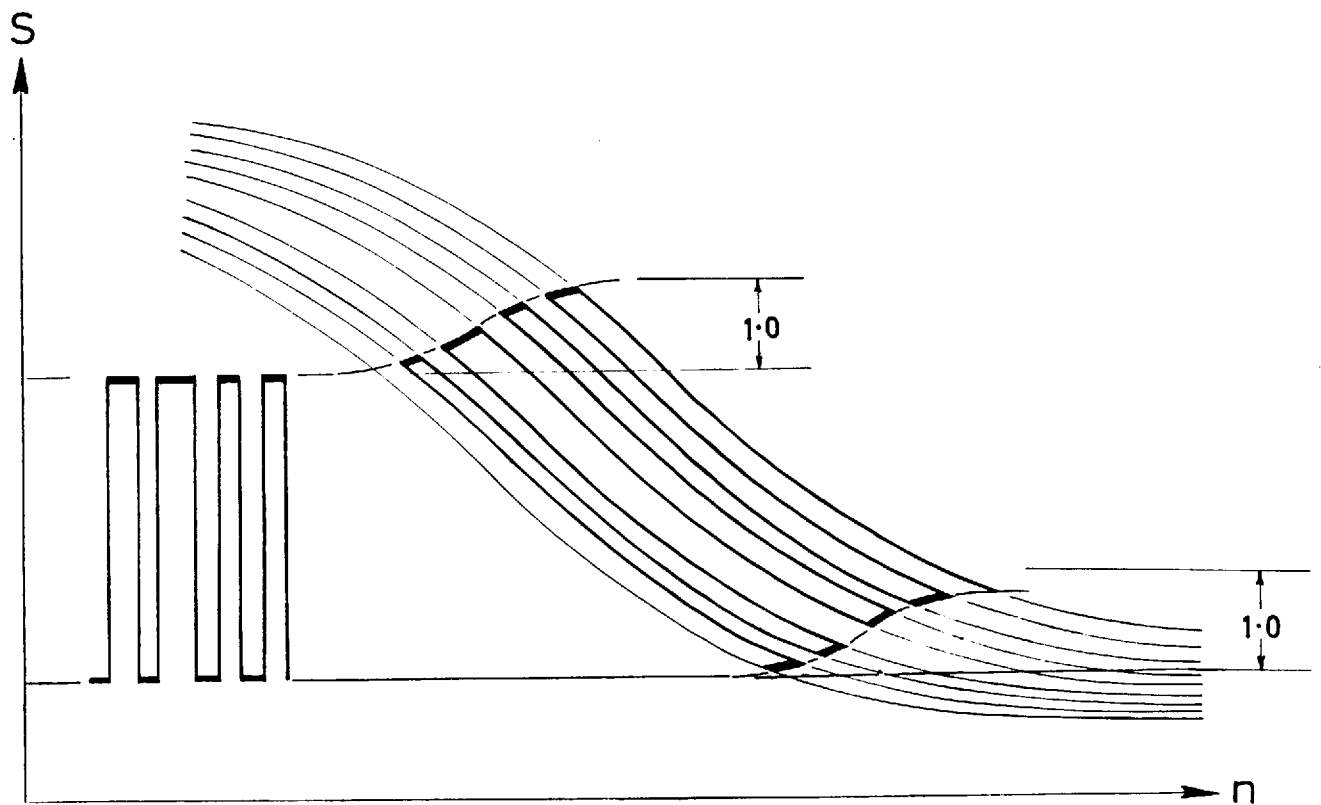
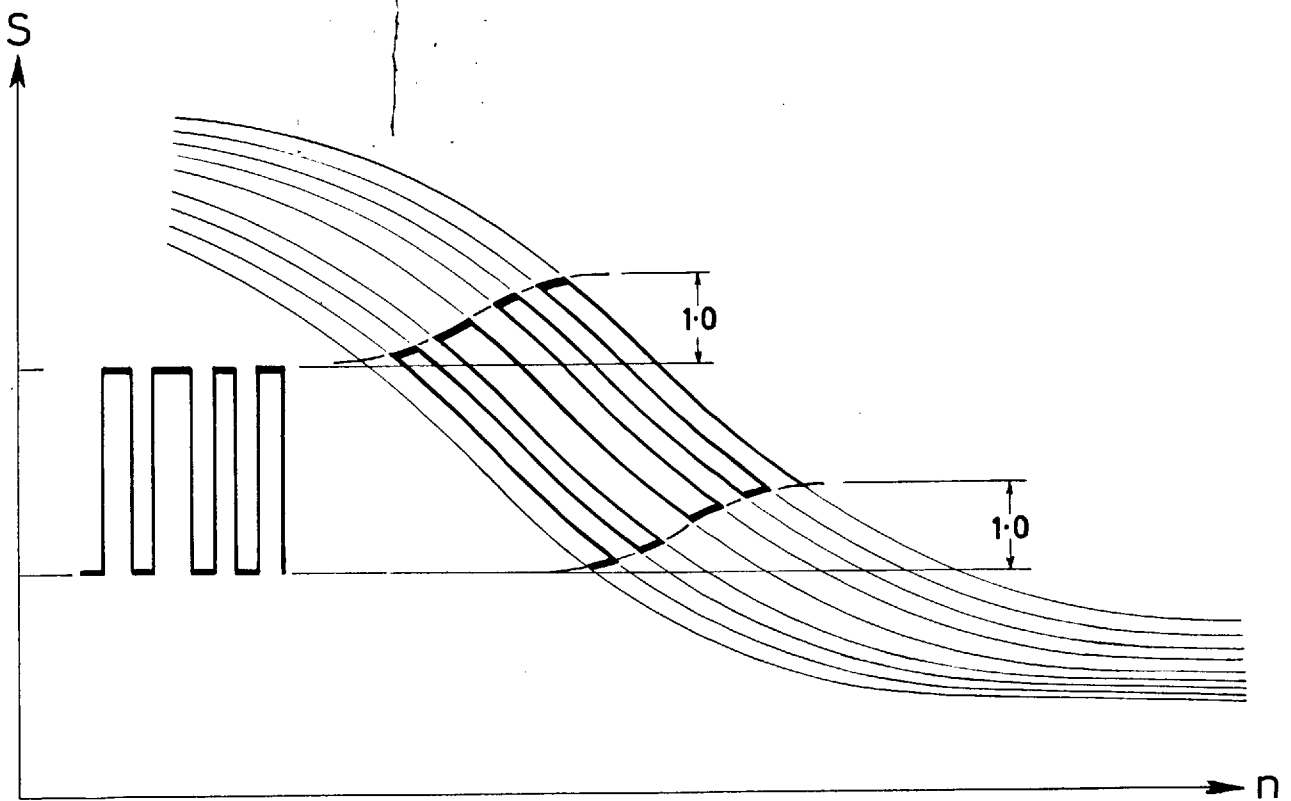


FIG. 1 DAMAGE BELOW ENDURANCE LIMIT

be simulated by having

$$F(n|S < E) \rightarrow p(S) < 1 \quad \text{as } n \rightarrow \infty.$$

For Miner damage the damage rate $1/n(S)$ becomes zero if $S < E$ but (6) indicates that for "short" lives

$f(n|S < E) > 0$, or for all lives $p(S)f(n|S < E) > 0$, so that damage can be done by programme loads below the endurance limit. This is not related to the development of cracks begun by higher loads for we have spoken only of initial failure. For a stress distribution independent of n we now investigate the effect of endurance limits on the log-normal damage of the previous section.

In (6) the second term becomes zero and since the distribution of u now becomes $p(S)\varphi(u)$, $\varphi(u)$ itself is no longer a damage. If E_* is the lower endurance limit (15) becomes

$$f(n) = \int_{E_*}^1 \varphi(u_o) \frac{e^{-u_o(S)}}{\sigma(S)n(S)} dF(S)$$

where u_o depends on S in such a way that

$$p(S)\varphi(u_o) = \varphi(u),$$

representing constant damage. This condition reduces to

$$u_o^2 = u^2 + 2 \ln p(S)$$

and we also know that

$$u = (N - N(S))/\sigma(S),$$

$N(S)$, $\sigma(S)$ referring to short lives if $S > E$. After these expressions are substituted into (15) as modified the r -th moment becomes

$$\mu_r = \int_0^{\infty} \int_{E_*}^1 \exp r\{\sigma(S)\sqrt{u_o^2 - 2\ln p(S)} + N(S)\} \frac{\varphi(u_o)e^{-u_o\sigma(S)}}{\sigma(S)n(S)} dF(S)dn$$

$$= \int_{E_0}^1 \int_0^{\infty} \exp r \{ u_0 \sigma(S) + N(S) + \overline{u - u_0} \sigma(S) \} \frac{\varphi(u_0) e^{-u_0 \sigma(S)}}{\sigma(S) n(S)} du_0 dF(S)$$

where $n(S) = \exp(N(S))$. Changing the variable to u_0 produces

$$u_r = \int_{E_0}^1 \int_{-\infty}^{\infty} \varphi(u_0) e^{ru_0 \sigma(S)} e^{rN(S) + r+1 \sigma(S) \overline{u - u_0}} (u_0/u) du_0 dF(S) \quad \dots \quad (19)$$

From the mean value theorem, the inside integral can be written

$$e^{rN(S)} \int_{-\infty}^{\infty} \varphi(u_0) e^{ru_0 \sigma(S)} du_0 \cdot \frac{\overline{u_0}(S) \cdot \exp r+1 \sigma(S) [u(S) - u_0(S)]}{\sqrt{\overline{u_0}^2(S) - 2 \ln p(S)}}$$

where $\overline{u_0}(S)$ is the typical value. The factor may now be interpreted as $\exp(r\overline{N}(S))$ where $\overline{N}(S)$ is another fictitious S-n curve differing for each moment.

When $p(S)=1$ $\overline{u_0}$ is obviously zero and in other cases one may increase u_0 until $\varphi(\overline{u_0}) = p(S)/\sqrt{2\pi}$. In this case the rate of damage increase for the approximating problem, using u_0 or N but ignoring infinite lives, is roughly the same as in the original problem. From these approximations

$$\overline{u_0}^2 \approx -2 \ln p(S)$$

and $\overline{u} \approx 0$

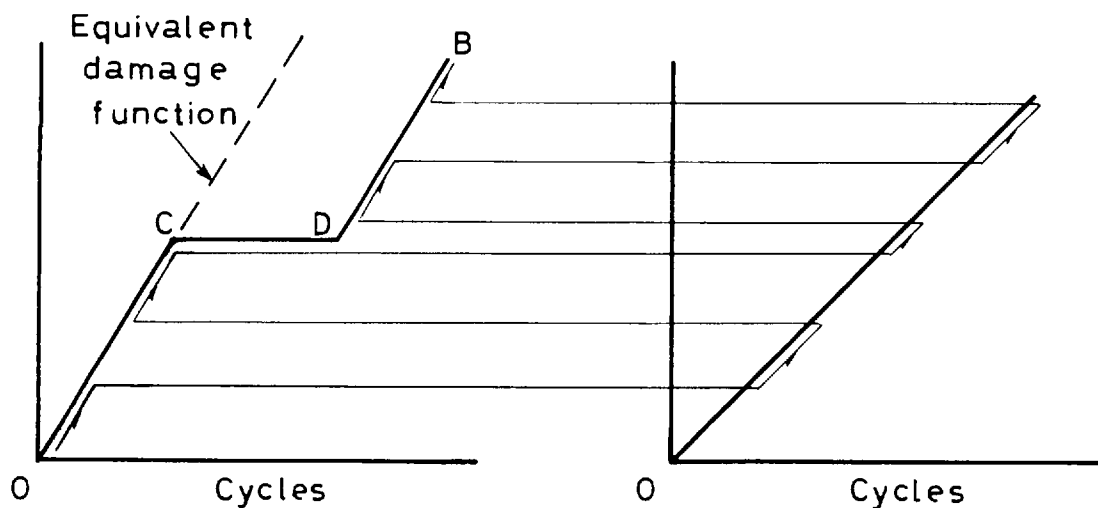
and the fictitious S-n curve becomes

$$\overline{N}(S) \approx N(S) - \frac{r+1}{r} \sigma(S) \sqrt{-2 \ln p(S)} - \ln 2 \quad \dots \quad (21)$$

in terms of log lives.

This example illustrates the predominant effect in Bastenaire theory of the higher damage rates. Damage

occurred below the endurance limit because, although the mean life was infinite together with the overall variance, the first mode (in (6)) produced a finite probability density, i.e. a finite damage rate. Because damage is retained during a programme dormant periods at particular loads tend to be bypassed. Thus the two (constant load) damages below have the same effect in a programme because the horizontal section CD will be passed as soon as any different load is applied and only the sections OC, DB contribute to the damage.



3.0 Correlation Effects

It has been shown⁹ that the correlation between the possible fatigue lives of the same specimen at different loads may have a marked effect on the variance of lives under random load. This conclusion arises from an extension of Miner damage in a direction foreign to Bastenaire theory and the approximate effect was that standard deviation was proportional to correlation.

For Bastenaire theory let us divide the specimens into groups K with probabilities $dF(K)$ (see Figure) within which the conditional life distributions are independent (we assume this to be possible) with densities

$$f(n | F, S, K)$$

so that
$$f(n | SF) = \int f(n | F, S, K) dF(K) \quad \dots \quad (22)$$

Taking expectations over S we find the conditional damage rate

$$f(n | F, K) = \int f(n | S, K, F) dF(S)$$

which itself has the expectation

$$f(n | F) = \int f(n | F, K,) dF(K)$$

all of which is entirely consistent with the laws of probability. The unconditional damage must therefore be identified with the marginal distribution of all specimens. Any reduction in the variance under random loads must therefore be attributed to further parameters.

4.0 Corrosion Fatigue

From the obvious generalisation of (3) it is possible to set up multidimensional damage by making the life distribution a function of the damage vector. For a less abstract approach we first consider a hypothetical case of corrosion fatigue in which fatigue and corrosion form two components of the damage vector.

Let D denote Miner damage and by C denote a fraction of material corroded so that if the nominal applied stress is S : $f(S)$ the stress for the purposes of Miner damage is

$$\sigma = s/(1-C).$$

Suppose further that

$$dC/dt = c(\sigma) + c(S/(1-C))$$

and in the usual manner

$$dD/dn = \int \frac{f(\sigma)d\sigma}{N(\sigma)} .$$

Let ω be the frequency of loading so that in unit time $k\omega$ say is spent at high load and the remainder at normal. A more refined time-integration procedure is not suited to this rudimentary investigation.

Thus

$$dC/dt = k\omega E(c(\sigma)) + c_o(1-k\omega), \quad \text{say,}$$

where E is the expectation. Now

$$f(\sigma) = (1-C)f_s(\sigma, \overline{1-C})$$

and the two damage equations become

$$dD/dn = (1-C) \int_0^1 f_s(S)d\sigma/N(\sigma) \quad \dots \quad (23)$$

$$= \int_0^{1-C} \frac{f(S)dS}{N(S/1-C)}$$

$$dC/dN = k \int_0^{1-C} f(S)dS \cdot c(S/1-C) + \frac{1-k\omega}{\omega} c_o$$

We have tacitly assumed that the upper limit

$$S = 1-C$$

is not exceeded or that its effect is negligible. In this case the second equation can be solved numerically and the result substituted into the first (by using a fixed upper limit). The equations themselves are simply a two-dimensional form of (3) but from the formulation here the mode of failure is necessarily by fatigue if we use the Life distribution based on the Miner damage of Sec. 1.1

However if this is done then the two equations above are merely a way of calculating a single damage and as we have seen one can, in principle, eliminate all damages but the one of interest. We conclude that true multi-dimensional damage must produce life distributions depending on all the parameters and in many cases there are several possible modes of failure (e.g. corrosion in the case above) which must be considered in the initial failure distribution. This will be considered when we return to corrosion fatigue.

5.0 Two Parameter Damage

The direct generalisation of (3) takes the form

$$dD/dn = A(D, S) \quad \dots (24)$$

where the notation indicates that each component of A depends on all the components of D .

It has been postulated by Bastenaire¹ that D defines an equivalent state based on a vector with

$$f(n) = f_n(D). \quad \dots (25)$$

In this system the equivalence

$$(S \nu) = (g(N) \nu_0)$$

defines a class of programme functions $g(n)$ which contain S, ν, ν_0 as parameters, presumably in a continuous and differentiable manner. More generally if

$$(g(n)\nu_1) = (h(n)\nu_2)$$

then $g(n)$ is a functional of $h(n)$ with parameters ν_1, ν_2 .

The damage increment along a programme is then (24) generalising (3). If required, the load S may also be extended to include the mean load as well.

If the other measures of the damage are obvious, e.g. corrosion or creep it may be possible to modify the one-parameter equations in a physically reasonable way to account for further effects. This has been done already for corrosion fatigue and we return to this example for further development.

5.1 Generalised Corrosion Fatigue

We now suppose that the stresses effective in fatigue and in corrosion are different so that for example the first is mostly affected by alternating loads, or range pairs for random loads, while the second is probably a function of maximum loads. For the processes generally occurring it is likely that even the frequencies of the two loads would be different. Suppose that

$$S : F(S)$$

relates to fatigue damage while for corrosion

$$P : F(P)$$

The first of these is set in discrete time while the latter loads are continuous in time. To relate the two let the average frequency of fatigue loads be \bar{w} .

Then the rate of corrosion is on the average

$$\begin{aligned} dc/dt &= \int c(P/\sqrt{1-C})dF(P) \\ &= \frac{1}{\bar{w}} \frac{dC}{dN} \quad \dots \quad (26) \end{aligned}$$

where the upper limit corresponds to the assumption that (initial) corrosion failure occurs when

$$P > 1 - C.$$

Now let us use the canonical damage $F = F_d + F_c$ as the

second parameter where F_c , F_d are the partial distributions of either fatigue or corrosion failure. In the absence of corrosion suppose that F_d is the solution of the equation for pure damage

$$\frac{dF_d}{dn} = H(S, F_d)(1-F_d) \quad , \quad \dots \quad (27)$$

in the reliability form. When corrosion is present the stresses increase to

$$\sigma = S/(1-C)$$

This expression is rather crude in order to simplify the illustration. However C , like D previously, belongs to a class of equivalent damages related by monotonic transformations so that it is more general than appears at first sight. When the mode of failure is uncertain the factor $(1-F_d)$ in (27), excluding prior fatigue failures, must now exclude all types of failure and accordingly it must become $(1-F)$.

If we also take the expectation over S then (27) becomes

$$\begin{aligned} dF_d/dn &= (1-F) \int_0^{1-C} H(S/1-C, F_d) dF(S) \quad \dots \quad (28) \\ &= (1-F) \int_0^{1-C} H(S/\sqrt{1-C}, F-F_c) dF(S) \end{aligned}$$

For corrosion failure

$$dF_c/dn = (1-F) \int_{1-C}^1 dF(P) = (1-F)H_c \quad \text{say} \quad \dots \quad (29)$$

where once more the factor outside excludes both kinds of failure. In (26) the only corrosion of interest is that occurring on unfailed specimens so that the proper equation to use is

$$dC/dn = (1-F) \int_0^{1-C} c(P/1-C) dF(P) \quad \dots (26A)$$

Adding (28) and (29),

$$dF/dn = (1-F) \left\{ \int_0^{1-C} H(S/1-C, F_d) dF(S) + \int_{1-C}^1 dF(P) \right\} \dots (30)$$

The equations (26), (27) and (30) may now be solved for C, F and F_d . In (29) the variables are separable from F and if we put $F(0) = 0$ we find

$$F = 1 - \exp \left(- \int_0^n \{ \} \right)$$

and by subsequent substitution into (28)

$$F_d = 1 - \exp \left(- \int \{ \} \right) - \int_0^n \exp \left(- \int \{ \} \right) \int_{1-C}^1 dF(P) dn$$

Treating the modified form of (27) similarly, (factor (1-F)),

$$C = \bar{w} \int_0^n \exp \left(- \int \{ \} \right) \int_0^{1-C} c(P/1-C) dF(P) dn. \quad \dots (31)$$

These are the formal solutions but only in the sense that the differential equations have been replaced by transcendental ones. In practice numerical solution of the original equations is probably the simplest course.

To allow for small rates of corrosion let us expand \bar{H} in (26A), (29) and (30) as a Taylor series in F_c .

Then

$$H(S/\sqrt{1-C}, \overline{F-F_c}) = \bar{H} - F_c F_F + \frac{1}{2} F_c^2 H_{FF} - \dots$$

$$\text{and } 1-F = e^{-\int H_c dn} \exp \left\{ - \int \bar{H} dF(S) dn + F_c \int H_F dF(S) dn - \dots \right\}$$

whence by (33)

$$dF_c/dn = H_c e^{-\int H_c dn} \exp \left\{ - \int \bar{H} dF(S) dn + F_c \int H_F dF(S) dn \dots \right\}$$

The corrosion C is still given by (31) with the appropriate modifications to $\{ \}$.

5.2 Canonical Form of Multidimensional Damage

For simple damage the canonical form was found to be equivalent to the life distribution function $F(n)$ for the programme in question. In symbols

$$dD/dn = A(D, S) \quad \text{and} \quad F(n) = F_n(D) \quad \text{say.}$$

In the more general case let us put $F(n)$ in the form

$$F_r(n) = F_o(n)G_1(n)G_2(n) \dots G_r(n) \dots \quad (32)$$

where $F_o(n)$ is the canonical form of the one parameter approximation so that

$$0 \leq F_o(n) \leq 1.$$

Now consider the two-dimensional case where the properties of probability distribution functions assure that

$$0 \leq F_1 < F_o^{-1}.$$

Let $F_r(n)$ ($=F_r$) be the r -dimensional damage in the canonical form

$F_r(n) = P_r(\text{Failure has occurred before } n | r \text{ parameters}).$
Obviously as a distribution

$$0 \leq F_r \leq 1$$

and if successive damage parameters are deleterious

$$F_{r+1} > F_r$$

or

$$G_r > 1.$$

The two inequalities together are

$$F_r < F_{r+1} < 1,$$

or on dividing

$$1 < G_{r+1} < F_r^{-1}.$$

Now consider the meaning of the expression

$$F_r = F_{r+1} G_{r+1}^{-1} \dots \quad (33)$$

i.e. P_r (failure|r parameters) = P_r (failure|r+1) G_{r+1}^{-1} .

Since $F_r < G_{r+1}^{-1} < 1$ it may be interpreted as a (Bayesian) probability that the (r+1)-th parameter is not needed to describe the damage. It will also be noted that

$$G_{r+1} > G_r$$

which agrees with the plausible idea that, as more damage parameters are introduced, the need for others will decrease.

As we have noted it often happens that two or more mechanisms acting together will partially cancel each other such as stress relief caused by creep.¹⁰ This contrasts with the case above which we can distinguish as pure damage. Because all cases of improvement (except coaxing) can be ascribed to stress relief it is possible that in the strict sense pure damage is the only kind.

5.3 Variance under Programme Loading

When considering simple damage (correlation effects) it was decided that the reduction in the variance of lives observed by several investigators¹¹ associated with random loading was caused by an additional component of damage.

For increasing orders of pure damage above, the probability of prior failure and the subjective probability that the number of parameters (i.e. the order of damage) is sufficient both increase uniformly over the life n as the order r increases.

If the logarithmic variance σ^2 of life depends only on the programme $S(n)$ and not on the order of damage r and if also the log-life is normally distributed $N(\mu, \sigma^2)$ then the inequality

$$F_{r+1} > F_r \quad 0 < n < \infty$$

is equivalent to

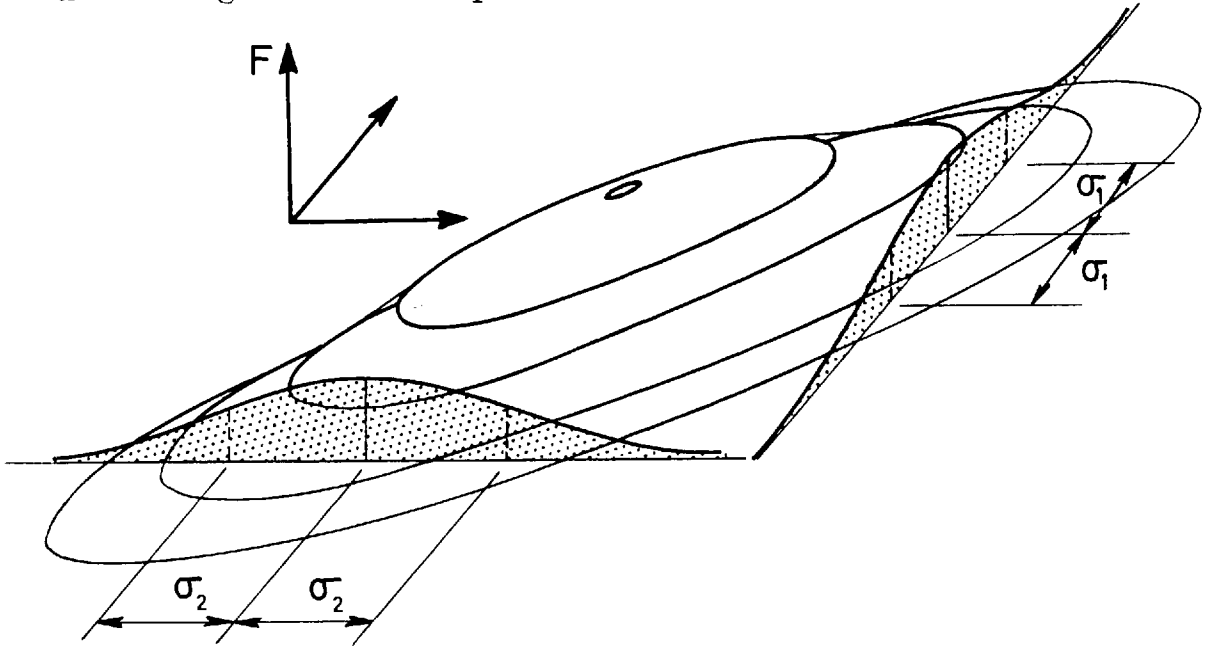
$$\mu_{r+1} < \mu_r$$

and the whole question reduces to a general linear regression problem.

With these restrictions the treatment of r -dimensional damage becomes more manageable. In addition, since all the information now concerns the mean μ , testing and analysis can be made much more efficient. Finally there is now no need (in this case) for the restriction (34) which confines us to pure damage.

The success of this approximate theory depends on the measurement or prediction of σ^2 which itself involves some of the damage components. It has been surmised that the reduction in variance is associated with correlation between the constant load lives of the same specimen, i.e. a specimen "strong" at one load will also be strong at another. This explanation will be retained but we now imagine that the random loading $S(n)$, $S:F(S)$ will average the minimum variances of each load in the programme.

One of the essential effects of correlation is the reduction of variation in conditional distributions as compared with the joint distribution. For the bivariate distribution in the sketch for example the conditional standard deviations σ_1 , σ_2 are obviously smaller than their marginal counterparts.¹²



If this figure is appropriate to the two load programme

$$f(S_1) = p \quad , \quad f(S_2) = 1 - p$$

then the simplest case of our theory for the random load variance will give

$$\text{Var}(n \text{ under random load}) = p \sigma_1^2 + (1-p) \sigma_2^2 \dots (35)$$

Strictly speaking (35) is meaningless unless σ_1 and σ_2 are independent of the load or variate which has been fixed. This is a characteristic of the multivariate normal distribution and we now generalise (35) to programmes whose loads are associated with lives (or log lives) following the k -fold normal density

$$f(\mathbf{x}) = (2\pi)^{-\frac{1}{2}k} |\mathbf{A}|^{-\frac{1}{2}} \exp(-\frac{1}{2}(\mathbf{x} - \boldsymbol{\xi})^t \mathbf{A}(\mathbf{x} - \boldsymbol{\xi}))$$

where \mathbf{A}^{-1} is the matrix of covariances. Now let us fix all variates except x_1 say and suppose that the remaining variates x_1 have the covariance matrix \mathbf{A}_1^{-1} which must be a submatrix of \mathbf{A}^{-1} . The conditional density is

$$f(x_1 | \mathbf{x}_1) = f(\mathbf{x}) / f(\mathbf{x}_1)$$

which is also normal with the exponent

$$-\frac{1}{2}(\mathbf{x} - \boldsymbol{\xi})^t \mathbf{A}(\mathbf{x} - \boldsymbol{\xi}) - \frac{1}{2}(x_1 - \xi_1)^t \begin{bmatrix} 0 & 0 \\ 0 & \mathbf{A}_1 \end{bmatrix} (x_1 - \xi_1)$$

where \mathbf{A}_1 is not a submatrix of \mathbf{A} . The inverse of the element $\mathbf{A} - \begin{bmatrix} 0 & 0 \\ 0 & \mathbf{A}_1 \end{bmatrix}$ then supplies the conditional variance and this can be done for each variate in turn.

Removing the factor \mathbf{A} this becomes

$$\begin{aligned} & \mathbf{A} \left(\mathbf{I} - \mathbf{A}^{-1} \begin{bmatrix} 0 & 0 \\ 0 & \mathbf{A}_1 \end{bmatrix} \right) \\ &= \mathbf{A} \left(\mathbf{I} - \begin{bmatrix} \mathbf{A}_{11} & \mathbf{b}' \\ \mathbf{b} & \mathbf{A}_1^{-1} \end{bmatrix} \begin{bmatrix} 0 \\ \mathbf{A}_1 \end{bmatrix} \right) \\ &= \mathbf{A} \begin{bmatrix} 1 & 0 & \dots & 0 \end{bmatrix} \\ &= a_{11} \text{ say.} \end{aligned}$$

The reduced variance is therefore a_{11}^{-1} so that the rule for the k loads is to invert the diagonal matrix formed from the diagonal of the inverted covariance matrix.

The logarithmic variance of life is then

$$\sum_{i=1}^k a_{ii}^{-1} f(S_i) \quad \dots (36)$$

where the notation emphasises the discreteness of the programme $f(S)$. For continuous distributions this method

obviously fails but it is possible that there is an equivalent one based on the theory of Fredholm integral equations.

Because this reduction of variance is still uncertain and has never been properly verified even for the one-dimensional theory described here there is no point in discussing its physical nature.

5.4 Log-normal Damage with Several Parameters

Before leaving this chapter let us extend the log-normal model described above to a stage amenable to statistical analysis.

Suppose we have several recognisable and observable damage parameters as well as the fatigue life and the constant logarithmic variance. Then in order to avoid confounding we need at least as many distinct programmes as there are parameters and preferably several more for practical results.

Let there be N programmes P_i say, each producing a logarithmic life $n_i : N(\eta_i, \sigma^2)$ by our assumptions. For each of these (which need not all be different) we also observe or calculate the set of parameters x_i . If we also assume that the mean lives depend linearly on x then for all programmes

$$X\beta = y + e \quad \dots \quad (37)$$

where $y = n - n_0$, the change in life caused by the extra parameters,

$X = [x_i]$, the parameters for all programmes, and e is a vector of errors. This is the general linear hypothesis in analysis of variance¹³ and the effects β can be fitted to this model by minimising the error sum of

$$e^t e = (\beta^t X^t - y^t)(X\beta - y)$$

with respect to β . The solution is

$$\hat{\beta} = (X^t X)^{-1} X y \quad \dots (38)$$

with the error sum of squares

$$e^t e = y^t y - y^t X \hat{\beta} \quad \dots (39)$$

Further details may be found in Kempthorne¹³ or any other statistical text but the essential point here is its applicability. With good experimental design simple standardised analyses can be substituted for (38) and (39). It is also important to remember that the "linearity" refers to the role of $\hat{\beta}$ in (37) and a non-linear relation between life and the damage parameters is perfectly feasible, if further parameters are introduced. For example if

$$y = a + bx + cx^2 + e \quad \dots (40)$$

then $\{a \ b \ c\}$ is the vector β of (37).

In practice it is likely that the presence of higher damages will be noticed only by the effect on the life and there will be no obvious effects to measure. In such cases we will show that arbitrary functions of the load may be chosen as damage parameters to any degree of approximation. This is obviously no substitute for physical insight which would be reflected in the present framework by a need for very few parameters combined with a truly minimal error variance.

We again postulate the parameters x which are now unknown but we now suppose that they can be written in the form

$$x_{jn} = \int \xi_i(S) dF_j(S) \quad \dots (41)$$

where $F_j(S)$ describes the j -th programme and $\xi_i(S)$ is a constant load relation for the parameter in question. The problem previously described by (37), (38) and (39) now includes the estimation of the ξ 's. To get any further it is necessary to restrict ξ to forms (not necessarily polynomial) like (40) which depend on a certain number of parameters. Thus

$$\xi_i(S) = a_{i1}s_1(S) + \dots + a_{im}s_m(S) \dots \quad (42)$$

and without loss of generality the $s_1(S)$ can be taken as linearly independent. Substituting in (41)

$$\begin{aligned} x_{ji} &= \int [a_{i1}s_1(S) + \dots + a_{im}s_m(S)] dF_j(S) \\ &= a_{i1}S_{ij} + \dots + a_{im}S_{mj} \\ &= \mathbf{S}_j^t \mathbf{a}_i, \text{ say,} \end{aligned}$$

where $S_{kj} = \int s_k(S) dF_j(S)$,

the expectation of $s_k(S)$ in the j -th programme and a known quantity in the present context. In (37) then

$$\begin{aligned} &= [\mathbf{S}_j^t] [\mathbf{a}_i] \\ &= \mathbf{S} \mathbf{a}, \text{ say,} \end{aligned}$$

so that

$$\mathbf{y} + \mathbf{e} = \mathbf{S}^t \mathbf{a} \hat{\beta} \dots \quad (43)$$

with $\hat{\beta}$ of order m . Except that $\mathbf{a} \hat{\beta}$ has replaced $\hat{\beta}$, this is exactly the same problem as (37) but the solution there supplies only $\mathbf{a} \hat{\beta}$ as a whole. No further equations to find \mathbf{a} can be found. For the error sum of squares is now

$$\mathbf{e}^t \mathbf{e} = (\hat{\beta}^t \mathbf{a}^t \mathbf{S} - \mathbf{y}^t) (\mathbf{S}^t \mathbf{a} \hat{\beta} - \mathbf{y})$$

and if the variation of this with respect to a alone is considered we find that

$$d(e^t e) = 2(\beta^t a^t S - y^t) S^t da \beta + 40^2 (da)$$

which is automatically zero for the given solution $a \hat{\beta}$. The form (42) is therefore no better than (41) in which the ξ_i may be arbitrary. In (41) however the effect of using further ξ 's can be assessed by an analysis of variance.

6.0 Final Note on Applicability

Because it seems more fundamental physical damage in the sense of this chapter has been taken to describe processes before initial failure which is here the sudden appearance of a crack. However this is ambiguous and for different purposes the initial crack length can be made roughly equal to the grain size, as we argue later, or lengths such as the distance from the edge to the opposite side of a rivet hole which could be used for aircraft structures.

Similarly the loads which form the programmes can also be generalised. In a fatigue context two such possibilities are programmes of the stress intensities defined in fracture mechanics and programmes of different rms values of random noise loading for which Kirkby¹⁴ has produced S-n curves. He suggests that Miner damage calculations based on such data are more accurate. That the results are only partly better may be due more to the inherent limitations of Miner damage than to the use of rms loads and it is possible that a one parameter Bastenaire damage may suit this case and not that of constant load S-n curves.

Chapter II

FINAL FAILURE,

HAZARDS AND RELIABILITY

In the first chapter it was stated that the life distribution to ultimate failure was a subsidiary problem which could be solved separately after the general fatigue problem, whose solution described the random growth of cracks, taking cumulative damage into account. The method of doing this belongs to the theory of reliability and the relevant analysis will be developed below.

1.0 Failure Rate and Hazards

Suppose we have a structure whose ultimate strength changes with time (or cycles) in a known manner. This is subjected to a series of loads (the same ones that indirectly reduce the strength by starting fatigue cracks) which may exceed this strength. In this way the structure will fail and the probability of this event is

$$\Pr(\text{failure on } n\text{-th cycle}) = \Pr(\text{no previous failure}) \times \Pr(S_N > U_n | \text{n.p.f}) \dots \quad (1)$$

where $S_n = n\text{-th load}$

$U_n = \text{strength at } n\text{-th cycle.}$

Now the left hand member is merely the probability density $f(n)$ of cycles to ultimate failure so that (1) may be abbreviated as

$$f(n) = [1 - F(n)] h(n) \dots \quad (2)$$

where $H(n) = \Pr(S_n > U_n | \text{no previous failure})$

is commonly called the hazard rate or hazard. If we allow cycles to be continuous variables then (2) becomes the separable equation

$$d(\log\{1-F(n)\}) = -h(n) \quad \dots \quad (3)$$

with the solution

$$F(n) = 1 - \exp(-H(n)) \quad , \quad F(0) = 0, \quad \dots \quad (3A)$$

where

$$H(n) = \int_0^n h(t)dt \quad ,$$

the total hazard. The corresponding density is

$$f(n) = h(n) \exp(-H(n)) \quad \dots \quad (4)$$

and if $h(n)$ is a constant, as it is in many applications,¹⁵ the life distribution is exponential. For aircraft such a case would be ultimate failure by gust loading in the absence of weakening from fatigue. If there are two independent modes of failure then (2) becomes

$$f(n) = [1-F(n)](h_1(n)+h_2(n))$$

so that independent hazards, as independent probabilities, are additive.

Since $F(n)$ and $h(n)$ or $H(n)$ are equivalent one need only find $h(n)$ which depends solely on the current size of all cracks, which is known from the solution of the general fatigue problem.

If $a : F(a | n)$ is random together with the applied loads $S : F(S)$ then from the definition

$$\begin{aligned} h(n) &= \Pr(\text{Applied load} > \text{Ultimate} \mid \text{npf}) \\ &= \int_{U(a) < S} dF(a | n) dF(S) \quad \dots \quad (5) \end{aligned}$$

where $U(a)$ is the ultimate strength as a function of the various crack lengths. For a constant loading $S=S_0$

$$dF(S) = \delta(S - S_0),$$

and this becomes

$$h(n) = \int_{S_0}^{\infty} dF(a | n) \quad \dots \quad (6)$$

2.0 Effect of Inspection and Repairs

A structure which is periodically inspected and repaired will last longer than a neglected one. This has been considered by von Sydow¹⁶ who considered a single crack which if necessary was repaired at preset inspection times T_v . We outline the analysis below, adding another term to include static failure in the absence of fatigue cracks.

Let $F(t)$ denote the life distribution obtained by (3) or (4) if the crack begins at $n=0$. In any interval (T_{v-1}, T_v) a crack may start at time t , say, and if these starting times have the density $f(t)$ then

$$\begin{aligned} \text{Pr}(\text{First fatigue failure during } (T_{v-1}, T_v)) &= \\ &= \int_{T_{v-1}}^{T_v} F(T_v - t) dF_0(t) \quad \dots \quad (7) \end{aligned}$$

where $F_0(t)$ is the distribution of initial failures. This includes only those failures in the interval (t, T_v) and not any static failures during (T_{v-1}, t) . Let this possibility be denoted by A and its absence by \bar{A} while B, \bar{B} refer to the fatigue failure when the structure is intact at time t . There are then four possibilities in the combination of these events and using the same symbols their probabilities are as follows

$$\begin{aligned} AB &= C \quad (\text{Two failures in succession}) \\ \bar{A}\bar{B} &= 1 - e^{-h_s(t-T_{v-1})} \quad (\text{Static failure with hazard } h_s) \\ \bar{A}B &= e^{-h_s(t-T_{v-1})} F(T_v - t) \end{aligned}$$

$$\overline{AB} = e^{-h_s(t-T_{v-1})} (1-F(T_{v-t}))$$

To include static failure we replace the integrand in (7) by $\overline{AB} + \overline{AB}$ obtaining

$$\begin{aligned} \text{Pr(Any first failure in } (T_{v-1}, T_v)) &= \\ &= \int_{T_{v-1}}^{T_v} [1 - e^{-h_s(t-T_{v-1})} \{1 - F(T_{v-t})\}] dF_o(t) \quad \dots (8) \end{aligned}$$

Failures in any interval are mutually exclusive and these probabilities can be added to obtain the chance of failure any time before T_v . When the hazard $H(t)$ corresponding to $F(t)$ is used this sum takes the form

$$\begin{aligned} F(T_k) = F_o(T_k) - \sum_{v=1}^k \int_{T_{v-1}}^{T_v} e^{-h_s(t-T_{v-1})} e^{-H(T_v-t)} dF_o(t) \\ \dots (9) \end{aligned}$$

where the second term is the improvement effected by the inspections. Part of this improvement is illusory however because $F_o(t)$ refers to the material present at the beginning and not to the possibility of cracks developing in the material used in repairs. If the failures arising from repairs are also considered then the situation is similar to that obtaining in statistical renewal theory. This extension will now be treated by the theory of recurrent events.¹⁷

Let us first regard a failure during (T_{v-1}, T_v) as a discrete event at time T_v with a concentrated probability, still called a density for convenience. Consider a structure which has failed at T_v and which was last repaired at T_r . Then if the origin is moved to T_r , (8) still supplies the probability for this condition which

can be written

$$\begin{aligned}
 f_{\nu r} &= [F_o(T_\nu - T_r) - F_o(T_{\nu-1} - T_\nu)] - \\
 &\quad - \int_{T_{\nu-1}}^{T_\nu} e^{-h_s(t - T_{\nu-1})} e^{-H(T_\nu - t)} dF_o(t - T_r) \dots \quad (10) \\
 &= f_{o\nu r} - g_{\nu r}, \text{ say.}
 \end{aligned}$$

The probability q_ν of catastrophic failure at T_ν is therefore

$$q_\nu = f_{\nu o} + \sum_{r=1}^{\nu-1} p_r f_{\nu r} \quad \dots \quad (11)$$

where

$$\begin{aligned}
 f_{\nu o} &= \text{Prob. of final failure from first crack.} \\
 p_r f_{\nu r} &= \text{" " " " from crack repaired at} \\
 &\quad \text{time } T_r.
 \end{aligned}$$

For equal intervals it is convenient to define the generating function

$$\begin{aligned}
 Q(s) &= 1 + \sum_{\nu=1}^{\infty} q_\nu s^\nu \\
 A_o(s) &= \sum_{\nu=1}^{\infty} f_{\nu o} s^\nu
 \end{aligned}$$

which are retained temporarily for all cases. From (11)

$$Q(s) - 1 = A_o(s) + \sum_{\nu=1}^{\infty} \sum_{r=1}^{\nu-1} p_r s^r f_{\nu r} s^{\nu-r}$$

and if we change the order of summation

$$\begin{aligned}
Q(s)-1 &= A_0(s) + \sum_{r=1}^{\infty} \sum_{v=r+1}^{\infty} p_r s^r f_{vr} s^{v-r} \\
&= A_0(s) + \sum_{r=1}^{\infty} p_r s^r \sum_{v-r=1}^{\infty} f_{vr} s^{v-r} \\
&= A_0(s) + \sum_{r=1}^{\infty} p_r s^r A_r(s)
\end{aligned}$$

where $A_r(s) = \sum_{t=1}^{\infty} f_{t+r} r s^t$

may be regarded as a retarded generating function. If the T_v are evenly spaced then

$$A_r(s) = A_0(s)$$

and then

$$Q(s) = 1 + A_0(s)P(s) \quad \dots \quad (12)$$

where $P(s)$ is the generating function of minor cracks,

$$P(s) = 1 + \sum_{v=1}^{\infty} p_v s^v \quad \dots \quad (13)$$

We now return to p_v which is the probability of a minor crack in the intervals (T_{v-1}, T_v) . This is an event similar to final failure and the previous analysis is largely repeated. Corresponding to (8) we have the event

$$\text{Pr}(\text{Minor first crack during } (T_{v-1}, T_v))$$

$$= \int dF_0(t) \text{Pr}(\text{No failure} < t) \cdot \text{Pr}(\text{No failure} > t)$$

$$= \int_{T_{v-1}}^{T_v} e^{-h_s(t-T_{v-1})} [1-F(T-t)] dF_0(t) \quad \dots (14)$$

Thus

$$g_{vo} = \int_{T_{v-1}}^{T_v} e^{-h_s(t-T_{v-1})} e^{-H(T_v-t)} dF_0(t) \quad (\text{cf (10)})$$

for first occurrences and as in (11)

$$p_v = g_{vo} + \sum_{r=1}^{v-1} p_r \overline{g_{v-r}}_o \quad \dots (15)$$

with the generating function

$$\begin{aligned} \sum_{v=1}^{\infty} p_v s^v &= G_o(s) + \sum_{v=1}^{\infty} \sum_{r=1}^{v-1} p_r s^r \overline{g_{v-r}}_o \\ &= G_o(s) + \sum_{r=1}^{\infty} \sum_{v-r=1}^{\infty} p_r s^r \overline{g_{v-r}}_o s^{v-r} \end{aligned}$$

after changing the order of summation. This can be written in the form

$$P(s)-1 = G_o(s) + \sum_{r=1}^{\infty} p_r s^r G_r(s) \quad \dots (16)$$

resembling (12) where $G_r(s)$ is another retarded generating function. If the inspection intervals are constant

$$G_r(s) = G_o(s)$$

and

$$P(s) = 1/(1-G_o(s)).$$

Substituting into (13)

$$Q(s) = (1+A_o(s) - G_o(s))/(1-G_o(s)) \quad \dots (17)$$

$$\text{and } A_0(s) - G_0(s) = \sum_{r=1}^{\infty} (f_{0v_0} - 2g_{v_0}) s^r$$

Now $A_0(s)$ and $P_0(s)$ can be found from (10) and (14) and in this case $P(s)$ and $Q(s)$ can be expanded to give the repair and failure rates.

With unequal intervals the generating function method can be used by considering fixed values of s but it is better to find p_v and q_v recursively from (15) and then (11).

For continuous lives we have obtained essentially the life distribution at $T_1 \dots T_v$. To obtain the density of failures suppose that the last inspection interval is infinitesimal so that, with $n=T_v$, (11) becomes

$$f(n)dn = f_0(n)dn + \sum_{r=1}^{v-1} p_r e^{-h_s(t' - T_{v-1})} e^{-H(n-t')} f_0(n-T_r)$$

where $T_{v-1} < t' < n$. To the first order

$$f(n) = f_0(n) + \sum p_r f_0(n-T_r) \dots \quad (18)$$

For a linearly decreasing strength and log normally distributed initial failures various results calculated from (9) can be found in ref. 16.

The hazard $H(n)$ on which (9) and all other results are based is that found through (5) by a fatigue analysis, however crude the approximations used.

When there are several cracks the initial failure here can be approximated as the first one (a least value distribution), or the second or a similar event. The essential simplicity of having only one crack is that, once started, its growth is roughly deterministic.

2.1 Several Initial Failures

With several possible types of crack it is most convenient to consider the average size, including those not yet begun, and let this be zero at $n=0$. All hazards are then based on the origin and the first failure probability (7) becomes simply

$$\begin{aligned} \Pr(\text{f.f.} \subset (T_{v-1}, T_v)) &= F(T_v) - F(T_{v-1}) \\ &= e^{-H(T_v)} - e^{-H(T_{v-1})} \end{aligned}$$

and (9) reduces to $F(T)$. Similarly (10) is now

$$f_{vr} = F(T_v - T_r) - F(T_{v-1} - T_r).$$

Now consider the probability of a minor crack appearing for the first time at T_v . It will be shown later that the initial life distributions of a set of cracks are independent and therefore

$$1 - F_0(t) = (1 - F_1(t)) \dots (1 - F_n(t)) \dots \quad (19)$$

is the probability that no appreciable cracks have appeared by t cycles, $F_0(t)$ playing the same role as before. Thus g_{vr} is still given by (14), using the failure distribution from (19). This is still tantamount to assuming that a repaired structure is completely restored when a crack is discovered whereas the uncracked parts are left, still containing a certain amount of fatigue damage.

The problem can be circumvented by solving the crack-damage equations (Chapter IV) in a piecewise fashion with the added boundary conditions that all cracks return to zero lengths at each inspection. For parts not needing repair the damages are retained, becoming zero for those repaired. Overall then it is necessary to average the canonical damage at each inspection, a process similar to

that above but rather more complex because of the interaction between the differential equations and the boundary conditions which depend on an earlier part of their solution.

3.0 Hazards from Several Cracks

The hazard $H(n)$ on which the failure distribution depends is related to a complete structure but it is plain that an analysis broken into independent sections is more efficient. This is possible if the different cracks are sufficiently separated to allow independent structural analyses. If this is so there is still a statistical interaction between the different areas of failure which we shall investigate below.

Let the external loads be R which is a vector of magnitudes applied to a set of external load systems b_o in equilibrium (in accordance with the matrix methods of analysis). Any linear combination of these systems is also in equilibrium so that if A is of full rank the loads $b_o A^{-1}$ are also a suitable basis* and the applied loads are

$$b_o R = b_o A^{-1} \cdot AR$$

Thus any linear transformation of b_o is equivalent to it when R is correspondingly altered. We now suppose that the elements of R , but not those of b_o , are random variables, generally correlated with each other, and having the covariance matrix Σ_R . For the new vector

$$K = A^{-1} R$$

the covariance matrix is

* A^{-1} is chosen to agree with the next section. Strictly speaking the order of K can exceed that of R and the analysis can be extended but one expects one crack to be critical for each load vector.

$$\Sigma_K = \mathcal{E}(KK^t) = \mathcal{E}(A^{-1}RR^t A^{-t}) = A^{-1} \Sigma_R A^{-t} \dots \quad (20)$$

It is obviously convenient if Σ_R is diagonal and without loss of generality the variances (on the diagonal) can be unity so that

$$\Sigma_K = A^{-1} A^{-t} \dots \quad (21)$$

This is quite general since Σ_R can always be diagonalised by another preliminary transformation. Let us now consider A^{-1} , remembering (3A). By definition

$$A^{-1} A = I \dots \quad (22)$$

$$= [\tau_i^t][A_j] \text{ say,}$$

and for $j = 2, \dots, N$

$$\tau_1^i A_{1j} = 0$$

which is a restatement of (22). Considered as a vector τ_1 is perpendicular to the subspace spanned by A_j , $j=2, \dots, N$, and if this is also the case for A_1

$$A_1 = \tau_1$$

within a constant factor. By the same reasoning

$$A_1^t \tau_j = 0$$

from (22) and hence

$$\tau_1^i \tau_j = 0, \quad j = 2, \dots, N.$$

From (21) it now follows that K_1 is not correlated with K_2, \dots, K_N and if the loads are normally distributed this also implies independence. We shall show below that this is also true in the important case of exponential distributions.

3.1 Exponential Distributions

These are a close approximation to the load distributions experienced by aircraft structures and therefore warrant closer consideration. The range of application of any distribution can also be extended by transformations such as logarithmic loads etc.

For normal distributions it is well known that the covariance matrix (21) and the means $\mu_K = A^{-1} \mu_R$ completely define the new variates. We now try to find a similar generalisation of the exponential distribution

$$f(x) = a e^{-ax}, \quad F(x) = 1 - e^{-ax}.$$

The simplest generalisation is the product of several such factors,

$$f(x) = a_1 \dots a_N \exp(-a^t x), \quad x_i > 0, \dots \quad (23)$$

representing independent variates. Now suppose that $x = Ay$ where A is constant. The Jacobian of the transformation is

$$\frac{\partial x}{\partial y} = |A|$$

so that the density of y is

$$\begin{aligned} f(y) &= f(x) |\partial x / \partial y| \\ &= A a_1 \dots a_N e^{-a^t Ay} \end{aligned} \quad \dots \quad (24)$$

If e_N^t represents a row matrix of ones and a is changed to a diagonal matrix then it can be seen that this belongs to the set of densities

$$\begin{aligned} f(y) &= |A| e^{-e_N^t Ay} \\ &= |A| \exp\{-y_1 \sum_i a_{i1} - y_2 \sum_i a_{i2} \dots - y_N \sum_i a_{iN}\} \end{aligned} \quad \dots \quad (25)$$

We know that the components of x are independent. Let us consider their correlations and those of y . The moment generating function of x is

$$\begin{aligned}
 M_x(t) &= \int e^{x^t t} dF(x) \\
 &= \int_0^\infty \dots \int_0^\infty a_1 \dots a_N e^{-(a-t)^t x} dx \\
 &= \prod_{i=1}^N \frac{a_i}{a_i - t_i} \dots \quad (26)
 \end{aligned}$$

The logarithm of $M_x(t)$ is the cumulant generating function $\Psi_x(t)$ and since covariances are second cumulants and (25) is a product all correlations are zero. After a change of variable the corresponding MGF of y becomes (from (24))

$$\begin{aligned}
 M_y(t) &= \int e^{t^t y} dF(x) \\
 &= \int_0^\infty \dots \int_0^\infty a_1 \dots a_N e^{-(a^t - t^t A^{-1})x} dx \\
 &= \prod_{i=1}^N \frac{a_i}{a_i - u_i} \dots \quad (27)
 \end{aligned}$$

where $u = [u_i] = A^{-t} t$. The cumulant generating function is therefore

$$\Psi_y(t) = \sum_{i=1}^N \log \left(1 - \frac{u_i}{a_i} \right) + \text{constant}$$

and the correlations depend on which elements of t are involved in those of u or equivalently, on the relation between y and x . Expanding,

$$\Psi_y(t) = \sum_{i=1}^N \left\{ \frac{u_i}{a_i} + 2\left(\frac{u_i}{a_i}\right) + \dots \right\}$$

and the covariance $\text{cov}(y_i, y_j)$ is represented by the corresponding terms in

$$\begin{aligned} \sum_{i=1}^N (u_i/a_i)^2 &= u^t a^{-2} u \\ &= t^t A^{-1} [a]^{-2} A^{-t} t \end{aligned}$$

or in other words the covariance matrix is

$$\Sigma_y = A^{-1} [a]^{-2} A^{-t} \quad \dots \quad (28)$$

If A consists of diagonal submatrices then (28) may be correspondingly split and after retracing our steps we find that (27) also splits into a number of factors which thus represent independent vectors.

Therefore, remembering (10), it has been shown that zero correlation is necessary and sufficient for the corresponding variates to be independent. Equation (28) corresponds to (24), which is convenient here, but its form shows that the covariance matrix corresponding to the form (25) is

$$\Sigma_y = A^{-1} A^{-t} \quad \dots \quad (29)$$

In (20) now, K_1 represents the stress intensity (on which the rate of crack growth depends), the components of R can be made uncorrelated and therefore independent and finally

$$K = A^{-1} R \quad , \quad [\tau_i] = A^{-1}.$$

If also the other column vectors of A^{-1} are orthogonal to τ_1 then by (29)

$$\text{Var(Intensity)} = \tau_1^t \tau_1$$

In our derivation of the moment generating function reference

to the limits of y was avoided by integrating over x . Apart from simplicity this was forced upon us by ignorance of the values of these limits. For the independent distribution here, which by (25) is still exponential, we have the variance above and the mean value $e^t \tau_1$ corresponding to (25) or to $y = A^{-1}x$. Since the distribution is exponential we might expect that

$$\sigma^2 = \mu^2$$

which is clearly not so. The difference arises from a change in the range of the variate which for x_i is $(0, \infty)$. If the minimum of x , say, becomes b the variance is not altered but the mean becomes

$$\mu \rightarrow \mu + b$$

in which case

$$\sigma^2 = (\mu - b)^2 \quad \text{or } b = \mu - \sigma \text{ (+ve roots).}$$

In this instance the formulae can be written

$$b = e^t \tau_1 - \sqrt{\tau_1^t \tau_1} \quad \dots \quad (30)$$

and by taking the relevant factor from (25)

$$f(K_1) = ae^{ab} \cdot e^{-aK_1} \quad \dots \quad (31)$$

where $a = e^t A_1$ = Sum of elements in 1st (say) column of A and b is given above with

$e^t \tau_1$ = Sum of elements in corresponding ROW of A^{-1} . If K_c is the stress intensity critical for fracture then from (31) the probability of fracture is

$$\begin{aligned} \Pi &= \Pr(K_1 > K_c) \\ &= \exp\{-a(K_c - b)\}. \end{aligned} \quad \dots \quad (32)$$

When K_1 is normally distributed this hazard has of course the form

$$H = 1 - \Phi(u) \quad \dots \quad (32A)$$

where

$u = (K_c - \mu_{K_1})/\sigma_{K_1}$ and $\Phi(u)$ is the normal integral.

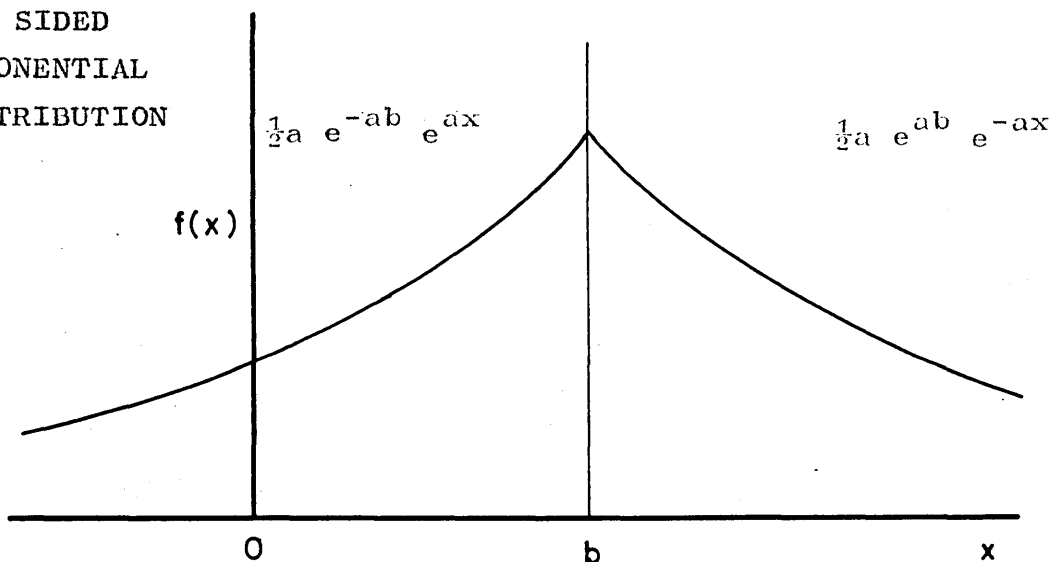
3.2 Two Sided Exponential Distribution

The gust loading of aircraft usually occurs in either sense and to a first approximation the practical distribution is that shown, each part of the curve being exponential.

The multivariate distribution will be approached as before, starting with independent variates x which are transformed to $y = A^{-1}x$. We then consider the characteristic functions of x and y using t, u as the parameters of Φ . For the single variate x the characteristic function is

$$\varphi_x(t) = \frac{1}{2}a \left\{ e^{-ab} \int_{-\infty}^b e^{x(it+a)} dx + e^{ab} \int_b^{\infty} e^{x(it-a)} dx \right\} \quad \dots \quad (33)$$

TWO SIDED
EXPONENTIAL
DISTRIBUTION



which reduces to

$$\varphi_x(t) = ae^{it/b}/(a^2+t^2),$$

or as a moment generating function ($it \rightarrow t$)

$$M_x(t) = ae^{bt}/(a^2-t^2).$$

The cumulant generating function is therefore

$$\begin{aligned} \psi_x(t) &= \log a + bt - \log(a-t) - \log(a+t) \\ &= \log a + bt + (t/a)^2 + \frac{1}{2}(t/a)^4 + \frac{1}{3}(t/a)^6 + \dots \end{aligned} \quad \dots (34)$$

and if x , a , b and t generalise to x , a , b , t the C.G.F. of x is merely the sum of such expressions with these parameters.

If we define

$$x_s \equiv (x-b)\text{sgn}(x-b)$$

and x_s as the corresponding vector then the joint density of x is

$$f(x) = \frac{1}{2} |a| \exp(-e_N^t a x_s), \quad \dots (35)$$

a being diagonal with e_N defined as before.

In the same way as before

$$M_y(t) = \int_{-\infty}^{\infty} \dots \int e^{t^t y} dF(x)$$

or, on changing the variable,

$$\begin{aligned} M_y(t) &= \int_{-\infty}^{\infty} \dots \int e^{t^t A^{-1}x} dF(x) \quad (x = Ay) \\ &= M_x(u) \text{ say} \end{aligned} \quad \dots (36)$$

where

$$u = A^{-t} t.$$

From (34) therefore

$$\Sigma_y \Leftarrow 2 u^t a^{-2} u \Rightarrow 2A^{-1} a^{-2} A^{-t}$$

as in (28). This covariance matrix is the same as that for the one-sided exponential density and therefore the same argument as before shows that zero correlation implies independence and vice-versa.

Now consider the joint density

$$f(y) = \exp(-e_N^t a x_S)$$

where

$$\begin{aligned} x_S &= [\text{sgn}(x - b)] (x - b) \\ &= [\text{sgn}(x - b)] (Ay - b) \\ &= [\text{sgn}(Ay - b)] (Ay - b) \quad \dots (37) \end{aligned}$$

Thus

$$\begin{aligned} 2f(y) &= |A \cdot a| \exp\{-e_N^t a (Ay - b) [\text{sgn}(Ay - b)]\} \\ &= |a A| \exp\{-e_N^t a A (y - A^{-1}b) [\text{sgn}A(y - A^{-1}b)]\} \\ &= |A| \exp\{-e_N^t A (y - \mu_y) [\text{sgn} a^{-1}A (y - \mu_y)]\} \\ &\quad \text{if } aA \rightarrow A. \end{aligned}$$

So far the manipulations of the sign matrix $[\text{sgn}(\)]$ have been purely formal. In the last formula one manipulates $a^{-1}A(y - \mu_y)$ and chooses elements of ± 1 according to the sign of each row. As standard deviations, the elements of a^{-1} are essentially positive however and a^{-1} is therefore immaterial to the value of the sign matrix. Thus the general two-sided exponential distribution has the form

$$f(y) = \frac{1}{2} |A| \exp\{-e_N^t A (y - b) [\text{sgn}A(y - b)]\} \quad \dots (38)$$

At failure, the stress intensities should be high compared with b so that the sign matrix should be the unit matrix. For one crack, the hazard is then half that of (15), using the same definitions and notation.

3.21 Several Cracks

If there are several cracks the event of no failure (\bar{F}) has the form

$$\begin{aligned}\bar{F} &= \sum_{i=1}^N \bar{F}_i \quad (F_i = \text{failure at crack } i) \\ &= 1 - \prod_{i=1}^N F_i \quad (1 \equiv \text{All possibilities}).\end{aligned}$$

This formulae also applies to the probabilities if the F_i are independent events and there is then a formal resemblance to the distribution of the least of N variates. Where there is correlation the product represents the joint probability

$$\int_{K_{ci}}^{\infty} \dots \int dF(K) \quad \dots \quad (39)$$

of no failures anywhere, where $K_c = \{K_{ci}\}$ are the relevant critical stress intensities. For practical purposes the sign matrix has positive elements and the one-sided and two-sided distributions are both equivalent to (25) apart from a factor of a half. Substituting (38) into (39), with these provisions,

$$\begin{aligned}F &= \frac{1}{2} |A| \int_{K_{ci}}^{\infty} \dots \int e^{-e_N^t A(y-b)} dy \\ &= \frac{1}{2} |A| \prod_{i=1}^N \int_{K_{ci}}^{\infty} e^{-(y_i-b_i)} \prod_{i=1}^N a_{ij} dy_i\end{aligned}$$

$$\begin{aligned}
&= \frac{1}{2} \left\{ |A| / \prod_{i=1}^N \left(\sum_{j=1}^N a_{ji} \right) \right\} \cdot \prod_{i=1}^N \exp \left\{ - (K_{ci} - b_i) \sum_{j=1}^N a_{ji} \right\} \\
&= \frac{1}{2} \left\{ |A| / \prod_{i=1}^N \sum_{j=1}^N a_{ji} \right\} \cdot e^{-e_N A (K_c - b)} \dots (40)
\end{aligned}$$

A similar result holds for the one-sided distribution and if the sign matrix is important a term similar to this must occur nevertheless in F together with other terms corresponding to regions bounded by the discontinuities of $f'(y)$. Because of its relative practical unimportance the more general case will not be investigated.

Chapter III

CRACK PROPAGATION AND FAILURE

1.0 Introduction

In this chapter we present a unified review of crack propagation and failure with the emphasis on thin sheets. Attention is confined to Griffith-Irwin theory of static failure and the related approach of Paris or Liu¹⁹ to crack propagation. The most important new results arise from a non-dimensional presentation of fatigue crack data. This leads to a treatment for random loads and we have also considered (for 7075-T6 and 2024-T3) a wider range of conditions than Paris allowing a better inclusion of mean load and some discussion of work hardening effects. In an approximate fashion there is also some discussion of the plastic stress system.

We have already identified microcracking or Forsyth's²⁰ Stage I with the older concept of cumulative damage and this chapter is entirely concerned with visible or Stage II cracks where the (main) direction of propagation is perpendicular to the principal stress. The transition depends²¹ on stress (or actually stress intensity) and the presence of corrosion and there is also evidence, added to here, that grain boundaries are important. The basic difference between the two stages is that microcrack propagation continually exposes fresh material whereas "damage" implies the continual fatiguing of the same small part of the structure.

2.0 Elastic Stresses

Inglis²² presented the first treatment of elliptical holes in 1913, and obtained the now standard formulae

$$K_T = 1 + 2b/a = 1 + \sqrt{2l/r} \quad \dots \quad (1)$$

where a , b are the semi-axes and r the minimum radius of curvature. The analysis proceeded by the use of confocal elliptical coordinates.

For sharp cracks the next major step was the presentation of a semi-inverse complex variable method by Westergaard²³ which formed a basis for much of Irwin's²⁴ work later.

If the crack coincides with the x -axis and

$$z = z(\zeta) \quad \text{where } \zeta = x + iy$$

then in Westergaard's method

$$\sigma_y = \mathcal{R}(z) + y \mathcal{I}(z') \quad \dots \quad (2)$$

$$\sigma_x = \mathcal{R}(z) - y \mathcal{I}(z')$$

$$\tau_{xy} = -y \mathcal{R}(z')$$

In plane stress

$$Eu = (1-\nu) \mathcal{R} \int z d\zeta - (1+\nu) y \mathcal{I}(z) \quad \dots \quad (3)$$

$$Ev = 2 \mathcal{I} \int z d\zeta - (1+\nu) y \mathcal{R}(z)$$

For an infinite row of equal collinear cracks

$$z(\zeta) = \sigma \left\{ 1 - \frac{\sin^2 \pi a/W}{\sin^2 \pi \zeta/W} \right\}^{-\frac{1}{2}} \quad \dots \quad (4)$$

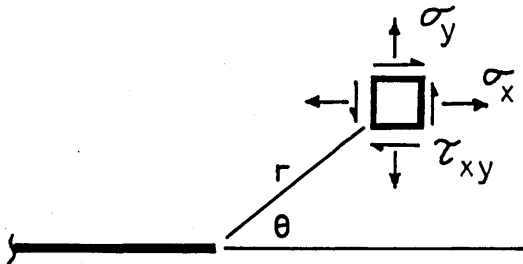
where σ = stress at infinity

$2a$ = crack length

and W = width of strips which contain each crack.

2.1 Tip Stresses and Intensities

There are three basic²⁴ stress fields near the tip of a crack corresponding to two edge dislocations and a screw. Except where noted the discussion is related to cracks opening under pressure or the effect of stress perpendicular to the crack.



In such cases when r is small, the tip stresses always take the form

... (5)

$$\sigma_y = \frac{K}{\sqrt{2\pi r}} \cos \frac{\theta}{2} \left\{ 1 + \sin \frac{\theta}{2} \sin \frac{3\theta}{2} \right\}$$

$$\sigma_x = \frac{K}{\sqrt{2\pi r}} \cos \frac{\theta}{2} \left\{ 1 - \sin \frac{\theta}{2} \sin \frac{3\theta}{2} \right\} - \sigma_{ox}$$

$$\tau_{xy} = \frac{K}{\sqrt{2\pi r}} \cos \frac{\theta}{2} \sin \frac{\theta}{2} \cos \frac{3\theta}{2}$$

$$\sigma_z = \nu(\sigma_x + \sigma_y) \quad \text{Plane strain}$$

$$= 0 \quad \text{Plane stress}$$

where $K = \sqrt{\pi} k_a = \sqrt{\pi} \mathcal{K}$, depending on the stress and geometry, is called the Stress Intensity Factor.

The square root singularity applies to all types of elastic cracks, and we will present some evidence that it holds for plastic systems also.

Now consider any crack made in a previously stressed body. (Fig. 2).

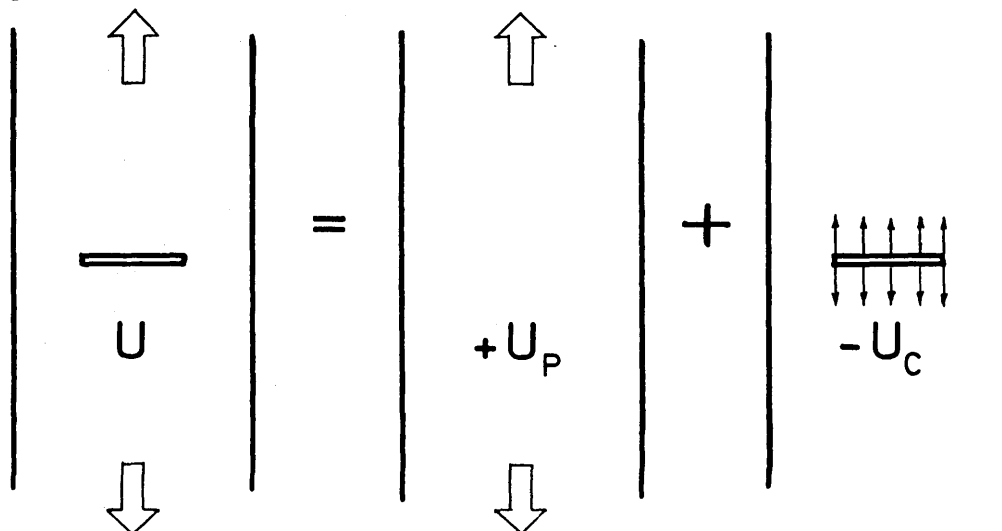


FIG.2.

Because the crack opens, negative work will be done by the previously internal stresses along the crack edge and the total strain energy is reduced. Moreover, the reduction is equal to the strain energy for the crack under pressure (see Fig.2). This energy U_c powers the crack growth in static failure and in fatigue and it appears that on a unit thickness basis

$$\frac{\partial U_c}{\partial a} \stackrel{\text{def}}{=} \mathcal{G} = \begin{matrix} K^2/E & \text{Plane stress} \\ (1-\nu^2)K^2/E & \text{Plane strain} \end{matrix} \quad \dots (6)$$

where \mathcal{G} is the crack driving force of fixed-grip energy release rate. For a crack of length $2a$ in a infinite plate

$$\mathcal{G} = \pi a \sigma^2 / E$$

and this is the order of magnitude in any other system.

Consider the contours of a stress σ_y , say. When $\theta = 0$ we have from (5) and (6)

$$r_y = E\ell/2\pi\sigma_y^2 \quad \dots \quad (7)$$

so that ℓ may be regarded as a scale parameter. When plastic flow occurs this is still true, for if the plastic region is much smaller than the region where (5) is valid, then the truth of (7) when ℓ is large and uniqueness of the solution of the elasto-plastic problem lead to the tentative conclusion that (7) becomes

$$r_y = \ell \cdot f(\sigma_y) \quad \dots \quad (7a)$$

The manner in which this breaks down and the strict conditions of its validity do not concern us here, although they form an unsolved problem requiring investigation.

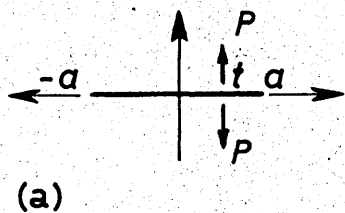
2.2 Special Cases

To form a reference the driving forces for some common cases have been shown in Fig.3. The cases of elliptical and circular cracks apply to small fatigue cracks in heavy sections provided the edge is not too close to the other boundaries.

As an example, Irwin has stated that the formula for a semi-elliptical crack in a plate is reasonable if the crack is less than half-way through the thickness. From the actual behaviour of fatigue cracks²⁵, stress concentrations and the growth of static cracks, it seems that the nearness of other boundaries accentuates the driving force.

3.0 General Solutions

When the shear stresses τ_{xz} , τ_{yz} on the x,y plane vanish, it can be shown that^{26, 28} problems in three-dimensional elasticity may be reduced to dependence on one harmonic function ϕ . Sneddon²⁶ has shown that the



Infinite Plate $\mathcal{G} = \frac{P^2}{\pi a E} \left(\frac{a+t}{a-t} \right)$ at end +a

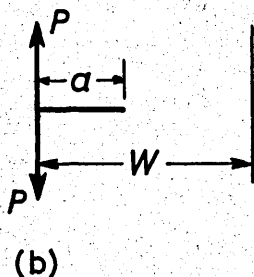
Width W $\mathcal{G} = \frac{P^2}{EW \sin(\pi a/W)} \left(\frac{\lambda + \tau}{\lambda - \tau} \right)$

Where $\lambda = \sin \pi a/W$
 $\tau = \sin \pi t/W$

Uniform Pressure $\mathcal{G} = \pi a \sigma^2$
 or $\mathcal{G} = \sigma^2 W \tan \pi a/W$

Accurate Results Srawley et al NASA TN-D 2395
 NASA TN-D 2396

$$\mathcal{G} \approx \frac{4P^2}{\pi a E} \left\{ 1 + \left(\frac{a}{W} \right)^2 \left[2 + 12 \operatorname{arcosh} \frac{W}{a} \right] \right\}$$



Uniform Pressure σ

$$\mathcal{G} \approx \pi a \sigma^2 \left\{ 1 - \left(\frac{a}{W} \right)^2 \left[6 \operatorname{arcosh} \frac{W}{a} - 2 \right] \right\}$$



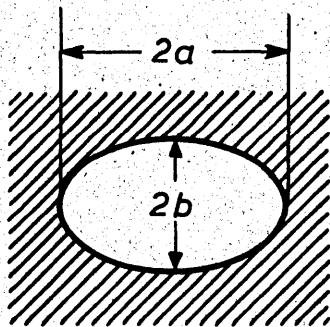
Near ends $\mathcal{G} = \frac{\pi \sigma^2}{a} \frac{(b^2 E(k) / (k) - a^2)^2}{b^2 - a^2}$

Far ends $\mathcal{G} = \pi b \sigma^2 \left[\frac{1}{k} - \frac{E(k)}{kK(k)} \right]$

where $k = \sqrt{1 - a^2/b^2}$ and $E(k), K(k)$ are complete elliptic integrals of the first and second kind.

Erdogan 4th U.S. Nat. Cong. App. Mech. 1962.

Barenblatt Ad. in App. Mech. VII Academic 1962.



Uniform Pressure σ

$$E \mathcal{G}_{max} = 3.77 b \sigma^2 / \left\{ \Phi^2 - 0.212 \left(\frac{\sigma}{\sigma_y} \right)^2 \right\}$$

$$\Phi = E(1 - b^2/a^2)$$

$$= \int_0^{\pi/2} \left\{ 1 - (1 - b^2/a^2) \sin^2 \theta \right\}^{1/2} d\theta$$

FIG. 3 SOME CRACK EXTENSION FORCES

stresses near an elliptic crack under uniform pressure in an infinite isotropic medium, can be described in terms of the gravitational potential of a uniform elliptical disk. Since the boundary shape is not used, the analogy holds for any crack or set of cracks.

It is probable that it can be extended to non-uniform pressures on cracks in prismatic elements such as aircraft spar booms. In this most general case the density of our disk would be proportional to stress or pressure and we require $\frac{\partial \phi}{\partial x} = 0$ on the surface of our prismatic boom.

If the crack is in the x-y plane of an infinite medium, then $\sigma_{xx} + \sigma_{yy} = \sigma_{zz}$ and in thin sheets the stress σ_{xx} may lead to buckling.

As the potential problem can be solved by Green's functions, it also seems possible that this approach may be usable to find stress intensities directly using numerical methods in the most general case. From the case of the elliptic crack, it appears²⁷ that the maximum intensity occurs on the straightest part of the crack boundary, if the pressure is uniform.

3.1 Two-Dimensional Case

In this case a complex variable procedure is appropriate. We have already mentioned that of Westergaard, but here will choose a particular case of the general theory. From Green and Zerna²⁸, if $\tau_{xy} = 0$ when $y = 0$ then

$$G(u_x + iu_y) = \kappa \Omega(z) - \Omega(\bar{z}) + (z - \bar{z}) \Omega'(z) \quad \dots \quad (8)$$

$$\sigma_{xx} + \sigma_{yy} = 4 \{ \Omega'(z) + \Omega'(\bar{z}) \}$$

$$\sigma_{xx} - \sigma_{yy} + 2i\tau_{xy} = 4 (z - \bar{z}) \Omega''(\bar{z})$$

where

$$\begin{aligned} \mu &= 3-4\nu && \text{for plane strain} \\ \text{or} &&& (3-\nu)/(1+\nu) && \text{in plane stress.} \end{aligned}$$

It will be noticed that the last two equations give vectors defining the Mohr circle for stress. These equations relate to infinite sheets and if we have a single crack $a < t < b$ loaded by a pressure $p(t)$ (zero stress at infinity) then

$$\Omega'(z) = \frac{-1}{4\pi i \sqrt{R(z)}} \int_a^b \frac{p(t) \sqrt{R(t)}}{t-z} dt \quad \dots \quad (9)$$

where

$$R(z) = (z-a)(b-z)$$

3.2 Lyell-Sanders' Method

By considering the work done by boundary tractions during crack extension $(\partial a / \partial \alpha) d\alpha$ defined by some parameter α , Lyell-Sanders²⁹ has obtained the driving force in the form of a line integral.

$$\begin{aligned} \oint \frac{\partial a}{\partial \alpha} &= -\frac{2}{E} \mathcal{I} \left\{ \left[\bar{z} \omega' \Omega_{\alpha} \right]_A^B \right. \\ &\quad \left. + \int_A^B (\omega'_{\alpha} \Omega' + \omega'' \Omega_{\alpha}) dz \right\} \quad \dots \quad (10) \end{aligned}$$

in the general two dimensional case described by two complex potentials $\Omega(z)$, $\omega(z)$. In this expression

$$\omega' = \frac{\partial \omega}{\partial z}, \quad \Omega_{\alpha} = \frac{\partial \Omega}{\partial \alpha} \quad \text{etc.}$$

and the integral is independent of the path AB surrounding the crack tip(s). When the crack is straight

$$\omega(z) = 0.$$

3.3 Experimental Methods

As \mathcal{G} is a derivative of strain energy, it follows that it is obtainable from a series of experimental flexibility measurements with cracks of differing lengths. Let the total load on any specimen (of unit thickness) be P and let x be the corresponding extension. Then

$$x = FP \quad \text{and} \quad U = \frac{1}{2}FP^2$$

where F is the flexibility. Thus,

$$\mathcal{G} \equiv \frac{\partial U}{\partial a} = \frac{1}{2}P^2 \frac{dF}{da}$$

or in non-dimensional terms

$$\frac{EW\mathcal{G}}{P^2} = \frac{1}{2} \frac{d(EF)}{d(a/W)},$$

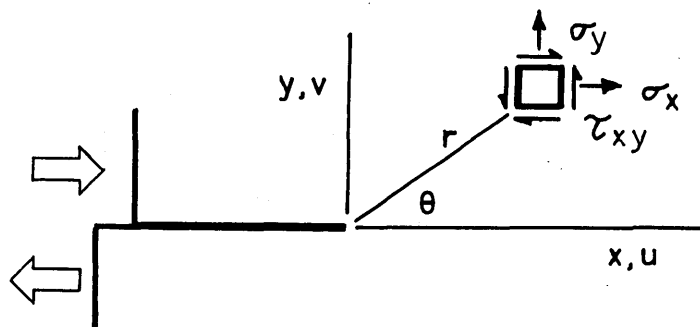
where a = crack length and W is a fixed dimension of the specimen.

Accurate results can be obtained in this way, provided one takes extreme care with the measurements³⁰ using the same specimen continually with the crack approximated by keyhole slots. These reduce the stress concentration so that, after shakedown, there is no plastic flow. From the form of the singularity, it follows that the end radius of the keyhole does not greatly affect the stiffness if it is referred to a crack reduced by half the end radius from its actual total length. If we assume that the keyhole slot approximates an ellipse, then this effective crack length is measured from the focus and confocal ellipses form a natural set of coordinate lines for crack problems^{22,26}. Generally, the stresses approximate a state of plane stress.³¹

4.0 Other Modes of Fracture

So far we have only considered cracks under stresses perpendicular to their surfaces. Irwin²⁴ has also described two other modes of fracture which correspond to edge and screw dislocations. In these cases, the surfaces slide against each other but do not separate.

4.1 Edge Sliding



This system is produced by forces such as that shown, or by crack surfaces under shear in the same direction.

Near the crack tip

$$\sigma_x = \frac{-K_2}{\sqrt{2r}} \sin \frac{\theta}{2} \left\{ 2 + \cos \frac{\theta}{2} \cos \frac{3\theta}{2} \right\} \quad \dots \quad (12)$$

$$\sigma_y = \frac{K_2}{\sqrt{2r}} \sin \frac{\theta}{2} \cos \frac{\theta}{2} \cos \frac{3\theta}{2}$$

$$\sigma_z = -2\nu \frac{K_2}{\sqrt{2r}} \sin \frac{\theta}{2} \quad \text{for plane strain}$$

or zero for plane stress. In addition

$$\tau_{xy} = \frac{K_2}{\sqrt{2r}} \cos \frac{\theta}{2} \left\{ 1 - \sin \theta \sin \frac{3\theta}{2} \right\} \quad \dots \quad (13)$$

$$u = \frac{K_2 \sqrt{2r}}{2G} \sin \frac{\theta}{2} \left\{ 2(1-\nu) + \cos^2 \frac{\theta}{2} \right\}$$

$$v = \frac{-K_2\sqrt{r}}{\sqrt{2G}} \cos \frac{\theta}{2} \left\{ 1 - \sin^2 \frac{\theta}{2} \right\}$$

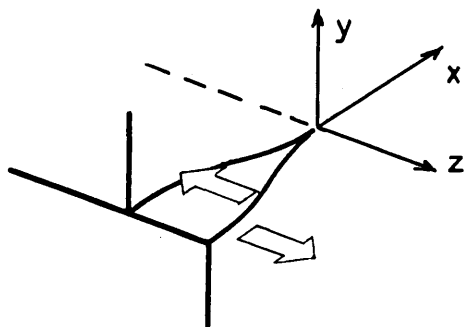
and $\tau_{yz}, \tau_{xz}, w = 0$.

Finally, the driving force is given by

$$\begin{aligned} K_2^2 &= E\ell_2/\pi(1-\nu^2) && \text{for plane strain} \\ &= E\ell_2/\pi && \text{for plane stress} \quad \dots (14) \end{aligned}$$

4.2 Screw Sliding

In this case the crack faces slide in a direction parallel to the edge of the crack.



This is a special case of St. Venant torsion so that by the sandheap or roof analogy³⁴ it is also the only case with a complete elastoplastic solution.³⁵

In the purely elastic case, using the previous notation,

$$\begin{aligned} \tau_{xz} &= \frac{-K_3}{\sqrt{2r}} \sin \frac{\theta}{2} && \dots (15) \\ \tau_{yz} &= \frac{K_3}{\sqrt{2r}} \cos \frac{\theta}{2} \end{aligned}$$

The warping and driving forces are given by

$$Gw = K_3 \sqrt{2r} \sin \frac{\theta}{2} \quad \dots (15a)$$

and $G_3 = \pi K_3^2 / 2G$.

At any point, the maximum shear stress is $K_3/\sqrt{2r}$ and these follow trajectories defined by-

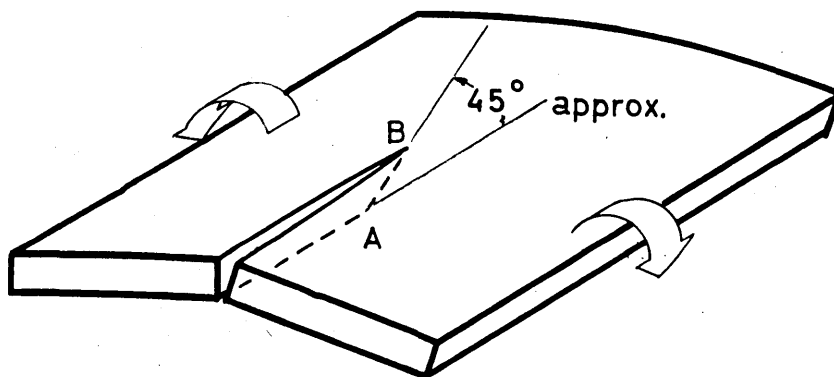
$$\frac{dy}{dn} = -\cot \frac{\theta}{2}$$

Recently G.C. Sih⁷⁹ has presented general complex variable methods for this type of crack including a relation between intensity and the residue of the potential function near the tip, similar to Lyell-Sanders' result.

4.3 Effects of Other Modes

Many of the particular cases described in Section 2.2, have obvious analogies when the plates are in bending. Williams^{36,37} has described some of these cases and points out that if the effects of shear are allowed for, the stress field near the crack corresponds to the opening mode.

However, in this case the calculated stresses are unlikely to be achieved because on the compressively stressed side, the crack will close and the edge will act as the fulcrum of a lever tending to further increase θ on the tension side.



In practice³⁸ the edge AB also becomes inclined to the surface as one might expect.

We will not mention plates again but similar complications arise with sheets in pure tension. In static fracture and fatigue, the plane of the crack faces often rotates until it makes an angle of approximately 45° with the sheet surface.

We have also seen that there are compressive stresses along the crack face equal to the local pressure (or its equivalent) and these often cause buckling when the sheets are thin.

This buckling tends to increase the driving force and, in these cases, the crack face is usually inclined to the surface so that a screw sliding component is added also.

In fatigue problems, buckling³⁹ seems to have little effect (probably because of the lower stresses) but there is evidence²¹ that the crack front is curved, "tunnelling" ahead in the centre of a sheet.

4.4 Additivity of Driving Forces

The intensity K is proportional to stress so that intensities corresponding to the same mode of failure are additive. The driving force is then obtained from the square of this total.

Let us consider elastic cases where different modes of failure operate together, for example where the tractions on a crack surface are inclined. These tractions may be resolved into components associated with the opening, edge and screw-sliding modes, and to this extent the stress problem is easily solved. It can be shown that the strain energies of the three modes associated with a crack are simply additive.

First consider screw sliding* and the other two modes. The cross-product terms in the strain energy integral are zero. The opening and edge sliding modes give rise to systems which are respectively symmetric and antisymmetric about the crack and the integral of cross-product terms again vanishes. Since the strain energies are additive, the driving forces or any other derivatives are also additive.

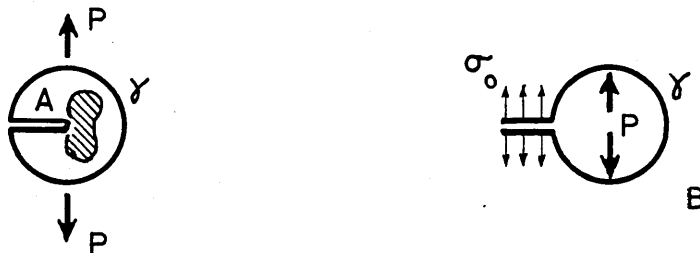
5.0 Effect of Non-Linearities and Local Geometric Changes.

Inside a small circle of radius r enclosing the crack tip, the total strain energy

$$U_r = O\left(\frac{r\sigma_o^2}{E}\right) \quad \dots \quad (16)$$

so that the orthogonality relations are little affected by small amounts of plastic flow or local departures from the straight crack front perpendicular to the surface. This argument is essentially that of Irwin²⁴ but as it seems vaguely unconvincing, we shall use a similar one more capable of rigorous development.

Consider separately the circular region mounting the crack tip and the remainder of the structure which is supposed elastic. In general, the tip region contains both elastic and plastic parts. For simplicity suppose that the (self-equilibrating) tractions across the mutual



*For thin sheets, the particular system shown seems inappropriate, being related to a crack along the z -axis of an infinite medium.

boundary of A and B can be summarised as two equal and opposite forces as shown. Suppose that the actual stress system is achieved by having the material behaving elastically until the maximum load is reached, and then allowing the stresses in A to decrease to their correct values. In the purely elastic case the strain energy is

$$\begin{aligned} U &= U_0 + \frac{1}{2}F_A P^2 + \frac{1}{2}F_B P^2 \quad (\text{Unit thickness}) \\ &= U_0 + U_{AE} + U_{BE} \quad \text{say,} \quad \dots \quad (17) \end{aligned}$$

where U_0 is the energy of region B when the circular part γ is not loaded.

From the previous results

$$\begin{aligned} U_{AE} &= \frac{1}{2}O\left\{\frac{\sigma_0^2}{E} \int \frac{r \, dr \, d\theta}{(\sqrt{r})^2}\right\} \quad \dots \quad (18) \\ &= O\left(\frac{r\sigma_0^2}{E}\right), \quad \sigma_0 = \text{Stress on crack face,} \end{aligned}$$

and we can therefore assume that

$$\begin{aligned} P &= O(r\sigma_0) \\ F_A &= O(rE)^{-1}. \end{aligned}$$

Now consider F_B . Here again r is the only dimension of interest, and it follows from dimensional considerations that

$$F_B = O(rE)^{-1} \quad \dots \quad (18a)$$

or
$$U_B = O(r\sigma_0^2/E)$$

and
$$U = U_0 + O(r\sigma_0^2/E)$$

When A becomes plastic the work U_{AE} becomes

$$U_A = O(PF_B) = O(r\sigma_o^2/E)$$

From (18) and (18a) however, it can be seen that at most the unloading of A cannot affect the total work done by a term greater than $O(r\sigma_o^2/E)$ which proves that small amounts of plastic flow do not greatly affect the stress distribution.

Local changes in geometry can be simulated by local self-equilibrating stress systems and by St. Venant's principle these are also unimportant.

5.1 Cracks in Cylinders

As in the case of buckling, the bowing at the edges of cracks in pressurised cylinders invalidates our assumed stress systems causing a severe reduction in strength.

For static fracture of pressurized cylinders, Kuhn⁴¹ suggested the empirical formula

$$\sigma_R = \sigma_u / (1 + 9(2a/R)) \quad \dots \quad (19)$$

where $2a$ = crack length

R = radius of cylinder

and σ_R , σ_u are the nominal (hoop) stresses at failure in the cylinder and an infinite flat sheet containing the same crack. The factor 9 is that suggested by Williams⁴². Eq. (19) suggests as a driving force on cylinders

$$g_R = (1 + 18a/R)^2 g_o$$

but it must be remembered that it only applies to static failure of unstiffened cylinders. For stiffened shells

For recent work on this subject see

E.S. Folias "A finite line crack in a pressurised spherical shell"

International Journal of Fracture Mechanics 1 1965

or fatigue, it is probably too severe but experimental checks are needed.

6.0 Plastic Stress Systems

Excepting the special case of torsion treated by Hult³⁵, there are no closed solutions and work in this field is either photo-elastic or numerical. In ductile failure, fracture occurs along the slip systems radiating at $\pm 45^\circ$ from the crack tips so that one expects partly plastic sheets to behave similarly. This effect is shown in plane strain by the numerical results of Williams³⁶ and by the results of Rolfe and Munse⁴³ from photo-elastic coatings. From the latter it seems likely that the maximum shear strain (and hence the other strains) have the form

$$\epsilon_1 - \epsilon_2 = f(v)/\sqrt{r} \quad \dots \quad (20)$$

and we will take these results as a tentative standard.

In plane strain conditions, the slip field is apparently 45° to the sheet surface. According to Dugdale⁴⁴ of Liu⁴⁵ the plastic regions have the form shown in Fig. 7, where it is possible that 7(a) is a case between plane stress and plane strain.

If the tensile yield stress is σ_y then (7) supplies an approximation to the width of the plastic region. For convenience, we now define the plastic length p as

$$p = E/2\pi\sigma_y^2 \quad \dots \quad (21)$$

for plane stress and plane strain alike.

If the Mises yield criterion is applied⁴⁶ to the elastic stresses (5) then in polar coordinates the nominal plastic zone has the boundary

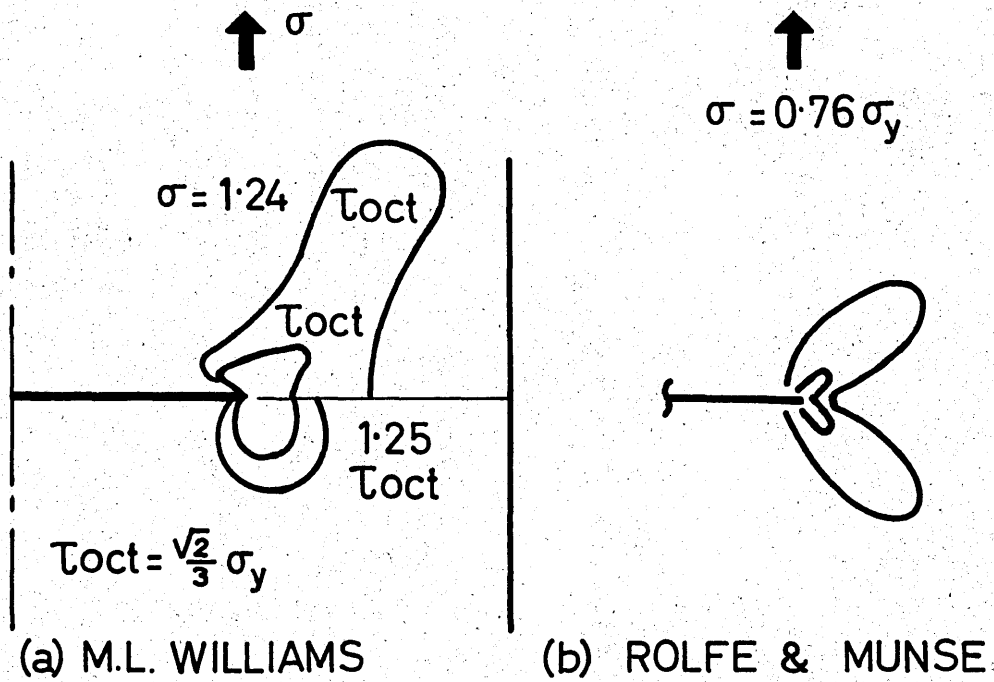


FIG. 4 REGIONS OF PLASTICITY IN PLANE STRAIN

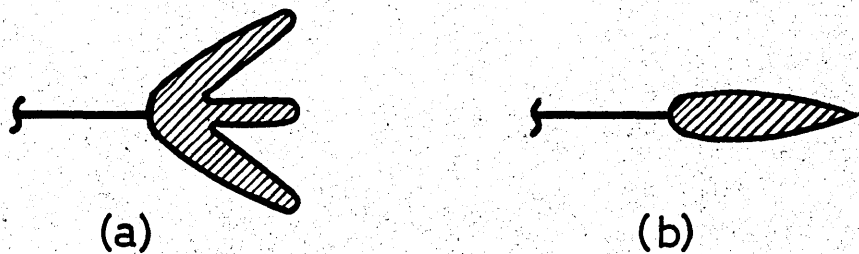


FIG. 5 PLASTIC REGIONS WITH PLANE STRESS

$$p(\theta) = \frac{E\ell}{2\pi\sigma_y^2} \cos^2 \frac{\theta}{2} \left\{ (1-2\nu)^2 + 3\sin^2 \frac{\theta}{2} \right\} \dots \quad (22)$$

where the plane stress case is obtained by putting $\nu = 0$. In plane stress then, (21) and (22) agree. Now let us consider the true width of the plastic region.

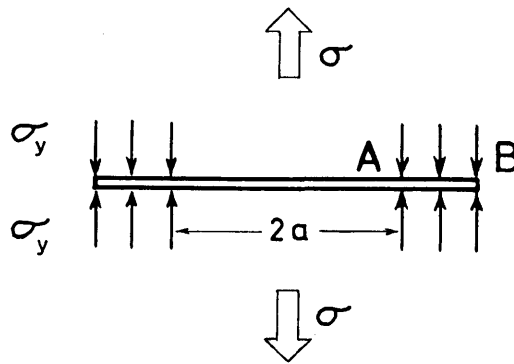


Fig. 6. Dugdale's Approximation

The form of plastic region shown in Fig. 5(b) led Dugdale to conjecture that the stresses in such a case could be approximated by an elastic crack in a loaded sheet with each end of the crack loaded by a tensile stress σ_y . The length AB in Fig. 6, was then obtained from the further condition that the stress at the tip (B) was finite. Thus, AB was regarded as the plastic width for a crack ending at A. For an infinite sheet, the only case considered, Dugdale found that

$$AB = \frac{2a \sin^2(\pi\sigma/4\sigma_y)}{1 - 2\sin^2(\pi\sigma/4\sigma_y)}$$

in excellent agreement with experiment.

For small stresses, this becomes, in our notation,

$$\begin{aligned}
 AB &= \frac{1}{8} \pi E \ell / \sigma_y^2 \quad \dots \quad (23) \\
 &= 2.46p .
 \end{aligned}$$

The same case for sheets of finite width has been treated by Bilby, Cottrell and Swindon⁴⁷ in terms of dislocation theory.

For plane strain consider the results of Rolfe and Munse⁴³ obtained from mild steel. Although the net stresses were very close to yield, the behaviour of the plastic regions closely paralleled that of the stress intensity and in the conditions appropriate to their Fig.9.

$$p = 0.1078''$$

From the figure one can obtain the admittedly approximate plastic width of 0.065'' based on the Tresca yield criterion. This is the narrowest part of the yielded zone in the line of the crack. Thus, in plane strain it seems that

$$\begin{aligned}
 \text{True plastic width} &\approx \frac{0.065}{0.1078} p \\
 &= 0.6p
 \end{aligned}$$

or roughly 3.75 times the value indicated by (22).

It is therefore almost certain that p has the correct order of magnitude especially in the plane strain case which is more important in fatigue. The definition is justified by the simplicity of (21) and the arguments of Section 2.1.

6.1 Work Done During Extension

It is convenient to anticipate here and consider the work done in plastic flow as a plastic zone moves across a plate. The results of Rolfe and Munse can be put in the form

$$\epsilon_s = \epsilon_y \sqrt{pf(\theta)/r}$$

where ϵ_s = maximum shear strain

ϵ_y = yield shear strain

and $f(\theta)$ = r/p along the experimental yield contour
(see Table I).

θ	r/p
0	.60
15	1.00
30	3.06
45	4.23
60	3.58
75	2.35
90	1.74
105	1.21
120	.89
135	.69
150	.46
165	.23
180	0

TABLE I

The plastic strain is now

$$\epsilon_p = \epsilon_s - \epsilon_y = \epsilon_y (\sqrt{pf(\theta)/r} - 1)$$

and we assume a linear work hardening, leading to the shear stress

$$\tau = \frac{1}{2}(\sigma_y + E_t \epsilon_p)$$

with the plastic work element

$$\frac{1}{2}(\sigma_y + E_t \epsilon_p) d\epsilon_p$$

Now consider the strain at a point A in Fig. 7 as the crack extends by an amount Δa .

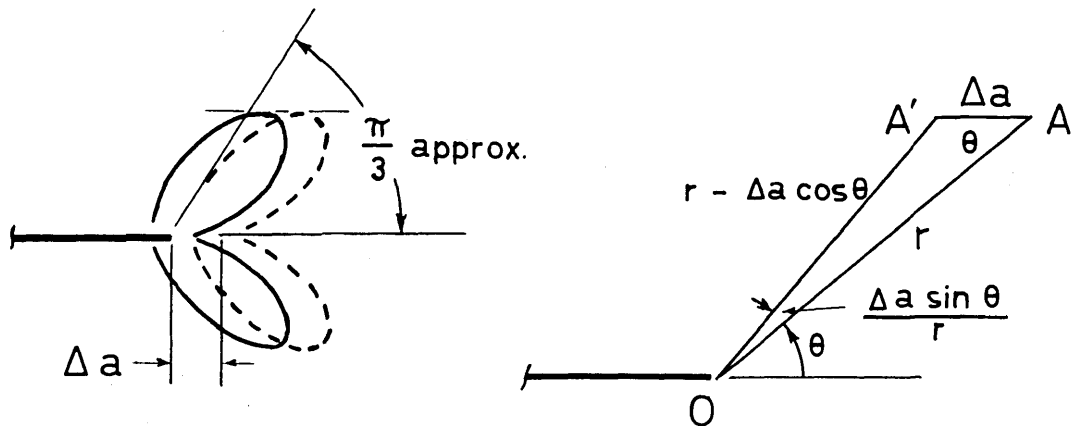


Fig. 7. Moving Plastic Region

If the crack and the flow field are held stationary, this is equivalent to moving A to A' and to the first order the new position is

$$(r - \Delta a \cos \theta, \theta + \frac{\Delta a}{r} \sin \theta)$$

and the corresponding change in plastic strain is

$$\frac{1}{2} \Delta a \epsilon_{yp}^{\frac{1}{2}} r^{-3/2} \{ \cos \theta \sqrt{f(\theta)} + \sin \theta f'(\theta) / \sqrt{f(\theta)} \}$$

To obtain the work corresponding to the extension Δa this is multiplied by the stress and integrated. When $|\theta| \approx \pi/3$ it will be seen from the figure that $A'A$ is tangential to the contours of maximum strain, so that $|\theta| > \pi/3$ corresponds to the region of elastic unloading. The radial limits of integration correspond to the onset of yield

$$r_y = p f(\theta)$$

and the maximum strain ϵ_u for which

$$r_u = \left(\frac{\epsilon_y}{\epsilon_u} \right)^2 p f(\theta)$$

(The lower limit is needed for convergence.)

Integrating over (r_u, r_y) we find the total rate of plastic work reduces to

$$\Delta W = p \Delta a \varepsilon_y^2 \left\{ (E_y - E_t) \left(1 - \frac{\varepsilon_y}{\varepsilon_u} \right) + E_t \log \frac{\varepsilon_u}{\varepsilon_y} \right\} \\ \times \int_{-\pi/3}^{\pi/3} \{ \cos \theta f(\theta) + \sin \theta f'(\theta) \} d\theta \quad \dots (23A)$$

The indefinite integral reduces to $f(\theta) \sin \theta$ and if we substitute for p and ε_y (23A) takes the more convenient form

$$\Delta W = 0.493 \Delta a \left\{ (1 - E_t/E) (1 - \varepsilon_y/\varepsilon_u) + \frac{E_t}{E} \ln \frac{\varepsilon_u}{\varepsilon_y} \right\}$$

The parameters here can be estimated from the true fracture stress σ_f (for ε_t) and the true ductility (for ε_u)

$$D = \ln A_o/A_f$$

where A_o , A_f are the initial and final cross-section areas of a specimen. In a paper on low cycle fatigue, Manson⁴⁸ gives the following values

	D	σ_f	σ_y
2024-T3	0.402	103 k.s.i.	51 k.s.i.
7075-T6	0.327	121	74

leading to the results

$$\Delta W = 0.493 \Delta a \begin{matrix} (1.027) \\ (1.017) \end{matrix} \text{ for } \begin{matrix} (2024-T3) \\ (7075-T6) \end{matrix}$$

These are respectively 3% and 9% larger than values obtained by using parameters from a simple tensile test. If this procedure is repeated using elastic octahedral shear strains⁴⁶ and stresses corresponding to linear work hardening we find the smaller values

$$\Delta W \approx \Delta a \begin{matrix} (0.210) \\ (0.072) \end{matrix} \text{ for } \begin{matrix} \text{(plane stress)} \\ \text{(plane strain)} \end{matrix}$$

In Griffith-Irwin theory it will be seen later that $\Delta W \equiv \Delta a$ so that these equations reflect the errors of the analysis and assumptions.

In contradiction to these results (and to fracture theory) Paris has based an explanation of his fourth power law⁴⁹ on the assumption that ΔW here is proportional to the area of the plastic zone, i.e. to g^2 .

From Fig.7 it can be seen that the plastic problem of a moving crack has a close resemblance to steady flow or die penetration problems except for the sign of the hydrostatic pressure.

6.2 Correction to g

If the case of Section 5.0 is considered again it will be seen that plastic yielding of the crack tips will allow the crack to open further or, in other words, the external forces do more work. If this additional work is available as elastic energy upon unloading, we may select an increased driving force.

This correction has been estimated by Irwin⁵⁰ by assuming that the crack behaves as if the length were $2(a+p)$. The yielding is thereby assumed to displace the stress field at the tip through a distance p . Since this correction successfully correlates⁵⁰ critical g_c values in fracture tests, we must conclude that it is reasonable. It is only appreciable when cracks are very short. In these cases plane strain plastic flow is more likely and we have also seen that p is then most realistic.

For fatigue the correction is unimportant, and we will henceforth ignore the correction except possibly for static failure of heavy sections.

7.0 Griffith-Irwin Theory

The earliest work on fracture mechanics was by Griffith⁵¹ who postulated that

$$g(a, \sigma^2) = W, \quad W \text{ constant}, \quad \dots \quad (24)$$

for brittle solids at incipient failure. By definition $g da$ is the elastic energy made available by an extension da , hence the term driving force. The right hand side is a dissipation term which is constant for brittle materials. Eq. (24) is a special case of the more general⁵²

$$\mathcal{H}(a, \sigma^2) + E(\theta) = W(a, t, \theta \dots) + dT \quad \dots \quad (25)$$

where $\mathcal{H}(a, \sigma^2) =$ energy available per unit crack extension

$E(\theta) =$ thermodynamic free energy

$W(a, t, \theta \dots) =$ rate of mechanical dissipation

$dT =$ increase of kinetic energy.

In (24) g is obtained from the solution of problems in elasticity with infinitesimal strains and displacements. It is implicit that energy is dissipated at a point "outside" the material. More generally the driving force, although elastic, comes from systems where the simple solutions have been invalidated by large amounts of previous plastic flow. This is actually the case when the above correction for g is needed.

In practical cases there is at least an order of magnitude difference between the scale of the plastic region

and the elastic stress systems of Section 2.0. It is therefore quite possible that the right hand side of (24) requires plane stress conditions while on the left hand side, plane strain is appropriate. This reflects the fact that we are approximating a basically three-dimensional problem. For edge notched specimens of cross-section $2\frac{1}{2}'' \times \frac{1}{2}''$, Srawley³⁰ et al. found that plane stress gave excellent agreement between theoretical and experimental measurements of \mathcal{G} .

For the ductile materials of interest, the work function W is not constant⁵³. We describe special cases later and also propose that (24) applies to fatigue fracture. It is often wrongly supposed that this is a condition for instability. The source of this notion is the fact that extension and instability are simultaneous when W is constant. Before proceeding let us extend* (24) to apply to variable work functions.

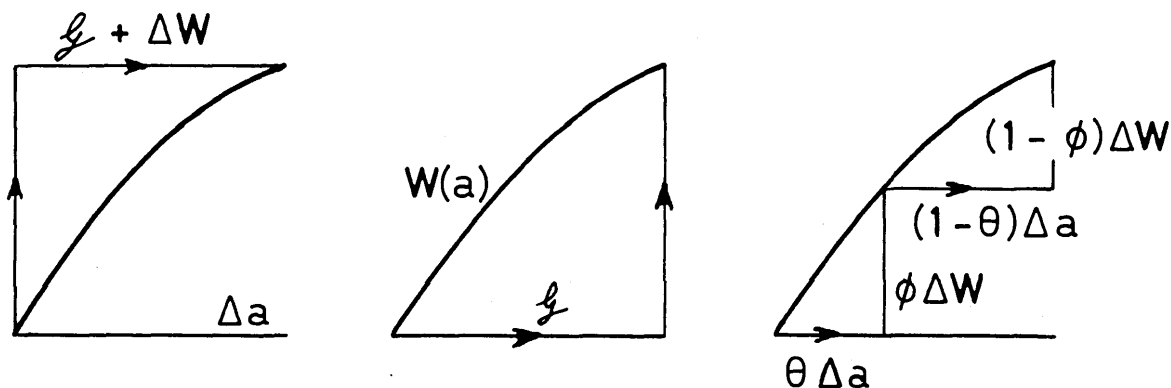


Fig. 8. Propagation with Variable Work Function

*This generalised form was mentioned by Irwin in a letter, but I have not seen any other discussion.

In Fig. 8 consider an extension Δa and suppose that during the extension $W(a)$ follows one of the polygonal paths shown. In Fig. 8(a) for example, the load is allowed to increase to the new value before extension is allowed.

In (a), (b) and (c) then

$$\text{Dissipation} = W\Delta a + O(\Delta a\Delta W)$$

while the available energies are

$$(a) \quad (\mathcal{L} + \Delta W)\Delta a$$

$$(b) \quad \mathcal{L}\Delta a$$

and (c) $(\mathcal{L} + \varphi(1-\theta)\Delta W)\Delta a$

intermediate between (a) and (b). Thus, to the first order

$$\mathcal{L}(a, \sigma^2) = W(a, \sigma^2) \quad \dots \quad (24A)$$

and if \mathcal{L} , W are known functions one has an implicit relation

$$a = a(\sigma^2).$$

There is obviously an upper bound to $W(a, \sigma^2)$ and with sufficient load $\mathcal{L} > W$ and failure is rapid. The start of this instability is marked³³ by

$$\frac{\partial \mathcal{L}}{\partial a} = \frac{\partial W}{\partial a} \quad \dots \quad (26)$$

Eqs. (24A) and (26) can be solved for σ and a i.e. the ultimate strength and the corresponding crack length, When W is constant, there is no extension before instability and (24) gives $\sigma(a_0)$.

7.1 Static Fracture

The essential features of the static fracture of sheets have been clarified by Irwin and his colleagues⁵⁰.

As the load increases, there is usually a period of slow growth governed by (24A) until instability occurs, followed by rapid fracture. During the slow cracking, the sizes of the plastic zone and the shear lips increase and the additional plasticity accounts for the increased work function. If fracture is sufficiently delayed, W reaches a maximum when the shear lips meet. There is also a corresponding minimum, the plane strain toughness, denoted by \mathcal{G}_I by Irwin which is appropriate to very thick plates or semi-elliptic cracks in heavy sections.

Now consider the effect of sheet thickness on the driving force at failure. In section 6.1, we have seen that the work function is proportional to p . In this respect the argument there applies to plane stress also and we assume further that in a plate

$$W \propto \text{average width of plastic zone.}$$

Using the results of Section 6.0, let us assume that the plastic zone of Fig. 9 has the cross-section shown where the $1.86p$ is also the width of the shear lip. In accordance with observation, we also assume that the line AB in Fig. 9 makes an angle $\arctan 0.2$, to the surface of the sheet.

If we also remember that W is defined as work per unit width and postulate that a zone width of $0.6p$ implies

$$W = \mathcal{G}$$

then some elementary calculations lead to the stepwise formulae ABC in Fig. 10.

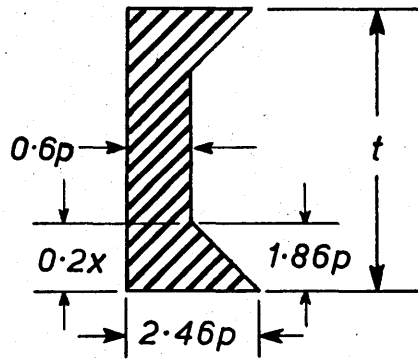
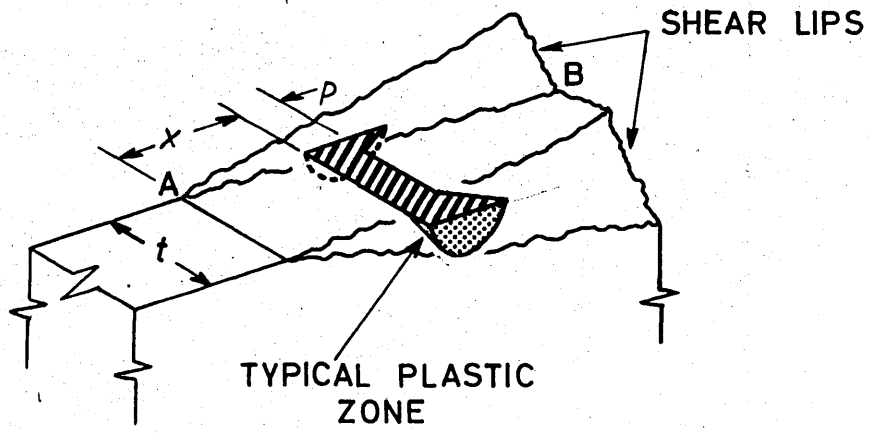


FIG. 9 GROWTH OF PLASTIC ZONE

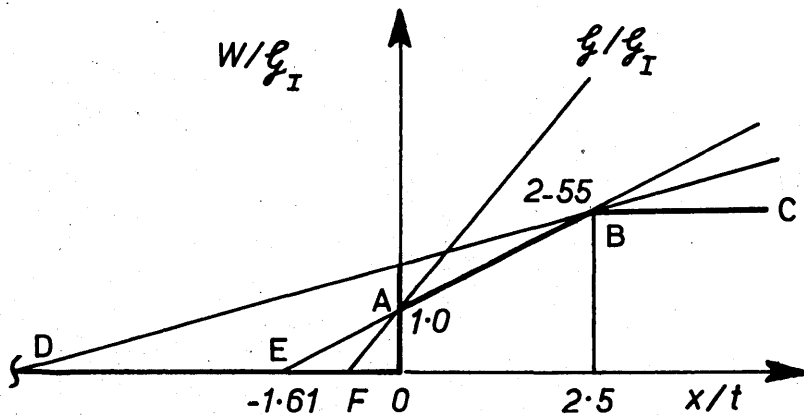


FIG. 10 APROXIMATE FORM OF WORK FUNCTION

Now let D, E and F be the centres of three cracks of different length while DB, EAB and FA represent their reduced driving forces at failure. If the half crack is larger than OE then from (24A) and (26) failure occurs (point B) after some slow growth and against a large resistance $2.55 \frac{t}{I}$. On the other hand, if the half crack is shorter than OE there is no slow growth and failure occurs under plane strain conditions. At E when $a = 1.61t$ there is a stepwise transition. These effects can also be achieved by having a constant crack length and increasing the thickness which is the way Irwin first discovered the effect experimentally. In practice, of course, OABC is a smooth curve (parabolic according to Kraft and Sullivan⁵³) and the transition is rapid rather than instantaneous.

7.2 Multiply Cracked Structures

Although most of the cracks discussed so far have two tips, their symmetry has obviated the need of detailed treatment of their interactions. In very many cases also different cracks are so far apart that their stress systems are independent.

When the extension of one crack affects the stress system of another, it is not clear how to generalise (24A) and (26) since it is possible to imagine several modes of extension corresponding to the same overall decrease in elastic energy. More generally, a single crack front which is curved is a similar problem with modes corresponding to varying speeds of advance on different parts of the crack front.

These problems have been discussed by the author, but as the result are uncertain, we will assume all cracks

to be independent. For a typical crack a_i then (24A) becomes

$$f_i(a, \sigma) = W(x_i/t_i) \quad \dots \quad (27)$$

where

$$a = \{a_j\}, \quad \sigma = \{\sigma_j\}$$

and (26) becomes

$$\frac{\partial f_i}{\partial a_i} = \frac{\partial W_i}{\partial a_i} \quad \dots \quad (27A)$$

failure being determined according to the crack first satisfying (27A).

8.0 Fatigue Cracks

Fatigue cracking like fracture depends on local conditions which we have seen to be defined by f or K . This view was first advanced by Paris^{49,54} who has also shown that the rate of growth per cycle does not introduce further complications. The physical processes in crack growth have been discussed by Forsyth²¹ and Schijve²⁵ and it is generally agreed that, apart from inhomogeneities and cases bordering on static failure, the crack extends by a sensibly constant amount in each cycle which depends⁴⁹ on f and other variables.

In sheet materials it has sometimes²¹ been noticed that the crack front "tunnels" ahead in the centre until the sides catch up by static fracture. This can also be regarded as a steady process.

8.1 Non-Dimensional Variables

The multiplicity of possible effects suggests the use of non-dimensional presentation. The basic parameters

can be divided into four classes, namely:

Geometric

$$\frac{dx}{dn} = \text{crack rate (extension per cycle)}$$

$$t = \text{thickness}$$

g, K or p (based on maximum load). These summarise the combined effects of load and the form of structure and crack ($p \equiv E g / 2\pi \sigma_y^2$)

$$\rho_o = \text{average grain size}$$

$$\rho_1, \rho_2, \dots = \text{other metallographic distances}$$

Stress

$$E, \nu$$

$$\sigma_y = \text{Yield stress (Here we use 0.2% proof)}$$

$$\sigma_u = \text{Ultimate stress}$$

$$g_I = \text{Critical work function for plane strain}$$

Fatigue

Mean load: Characterised by

$$\gamma^{\frac{1}{2}} = \text{Mean Load/Alternating Load}$$

$$\text{or} \quad \text{Maximum Load/Minimum Load}$$

Damage: Cycle ratio $\Sigma n/n$ etc.

S-N curve and statistical load parameters

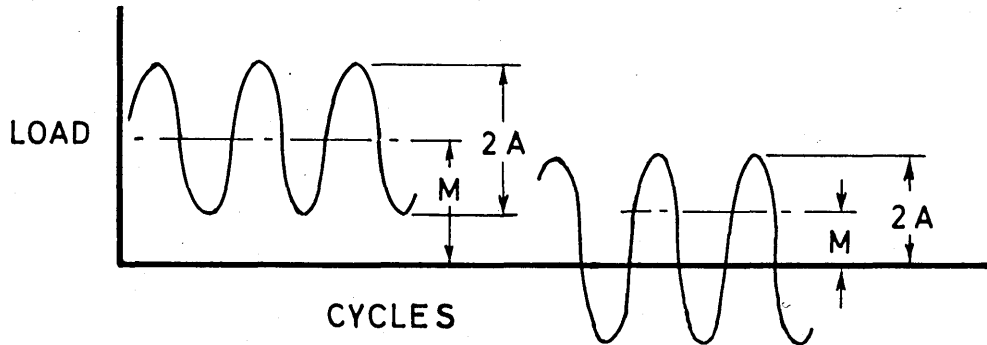
Time and Temperature

including frequency.

For a fixed material and conditions these variables reduce to

$$p = E g / 2\pi \sigma_y^2, \quad \frac{dx}{dn}, \quad t, \quad \rho_o$$

and g_m/g_a where g_m and g_a are the driving forces which correspond to the mean and alternating loads. This choice is not unique but we shall anticipate the experimental results.



Definition of Effective Mean and Alternating Loads

At this stage we recall that the important parameter in fatigue is the alternating rather than the mean load. When the minimum stress is compressive and the crack closes, it has also been found that the crack rate depends essentially on the tensile^{55,56} part of the fatigue cycle. Accordingly g_a and g_m are based on the loads A and M as shown in the sketch, and we use the non-dimensional variables

$$\frac{d\xi_a}{dn} = \xi_a' = \frac{2\pi\sigma_y^2(dx/dn)}{Eg_a} \quad \dots \quad (28)$$

$$= \frac{1}{p} \frac{dx}{dn} (1 + \sqrt{\gamma})^2, \quad \gamma \text{ below,}$$

$$\tau_G = t/p \text{ Relative thickness}$$

$$\rho = \rho_o/p \text{ Coarseness}$$

and finally

$$\gamma = g_m/g_a \text{ for mean loads.}$$

For large stresses $\frac{K}{\sqrt{a}}$ may also be important if the crack growth has a component of static failure.

8.2 Experimental Results

Three sets of results have been analysed in terms of the quantities just defined. The first two sets are compendiums of results for 2024-T3 and 7075-T6 by McEvily & Illg, Weibull and Boeing Aircraft, which have been assembled by Anderson⁵⁷ and Donaldson. These have the advantage that stress intensities are already calculated, the results having been used in Paris's thesis. A short test series of Moag⁵⁸ has also been analysed to investigate the effect of prior work hardening.

For the stronger aluminium alloys, Figs. 11, 12, 13 and 14 show $\log \xi_a'$ vs $\log p^{-1}$ which is essentially the correlation used by Paris⁴⁹. However, by basing ξ_a' on alternating load and the coarseness ρ on maximum load, the additional effect of mean load is almost completely accounted for. Both graphs are stepped but elsewhere the slope is about -1, corresponding to Paris's fourth power law. Where the curves are flat

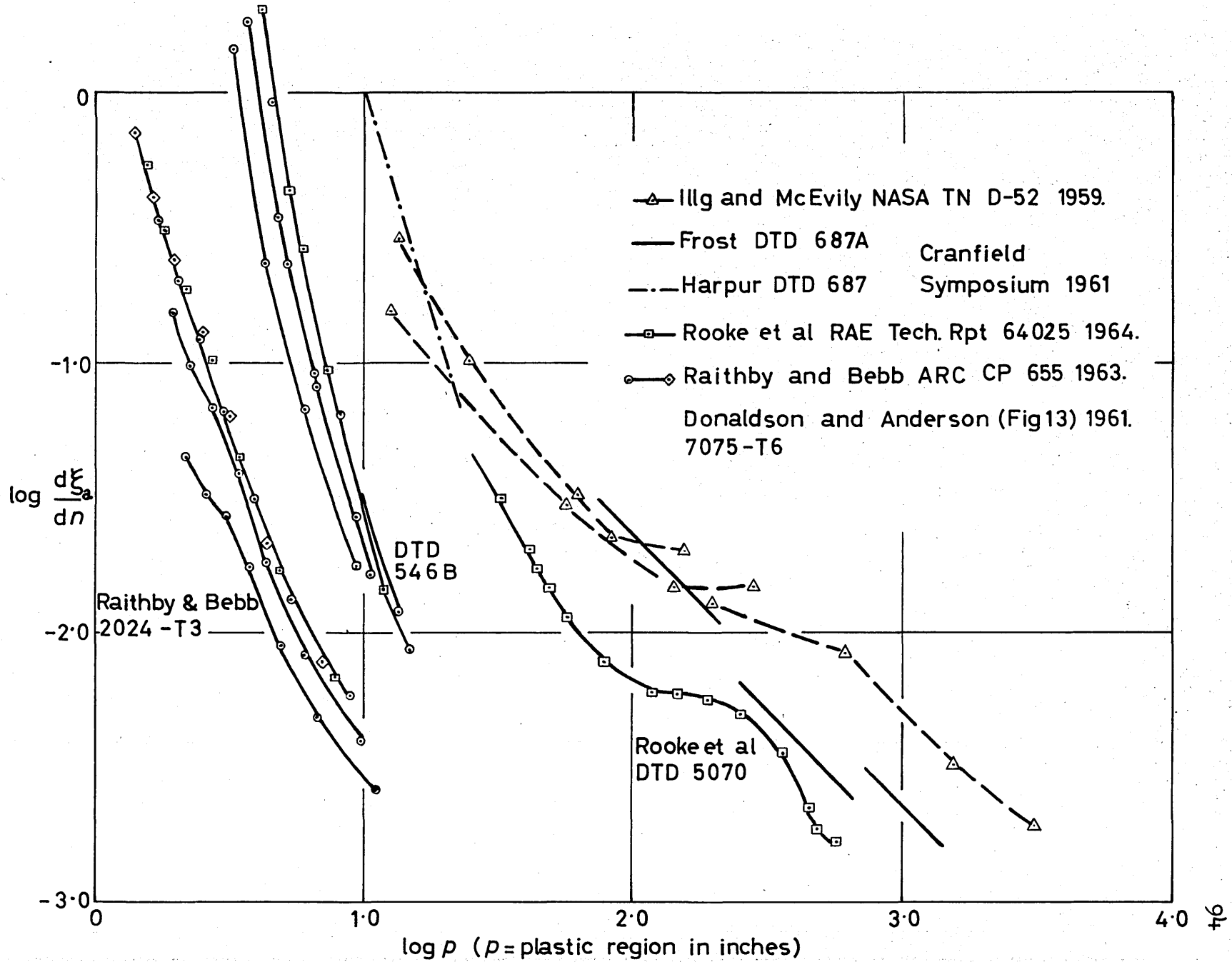
$$\frac{dx}{dn} \propto g_a$$

the similarity rule of Liu⁴⁶.

8.21 Discussion

Apart from details to be discussed below, the practical information here is no more than Paris has shown. However, the avoidance of high powers of stress means that the presentation is more accurate and has more fundamental significance. Even with non-dimensional pre-

FIG. 12 COMPARISON OF RESULTS



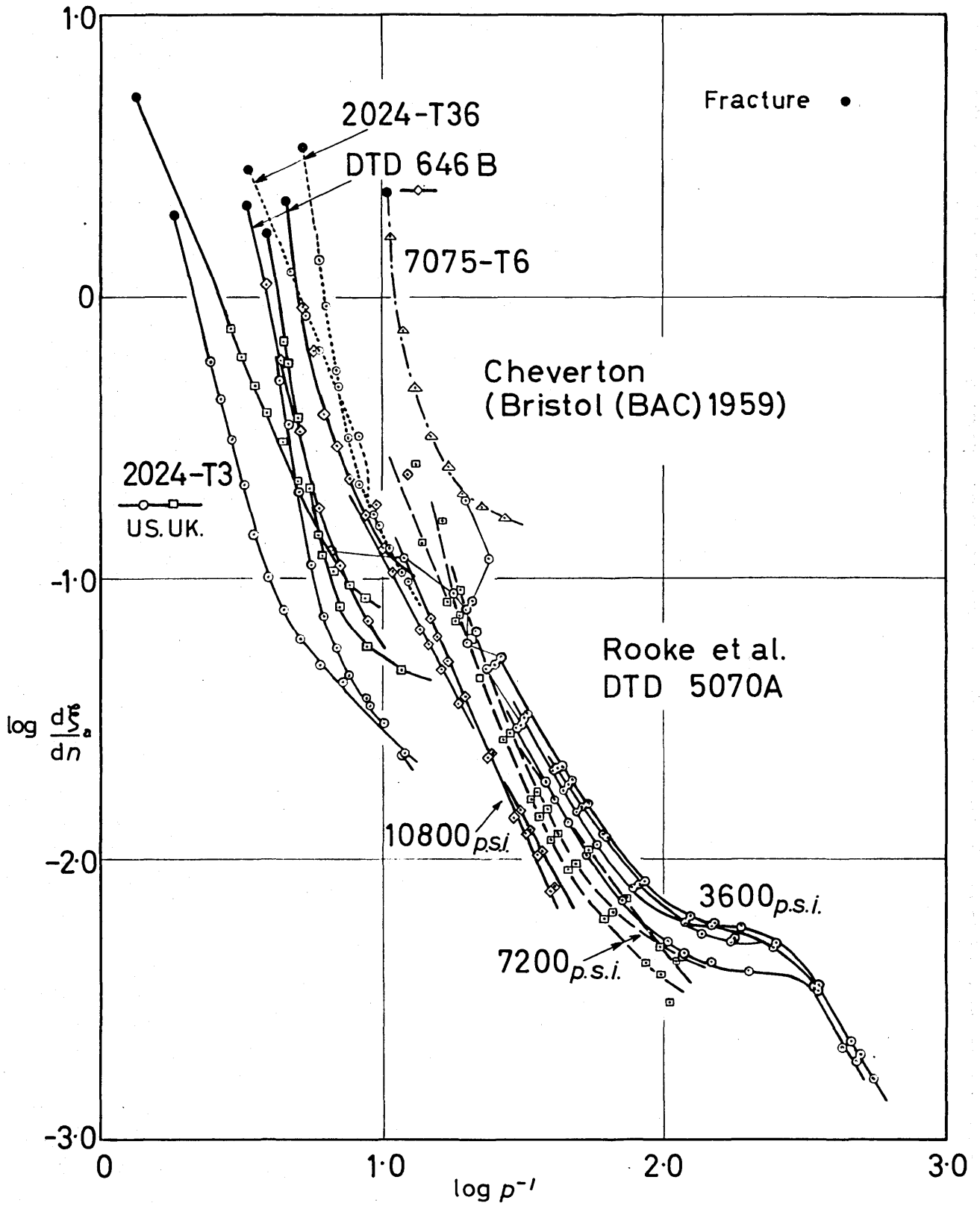


FIG. 14 CRACK GROWTH FOR HIGH STRESSES

sentation, it is obvious that different materials must be treated separately. Since ρ includes the grain size, a rarely measured material constant, it can be objected that the concept of coarseness is artificial and indeed we have been forced to use $\log p^{-1}$ as an abscissa which is equivalent, of course, to l or K .

It will be noticed however, that the flat parts of Figs. 11, 12 or 13 do include or lie near the point $\rho = 1$ (grain size 0.010" - 0.002"). If crack growth is a physical process then non-dimensional presentation should be possible. Furthermore, the excellent correlation obtained here suggests that the appropriate variables have been used. Thus, the formation of suitable non-dimensional variables requires an extraneous length. Any material constant is adequate but the evidence of the flat part indicates grain size. Forsyth²¹ has suggested that the transition from Stage I to Stage II cracking is associated with the penetration of a grain boundary by the initial crack.

The fourth power law of Paris agrees in a vague way with the present results but his supporting argument relates the work function to the area of plastic region (viewed at right angles to the sheet). We have seen in Section 6.1 that this contradicts Griffith-Irwin theory and experimental results.

8.3 The Role of Grain Boundaries

We now make some tentative suggestions regarding the effect of grain size on crack growth.

Consider the sloping parts of the curves in Figs. 11, 12 and 13. If for convenience the slope is taken

as -1 then

$$\frac{dx}{dn} = A \frac{g_a g}{\rho_o \sigma_y^4} \dots \quad (29)$$

where E is assumed constant but the yield stress σ_y can vary. It is reasonable to presume that σ_y increases for fine-grained materials and if

$$\sigma_y > A' \rho_o^{-1/4},$$

a rather mild dependence, this is achieved, but dx/dn also decreases with ρ_o .

Now let

$$\frac{dx}{dn} = A'' g g_a$$

on the sloping parts of the curve and consider the behaviour of the actual plastic zone z_p (i.e. g) increases. As $p \rightarrow \rho_o$ the grain boundary will often be loaded and will tend to hold the crack tips together so that, until g is sufficient to break the boundary, the actual plastic zone width will be approximately constant.

If the actual width is assumed to control ξ'_a then the flat part of the curves is explained. This view will be supported by the theory (Section 9.4) concerning random loads.

8.4 Statistical Analysis of Results

The data of Anderson and Paris is sufficiently varied to allow a guess at the effects of mean load, frequency and relative thickness. These effects and the smoothness and repeatability of individual results can be obtained by the help of an analysis of variance or regression

analysis which must be attacked piecemeal owing to the complexity of the overall pattern.

It is planned to perform two separate analyses on the flat parts and where the growth rate increases again. Preliminary results indicate that although the crack propagation is fairly smooth for a particular case, different specimens or structures which are nominally identical have significantly different $\log \xi'_a - \log p^{-1}$ curves with the associated component of standard error 0.1773 (log 1.5, 20 d.f.).

8.5 Work Hardening

The results ξ'_a vs. τ_G of tests done by Moag⁵⁸ are shown in Fig. 15. The thickness was a constant 1/8" and different mean loads have been obtained by interpolation. The relative rate ξ'_a is little affected by work hardening (c.f. 1/4 II, 1/2 II and fully hardened materials) but an increase in mean load decreases it.

At the high stresses used, the size of plastic zone is no doubt very sensitive to maximum stress and this increases the work function thus reducing the growth rate.

When $\tau_G > 1.5$, ξ'_a seems more constant possibly because of an approach to plane strain conditions.

9.0 Crack Growth under Random Loads

As in all random load questions one must first set up a consistent definition of a load cycle. In room temperature fatigue the effects of time such as frequency, rest periods and the wave form of the loading, are relatively unimportant but some variable is still required to mark the sequence of events. This is obviously the

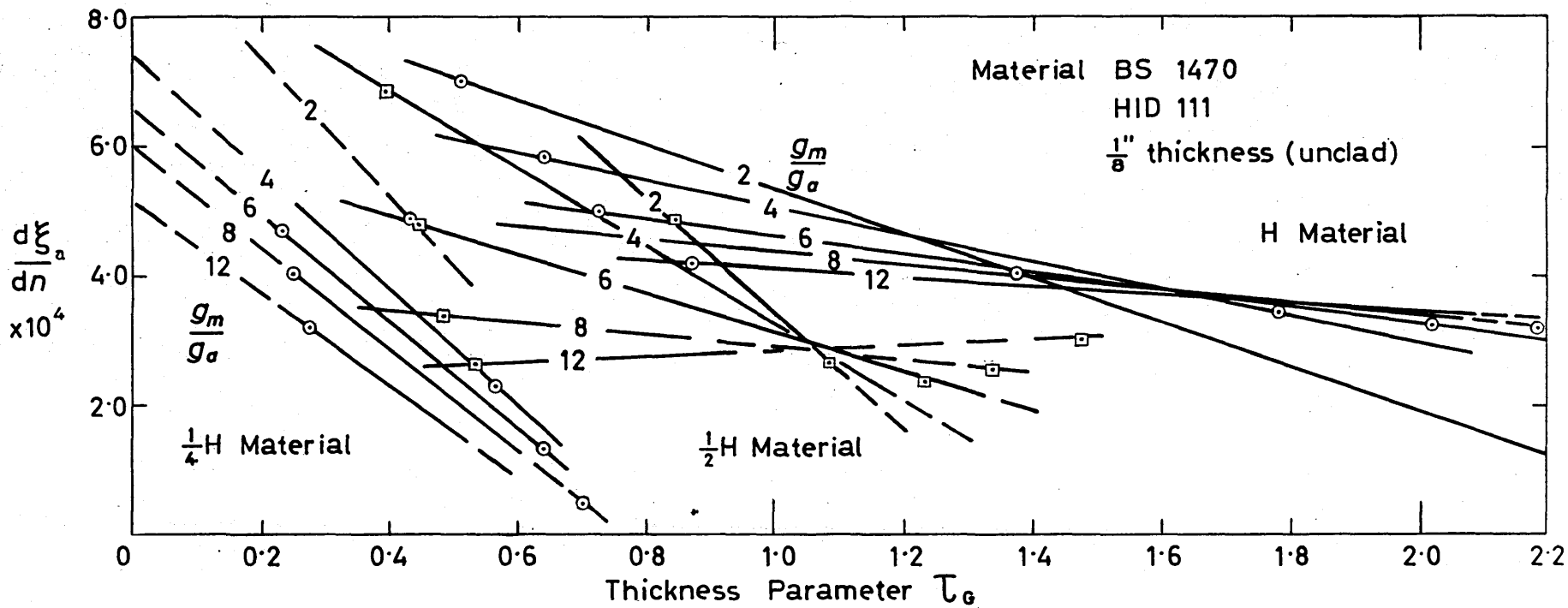
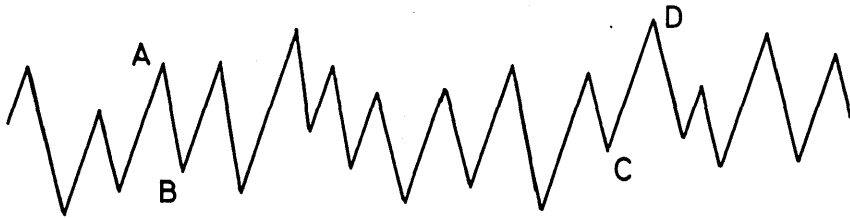


FIG. 15 EFFECT OF WORK HARDENING

number of peaks and troughs which, for consistency, should equal the number of cycles.

This question can be evaded by a theory based on the properties of small specimens under random load.¹⁵ Since "random load" implies e.g. an infinite choice of power spectra, any analysis would involve either interpolation or further testing. The first would probably require the concept of a cycle while the second would destroy the practical justification for any theory. In particular, the undoubtedly necessary technique of spectral analysis should be regarded, like aeroelastic analysis, as a type of stress calculation supplying input data for fatigue work.

From the results of Jones⁵⁵ and Paris⁶¹ it would seem that the best definition of a cycle is the load change (such as AB or CD in the sketch) between successive cycles.



Restricting ourselves to the tensile part of the cycle (Section 8.1) each load change can be defined by a mean and alternating load or some equivalents.

When speaking of a cycle one imagines a full wave returning to the same position. The present case shows that this restriction is unnecessary and indeed a load rise such as CD need never have a corresponding fall. If there is one it would probably occur when the crack has extended so that the two halves of such a wave would be unrelated physically.

However, it is a useful convention to define these load changes (AB or CD in the sketch) as half cycles.

9.1 Some Feasible Residual Stresses

The title indicates that a loading $0 - f - 0$ has occurred ab initio and that the strains have been assumed at first to rise and fall like those of the elastic system.

If the elastic stresses at any stage are now modified by disallowing those exceeding σ_y the equilibrium conditions (and others) or zero load and moment along the crack axis after unloading will be violated. This has been corrected by adding an arbitrary set of stresses and the total forms the required feasible system.

The aim of this procedure is to obtain an order of magnitude estimate of the amount of reversed yielding, which will be used as supporting evidence elsewhere.

As a preliminary check, let us compare this approximation with the numerical results of Stimson and Eaton⁶² who treated the edge notched plate of Fig. 16 (a).

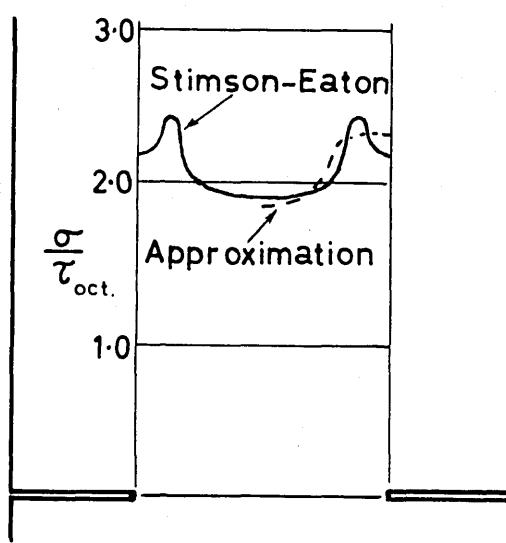


Fig. 16(a). Check of Approximation

By integrating their stresses we find the average gross area stress

$$0.43 \tau_{\text{oct}}$$

By trial and error the stress system

$$\sigma = \min \{A/\sqrt{x}, 1.8 \tau_{\text{oct}}\}$$

was fitted to give the same total load and it can be seen that the agreement is good for such a crude approximation.

We now return to the original example and for convenience assume that the stresses corresponding to maximum load are

$$\sigma_0(x) = \min \{1, x^{-\frac{1}{2}}\}$$

where the first term refers to yielding.

If reversed yielding is ignored then the corresponding stresses after unloading are

$$\sigma_1(x) = \sigma_0(x) - x^{-\frac{1}{2}} - \min \{0, 1-x^{-\frac{1}{2}}\}$$

which violates equilibrium conditions. These may be corrected in the range $0 < x < 1$ by assuming that the actual stresses are

$$\sigma_2(x) = 1 - x^{-\frac{1}{2}} + (ax^3 + bx^2 + cx + d).$$

The coefficients of the polynomial are determined by equilibrium and by tangency at $x=1$. The results indicate that reversed yielding occurs at $x = 0.0242$ and the final system $\sigma_3(x)$ in Fig. 16 (b) is that obtained by reducing $\sigma_2(x)$ ($x > 0.037$) by the ratio of the yielded system ($x < 0.037$) to $\int_0^{0.037} \sigma_2 dx$.

The region of reversed yield is extremely narrow and of the same order as the crack growth in each cycle. By Griffith-Irwin theory, we show later that they are equal.

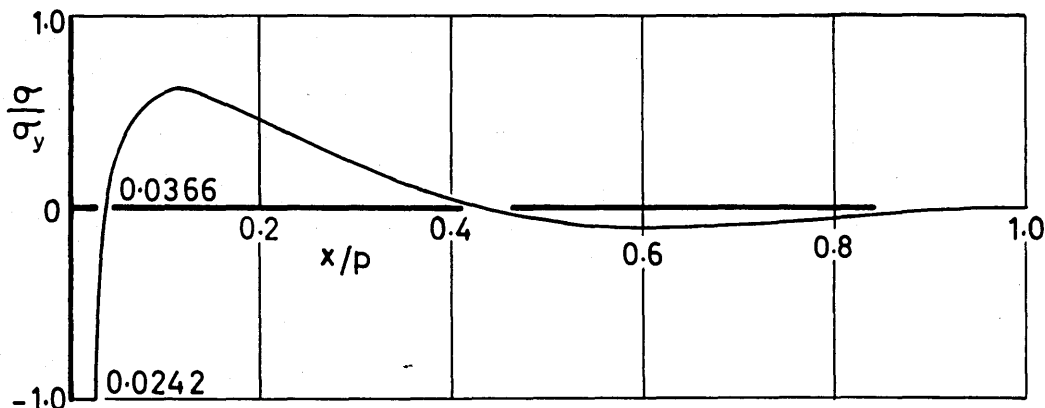


Fig. 16 (b). Form of Residual Stress System

9.2 Effect of Load Sequence

At considerable risk, let us extend the previous section to the load sequence

$$0 - \frac{1}{2} - 0 - \frac{1}{2}$$

by forming

$$\sigma_{1/2}(x) = \min \{1, ax^{-\frac{1}{2}} + \sigma_3 x\}$$

When $a = 0.3112$ ($a^{-1} = 3.22$)

$$\sigma_{1/2}(0.0242) = 1.$$

The figure a^{-1} may be interpreted as a rough guide to the magnitude of preloading necessary to inhibit subsequent crack growth at lower loads. Thus, if a load exceeding

$$(3.22)^2 \frac{1}{2} = 10.3 \frac{1}{2}$$

is introduced into a sequence of loads $\frac{1}{2}$ then crack growth should decrease.

This conflicts with the experimental results of Hardrath⁶³ who measured the delay of crack propagation in 2024-T3 after the constant loads of a sequence were suddenly reduced to a lower constant load (two step

test). However, the estimates above are claimed to be orders of magnitude only and are not used in further analysis.

On the other hand, Hardrath's result cannot represent a typical situation. This is easily shown by considering a typical numerical case from his data.

Let there be a structure loaded by a random sequence of the two stresses 40 k.s.i. and 37 k.s.i. where it is claimed that a preload of 40 k.s.i. delays growth at 37 k.s.i. by 100 cycles. Let us use the probabilities

$$\Pr(40 \text{ ksi}) = p \quad 0 < p < 1$$

$$\Pr(37 \text{ ksi}) = q = 1 - p$$

$$\text{and } \left. \frac{dx}{dn} \right|_{40} = R \text{ say.}$$

There are three relevant possibilities for each load namely:

37 and more than 100 previous loads of 37; step $0.768R$

37 and less than 100 previous loads of 37; no growth

40 k.s.i.; growth R .

Assuming Bernouilli trials and the fourth power law, these lead to the expected rate

$$\mathcal{E}(dx/dn) = R(0.768q^{101} + p)$$

with the minimum $0.05R$ when $p = 0.05$.

This defies common sense and, more rigorously, contradicts the random load experiments of Paris⁶¹ which would predict

$$\mathcal{E}(dx/dn) > R(0.768q + p).$$

The preload stresses in these experiments are always greater than 30 k.s.i. which implies extensive yielding

($\sigma_y \approx 51$ k.s.i.) when driving forces are also considered.

9.3 Form of Preload Delay

Since the load l is a scale factor, linear when l is small enough, it is apparent that the effect of a preload such as those described, depends on the ratio

$$(\text{Preload/Following Load}) = r, \text{ say.}$$

From the previous section it seems possible that unless $r > 10$, the occurrence of large driving forces (abbreviated to "preload" here) has little effect on subsequent crack growth.

In contrast to Hardrath's result, when growth stopped completely, fractographic measurements on Vampire⁶⁴ spar booms indicated that for a short period (≈ 100 cycles) the subsequent rate was roughly half that corresponding to the load. There was a corresponding increase when the subsequent loads exceeded the preload.

If the crack tip is a singularity when plastic flow occurs, then the latter behaviour is more likely although there is no obvious cause for the increased rate.

9.4 A Fourth Power Model of Random Growth

Barnard's results⁶⁴ indicate the possibility that a series of random "preload" effects may cancel. This is the actual behaviour observed by Jones⁵⁵ and Paris⁶¹ except that when the average driving forces were below those of the flat parts of Figs, 11, 12 and 13, the rates observed by Paris were about ten times greater than those predicted by simple addition.

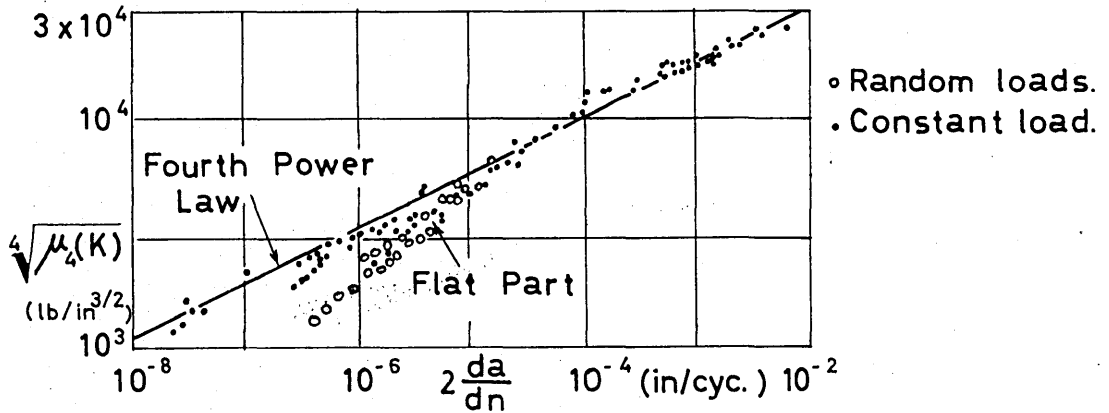


Fig. 17. Paris's Results for Random Load

In his experiments which employed random noise, Paris defined load cycles in terms of zero crossings. For a wide band noise which he sometimes uses, the number of zero crossings is considerably less than the number of load changes and this accounts for part of the discrepancy.

To account for the remainder, let us write Paris's fourth power law¹⁹ in the form

$$\frac{1}{p_a} \frac{dx}{dn} = A \frac{p}{p_o} \quad \dots (30)$$

where

$$p_a = E y_a / 2\pi \sigma_y^2$$

$$p = E y / 2\pi \sigma_y^2 \text{ the plastic length.}$$

If p_m is similarly defined in terms of mean stress

$$p = p_a + 2\sqrt{p_a p_m} + p_m$$

Now, let p be a random variable

$$p : f(p)$$

with mean \bar{p} and variance V .

Then, in a purely additive case (30) becomes

$$\begin{aligned} \mathcal{E}\left(\frac{dx}{dn}\right) &= A \mathcal{E}\left(\frac{pp_a}{\rho_o}\right) \quad (\mathcal{E} \equiv \text{Expectation}) \\ &\approx \frac{A}{\rho_o} \mathcal{E}(p_a^2 + 2p_m^{\frac{1}{2}} p_a^{3/2} + p_a p_m) \quad \dots (31) \end{aligned}$$

To explain a growth more rapid than this, assume that p in (30) is determined by the (average) maximum load during the time that such a plastic region takes to pass the relevant crack tip position. This generalisation is in the same spirit as our presentation of constant load results. When the average growth is rapid, the maximum will be chosen from fewer members so that it will not greatly differ from p in (31). If the locally maximum plastic length is p_f then the number of cycles to cross it is clearly

$$p_f / \mathcal{E}_f \left(\frac{dx}{dn} \right) = n_f, \text{ say} \quad \dots (32)$$

Thus, (31) is replaced by

$$\rho_o \mathcal{E}_f \left(\frac{dx}{dn} \right) = A \mathcal{E}(p_a p_f) \quad \dots (33)$$

where p_f is the n_f^{-1} -th fractile of $f(p)$.

A knowledge of $f(p)$ will now allow the solution of (32) and (33) as transcendental equations for $\mathcal{E}_f(dx/dn)$ and p_f . If n_f is large, p_a and p_f will be statistically independent and (33) becomes

$$\begin{aligned} \frac{\mathcal{E}_f(dx/dn)}{\mathcal{E}(p_a)} &\equiv \frac{d\mathcal{E}_f}{dn}, \text{ say,} \quad \dots (34) \\ &= \frac{A}{\rho_o} p_f \\ &= n_f^{-1} p_f / \mathcal{E}(p_a) \text{ from (32)} \end{aligned}$$

$$\text{i.e.} \quad n_f = \rho_o / A \mathcal{E}(p_a) \quad \dots \quad (34A)$$

and by comparison with (31) the rate increases by a factor of approximately p_f/ρ_o .

9.5 Generalisation

When the flat part is approached, the actual plastic region tends to be constant by our hypothesis of Section 8.3. Thus, the use of p_f (i.e. of maximum driving force) should not increase the rate. Above the flat part the rate is such that the expected increase is small. This explains why Paris's results (Fig. 17) start to diverge at the beginning of the flat part.

Let us generalise (30) in the form

$$\frac{1}{p_a} \frac{dx}{dn} = A \frac{p}{\rho_o} G\left(\frac{p}{\rho_o}\right)$$

where $G = O(1)$ is a slowly varying function.

As above, this immediately generalises to

$$\rho_o \mathcal{E}_f \left(\frac{dx}{dn} \right) = A \mathcal{E}_f \left\{ p_a p_f G\left(\frac{p_f}{\rho_o}\right) \right\} \quad \dots \quad (35)$$

with p_f still given by (32). When the relative rate is small then, as before,

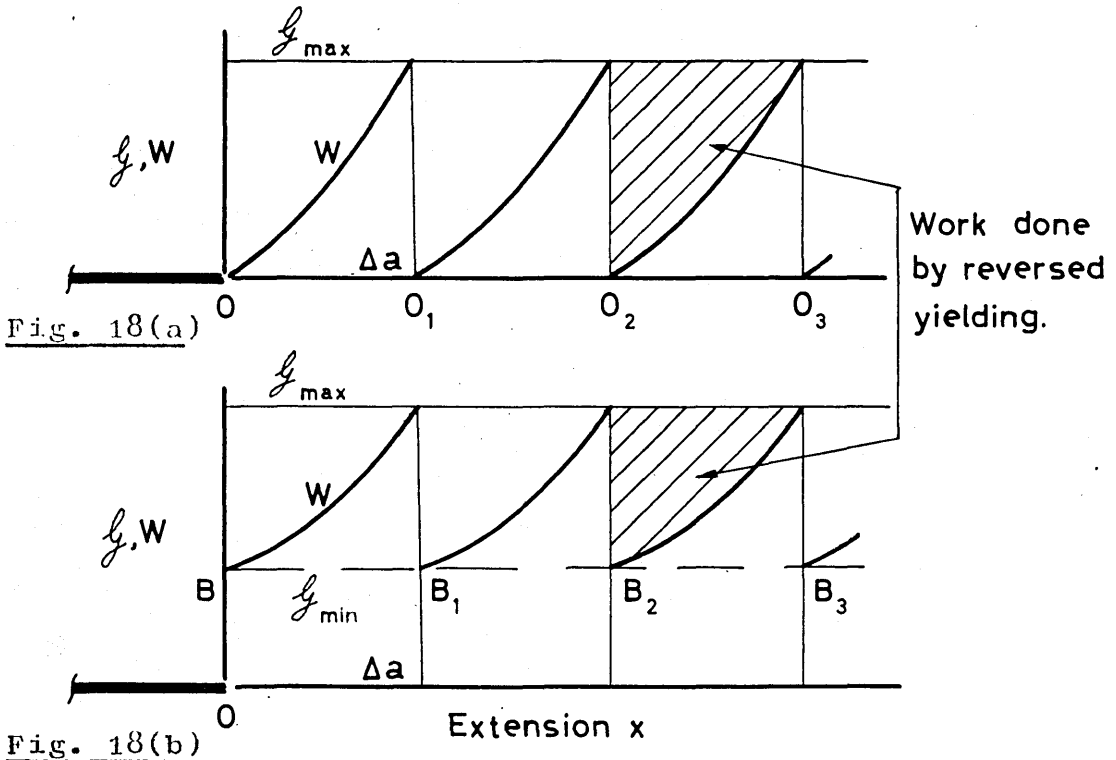
$$\frac{d\mathcal{E}_f}{dn} = \frac{A}{\rho_o} p_f G\left(\frac{p_f}{\rho_o}\right) \quad \dots \quad (36)$$

$$\text{and} \quad n_f = \rho_o / A \mathcal{E}(p_a) G(p_f/\rho_o) \quad \dots \quad (36A)$$

which can be solved for n_f or p_f when $f(p)$ is known.

9.6 Behaviour of Work Function

Apart from environmental conditions the work function W for static failure depends on the extension from the original crack length. As constant load fatigue cracking is a steady process, it is a reasonable hypothesis that W depends on the distance from the current crack tip.



Form of W For Fatigue Cracks

In Fig. 18(a) let O, O_1, O_2, O_3 be successive crack tip positions, while OA, O_1A_1 etc., represent W at the start of each cycle when the load is zero. At any stage of loading

$$l = W \dots (37)$$

which is also the case at l_{max} . (Here l represents all intermediate loads in the cycle $O-l_{max}-O$). Eq. (37) defines the crack length at any stage of loading so that

$$W < \dot{g}_{\max} \dots \quad (38)$$

It also follows that AO_1 etc. are vertical. The plastic work corresponding to each point on OA_1 ... is done over a much longer region* than the crack extension so that as a first guess one may suppose that the total work done for each element of crack growth is a constant and this total work rate must be \dot{g}_{\max} .

During each crack extension, the work done however is the area $O_1A_1O_2$ leaving areas such as O_1AA_1 . The only possibility is that work represented by the shaded area is done by the reversed plastic flow from the previous cycle which implies that the crack extension in each cycle is less than the width of the region of reversed yielding.

The force causing reversed yielding cannot be related to crack extension since none occurs. It may therefore modify W over a distance $O(p)$ from the crack tip. However, from (37) and (38) this effect must be zero at the points A, A_1, A_2 so that

$$\text{Crack Extension} = \text{Width of reversed yield.}$$

When the minimum load $\dot{g}_{\min} > 0$ the figure 18(b) applies but the argument is not affected. As \dot{g}_{\max} is less than the critical static driving force \dot{g}_c we may note in passing that repeated loading is in a sense a more efficient way of separating materials than static fracture.

The idea of an effectively periodic work function such as that in Fig. 18 has also been suggested by Cotterell⁸² but in his case W is the appropriate section of the static function so that fatigue fracture is taken as an incomplete static failure. This approach does

* From Section 6.1 or merely the fact that $\xi_1' \approx 10^{-2} \rightarrow 10^{-1}$.

not seem to make any allowance for the work done by reverse yielding.

9.7 Very Small Driving Forces

According to Griffith's original theory

$$W = 2T$$

where T = surface tension of material, and this refers to purely brittle fracture where the only lasting disturbance is the separation of two atomic planes. For metals there is always a little plastic flow⁶⁵ even in true cleavage.

The corresponding W is a lower bound albeit very small so that in Section 9.6, Fig. 23(b) is always the appropriate one. This lower bound implies the existence of non-propagating cracks as discussed by Frost⁶⁶ and Coffin⁶⁷.

Forsyth²¹ has suggested that non-propagating cracks have returned to the slower Stage I type of growth, along planes of maximum shear, which we regard as cumulative

damage. Obviously as ξ'_a decreases, the number of significant stress cycles suffered by a particular element of material i.e. $O(\xi'_a)^{-1}$ can cause significant cumulative damage which may hasten crack growth in comparison to the fourth power law. Figs. 11, 12 and 13 show evidence of such an effect, indicated by a departure from the fourth power law at low rates.

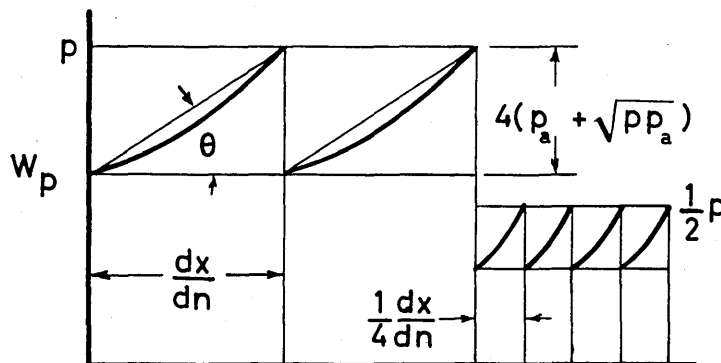
9.8 Possible Form of W

Before describing some possible experiments, we shall remark on the form of W in the light of the fourth power law and others, and of the discussion of residual stress in Sections 9.1 and 9.2.

Let us redraw Fig. 18(b) regarding p_a and p as alternating and maximum load. If the corresponding work function is

$$W_p = EW/2\pi\sigma_y^2$$

the new figure will be non-dimensional.



The fourth power law has the form

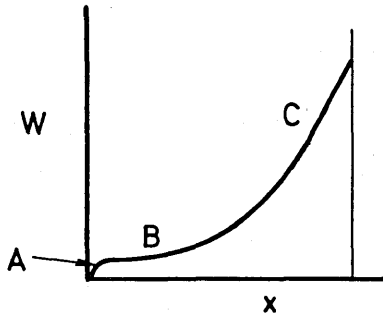
$$\frac{1}{p_a} \frac{dx}{dn} = A \frac{p}{p_o}$$

or in terms of the figure

$$\tan \theta = A^{-1} \rho_0 (1 + \sqrt{p/p_a})/p$$

The effect of halving p has been illustrated ($p/p_a =$ constant) and there is obviously no geometric similarity. In the flat parts, however, geometric similarity is preserved.

We now consider the form of W qualitatively. There is a residual compressive stress to be overcome and then according to Forsyth²¹ about half the crack extension is brittle ending with ductile fracture. This is consistent with the sketch, where A, B and C represent these three stages.



9.9 Some Possible Experiments

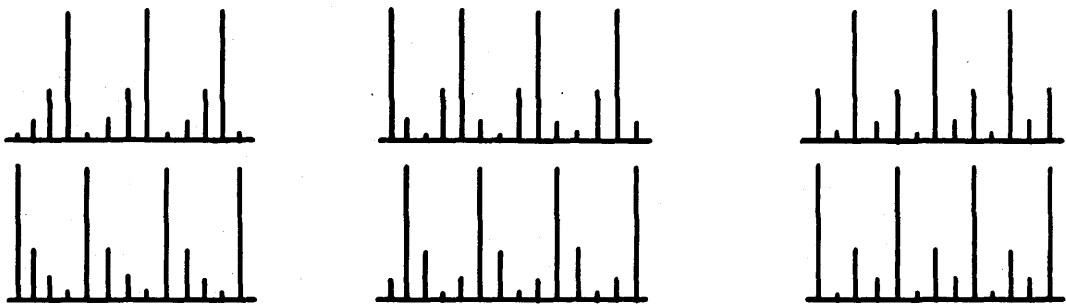
Although there are quite good empirical correlations, the detailed knowledge of crack growth under random loads is very meagre. It is quite possible that the happy results of Jones or Paris and their extensions of Sections 9.4 and 9.5 are purely fortuitous results of the probability distributions of the loads $f(p)$, $f(p_a)$. In any case the random load applications of Griffith-Irwin theory are unclear.

It is also plain that the interactions of individual load cycles must be studied and that two steps or programme tests are not representative. Because of the regularity of macroscopic cracking, this type of testing is also extremely wasteful. From previous considerations, if ξ'_a is on the flat part of Figs. 16, 17 or 18 or above then, when the loading is changed, the new regime will

become established after an extension of order p . This will normally be less than 0.01 in. and accurate rate measurements require a base length⁶⁸ 0.05 - 0.2 in.

Thus, a single conventional specimen allows several different cases to be studied without variations arising from different specimens. In statistical parlance each specimen is a "block" and a test series a randomised block design.

A possible procedure would be to apply all six permutations of four loads in geometric progression as shown. The regular arrangement allows fractographic study and accurate growth measurements over short distances.



Chapter IV

THE CRACK DAMAGE EQUATIONS

Having established general frameworks for the description of damage and crack growth separately it is now time to consider them together. The damages of interest are of course in places where cracks begin and these are assumed to be known. It follows, as one might expect, that single cracks are a trivial case and the main emphasis is on the interactions between several cracks and the corresponding damages. However the single crack is a useful introduction to the more complex cases.

With some restrictions, we shall eventually establish differential equations for the non-trivial case, which is the general fatigue problem mentioned earlier, but because of this generality the treatment is rather abstract. This is no disadvantage because the functions used will always involve full scale stress analyses which can only allow an abstract representation in formulae if the structures are at all realistic. In a later chapter the applications of the matrix force method will be considered as a particular case of the theory here.

In the following it is supposed that there are N possible cracks of lengths $a_1, \dots, a_i, \dots, a_N(\mathbf{a})$ and that these begin at the times $t_1, \dots, t_i, \dots, t_N = \mathbf{t}$. It is convenient to assume for the moment that

$$t_1 < \dots < t_i < \dots < t_N$$

which is always possible for a given sequence or mode of failure by renumbering or permuting suffices. As these cracks progress the structure becomes weaker and at any stage one can estimate the hazard by comparing

the strength with the applied loads as in Chapter II or by other means. For any particular t , if the crack growth is deterministic, the life distribution

$$f(n|t) = h(n|t) \exp \{-H(n|t)\}$$

can thus be found. The actual life distribution is therefore

$$f(n) = \int f(n|t) dF(t), \quad \dots (1)$$

taking the expectation over all possible sets of initial failures t . There remains the problem of finding $f(t)$.

For any particular crack however this is simply the derivative of its canonical damage (one-dimensional here). This in turn is given by the damage equation

$$\frac{dF_i}{dn} = A(F_i, S_i) \quad \dots (2)$$

where the local stress S_i depends on all the crack lengths a and the distribution of the applied loads $F(R)$. This is usually constant but there is no reason why it cannot change with time or cycles.* Only the autonomous equations are considered below.

We are interested in the relatively slow growth of cracks over hundreds or thousands of cycles so that the applied loads may be adequately represented by their moments or cumulants. If these are constant then for all cracks the damages (2) can be written in the form

$$\frac{dF}{dn} = A(F, a) \quad \dots (3)$$

where the right hand side implies that all the stresses

*For our purposes these words are equivalent.

and the stress intensities are calculated for the set of crack lengths \mathbf{a} (including zeros) and then substituted into the damage equations (2). Together with the randomness of the loads this is the essential practical difficulty whose consideration is postponed till later. The effects of stress concentration factors, which essentially increase the damage rate, can be directly included in (2) and without further ado this is assumed to be done. In a form analogous to (2) the growth rate of each crack can be written

$$\frac{da_i}{dn} = R_i(E\ell_i[F(R), \mathbf{a}], \tau_i)$$

which has the more abstract form

$$\frac{d\mathbf{a}}{dn} = R(\mathbf{a}) \quad \dots \quad (4)$$

analogous to (2).

1.0 Direct Solution

At any stage suppose that r cracks have begun at time t (of order r) and have reached the lengths \mathbf{a}_r at n cycles so that the complete crack length vector is

$\mathbf{a} = \{\mathbf{a}_r \ 0\}$ say. During this r -th stage the governing equations are

$$\frac{d\mathbf{a}_r}{dn} = R_r(\{\mathbf{a}_r \ 0\}) \quad \dots \quad (5)$$

and $\frac{dF_{N-r}}{dn} = A_{N-r}(\{F_{N-r} \ 0\}, \mathbf{a})$, $F_{N-r} = \{F_{j+1} \dots F_N\}$,

where the subscripts indicate the number of relevant components and the $N-r$ also refers to positions where cracks have not yet begun. When another crack, say \mathbf{a}_{r+1} , starts then (5) is replaced by

$$\frac{da_{r+1}}{dn} = R_{r+1}(a) \quad \dots (5A)$$

$$\frac{dF_{N-r-1}}{dn} = A_{N-r-1}(F, a), \quad a = \{a_{r+1} \ 0_{N-r-1}\} \text{ etc.,}$$

which are the same as (5) except that there is one more equation of crack growth and one less for damage.

For (5A) the initial conditions at $n=t_r$ say, are

$$a_{r+1} = 0, \quad a_r = a_r(t_r) \text{ i.e. } a_{r+1} = \{a_r \ 0 \ 0\} \text{ say,}$$

$$\{F_{N-r-1} \ F_r\} = F_{N-r},$$

and for any given set of initial failures all such equations can be solved; without extreme difficulty on a computer. If the stress S_i at the beginning of the crack a_i is suitably defined the solutions for damage may also be formally extended over the full range of life considered and this forms the basis of our second method. A damage not in this extension will be known as active.

2.0 The Initial Crack

At the start any rate of crack growth is roughly exponential since the stress intensity is approximately proportional to the crack length.

Mathematically this means that the initial crack existing immediately after time t_i must have finite length in order to propagate further. This expresses our previous contention that, below a certain length, the growth of a crack follows different laws if indeed such cracks can exist in the engineering sense. From the viewpoint of both metal physics and engineering the

growth of cracks smaller than some critical length is best regarded as a process of cumulative damage to be described by damage equations.

It is now generally accepted that most of the scatter in fatigue life arises in the crack initiation described by the damage equations. More precisely, Schijve has found that the growth of extremely small cracks is much more erratic. His viewpoint agrees with ours if these small cracks are regarded as damage per se. For consistency it is then most plausible to suppose that all initial cracks have the same length a_0 and that immediately before this the crack length is zero or in more practical terms it is too small to effect the stress pattern.

From physical considerations a_0 must be related to the scale of inhomogeneity in the material. As a maximum this is represented by the average grain diameter. It has been shown by Forsyth that the change from "stage I" (damage in our case) to "stage II" or crack propagation proper is often associated with the crack penetrating the first or possibly second or third grain boundaries. Thus it seems reasonable to make a_0 roughly equal to the grain diameter.

There is another less fundamental argument which leads to the same model with rather different values for a_0 . It applies most aptly to aircraft structures and so will be discussed in terms of that case. For these it can be argued that, compared to the complete structure, the first order of inhomogeneity is represented by the sizes of rivet holes, edge distances, rivet spacings etc. which are therefore of the order of a_0 . Because the damage equations must now include some true crack propagation they are likely to be either more complex or less accurate. If multiparametric damages are avoided this

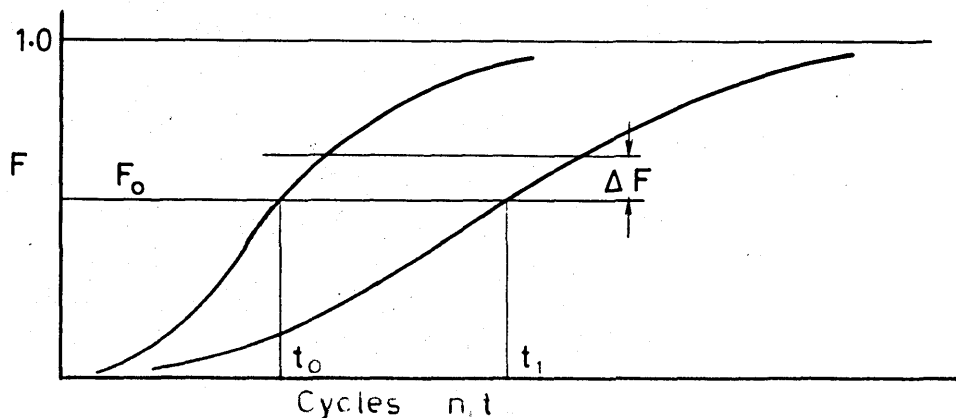
usage is intermediate between our previous postulate and the present day usage where in effect the damage equations must account for damage and cracking together. On the other hand the stress analysis is greatly simplified presaging its complete disappearance when damage is made to refer to final failure.

Both of these approaches should be equivalent if the equations are correspondingly adjusted and the ultimate choice depends on experience and experiment. The smaller a_0 can be inferred by noting the crack length at which the constant amplitude growth laws of Chapter III break down although a random load theory would be better if it were available.

3.0 The Role of Damage Equations

For physical reasons the accumulation of damage in any position cannot directly depend on the damages attained elsewhere, and the only possible coupling arises through the existence of cracks which are more likely in certain regions.

Consider a particular damage F for a crack a_0 (i.e. a crack not yet begun). Depending on the remainder of the structure, F takes several forms such as the two in the sketch.



Then F_0 corresponds to the same event, namely prior failure, because it is a damage also, but a damage corresponding to different initial lives t_0 and t_1 .

As the fatigue process develops and the (physical) damage functions increase then for each increment of damage the system in effect performs a Bernouilli trial in order to make the decision "Will the crack start now?". At any such time suppose that the canonical damage is F_0 and the increment ΔF . Then, using the statistical properties of canonical damage,

$$\begin{aligned}
 & \Pr(\text{Initial failure in the interval } (F_0, F_0 + \Delta F)) \\
 &= \Pr(\text{No previous failure}) \cdot \Pr(\text{Failure} \mid \text{No previous failure}) \\
 & \quad + \Pr(\text{previous failure}) \cdot \Pr(\text{Failure} \mid \text{Previous failure}) \\
 &= (1 - F_0) \cdot \{\Delta F / (1 - F_0)\} + F_0 \cdot 0 \\
 &= \Delta F. \qquad \qquad \qquad \dots (6)
 \end{aligned}$$

This is true for all increments so that this process of continuous experimentation until a single success occurs is equivalent to the choice of a single variate from the uniform distribution over $(0,1)$.

Now in (6) we have not used any relation between F and n and it follows that the distribution of F is independent of the initial life distribution which develops in the solution of the damage equations.

3.1 Monte-Carlo Solution

As the name implies this is a mathematical analogue of the physical fatigue process. In the result above we have shown that the starting times of the vector t need not be the outcome of the continuous experimentation implied by the damage equations. The N canonical damages

\mathbf{F} can be initially N independent selections from a uniform distribution, the independence arising from that of the physical damages. Similarly, mN selections can simulate the initial failures of m structures. The change from (5) to (5A) and the other changes are then made when F_{n-r} reaches its predetermined value.

Since the crack growth is deterministic any outcome is completely defined by, and the complete solution requires, the joint density $f(\mathbf{t})$. By appropriate renumbering let us suppose that any set of initial failures has the components

$$\mathbf{t} = \{t_1 \dots t_i \dots t_N\}$$

in order of magnitude. We also suppose that at each initial failure the solution of (5) and (5A) etc. give the damage densities

$$\frac{dF^j}{dn} = f(t_j | t_{j-1}) \quad \text{say,}$$

where, in general, the density for t_j depends on the existing cracks, starting at t_{j-1} . Then, for our randomly chosen point in \mathbf{t} -space, the joint density is

$$f(\mathbf{t}) = \prod_{j=1}^N f(t_j | t_{j-1}), \quad \dots \quad (7)$$

$t_0 = 0$. This simulation with mN selections will give m values of $f(\mathbf{t})$. From another viewpoint the fatigue process can also be regarded as a mapping or transformation of the equally likely points \mathbf{F} in the space of canonical damage into the initial failure vectors \mathbf{t} . In the Monte-Carlo method \mathbf{F} is directly obtained by the preliminary selection and the overall density $f(\mathbf{n})$ is

$$f(n) = \int f(n | t) dF(t)$$

which can be approximated by

$$f(n) = m_r^{-1} \sum_{i=1}^N f(n | t_i) \quad \dots \quad (8)$$

where m_r is the number of active solutions of the damage equations available at the time of interest. In t -space the grouping of the results gives a check of $f(t)$ which should agree (within the appropriate scatter) with (8). If the Monte-Carlo approach is used the approximation to (1) can be further improved by importance sampling and possibly by analytical values where $f(t)$ is small. Both these procedures are vastly more efficient using the independence proved below.

4.0 Independence of Initial Failure Times

Through equations (5) and (5A) we have formulated a transformation from the uniform damages F , reached at each initial failure, into the starting times t and this transformation is continuous and differentiable.

Suppose that $f(t)$ is known. Then F is simply the vector of marginal distribution functions, or,

$$F_i = \int_0^{\infty} \dots \int_0^{t_i} \dots \int_0^{\infty} f(t) dt \quad \dots \quad (9)$$

and $\partial F_i / \partial t_j = f(t_i)$, if $i = j$, $= 0$ if $i \neq j$,

where $f(t_i)$ is the marginal density. After our transformation

$$f(F) = \left| \partial t / \partial F \right| f(t) \quad \dots \quad (10)$$

and the Jacobian here is

$$\partial t / \partial F = \{f(t_1)f(t_2) \dots f(t_N)\}^{-1}$$

by (9A). Now

$$0 < F_i < 1$$

and it is of course uniformly distributed. In addition the physical damages are independent and hence the canonical damages have the joint density

$$\begin{aligned} f(F) &= 1 \\ &= f(\mathbf{t}) / \prod_{i=1}^N f(t_i) \end{aligned}$$

on substituting our Jacobian. From (9) onwards the same argument can be used for any subspace \mathcal{S} of \mathbf{t} whence

$$f(\mathbf{t}_{\mathcal{S}}) = \prod_{t_i \in \mathcal{S}} f(t_i).$$

Since \mathcal{S} is arbitrary and includes \mathbf{t} the different t_i must be independent.

This generalises the well known probability transformation. In words, we have shown that if the transformation to marginal distribution functions produces a uniform joint density of these in the hypercube $0 < F_i < 1$ then the original variates are independent (and of course the F_i).

For dependent variates the corollary follows that a transformation to marginal distributions cannot lead to a uniform joint density. A simple example is the two-dimensional case

$$f(x,y) = 2(x - 2xy + y), \quad 0 < x,y < 1, \dots (11)$$

with the marginal distributions

$$F(x) = x, \quad F(y) = y, \quad 0 < F < 1,$$

i.e. $f(x), f(y) = 1$.

Here (11) is also the dependent distribution of marginal density integrals.

Although they are independent it must not be supposed that the component densities are the same as one would obtain if fewer than N cracks were considered, i.e. if the problem were different. (In most similar applications of probability theory such a presumption would hold but independence never implies it.) It will transpire that the dependence of different crack growths arises, not by the sequence of failures, but through the differences in any particular crack caused by the presence or absence of the others. These effects determine the damage densities but leave them independent.

4.1 Improvement of Monte-Carlo Method

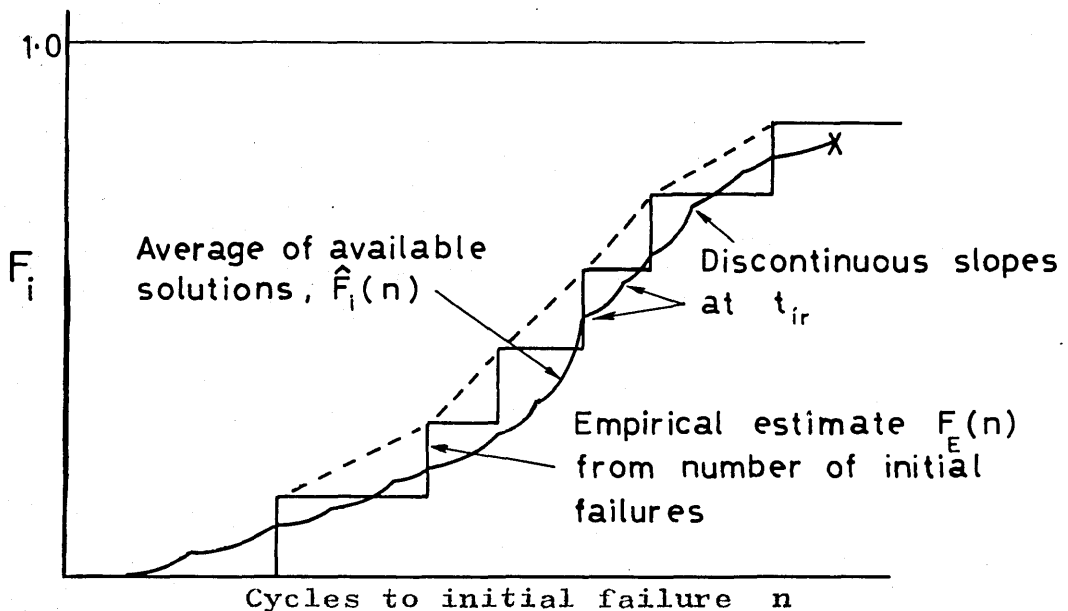
The independence of the initial failures can be used to improve the Monte-Carlo method already outlined. Suppose there are m simulations arising from mN initial failures $t_{ir} = t_r$ ($r=1,m$).

From the simulations the active solutions $A_r(F, a)$ of the damage equations in (5), (5A) provide estimates as in (8) for each crack and $m_r < m$, a function of the number of cycles and the particular crack, is the number of simulations with active solutions of the damage equations. For crack i let $\hat{F}_i(n)$ denote the distribution estimated from (8) at n cycles.

From the results we also have the stepped empirical distribution

$$F_E(n) = \left\{ \sum_{t_{ir} < n} t_{ir}^o \right\} / (m + 1) \quad \dots (12)$$

which also estimates $F(t_i)$. These two estimates are shown in the figure.



As n increases the results available for $\hat{F}_i(n)$ decrease to zero as n passes t_{i1} , t_{i2} etc. Thus although it is less satisfactory the information conveyed by F_E becomes more important as n increases. For practical purposes however the shorter lives have most interest. The right hand side of (12) represents the expectations of the standardised order statistics of which the r -th has variance

$$\sigma^2(F(r)) = \frac{r}{(m+1)^2} \frac{m-r+1}{m+2} \quad \dots (13)$$

As in the figure, the best continuous estimate of $F(t_i)$

based on (12) is the dashed polygon shown. This is the appropriate estimate to pool with the average of the solutions $\hat{F}_i(n)$ but it is not available outside the interval (t_{i1}, t_{im}) . Within any sub-interval $(t_{ir}, t_{i r+1})$ we have F_{r+1}, \dots, F_m say, $(m-r)$ solutions of (5), (5A) whose mean $F_i(n)$ has some sampling variance which can be approximated by the constant

$$s_r^2/(m-r), \text{ say.}$$

If the two estimators are independent then it follows that the combined minimum variance estimator in the interval $(t_{ir}, t_{i r+1})$ can be approximated by

$$F_{ti}(n) = \frac{\left| \left| \frac{s_r^2}{(m-r)} \frac{1}{m+1} r + \frac{n-t_{ir}}{t_{i r+1} - t_{ir}} + \frac{(r+\frac{1}{2})(m-r+\frac{1}{2})}{(m+1)^2(m+2)(m-r)} \sum_{j=r+1}^m F_j(n) \right| \right|}{\frac{(r+\frac{1}{2})(m-r+\frac{1}{2})}{(m+1)^2(m+2)} + \frac{s_r^2}{m+r}} \dots (14)$$

where the r in (13) has been arbitrarily moved to the midpoint $(r+\frac{1}{2})$.

4.2 An Identity

It is instructive to consider the continuous analogue of (14) as $m \rightarrow \infty$. Although the t_i are independent the sample distributions thereof will differ according to the t -vectors chosen in (5) and (5A). It is then convenient to denote these as

$$F_i(n|t),$$

whose active part is defined for $n < t_i$.

In the continuous case the average $F_i(n)$ becomes

$$F_i(n) = \int \dots \int F_i(n|t) dF(t) / \Pr(t_i > n)$$

the equality following from the law of large numbers.

The integral corresponds to the denominator and the formula can be written

$$\begin{aligned} F_i(n) \cdot (1 - F_i(n)) &= \int_{t_i > n} \int_{t_j > 0} \dots \int F_i(n|t) dF_1 \dots dF_i \dots dF_N \\ &= \int_{t_0} \int_n^\infty F_i(n|t) dF_i(n) dF(t_0), \end{aligned}$$

$$t_0 = \{t_1 \dots t_{i-1}, t_{i+1}, \dots, t_N\},$$

using the independence of t and integrating over the extraneous t_j ($j \neq i$).

If we write

$$\Delta F_i(n) = F_i(n) - F(n|t)$$

then this identity also takes the form

$$\int_{t_0} \int_{t_i=n}^\infty \Delta F_i(n) dF(t) = \frac{1}{2}(1 - F_i(n))^2.$$

5.0 The Development of Cracks

In the sections following we shall consider the growth of fatigue cracks as well as damage. At the start the Monte-Carlo standpoint will be adopted but it will become apparent that this can be discarded in favour of a set of explicit equations analogous to (5) and (5A).

It would be possible to display our final equations (35), (36) here and explain their significance quite simply but it is hoped that a more leisurely exposition will pro-

vide a more motivated derivation and indicate their relation to the Monte-Carlo method.

Consider the size distribution at n_0 cycles of a certain crack beginning at t . While this develops we suppose that the $N-1$ other cracks grow deterministically in some typical fashion. It is convenient if these "background cracks" all begin at $n=0$ and then grow continuously. This can be approximated by using the average of the Monte-Carlo solutions (equations (5), (5A)) for the crack lengths

$$\bar{a}_i(n) = m^{-1} \sum_{j=1}^m a_{ij}(n), \quad i=1, \dots, N, \quad \dots \quad (15)$$

where

$a_{ij}(n) = 0$ if $n < t_{ij}$ and these zero cracks have been included in the averaging. If da_{ij}/dn jumps from 0 to R say at $n=t_{ij}$ then in the average this discontinuity decreases to R/m which cannot be guaranteed if only non-zero cracks were included in the average (for example at t_{11} the jump would not alter). In the limit the growth rate is continuous and we assume that it is also differentiable. The background cracks in (15) then become the expectations

$$\tilde{a}_i(n) = \int_0^{\infty} \dots \int a_i(n|t) dF(t) \quad \dots \quad (16)$$

where we have adopted the notation of conditional probability. After changing the variable to a this becomes in vector form

$$\tilde{a}(n) = \int_0^{\infty} \dots \int a(n|t) dF(a|n)$$

with the derivative

$$\frac{d\bar{a}}{dn} = \int_a R(a) dF(a|n) \quad \dots \quad (17)$$

using (4). If R was linear in a then one could drop the integral sign and write

$$\frac{d\bar{a}}{dn} = R(\bar{a})$$

but consideration of Paris' fourth power law or the non-dimensional results of Chapter III will show that this linearity is unlikely, especially when the stress intensity is increased by finite width effects.

5.1 One Crack Illustration

It was found in Section 4.0 that the initial failures t_i were independent because of the one-one transformation from F to t . In (17) we have already extended this concept to regard the set of crack lengths $a(n|t)$ at n cycles given t as a transformation of t . However if any component of t is greater than n then it cannot affect these cracks and the transformation is therefore not unique unless all components of a exceed zero. (If the Stieltje integrals above are also based on Lebesgue measure the steps there are allowable.) If necessary uniqueness can be ensured by supposing that before initial failure a crack grows continuously up to the initial length previously discussed.

Let us approach the general case by considering the simple one-crack system (cf. (5))

$$\begin{aligned} \frac{dF}{dn} &= h, & 0 < n < h^{-1}, \\ \frac{da}{dn} &= Ka, & F(0) = 0, \quad a(t) = a_0, \end{aligned}$$

where initial lives are uniformly distributed over $(0, h^{-1})$ and, once begun, the crack grows exponentially. For an initial life t

$$a = a_0 e^{K(n-t)} \quad \dots \quad (18)$$

representing at transformation $t \rightarrow a$ with the parameter n . Using the rule for changing probability densities

$$\begin{aligned} f(a) &= f(t) \left| \frac{dt}{da} \right| \\ &= h/Ka_0 e^{K(n-t)} \\ &= h/Ka \quad , \quad a_0 < a < a_0 e^{Kn}. \end{aligned}$$

Obviously if $t > n$ then $\{t > n\} \rightarrow \{a = 0\}$ and the density $f(a)$ relates only to $\{a > 0\}$, integrating to hn .

Now consider the mean crack length given by

$$\begin{aligned} \bar{a} &= \int_{a_0}^{a_0 e^{Kn}} af(a) da + 0 \cdot (1-hn) \\ &= a_0 (e^{Kn} - 1) \end{aligned}$$

whence

$$\frac{d\bar{a}}{dn} = K\bar{a} + ha_0 \quad \dots \quad (19)$$

with the initial condition $\bar{a}(0) = 0$.

Thus the original homogeneous equation describing the growth of an initially finite crack now has a forcing term ha_0 while \bar{a} is initially zero. We now repeat the case using the distribution

$$t : f(t)$$

whence $\Pr(a=0) = 1 - F_t(n)$; $F(n) \equiv F(t)$ for $t = n$.

Using (18) again,

$$f(a) = f(t)/Ka$$

for finite cracks and

$$t = n - K^{-1} \log(a/a_0).$$

In addition

$$\begin{aligned} \bar{a} &= \int_{t=0}^n a dF(a) \\ &= \int_0^n a f(t) dt \quad \dots (20) \end{aligned}$$

Differentiating and remembering that $a(t) = a_0$,

$$\frac{d\bar{a}}{dn} = K \int_0^n a f(t) dt + a_0 f_t(n) = K\bar{a} + a_0 f_t(n), \quad \bar{a}(0) = 0,$$

generalising (19).

We now come to the general rate

$$\frac{da}{dn} = R(a), \quad a(t) = a_0,$$

for which (20) still holds. The average rate is now

$$\begin{aligned} \frac{d\bar{a}}{dn} &= \int_0^n R(a) dF(t) + a_0 f_t(n) = \int_{a_0}^{\infty} R(a) dF(a|n) + a_0 f_t(n), \\ &\bar{a}(0) = 0, \quad \dots (21) \end{aligned}$$

and unless R is linear in a this is the simplest form.

As an approximation let the rate be

$$K(a+m) + R(a)$$

where K, m can be chosen to minimise $R(a)$ in some sense.

Then

Then

$$a + m = (a_0 + m) \cdot e^{K(n-t)} \exp(I(a)) \quad \dots \quad (22)$$

where

$$\begin{aligned} I(a) &= \int_t^n \frac{R(a)dn}{a+m} = \int_{a(t)}^{a(n)} \frac{R(a)S}{a+m} \frac{dn}{da} da \\ &= \int_{a_0}^a \frac{R(a)da}{(a+m)[K(a+m)+R(a)]} \quad (\text{since } a(t) = a_0) \end{aligned}$$

a function of crack length only. The correction term in the solution is also obtainable by variation of parameters with the extra term $R(a)$ and the result can be iterated. The expected length is

$$\begin{aligned} \bar{a} &= \int_0^n a(n|t) f(t) dt \\ &= -mF_t(n) + (a_0 + m) \int_0^n e^{K(n-t) + I(a)} dF(t) \end{aligned}$$

from (22).

The derivative here is

$$\begin{aligned} \frac{d\bar{a}}{dn} &= a_0 f_t(n) + (a_0 + m) \int_0^n \left\{ K + \frac{R(a)}{a+m} \right\} e^{K(n-t) + I(a)} dF(t) \\ &= \int_0^n [K(a+m) + R(a)] dF(t) + a_0 f_t(n), \quad \text{from (22)}, \\ &= K\bar{a} + mKF_t(n) + \int_0^n R dF(t) + a_0 f_t(n) \\ &= K\bar{a} + mKF_t(n) + \int_0^\infty R(a) dF(a|n) + a_0 f_t(n), \quad \dots \quad (23) \end{aligned}$$

as one would expect. Each term here represents an important case and in the following it is convenient to combined them as above.

5.2 Several Cracks

For several cracks $\mathbf{a} = \{a_1 \dots a_N\}$ the rate above generalises to

$$\frac{d\mathbf{a}}{dn} = \mathbf{K}(\mathbf{a} + \mathbf{m}) + \mathbf{R}(\mathbf{a}) \quad \dots (24)$$

where \mathbf{K} is a constant square matrix while \mathbf{a} , \mathbf{m} , \mathbf{R} are column vectors. By definition each average length is

$$\begin{aligned} \bar{a}_i(n) &= \int_{t_j=0}^{\infty} \dots \int a_i(n|t) dF(t) \\ &= \int_0^{\infty} \dots \int_{t_i=0}^n \dots \int_0^{\infty} a_i(n|t) dF(t_1) \dots dF(t_N) \end{aligned}$$

since $a_i(n|t) = 0$ when $t_i > n$.

Differentiating,

$$\begin{aligned} \frac{d\bar{a}_i}{dn} &= \int_0^{\infty} \dots \int_0^n \dots \int_0^{\infty} \frac{da_i}{dn} dF(t) \\ &+ \int_0^{\infty} \dots \int_0^{\infty} a_i f_i(n) \prod_{j \neq i} dF(t_j), \quad (a_i(n|t_i=n) = a_i). \end{aligned}$$

The restricted range $0 < t_i < n$ allows for the fact that $a_i = 0$ and $da_i/dn = 0$ if $t_i > n$, i.e. if the crack has not begun at the time considered.

Using (24) carefully with $\mathbf{a} \equiv \mathbf{a}(n|t)$, $\mathbf{K} \equiv \{k_i\}$,

$$\begin{aligned}
\frac{d\bar{a}_i}{dn} &= \int_0^\infty \dots \int_0^n \dots \int_0^\infty \{ k_i(a+m) + R_i(a) \} dF(t) + a_0 f_i(n) \\
&= \int_0^\infty \dots \int_0^\infty \dots \int_0^\infty \{ k_i(a) + R_i(a) \} dF(a|n) + \\
&\quad + k_i m \int_0^\infty \dots \int_0^n \dots \int_0^\infty dF(t) + \\
&\quad + a_0 f_i(n) \\
&= k_i \bar{a} + k_i m F_i(n) + \int_0^\infty \dots \int_0^\infty \dots \int_0^\infty R_i(a) dF(a|n) + \\
&\quad + a_0 f_i(n).
\end{aligned}$$

For all cracks together this can be written ($\bar{a}(0) = 0$)

$$\frac{d\bar{a}}{dn} = K \bar{a} + [F_i(n)]K + \bar{R}(a|n) + a_0 [f_i(n)] e_N,$$

where the distributions and densities have been arranged as diagonal matrices. The general rate term arises from

$$\frac{d\bar{a}}{dn} = \int_0^\infty \dots \int_0^n \dots \int_0^\infty R(a) dF(t)$$

and since da_i/dn for example is zero if $n > t_i$ together with the length itself all the limits of integration may be extended to infinity so that the average rate includes unstarted cracks just as \bar{a} does.

If we put

$$y = T \bar{a}$$

where

$$K = T^{-1} [\lambda_i] T$$

then the homogeneous equation

$$\frac{dY}{dn} = KY, \quad Y(0) = I$$

has the solution⁶⁹

$$Y(n) = T^{-1} [e^{\lambda_i n}] T \stackrel{\text{def}}{=} \exp(nK) \quad \dots (26)$$

so that with the initial values $\bar{a}(0) = 0$ the solution is

$$Y \bar{a}(0) = 0.$$

For the particular solution let

$$\bar{a} = Yu \quad (\text{variation of parameters})$$

which leads to

$$u(n) = \int_0^n Y^{-1}(t) \{ [F_i(t)] Km + \bar{R}(a|t) + a_0 [f_i(t)] e_N \} dt \quad \dots (27)$$

Multiplying by $Y(n) (= e^{nK})$, from (26),

$$\bar{a}(n) = \int_0^n e^{(n-t)K} \{ \} dt = \int_0^n Y(n-t) \{ \} dt \quad \dots (27A)$$

In (27) the first term can be integrated by parts

$$\int_0^n e^{-tK} F_i dt = [-K^{-1} [F_i]]_0^n + K^{-1} \int_0^n e^{-tK} [f_i] dt$$

so that the linear part of (27) becomes

$$-K^{-1} [F_i(n)] Km + K \int_0^n e^{-tK} [f_i] dt Km + a_0 \int_0^n e^{-tK} [f_i] dt e_N$$

which can be iterated with (27A) in non-linear cases

(cf. equation (22)). The integrals in (27) have the form

of partial moment generating functions of $f(t)$ with the transformed variables Kt . Similar integrals occur later in the numerical solution.

5.3 Moment generating Function for Several Cracks

The transformed variables in the moment generating function are denoted by u so that at time n the MGF is

$$M(n, u) = \int_0^{\infty} \dots \int_0^{\infty} \exp\{u^t a(n|t)\} dF(t) \quad \dots \quad (28)$$

which includes concentrated probabilities of having no cracks.

The derivative of $M(n, u)$ divides naturally into

$$\frac{dM}{dn} = \int_0^{\infty} \dots \int_0^{\infty} \frac{d}{dn} e^{u^t a(n|t)} dF(t)$$

+ Terms associated with increase dn of each effective upper limit.

The latter are related to changes in the discontinuities of $\exp(u^t a)$ as a crack begins. Let the equations

$$u = \{u_i, u_i\}, \quad t = \{t_i, t_i\},$$

$$a = \{a_i, a_i\}$$

define the new notation here which, if convenient, may be associated with a renumbering of the elements. Now, most generally,

$$M = M(n_1, n_2, \dots, n_N; n)$$

where $n_1 = t_1$, ..., $n_N = t_N$ are the planes of discontinuity in the region of integration and n is still the parameter in the integrand.

Then

$$\frac{dM}{dn} = \frac{\partial M}{\partial n_1} \frac{dn_1}{dn} + \frac{\partial M}{\partial n_2} \frac{dn_2}{dn} + \dots + \frac{\partial M}{\partial n_N} \frac{dn_N}{dn} + \frac{\partial M}{\partial n}$$

and in our case $n_1 = n_2 = \dots = n_N = n$. We can now investigate $\partial M / \partial n_i$ and equation (28) is rewritten as

$$M(n, u) = \int_0^\infty \dots \int_0^n \dots \int_0^\infty \exp(u_i^t a_i + a_i a_i) dF(t_i) dF(t_i) \\ + \int_0^\infty \dots \int_n^\infty \dots \int_0^\infty \exp(u_i^t a_i) dF(t_i) dF(t_i)$$

and to the first order

$$M(n+dn, u) - M(n, u) =$$

$$f_i(n) dn \int \dots \dots \int \exp\{u_i^t a_i(n|t) e^{u_i a_i}\} dF(t_i) \\ - f_i(n) dn \int \dots \dots \int \exp\{u_i^t a_i(n|t)\} dF(t_i)$$

since $a_i = 0$ if $t_i > n$.

A comparison of integrals here with (28) shows that they are MGFs of a reduced system obtained by the suppression of the crack a_i . There are N such fatigue problems, one for each crack, which are denoted by $M_i(n, u_i)$. With this notation we have shown that

$$\frac{\partial M}{\partial n_i} = (e^{u_i a_i} - 1) f_i(n) M_i(n, u_i) \dots \dots (29)$$

Because the crack has been suppressed $M_i(n, u_i)$ cannot depend on t_i and the result does not depend on the independence of the t_j 's.

Finally

$$\begin{aligned}
 \frac{dM}{dn} &= \sum_{i=1}^N (e^{u_i a_0} - 1) f_i(n) M_i(n, u_i) + \\
 &+ \int_0^{\infty} \dots \int_0^{\infty} \frac{d}{dn} \exp(u^t a(n, t)) dF(t) \\
 &= \sum_{i=1}^N (e^{u_i a_0} - 1) f_i(n) M_i(n, u_i) \\
 &+ \int_0^{\infty} \dots \int_0^{\infty} \left(u_1 \frac{da_1}{dn} + \dots + u_N \frac{da_N}{dn} \right) \exp(u^t a) dF(t_1) \dots dF(t_N).
 \end{aligned}
 \tag{30}$$

Now if $t_i > n$ then as before $da_i/dn=0$ so that a typical component of the integral is

$$\begin{aligned}
 &\int_0^{\infty} \dots \int_0^{n_i} \dots \int_0^{\infty} u_i \frac{da_i}{dn} \cdot \exp(u^t a) dF(t_1) \dots dF(t_i) \dots dF(t_N) \\
 &= \int_0^{\infty} \dots \int_0^{n_i} \dots \int_0^{\infty} u_i \{ k_i(a+m) + R_i(a) \} \cdot e^{u^t a} dF(t) \dots \tag{31} \\
 &= \int_0^{\infty} \dots \int_0^{n_i} \dots \int_0^{\infty} u_i (k_i(a+m)) e^{u^t a} dF(t) + \\
 &\int_0^{\infty} \dots \int_0^{n_i} \dots \int_0^{\infty} u_i R_i(a) \cdot e^{u^t a} dF(a|n)
 \end{aligned}$$

again using the equivalence of probabilities in the spaces of t or $a(n)$.

The limits corresponding to $k_i a$ can be made infinite and if the matrix product is expanded and integrated then the result can be again abbreviated to the form

$$u_i k_i \partial M / \partial u^t \text{ say.}$$

The second term, in $k_i m$, decomposes into two integrals

$$\int_0^\infty \dots \int_0^\infty \int_0^\infty - \int_0^\infty \dots \int_{n_i}^\infty \int_0^\infty k_i m e^{u^t a} dF(t)$$

with the total value

$$M - (a - F_i(n)) \cdot M_i(n, u_i).$$

Finally the mean value theorem is used to simplify the general rate term by removing the factor

$$\bar{R}_i(a) / F_i(n).$$

This leaves the same integral as the second term. When these quantities are substituted into (30)

$$\begin{aligned} \frac{dM}{dn} &= \sum_{i=1}^N (e^{u_i a} - 1) f_i(n) M_i(n, u_i) + \sum_{i=1}^N u_i k_i \frac{\partial M}{\partial u^t} \\ &+ \sum_{i=1}^N u_i \left(k_i m + \frac{\bar{R}_i(a|n)}{F_i(n)} \right) \{ M - (1 - F_i(n)) M_i(n, u_i) \} \\ &\dots (32) \end{aligned}$$

From this equation it should be possible to derive (25) which supplies the mean rates. For this reason the notations for the average general rate terms are the same. To justify ourselves (25) will be derived from (32).

Thus

$$\begin{aligned} \frac{d}{du_i} \left(\frac{dM}{dn} \right) &= a_0 e^{u_i a} f_i(n) M_i + \sum_u^N u_j k_j \frac{\partial^2 M}{\partial u_i \partial u^t} + k_i \frac{\partial M}{\partial u^t} \\ &+ [k_i m + \bar{R}_i(a|n) / F_i(n)] \{ M - (1 - F_i(n)) \cdot M_i(n, u_i) \} + \dots \end{aligned}$$

and if $u = 0$ for $i = 1, \dots, N$ the results can be grouped as in (25). Therefore in (25) the term $\bar{R}(\mathbf{a} | n)$ must be the same as $\{\bar{R}_i(\mathbf{a} | n)\}$ in (32).

If we put

$$M = e^{\Psi} \quad \text{and} \quad M_i(n, u_i) = e^{\Psi_i} \quad \dots (33)$$

then if (32) is divided by M

$$\begin{aligned} \frac{d\Psi}{dn} &= \sum_{i=1}^N (e^{u_i a_i} - 1) f_i(n) \cdot e^{\Psi_i - \Psi} + \sum_{i=1}^N u_i k_i \frac{\partial \Psi}{\partial u_i} \\ &+ \sum_{i=1}^N u_i (k_i m + \bar{R}_i(\mathbf{a} | n) / F_i(n)) \cdot (1 - (1 - F_i(n))) \cdot e^{\Psi_i - \Psi}, \end{aligned} \quad \dots (34)$$

a differential equation for the growth of the cumulant generating function. As above, this depends on the CGF's of the reduced problems which depend in turn on still simpler problems. For a complete solution one thus requires 2^N CGF's, beginning with those for one crack only.

6.0 Complete Equations

On expanding the equations (32) or (34) it will be found that the higher moments or cumulants are determined recursively by first order differential equations which involve also the reduced systems from $M_i(n, u_i)$, $i = 1, \dots, N$. The average cracks for the $N+1$ systems, through the moments which must all exist as solutions of the extra differential equations, determine $f(\mathbf{a} | n)$.

In (25) one can now substitute for $f_i(n)$ and $F_i(n)$ from the damage equations (3). Because these now depend

on a random crack length the right hand side of (3) needs to be averaged over $f(a | n)$. After these changes have been made the crack growth and damage equations become

$$\begin{aligned} \frac{d\bar{a}}{dn} &= K\bar{a} + [F_i(n)]K_m + \bar{R}(a | n) \\ &+ a_0 \int_0^\infty \dots \int_0^\infty A(F, a) dF(a | n) \\ \frac{dF}{dn} &= \int_0^\infty \dots \int_0^\infty A(F, a) dF(a | n), \quad \dots \quad (35) \end{aligned}$$

corresponding to (5) and (5A) and the $F_i(n)$ are of course components of F . As in (25) the general rate term is

$$\bar{R}(a | n) = \int_0^\infty \dots \int_0^\infty R(a) dF(a | n) \quad \dots \quad (35A)$$

and in all these equations the length distribution $f(a | n)$ depends on the solution through (32) or (34) as described above. Even the linear rate case here is quite formidable and since this is not the practical situation and we later concern ourselves with matrix force methods we have elected to treat (35) as a system of differential equations, using predictor-corrector methods.

This requires a simultaneous knowledge of $f(a | n)$ so that the moment equations must be integrated at the same time. Although all moments (or an inversion integral) are required to find the distribution, if a suitable approximation is used only a few need to be calculated. With a computer a complete solution would be feasible if the rate function were sufficiently simple. For the general structure unfortunately $R(a)$ is the outcome of some type of structural analysis and, although one is prepared to repeat it for the iterations required by a predictor-corrector method, the large number of points in the expect-

ation integrals almost preclude the computation from present day computers. However it is possible to "remember" the results of prior structural analyses and use these instead. This will be discussed further in the chapter on numerical solutions.

6.1 General and Multiparametric Damage

The canonical damage in (35) may be replaced by any equivalent Bastenaire damage D and indeed there is no reason why this cannot be multidimensional, in which case A, D would be matrices with say rN elements. It is always true that there are physically independent damage vectors however and it follows that the proof that initial lives are statistically independent still holds. For the complete set of cracks the basic equations (35) generalise to

$$\begin{aligned} \frac{da}{dn} &= Ka + F_i(n)Km + \bar{R}(a|n) \\ &\quad + a_0 \int_0^\infty \dots \int_0^\infty A(F, a) dF(a|n) \\ F &= F(D) \\ \frac{dD}{dn} &= \int_0^\infty \dots \int_0^\infty A(D, a) dF(a|n), \quad \dots \quad (36) \end{aligned}$$

where the central equation is merely auxiliary. If the Monte-Carlo method is used (5) and (5A) may be similarly generalised.

In (35) or (36) each component of damage is meaningful only if the crack in question has not started. Each element of D (or A) thus has the more particular form

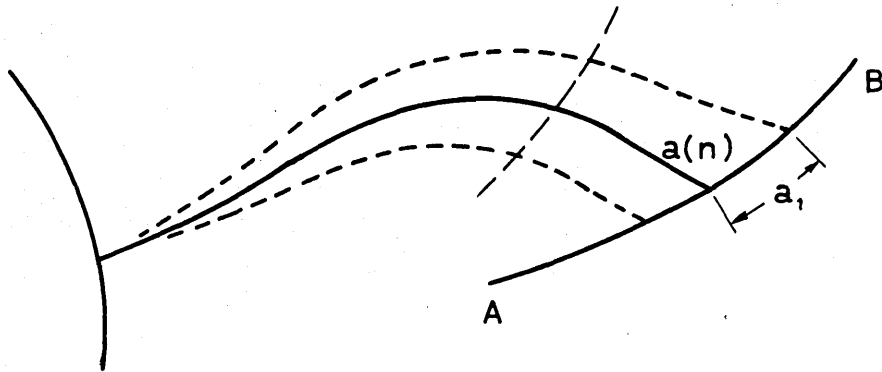
$$D_i = A(D_i, K_{T_i}, a) \quad \dots \quad (37)$$

where K_{T_i} is the stress concentration factor.

6.2 Nature of Cracks

So far all cracks have been described exclusively by their lengths but in general the crack path is also unknown and equally erratic. On the whole the average direction is that of the lesser principal stress (in sheet structures) and this may be found as part of the stress analysis.

From Chapter III it is most natural that (5), (5A), (35) or (36) should always be framed in terms of total lengths. If the average crack follows the principal stress then $R(a)$ relates to cracks in fixed positions and the crack damage equations still have meaning.



To generalise further consider the crack in the sketch. Let AOB be the locus of tip positions if $a = a(n)$. Then the standard deviation of the tip wandering a_1 can be regarded as another crack length. This need not be included in (36) however as it probably has the simple form

$$\frac{da_1}{dn} = g(x, y, \psi) \frac{da}{dn} \quad \dots (38)$$

where (x, y, ψ) are the tip position and orientation. In (36) then a_1 etc. as a function of a need not be speci-

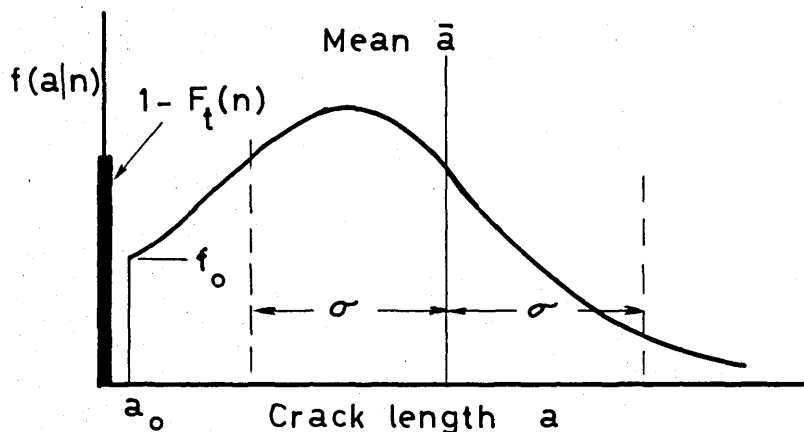
fically included and if the averaging also includes the distribution of a_1 then the result is suitably generalised. The density $f(a_1)$ is severely restricted with just one parameter (a normal distribution seems the obvious choice) and if desired other artificial crack lengths may be introduced but the practical improvement effected thereby is likely to be negligible.

In a similar fashion the primary notion of crack length can be extended to any geometric magnitude. For example an elliptical crack in a solid member can be characterised by its semi-axes and possibly the orientation. In aircraft structures it may often be possible to treat the failure of a succession of rivets as the continuous progress of a single crack, which cannot wander. If this is done a_0 and possibly other parts of (36) may require alteration but there is no essential difference.

There is also a need (in the theory) for crack propagation of a more general nature. In a practical structure for example the main failure may be just one or two cracks in essence but these will branch, sometimes stop at rivet holes or be delayed while subsidiary cracks grow in booms or stringers. Some of these small scale problems may possibly be idealised and analysed as simple fatigue problems and the results incorporated in more general crack growth laws. The most marked changes with such generalisations are likely to occur in the higher cumulants (Section 7.0).

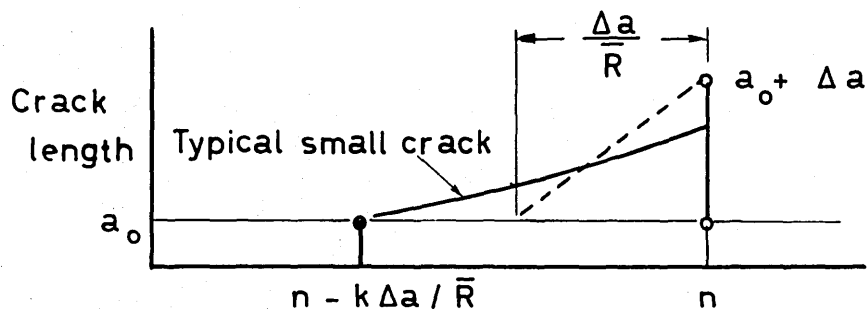
6.3 Initial Densities of Crack Lengths

At n cycles there is a finite probability $1-F_t(n)$ say that a crack has not started. The density must therefore have the general form shown with a concentrated probability at the origin.



The form of $f(a|n)$ must be known in order to solve (35) or (36) and we try to approximate it numerically using the mean and variance. For any realism however the initial density must also be included and for this reason it is considered here. To the first order if Δa is a small increment of growth

$$f_0 \Delta a = \Pr(a_0 < a < a_0 + \Delta a).$$



As shown, cracks in this neighbourhood can arise at any time between 0 and n cycles. Let a typical time be described by

$$n - k\Delta a/\bar{R}$$

where

$$\begin{aligned} \bar{R} &= \text{Average rate of initial propagation} \\ &= \int_0^{\infty} \dots \int_0^{\infty} R(a) dF(a_i | n, a_i = a_0) \quad \dots \quad (39) \end{aligned}$$

which is most closely related to the reduced problem.

In practice the small crack length a_0 has little effect on the reduced problems and in these it is convenient to give the suppressed cracks a length of a_0 and thus make \bar{R} more easily obtainable. If $a(n-t)$ represents the crack growth from t cycles and we substitute for t from above

$$f_0 \Delta a = \int_0^n f(t) \Pr(a(n-t) < a_0 + \Delta a) dt \dots (40)$$

Now $a(n-t)$ is a function of the starting time t and the propagation time $n-t$ and if both of these are written in terms of

$$k' = k \Delta a / \bar{R}$$

then the crack length can be expanded as a two-dimensional Maclaurin series. In this way we find

$$a(n-t) = a_0 + R_0 k' - O(k')^2$$

where R_0 is random. Similarly

$$f(t) = f(n) - (n-t)f'(n) + O(n-t)^2$$

and

$$f(a|t) = f(a|n) - k' \frac{\partial f}{\partial n} + O(k')^2$$

so that

$$\begin{aligned} \Pr\{R_0 k' - O(k')^2 < \Delta a\} &= \Pr(a(n-t) < a_0 + \Delta a) \\ &= \Pr\left\{R_0 < \frac{\bar{R}}{k}(1 + O(\Delta a))\right\} \\ &= \int_0^{\bar{R}/k} dF(R_0) = \int_0^{\bar{R}/k(1+O(\Delta a))} \frac{dF(R_0)}{\bar{R}/k} \end{aligned}$$

Because $dF(R_0)$ is a density the second integral is bounded and approaches zero with k . Thus for all values of

k the probability above is

$$\int_0^{\bar{R}/k} dF(R_0) + O(\Delta a)$$

and hence from (40), after some reduction,

$$\begin{aligned} f_0 \Delta a &= \int_0^n \{f(n) - [f(n) - f(t)]\} \left\{ \int_0^{\bar{R}/k} dF(R_0) + O(\Delta a) \right\} dt \\ &= \frac{\Delta a}{\bar{R}} \int_0^U \{f(n) - [f(n) - f(t)]\} \left\{ \int_0^{\bar{R}/k} dF(R_0) + O(\Delta a) \right\} dk \end{aligned}$$

where $U = n\bar{R}/\Delta a$. In the limit as $\Delta a \rightarrow 0$

$$f_0 = \frac{f(n)}{\bar{R}} \int_0^\infty \int_0^{\bar{R}/k} dF(R_0) dk \quad \dots \quad (41)$$

provided

$$\int_0^\infty [f(n) - f(t)] \int_0^{\bar{R}/k} dF(R_0) dk$$

vanishes. In terms of k this is

$$I = \int_0^{U(\varepsilon)} [f(0) - f\left(\frac{k\Delta a}{\bar{R}}\right)] \int_0^{\bar{R}/k} dF(R_0) dk + \varepsilon$$

and if $f(n)$ is bounded the integral converges with (41) uniformly in Δa . Thus

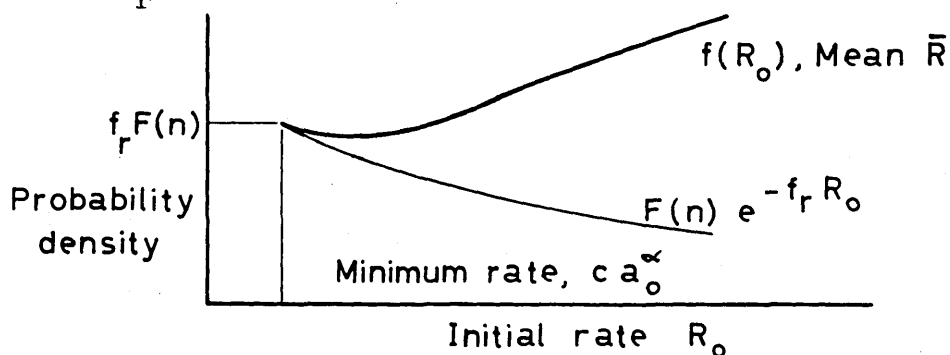
$$I = \int_0^{U(\varepsilon)} [f(0) - f(k\Delta a/\bar{R})] \int_0^{\bar{R}/k} dF(R_0) dk + \varepsilon$$

where $U(\varepsilon)$ does not depend on Δa . It then follows that

$$I \rightarrow 0 \quad \text{as} \quad \Delta a \rightarrow 0,$$

so that (41) is true if the integral there exists and if $f(t)$ is bounded in the closed interval $(0, n)$.

Returning to (41) it will be seen that its convergence depends critically on the behaviour of $f(R_0)$ near the origin. If the local stress (in the absence of a crack) is approximately linearly dependent on the other crack lengths and these have distributions similar to that shown above the local stress intensity should also have this distribution and be proportional to Δa_0 . Accordingly R_0 would also have a similar distribution with a finite density $f_r F(n)$ near the origin.



Let us now anticipate the next chapter and write the rate distribution as

$$F(R_0) = 1 + F(n)e^{-f_r R_0} (T(R_0) - 1)$$

where $T(R_0)$ is also a distribution function with tangential contact near the origin.

Substituting in (41), with ca_0^α as the minimum growth rate,

$$\begin{aligned} f_0 &= \frac{f(n)F(n)}{\bar{R}} \int_0^{\bar{R}/ca_0^\alpha} \left\{ e^{-f_r \bar{R}/k + f_r ca_0^\alpha} [T(\bar{R}/k - ca_0^\alpha) - 1] + 1 \right\} dk \\ &= \frac{f(n)F(n)}{\bar{R}} \left\{ \frac{\bar{R}}{ca_0^\alpha} - \int_0^{\bar{R}/ca_0^\alpha} e^{-f_r \bar{R}/k} dk + \int_0^{\bar{R}/ca_0^\alpha} e^{-f_r \bar{R}/k} T(\bar{R}/k) dk \right\} \end{aligned}$$

if $f_r ca_0^\alpha$ is small. By a change of variable and partial integration the first integral takes the form

$$-I(f_r ca_o^\alpha) = -\frac{\bar{R}}{ca_o^\alpha} e^{-f_r ca_o^\alpha} + \bar{R}f_r \cdot Ei(f_r ca_o^\alpha)$$

whose absolute value must exceed the other integral since $T(R_o) < 1$. Therefore an upper bound for f_o is

$$f_o \text{ max} = f(n)F(n)/ca_o^\alpha \quad \dots (42)$$

The second integral must also exceed

$$T(ca_o^\alpha) \frac{\bar{R}}{ca_o^\alpha} e^{-f_r ca_o^\alpha} - \bar{R}f_r Ei(f_r ca_o^\alpha)$$

but the factor in practice would be extremely small. For a more usable estimate $T(u)$ ($U=\bar{R}/k$) will be taken as the distribution relating to a triangular density, the answer being referred to its mean and variance. In terms of u the second integral is

$$\bar{R} \int_{ca_o^\alpha}^{\infty} e^{-f_r u} T(u) du / u^2$$

and we assume that the integrand is zero at ca_o^α . The integrations resemble those above and if the range of $T(u)$ is (a, b) then we can arrange the intermediate results in the form

$$\begin{aligned} \frac{\bar{R}}{(b-a)^2} & \left\| \left\| 8(f_r^{-1} + u) e^{-f_r u} \cdot \cosh^2(\frac{1}{2}f_r(b-u)) - 4(b-u) e^{-f_r u} \right. \right. \\ & \left. \left. \cdot \sinh(f_r(b-u)) + 2a(2-a/b) e^{-f_r b} + 4(b-a+u^2 f_r) Ei(f_r u) \right. \right. \\ & \left. \left. - 4(2+f_r a)[a Ei(f_r a) + b Ei(f_r b)] - 2u(b-a)f_r Ei(f_r b) \right\| \right\| \\ & \dots (43) \end{aligned}$$

Now the mean $\mu = (a+b)/2$ and the variance is

$$\sigma^2 = (b-a)^2/6 \quad \dots (43A)$$

This is not very good for computation and the simplest alternative is the upper bound (42) which is unconservative since it favours short cracks. However the form of f_o and of $f_o \max$ does suggest that the form of $F(R_o)$ is relatively unimportant except for the minimum growth rate which seems to be a function of local stress and the material.

7.0 Variance and Covariance

As well as having intrinsic interest these are important in the numerical method to be suggested in the next chapter. Their derivation is straightforward and illustrates the general procedure for all higher cumulants or moments.

For reference purposes we show a table of the general first and second derivatives of (34) with respect to the u_i 's. When these are made zero we obtain the differential equations

$$\begin{aligned} \frac{d}{dn} \sigma_{jj} &= a_o^2 f_j(n) - 2a_o f_j(n) a_j + 2 k_j \sigma_{.j} \\ &+ 2 [k_j m + \bar{R}_j(a|n)/F_j(n)] \cdot (1 - F_j(n)) a_j \end{aligned}$$

and

$$\begin{aligned} \frac{d}{dn} \sigma_{jk} &= a_o f_j(n) (a_{k|j} - a_k) + (a_o f_k(n) (a_{j|k} - a_j) \\ &+ k_j \sigma_{.k} + k_k \sigma_{.j} \\ &+ [k_j m + R_j(a|n)/F_j(n)] \cdot (1 - F_j(n)) (a_k - a_{k|j}) \\ &+ [k_k m + R_k(a|n)/F_k(n)] \cdot (1 - F_k(n)) (a_j - a_{j|k}) \end{aligned}$$

... (44)

where

$a_j|_k$ = Length of crack j (average) when crack k is suppressed,

$\sigma_{.j}$ = j -th column of covariance matrix Σ ,

and as before k_j is the j -th row of K .

If the small term in a_0^2 is ignored and we define $a_i|i = 0$ these two formulae can be combined. One can now obtain a single equation for the covariance matrix. In the first place we take j and k as row and column indices. We then rearrange (44) so that matrices with subscript j always appear first. After this the equation for a column and then for all of Σ becomes apparent. We obtain

$$\begin{aligned} \frac{d\Sigma}{dn} = & -a_0 f_i(n) A_c^t \quad -a_0 A_c f_i(n) + K \Sigma + \Sigma K^t \\ & + (I - [F_j(n)]) [K m + [F_j^{-1}(n)] \bar{R}(a|n)] A_c^t \\ & + A_c [m^t K^t + \bar{R}(a|n) [F_j^{-1}(n)]] (I - [F_j(n)]) \end{aligned} \quad \dots \quad (45)$$

where A_c is a square matrix with elements $(a_j - a_j|_k)$, i.e. each column is the solution of a subsidiary system.

For the general rate (44) and (45) both indicate a simple quadrature and the purely linear case is best solved in this way. Indirectly we can thus investigate the equation

$$\frac{da}{dn} = K a + \Sigma K^t$$

in terms of a where

$$\frac{da}{dn} = K a.$$

TABLE II.

DERIVATIVES OF CUMULANT GENERATING FUNCTION

$$\frac{d\Psi}{dn} = \sum_{i=1}^N (e^{u_i a_o} - 1) f_i(n) e^{\Psi_i - \Psi} + \sum_{i=1}^N u_i k_i \frac{\partial \Psi}{\partial u^t} + \sum_{i=1}^N u_i (k_i m + \bar{R}_i(a|n) / F_i(n)) \cdot [1 - (1 - F_i(n)) e^{\Psi_i - \Psi}]$$

$$\begin{aligned} \frac{\partial}{\partial u_j} \frac{d\Psi}{dn} &= a_o e^{u_j a_o} f_j(n) e^{\Psi_j - \Psi} + \sum_{i=1}^N (e^{u_i a_o} - 1) f_i(n) \left\{ \frac{\partial \Psi_i}{\partial u_j} - \frac{\partial \Psi}{\partial u_j} \right\} e^{\Psi_i - \Psi} + \sum_{i=1}^N u_i k_i \frac{\partial^2 \Psi}{\partial u_j \partial u^t} + k_j \frac{\partial \Psi}{\partial u^t} + \\ &+ \left\{ k_j m + \bar{R}_j(a|n) / F_j(n) \right\} \cdot \left\{ 1 - (1 - F_j(n)) e^{\Psi_j - \Psi} \right\} \\ &- \sum_{i=1}^N u_i \left\{ k_i m + \bar{R}_i(a|n) / F_i(n) \right\} \cdot (1 - F_i(n)) \left\{ \frac{\partial \Psi_i}{\partial u_j} - \frac{\partial \Psi}{\partial u_j} \right\} e^{\Psi_i - \Psi} \end{aligned}$$

TABLE II. (Continued)

$$\begin{aligned}
 \frac{\partial^2}{\partial u_j^2} \frac{d\Psi}{dn} = & e^{u_j a_0} f_j(n) e^{\Psi_j - \Psi} \left[a_0^2 + 2a_0 \left\{ \frac{\partial \Psi_j}{\partial u_j} - \frac{\partial \Psi}{\partial u_j} \right\} \right] \\
 & + \sum_{i=1}^N (e^{u_i a_0} - 1) f_i(n) e^{\Psi_i - \Psi} \left[\frac{\partial^2 \Psi_i}{\partial u_j^2} - \frac{\partial^2 \Psi}{\partial u_j^2} + \left\{ \frac{\partial \Psi_i}{\partial u_j} - \frac{\partial \Psi}{\partial u_j} \right\}^2 \right] + 2k_j \frac{\partial^2 \Psi}{\partial u_j \partial u^t} + \\
 & + \sum_{i=1}^N u_i k_i \frac{\partial^3 \Psi}{\partial^2 u_j \partial u^t} - 2[k_{j, m+\bar{R}_j}(\mathbf{a}|n)/F_j(n)](1-F_j(n)) e^{\Psi_j - \Psi} \left\{ \frac{\partial \Psi_j}{\partial u_j} - \frac{\partial \Psi}{\partial u_j} \right\} \\
 & - \sum_{i=1}^N u_i [k_{i, m+\bar{R}_i}(\mathbf{a}|n)/F_i(n)](1-F_i(n)) e^{\Psi_j - \Psi} \left[\frac{\partial^2 \Psi_i}{\partial u_j^2} - \frac{\partial^2 \Psi}{\partial u_j^2} + \left\{ \frac{\partial \Psi_i}{\partial u_j} - \frac{\partial \Psi}{\partial u_j} \right\}^2 \right]
 \end{aligned}$$

TABLE II (Continued)

$$\begin{aligned}
 \frac{\partial^2}{\partial u_j \partial u_k} \frac{d\Psi}{dn} &= a_o e^{u_j a_o} f_j(n) e^{\Psi_j - \Psi} \left\{ \frac{\partial \Psi_j}{\partial u_k} - \frac{\partial \Psi}{\partial u_k} \right\} + a_o e^{u_k a_o} f_k(n) e^{\Psi_k - \Psi} \left\{ \frac{\partial \Psi_k}{\partial u_j} - \frac{\partial \Psi}{\partial u_j} \right\} \\
 &+ \sum_{i=1}^N (e^{u_i a_o} - 1) f_i(n) e^{\Psi_i - \Psi} \left[\frac{\partial^2 \Psi_i}{\partial u_j \partial u_k} - \frac{\partial^2 \Psi}{\partial u_j \partial u_k} + \left\{ \frac{\partial \Psi_i}{\partial u_j} - \frac{\partial \Psi}{\partial u_j} \right\} \cdot \left\{ \frac{\partial \Psi_i}{\partial u_k} - \frac{\partial \Psi}{\partial u_k} \right\} \right] \\
 &+ k_k \frac{\partial^2 \Psi}{\partial u_j \partial u^t} + k_j \frac{\partial^2 \Psi}{\partial u_k \partial u^t} + \sum_{i=1}^N u_i k_i \frac{\partial^3 \Psi}{\partial u_j \partial u_k \partial u^t} \\
 &- [k_j m + \bar{R}_j(\mathbf{a}|n)/F_j(n)] (1 - F_j(n)) e^{\Psi_j - \Psi} - [k_k m + \bar{R}_k(\mathbf{a}|n)/F_k(n)] (1 - F_k(n)) e^{\Psi_k - \Psi} \\
 &- \sum_{i=1}^N u_i [k_i m + \bar{R}_i(\mathbf{a}|n)/F_i(n)] (1 - F_i(n)) e^{\Psi_i - \Psi} \\
 &\times \left[\frac{\partial^2 \Psi_i}{\partial u_j \partial u_k} - \frac{\partial^2 \Psi}{\partial u_j \partial u_k} + \left\{ \frac{\partial \Psi_i}{\partial u_j} - \frac{\partial \Psi}{\partial u_j} \right\} \cdot \left\{ \frac{\partial \Psi_i}{\partial u_k} - \frac{\partial \Psi}{\partial u_k} \right\} \right]
 \end{aligned}$$

The generalised cracks suggested in Section 6.2 would generally lead to extra terms in (44) or (45) which would depend on crack position and orientation like $g(x,y,\psi)$ in (38). There are likely to be similar additions for every cumulant.

8.0 Estimation of Initial Failures and Initial Crack Lengths

In this thesis the basic data are assumed to be all the S-N data relating to initial failure, the initial crack length a_0 and finally a minimum rate ca_0^α , dependent on stress distribution and material.

In practice S-N data refers to the complete failure of simple specimens and the measured lives comprise a nucleation or damage time and a time of crack growth. However the effect of stress concentrations should allow a quantitative estimate of initial failure data and the initial crack length.

Consider plain and notched sheet specimens and for simplicity let us make the conflicting assumptions that their maximum widths are the same and also, that the average distances travelled by a crack until failure at a given nominal stress S are equal.

Let the true S-N data be approximated as

$$f(N) = n(\mu(S), \sigma^2(S))$$

where

$$N = \log n$$

and $n(\)$ is the normal density function. If the notch radius is of larger order than the grain diameter then for true S-N data

$$K_f = K_T,$$

these being practical and theoretical stress concentration factors. For final failure

$$K_f < K_T$$

and we hypothesise that this alleviation arises because notched and plain specimens have the same residual life once a crack has started. Suppose the average crack propagation period is a definite function $n_c(S)$ of the nominal stress. Allowing for the logarithmic variance, the mean life is then roughly

$$e^{\frac{1}{2}\sigma^2(K_T S)} \bar{n}_{1c} = e^{\mu(K_T S)} + n_c(S)$$

for a notched specimen compared with

$$e^{\frac{1}{2}\sigma^2(S)} \bar{n} = e^{\mu(S)} + n_c(S)$$

for plain specimens and the variances can be estimated from the test results. The left hand sides are therefore known, iteratively at least, and we can find the difference between the two lives. For several levels of nominal stress it is then possible to build up an estimate of $\mu(S)$, using these life differences and the assumption that it is a smooth monotonically decreasing function of S . At the same time this will provide an estimate of $n_c(S)$ but both $n_c(S)$ and $\exp(\mu(S))$ thus estimated will be unknown to the extent of a constant. This constant can be bounded however by the knowledge that both these functions are essentially positive for all stresses.

Once a first estimate of $n_{1c}(S)$, $\mu_1(S)$ has been made the logarithmic variances $\sigma^2(S)$ can be recalculated with respect to the mean $\mu_1(S)$ and the process then

repeated. In designing a test series the requirements of fairly constant stress at the notch root, small numbers of specimens above yield and small stress increments all indicate moderate or low values of K_T . A compromise is necessary however because $K_T - K_f$ is small for low K_T values. It is also convenient if the stresses are in geometric progression with a ratio $(K_T)^{1/m}$ where m is an integer. In this way the same damaging stress $K_T S$ can be reached either by a notch effect $K_T(S)$ or in a plain specimen at a higher stress $1.(K_T S)$. Ford and Lewis⁷⁰ have also suggested that this is convenient for fitting curves to $\mu(S)$. Further improvements should also follow by using two or more K_T values.

This is a general description of the analysis needed to estimate $\mu(S)$, $\sigma^2(S)$ and $n_c(S)$. Assuming we have $n_c(S)$ let us now consider a_0 and the minimum rate ca_0^α . If measurements of crack growth are made then these quantities are relatively straightforward, providing the tester has the patience to wait for cracks at the lower stress levels. If this is not done it is usually possible to estimate crack lengths at final failure and if growth rates can be integrated from known data or from Paris' law, as in Chapter III, then a_0 can be estimated from $n_c(S)$. If it is assumed independent of stress such calculations should also provide information about the minimum rate (strictly speaking for constant stress only). For more realism S here can represent the scale parameter of a random process, as done by Kirkby.¹⁴

Chapter V

NUMERICAL SOLUTION

From the nature of the data alone it is plain that most practical solutions of (4.35) will be numerical. In essence these equations, with the reduced problems, constitute $2N(N+1)$ first order differential equations, becoming $(r+1)(N+1)N$ for the r -dimensional damage of (4.36). Calculation of the right hand sides involves simultaneous quadrature of sufficient moments of \mathbf{a} , the construction of $f(\mathbf{a} | n)$ therefrom and then its use in the expectation integrals. The random variables here involve the stress analysis of the structure (for random loads) and when one considers the number of point evaluations needed for a multidimensional expectation it can be seen that efficient stressing and economy of analysis are essential.

For this reason and the possibility of error checks the author favours predictor-corrector methods for the actual integration of the equations together with a finite difference starting method.⁷¹ There are several well known methods and this aspect is not discussed any further.

For the stress analysis it is best to use procedures which can incorporate simple modification techniques to modify the results of an overall primary stressing. The matrix force and displacement methods are of this type and there is a possibility that the two-dimensional complex variable methods also allow such an extension. In the later chapters we will investigate the use of a force method for reinforced flat sheet structures which are roughly rectangular. With the present progress of stress intensity results it is also possible that the theory will become applicable to thin-walled

beams and tubes.

Among the predictions in the integration of the differential equations will be included the form of the crack length density, expressed in the form of suitable parameters. However in the expectation integrals simple functional forms will be fitted to the damage and crack rates found by previous integration steps. For the present it seems that the expectations must ignore correlations between different cracks until suitable multivariate densities are developed.

In the following sections we first describe an empirical form of $f(a_i | n)$ and the fitting of appropriate parameters. Its use in the expectations will then be described using Gauss-Laguerre integration rules. Finally the fitting of functions to the known damage and crack rates is discussed.

1.0 A Class of Empirical Distributions

In this section we describe a way of approximating the crack length distributions $F(a_i | n)$. It is based on the decomposition shown in the figure or by equation (1). Briefly the truncated exponential distribution AB is chosen to satisfy the probability conditions at the origin and then the transition curve D is drawn in such a way that the final distribution AC has the required moments. The transition is obtained as shown by adding a term based on some standard distribution function $T(x)$ (x is the random variable here while a is a constant) preferably with tangential contact at the origin

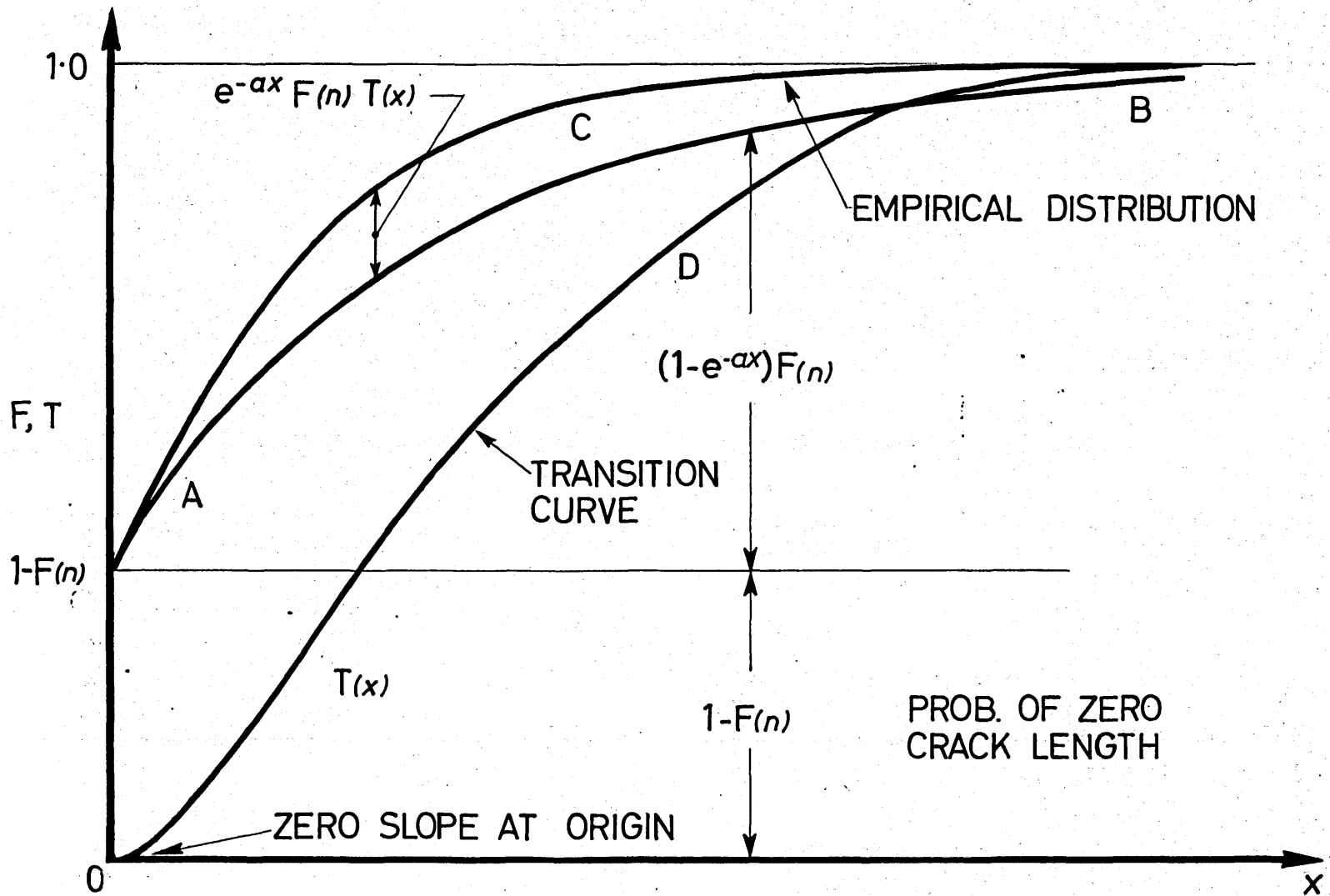


FIG. 19 EMPIRICAL FORM OF CRACK LENGTH DISTRIBUTION

Algebraically*

$$\begin{aligned} F(x) &= 1 - F(n) + F(n)(1 - e^{-ax}) + F(n) T(x)e^{-ax} \quad (1) \\ &= 1 + F(n)e^{-ax} (T(x) - 1) \end{aligned}$$

where

$$T(0), T'(0) = 0, \quad T(\infty) = 1 \text{ and for future reference}$$

$$f(x) = e^{-ax} F(n) T'(x) + a(1 - T(x)). \quad \dots \quad (1A)$$

The initial value of this density is the quantity f_0 discussed in Section 6.3 of the previous chapter. It is also convenient to define here

$$M_T = \int_0^{\infty} e^{xt} dT(x)$$

the MGF of the distribution function $T(x)$. Depending on the context this will be written as the function of a number of different arguments.

Now consider the MGF of $f(x)$

$$\begin{aligned} M(t) &= \int_0^{\infty} e^{tx} f(x) dx \\ &= \int_0^{\infty} e^{tx} d(F(x) - 1) \end{aligned}$$

since zero length cannot contribute to any moments. Integrating by parts this becomes

* Strictly speaking, the crack length belongs to the set $\{0; (a_0, \infty)\}$ but since a_0 is small with little physical effect elsewhere in the structure it is convenient to use the range $(0, \infty)$ and assign the initial density to lengths nearly zero.

$$\begin{aligned}
M(t) &= F(n) - F(n)t \int_0^{\infty} e^{(t-a)x} (T(x)-1) dx \\
&= \frac{aF(n)}{a-t} - \frac{tF(n)}{a-t} \int_0^{\infty} e^{(t-a)x} dT(x) \\
&= \frac{F(n)}{a-t} \{a - t M_T(t-a)\} \quad \dots (2)
\end{aligned}$$

Expanding this about $t=0$,

$$\mu = \frac{F(n)}{a} \{1 - M_T(-a)\} \quad \dots (3)$$

and

$$\mu_2 = \frac{2F(n)}{a^2} \{1 - M_T(-a) - aM_T'(-a)\}$$

whence

$$\sigma^2 = \frac{F(n)}{a^2} \{1 - M_T^2(-a) - 2aM_T'(-a) + (1 - F(n))(1 - M_T(-a))^2\}$$

If we now postulate a two parameter form for $T(x)$ these equations determine them. Here there are two possible approaches. In the first a specific form of $M_T(t)$ is known and (3) is duly solved. Otherwise $M_T(t)$ may be expanded in terms of its moments. This offers possibilities for an iterative solution so that even when the first method is available the second may be preferable.

In (2) or (3) a^{-1} is a scale parameter (as the mean of the exponential density $\exp(-ax)/a$) and to ensure a sort of similarity it will also be used as a scale parameter in $T(x)$. The β -distribution over $(0, \infty)$ will be chosen as a reasonable transition function, with the density

$$\frac{d\Gamma}{dx} = \frac{\Gamma(m+n)}{\Gamma(m)\Gamma(n)} \frac{a^m x^{m-1}}{(1+ax)^{m+n}} \quad \dots (4)$$

and the moments

$$\mu_r = a^{-r} \frac{m(m+1) \dots (m+r-1)}{(n-1) \dots (n-r)} \quad r < n \quad \dots \quad (4A)$$

In addition

$$\sigma^2 = a^{-2} \frac{m(m+n-1)}{(n-1)^2(n-2)}, \quad \mu = a^{-1} \frac{m}{n-1}$$

and there is a mode at $x = (m-1)/a(n+1)$.

1.1 Behaviour of $M_T(-a)$

As a Laplace transform $M_T(-a)$ must exist for any transition function although the series expansion based on (4A) diverges. It has also been found that the moments of log-normal and logistic forms become infinite.

After a change of variable, using (4),

$$\begin{aligned} M_T(-a) &= \frac{e}{B(m,n)} \int_1^\infty e^{-u} u^{-(n+1)} (1-u^{-1})^{m-1} du \\ &= M_T(m,n) \quad \text{say,} \end{aligned}$$

since a is immaterial. It can also be shown that

$$aM_T' = M_T(m+1,n)$$

and that

$$mM_T(m+1,n) = (m+n)M_T(m,n) - nM_T(m,n+1) \quad \dots \quad (5)$$

When $m = 1$ we have

$$e \int_1^\infty e^{-u} u^{-(n+1)} du = \frac{1}{n} \left\{ 1 - \int_1^\infty e^{-u} e^{-u} u^{-n} du \right\} \quad \dots \quad (6)$$

by partial integration. With the recurrence relation

above this leads to a terminating and asymptotic series.
In terms of M_T this is

$$M_T(1,n) = 1 - \frac{1}{n-1} M_T(1,n-1), \quad n \geq 2. \quad \dots (7)$$

Through (5) and (6) all integral values are derivable from

$$e \int_1^{\infty} e^{-u} u^{-1} du = 0.596\ 347\ 361$$

from the tables of Jahnke-Emde. It can also be seen that

$$M_T(1,n) \rightarrow 1 \quad \text{as } n \rightarrow \infty,$$

$$\lim_{m,n \rightarrow \infty} M_T(m,n) = \text{constant}$$

and when m or $n = 0$ M_T is zero as one can verify by direct substitution. If we substitute $M_T = 1$ into (7) we find the asymptotic formula

$$M_T(1,n) \sim 1 - 1/(n-1)$$

and successive substitution shows that

$$\begin{aligned} M_T(1,n) &\sim 1 - \frac{1}{n-1} + \frac{1}{(n-1)^2} - \dots + (-)^r (n-1)^{-r} \\ &= 1 - 1/n \quad n \geq 2. \end{aligned} \quad \dots (8)$$

From (5)

$$M_T(2,n) \sim M_T(1,n) - 1/(n+1).$$

For the purposes of induction suppose that

$$M_T(m+1,n) \sim M_T(1,n) - m/(n+1).$$

Then in (5) again

$$(m+1)M_T(m+2, n) = (m+n+1)M_T(m+1, n) - nM_T(m+1, n+1)$$

$$(m+1)M_T(1, n) - m/(n+1) - n m/(n+1) - m/(n+2)$$

i. e.

$$M_T(m+2, n) \sim M_T(1, n) - \frac{m}{n+1} \left\{ \frac{1}{m+1} + \frac{n}{n+2} \right\}$$

$$\sim M_T(1, n) - (m+1)/(n+1) \quad \dots \quad (9)$$

By plotting numerical results it was found that the contours of $M_T(m, n)$ tend toward a set of straight lines radiating from the neighbourhood of $(0; 0.4)$. This agrees with the asymptotic formulae (8) and (9) but suggests that the parameter

$$\vartheta = \arctan \left(\frac{n+0.4}{m} \right)$$

is more descriptive than (m, n) . Empirically (for $m, n \approx 10$) the best fitting parabola is

$$\vartheta = 0.230\ 921 + 1.641\ 871 M_T - 0.302\ 007 M_T^2 \quad \dots \quad (10)$$

which is $\pi/2$ if $M_T = 1$. The contours of M_T are shown in Fig. 20 and Fig. 21 shows some of the curves fitted by this parabola.

With this approximation it is now possible to solve (3) for the parameters m and n using simple trigonometry. Rearranging and remembering that

$$aM_T'(m, n) = M_T(m+1, n)$$

equations (3) become

$$M_T(m, n) = 1 - a\mu/F(n) \quad \dots \quad (11)$$

$$M_T(m+1, n) = \frac{a\mu}{F(n)} \left\{ 1 - \frac{a\mu}{2} - \frac{a\sigma^2}{2\mu} \right\}$$

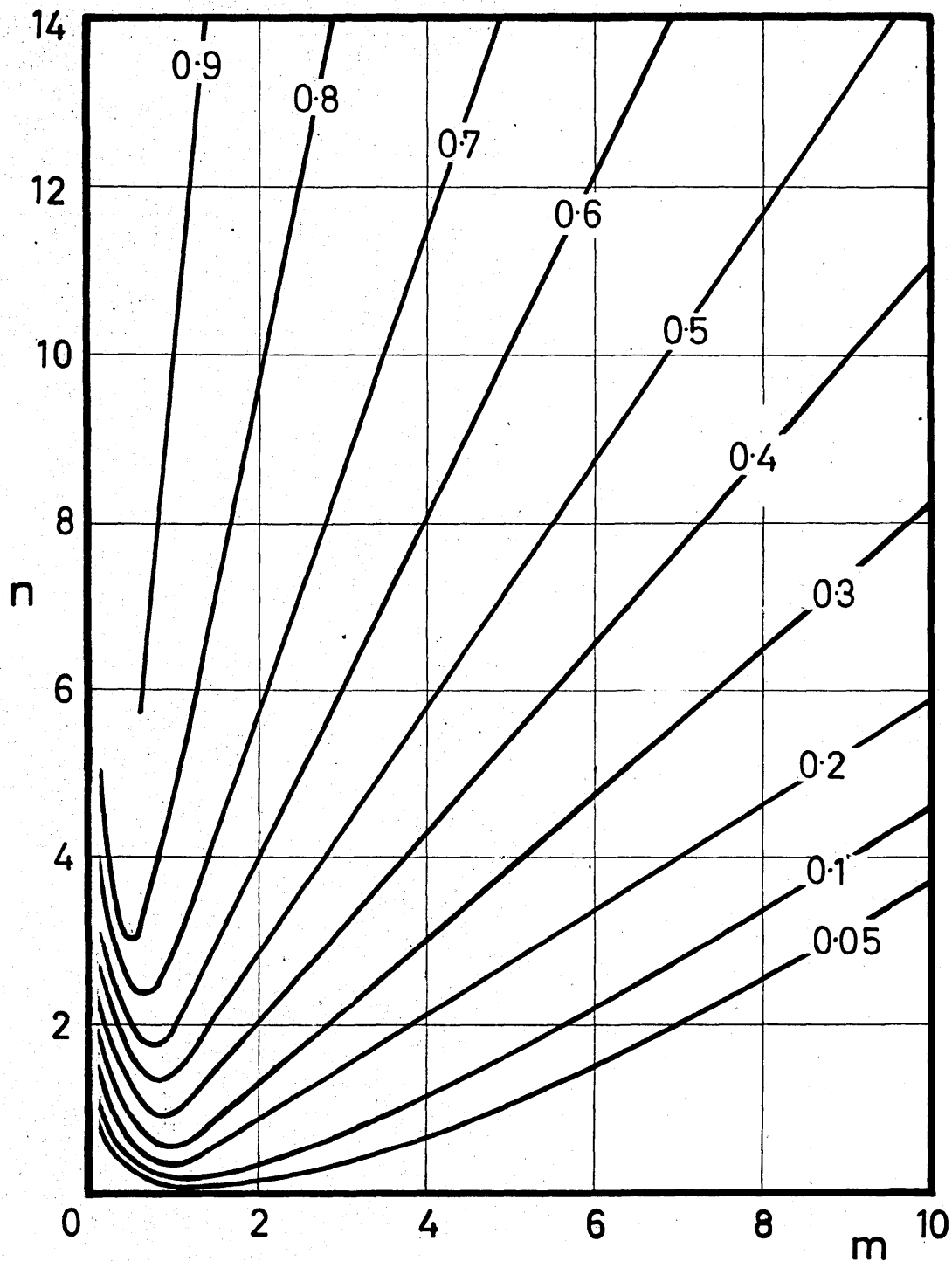


FIG. 20 VALUES OF $M_T(m, n)$

(Parameters of empirical crack length distribution)

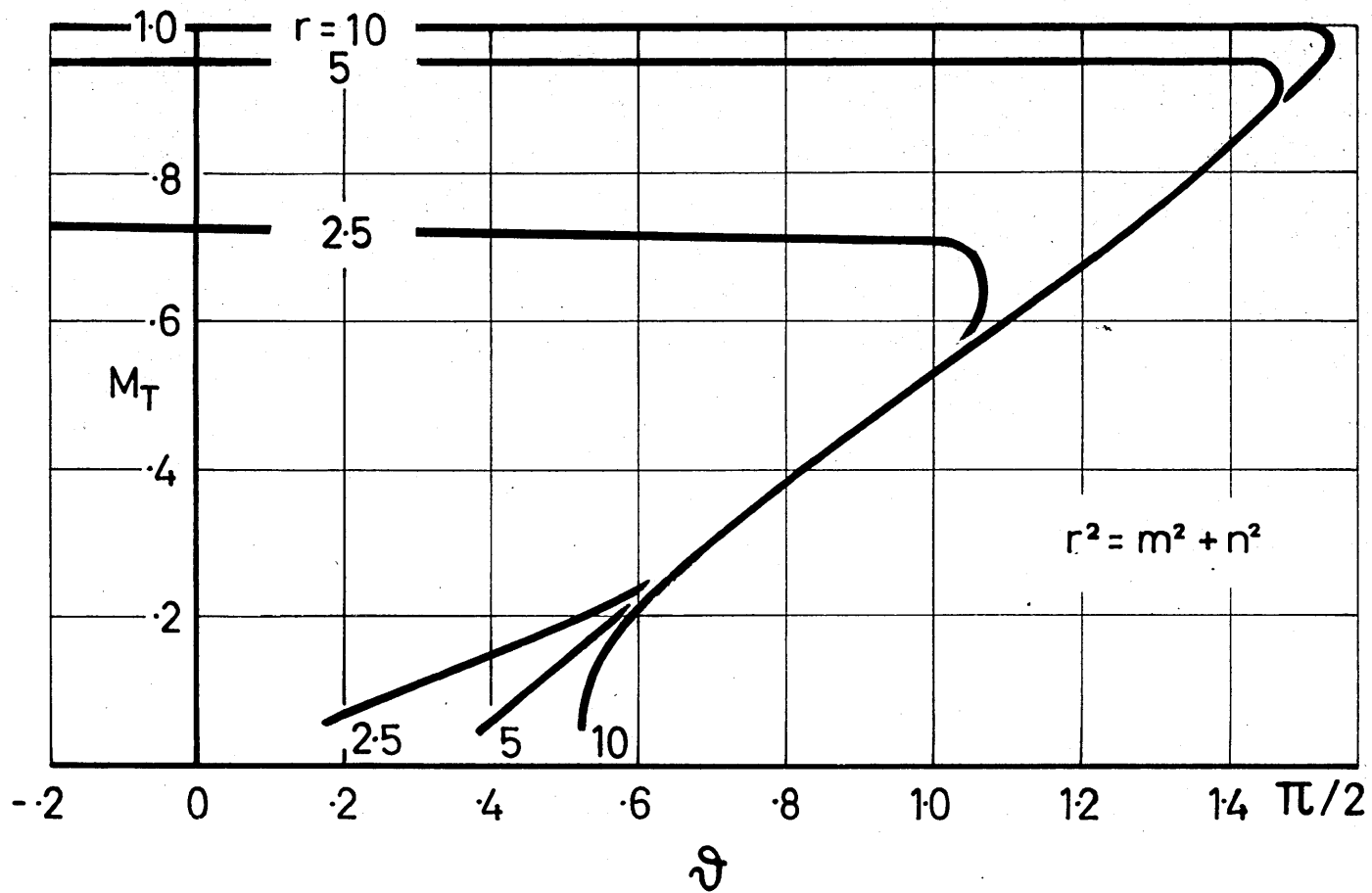


FIG. 21 M_T AS A FUNCTION OF CONTOUR GRADIENT

where the right members are known so that two angles ϑ_0 , ϑ_1 can be found by (10). It finally follows that

$$m = \tan \vartheta_1 / (\tan \vartheta_0 - \tan \vartheta_1) \quad \dots \quad (12)$$

$$n = m \tan \vartheta_0 - 0.4.$$

This seems to be the simplest method of fitting $f(x|n)$, the length distribution. However it is only suitable for independent distributions, making no allowance for the correlations appearing from the solutions of the crack-damage equations. An approximate allowance for these is considered below. From Fig. 21 it can also be seen that (10) is very inaccurate when $M_T < 0.2$.

2.1 Summarising Rates and Damages

Before discussing the expectation integrals in more detail we consider the fitting of formulae to the known rates and damages to give algebraic form to $R(\mathbf{a})$ and $A(\mathbf{a}, F)$.

Suppose that m steps of the overall integration have been completed. At the crack lengths corresponding to each of these we know the rates $R(\mathbf{a})$ by means of whatever structural analysis is employed. Each step, with the crack suppressed systems, will add $N(N+1)$ values of $R_i(\mathbf{a})$ so that there will be $mN(N+1)$ data altogether.

We now let the rate (or damage) depend quadratically on the crack lengths with zero length implying zero rate. For crack i

$$r_{ijk} = \sum_1^{\bar{}} c_{il} a_{ljk} + a_{ijk} \sum_1^{\bar{}} d_{il} a_{ljk} + e_{ijk} \quad \dots \quad (13)$$

where

$$i = 1, \dots, N$$

$$j = 0, \dots, N, \text{ the index of the suppressed crack,} \\ (0 \equiv \text{No suppression})$$

$$k = 1, \dots, m, \text{ the replication or step number,}$$

$$a_{ijk} = \text{crack length}$$

$$r_{ijk} = \text{calculated rate,}$$

$$e_{ijk} = \text{error in fitted formula.}$$

The crack rate r_{ijk} may also be interpreted as a damage rate and it may be an improvement to use logarithmic crack lengths a_{ijk} . For the damage rate a transformation to probits may also be helpful. In practice these questions can be decided after a preliminary solution of the problem.

From (13) one can now fit $2N^2$ constants which implies that $m \geq 2$. Using least squares, the error sum of squares is

$$E = \sum_{ijk} e_{ijk}^2$$

and proceeding directly

$$\partial E / \partial c_{il} = -2 \sum_{jk} a_{ljk} (r_{ijk}^{-c_{il}} a_{ljk}^{-d_{il}} a_{ljk}^{a_{ijk}})$$

$$\partial E / \partial d_{il} = -2 \sum_{jk} a_{ljk}^{a_{ijk}} (r_{ijk}^{-c_{il}} a_{ljk}^{-d_{il}} a_{ljk}^{a_{ijk}})$$

$$; \quad i, l = 1, \dots, N,$$

Setting their right members at zero, these equations may be arranged in the pairs

$$\begin{bmatrix} \sum_{jk} a_{1jk}^2 & \sum_{jk} a_{1jk}^2 a_{ijk} \\ \sum_{jk} a_{1jk}^2 a_{ijk} & \sum_{jk} a_{1jk}^2 a_{ijk}^2 \end{bmatrix} \begin{bmatrix} c_{il} \\ d_{il} \end{bmatrix} = \begin{bmatrix} \sum_{jk} a_{1jk} r_{ijk} \\ \sum_{jk} a_{1jk} a_{ijk} r_{ijk} \end{bmatrix} \dots (14)$$

with simple solutions. During a computation it is easy to add new terms to the five independent sums forming the coefficients and the right hand side.

In the summations of (14) all the data r_{ijk} has been given an equal importance. However since the largest contribution to the expectation comes from crack lengths near the means it would be preferable to give more weight to the corresponding results. Another reason for this is that the range of the expectation integral is $(0, \infty)$ whereas the data only go as far as the current solution of (35) or (36). Using moment methods, the expectation must therefore involve an extrapolation unless the entire problem is repeated, in which case the most recent information could be used in the first part of the range and the extrapolation would be replaced by data from the previous run.

To aid the choice of a weight function let us try to approximate the expectation

$$G(x) = \int g(x) dF(x)$$

by averaging

$$ax + b \approx g(x)$$

which has the error

$$e(x) = g(x) - ax - b.$$

For a perfect approximation

$$\int c(x) dF(x) = 0. \quad \dots (15)$$

If we fit a , b by minimizing the error

$$E = \int c^2(x) dF(x)$$

we find the normal equations

$$\begin{bmatrix} \int x^2 dF(x) & \int x dF(x) \\ \int x dF(x) & 1 \end{bmatrix} \begin{bmatrix} a \\ b \end{bmatrix} = \begin{bmatrix} \int xg(x) dF(x) \\ \int g(x) dF(x) \end{bmatrix}$$

analogous to (14). The coefficient matrix consists of moments and it will be found that (15) is also satisfied. Thus the density $f(x)$ is here the ideal weight function. This argument can be extended to any linear regression with the same result and the practical implication is that equations such as (14) should have weights similar to the joint density which in this context is of course unknown.

On a computer it is most economic in (14) to store only the complete sums and add to these as the solution progresses. At each stage $f(a | n)$ and therefore the ideal weight functions change and with only these sums in storage it becomes impossible to always, if ever, have an ideal weighting. The only usable weight is in fact a function of m , the step number, and since one expects the joint density to increase on the whole as the mean is approached the most obvious weight is

$$w(m) = m$$

or possibly a higher power m^α . The sums in (14) then take the form

$$\sum_{jk} w^{(m)} a_{1jk}^2 \quad \text{etc.}$$

2.2 Expectation Integrals

The approximation (13) is well suited to the form of solution envisaged because it transpires that the detailed form of $f(\mathbf{a}|\mathbf{n})$ is irrelevant. If the rates and damages are known explicitly in terms of crack length and more accurate estimates are desired then the joint density and the associated integration formulae are briefly discussed in Appendix A. These formulae are also required if the approximation (13) is used for logarithmic or other transformed crack lengths.

Without the subscript k the expectation of (13) is

$$\begin{aligned} \int r_{ij} dF(\mathbf{a}|\mathbf{n}) &= \int \left\{ \sum_1 c_{i1} a_{1j} + a_{ij} \sum_1 d_{i1} a_{1j} \right\} dF(\mathbf{a}|\mathbf{n}) \\ &= \sum_1 \left\{ c_{i1} \bar{a}_{1|j} + d_{i1} (\bar{a}_{i|j} \cdot \bar{a}_{1|j} + \sigma_{i1|j}) \right\}, \\ &\dots \quad (16) \end{aligned}$$

requiring means and also covariances of systems with suppressed cracks. In turn the latter require the solution of lower systems with two suppressed cracks and so on until there are 2^N systems. To the approximation here we can avoid this proliferation by putting

$$\sigma_{i1|j} \approx \sigma_{i1}$$

or more accurately

$$\sigma_{i1|j} \approx \sigma_{i1} (\bar{a}_{i|j} \bar{a}_{1|j}) / \bar{a}_i \bar{a}_1, \quad \dots \quad (17)$$

which includes a rough correction for scale.

Chapter VI

MATRIX FORCE METHODS

The preceding chapters on the statistical aspects are quite general, being applicable to any system whose decay can be described in two stages. The remainder will be devoted to illustrating the theory by a particular type of example. In the following the general use of matrix force methods is described and in Chapter VII we consider rectangular reinforced panels. However some of the methods used have a wider applicability which will be mentioned as the occasion arises.

The progress of a crack in a structure may be regarded as a process in which various loads in the structural elements become zero, or more briefly, a cutout process. For a general crack these loads are not the obvious ones arising from the idealisation of the structure but other intermediate loads which we assume to be linear transformations of them. For the original idealisation the loads are⁷⁵

$$\begin{aligned} S &= b_0 R + b_1 X \\ &= b R \end{aligned} \quad \dots (1)$$

- where
- S = Column vector of generalised stresses or internal loads.
 - b_0 = Matrix whose columns represent loads statically equivalent to some external force system.
 - b_1 = Matrix of self-equilibrating internal force systems
 - R = Column vector of magnitudes of external systems.

X = Column vector of magnitudes of internal systems or redundants.

The deflections of each element are now given by

$$v = fS + H \quad \dots \quad (2)$$

f being a square flexibility matrix while H is a column of initial strains. Since b_1 is a set of self-equilibrating systems

$$b_1^t v = 0$$

by the theorem of virtual work. If (2) and (1) are now substituted into this and the resultant equation solved for X then

$$X = -D^{-1} b_1^t f b_0 R - D^{-1} b_1^t H \quad \dots \quad (3)$$

so that by (1)

$$S = (b_0 - b_1 D^{-1} b_1^t f b_0) R - b_1 D^{-1} b_1^t H \quad \dots \quad (4)$$

where

$$D = b_1^t f b_1$$

1.0 General Modification Method

Using the standard initial strain technique⁷⁵ we consider the simultaneous treatment of cutouts and modifications. Mathematically we try to find initial strains to make the submatrix S_m of S zero while the remaining stresses are appropriate to an internal flexibility

$$f' = f + \begin{bmatrix} 0 & f_\Delta \end{bmatrix} .$$

Assume that initial strains are only needed in the affected elements and let H_m , H_c be the subvectors where the subscripts m and c refer to modifications and cutouts

respectively. From (4) after suitable partitioning

$$S = bR - b_1 D^{-1} \begin{bmatrix} b_{1c}^t & b_{1m}^t \end{bmatrix} \begin{bmatrix} H_c \\ H_m \end{bmatrix}.$$

Now

$$v = fS + H$$

and in the fully modified structure

$$\begin{aligned} v' &= f' S' \\ &= f' S \end{aligned}$$

since $S' = S$ by hypothesis. Equating v and v' over the rows appropriate to H_m we find that

$$H_m = f_{\Delta} \{ b_m R - b_{1m} D^{-1} \begin{bmatrix} b_{1c}^t & b_{1m}^t \end{bmatrix} \begin{bmatrix} H_c \\ H_m \end{bmatrix} \} \quad \dots (5)$$

From the cutout condition $S_c = 0$ we similarly find

$$b_c R - b_{1c} D^{-1} \begin{bmatrix} b_{1c}^t & b_{1m}^t \end{bmatrix} \{ H_c \ H_m \} = 0 \quad \dots (6)$$

and these two equations may be combined as

$$\begin{aligned} \left[\begin{bmatrix} 0 & f_{\Delta}^{-1} \end{bmatrix} + \begin{bmatrix} b_{1c} & b_{1m} \end{bmatrix} D^{-1} \begin{bmatrix} b_{1c}^t & b_{1m}^t \end{bmatrix} \right] \{ H_c \ H_m \} &= b_m R \\ &\dots (7) \\ &= S_m. \end{aligned}$$

Now consider the effect of changing the flexibilities in some members where the loads are to be made zero by the cutout method. If this is done b_c , b_m etc. above will have some elements in common and the number of equations represented by (5) and (6) will be excessive.

In addition the extra equations will be inconsistent. Thus the cutout conditions (6) must be allowed to dominate and if necessary exclude any of the loads in the modified

members. If some trivial equations are added for the unaffected members than (7) can also take the form

$$\begin{bmatrix} 0 \\ 0 \\ H_m \end{bmatrix} = \begin{bmatrix} 0 & & \\ & I & \\ & & f_\Delta \end{bmatrix} \left\{ bR - b_1 D^{-1} [b_{1c}^t \ b_{1m}^t] \begin{bmatrix} H_c \\ H_m \end{bmatrix} \right\} \quad \dots (8)$$

which is useful when considering the transformed loads of the next section.

1.1 Use of Transformed Loads

We now view a crack as the generalised cutout process $BS \rightarrow 0$ and to treat it one can repeat the analysis based on (1) with the corresponding transformed loads

$$T = c_0 R + c_1 X$$

where T etc. are defined by (1) in the alternative form

$$\begin{bmatrix} S_0 \\ BS \end{bmatrix} = \begin{bmatrix} b_{00} \\ Bb_0 \end{bmatrix} R + \begin{bmatrix} b_{10} \\ Bb_1 \end{bmatrix} X$$

amounting to a prefactor

$$\begin{bmatrix} I & 0 \\ & B \end{bmatrix} \equiv B_* \quad \text{say}$$

The load vectors T and S must be of the same order and as above we suppose the elements of S are rearranged to obtain this convenient partitioning. The rows of B (or B_*) must also be linearly independent and preferably well-conditioned. This is discussed in Section 2.1 of Chapter VII. It is also possible to approach linear dependence between rows of B and the unit elements elsewhere, and this is discussed below.

The deflections are still

$$\begin{aligned} v &= fS + H \\ &= fB_*^{-1} T + H \end{aligned}$$

and after the transformation

$$\begin{aligned} w &= B_*^{-t} v \\ &= B_*^{-t} f B_*^{-1} T + B_* H \\ &= g T + H_* . \end{aligned}$$

Equation (8) now becomes (D not changing)

$$\begin{bmatrix} 0 \\ 0 \\ H_{m^*} \end{bmatrix} = \begin{bmatrix} 0 \\ I \\ g \end{bmatrix} \left\{ cR - c_1 D^{-1} \begin{bmatrix} c_{1c}^t & c_{1m}^t \end{bmatrix} \begin{bmatrix} H_{c^*} \\ H_{m^*} \end{bmatrix} \right\} \quad \dots (9)$$

where $H_{m^*} = B_*^{-t} H$ etc. and

$$\begin{bmatrix} 0 & g_\Delta & 0 \end{bmatrix} = B_*^{-t} \begin{bmatrix} 0 & f_\Delta & 0 \end{bmatrix} B_*^{-1}$$

corresponding to the transformation. Note that f_Δ , g_Δ are of the same order and that H here has the same order as S , unlike $\{H_{c^*} H_{m^*}\}$.

The transformed cutout equation is next interpreted in terms of the original load system. Equation (9) is first premultiplied by

B_* , rearranged as $[I_o \ B^t \ I_m]$, and since the left hand side must then contain H_m (by returning to the original structure)

$$H_{m^*} = H_m .$$

With this change the right hand side becomes

$$\begin{bmatrix} 0 \\ 0 \\ H_{m^*} \end{bmatrix} = \begin{bmatrix} 0 \\ 0 \\ f_\Delta \end{bmatrix} \left\{ I + B^t B \right\} \left\{ bR - b_1 D^{-1} \begin{bmatrix} c_{1c}^t & c_{1m}^t \end{bmatrix} \begin{bmatrix} H_{c^*} \\ H_{m^*} \end{bmatrix} \right\} \quad \dots (10)$$

The equations not involving f_{Δ} may be abstracted in the form

$$\begin{bmatrix} 0 \\ 0 \end{bmatrix} = \begin{bmatrix} B_o^t \\ B_c^t \end{bmatrix} \left\{ BbR - Bb_1D^{-1} \begin{bmatrix} b_1^t B^t & b_{1m}^t \end{bmatrix} \begin{bmatrix} H_{c^*} \\ H_m \end{bmatrix} \right\}$$

and these have a rank equal to the number of independent load conditions, are consistent, and reduce to the formula

$$B \left\{ bR - b D^{-1} \begin{bmatrix} b_1^t B^t & b_{1m}^t \end{bmatrix} \begin{bmatrix} H_{c^*} \\ H_m \end{bmatrix} \right\} = 0 \quad \dots (11)$$

generalising the case of simple pure cutouts. The second term in (10) now vanishes and (10) and (11) combine in the form

$$\begin{bmatrix} 0 \\ f_{\Delta}^{-1} H_m \end{bmatrix} = \begin{bmatrix} BS \\ S_m \end{bmatrix} - \begin{bmatrix} Bb_1 \\ b_{1m} \end{bmatrix} D^{-1} \begin{bmatrix} b_1^t B^t & b_{1m}^t \end{bmatrix} \begin{bmatrix} H_{c^*} \\ H_m \end{bmatrix} \quad \dots (12)$$

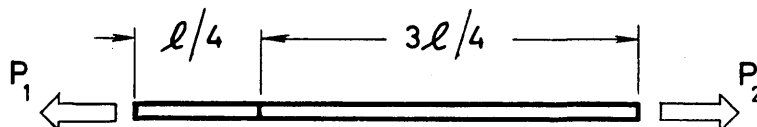
which is directly obtainable from (8) by substitution of transformed quantities as one would expect.

This expedient however gives no information about the independence of the various equations. In practical situations, when elements of flexibility corresponding to certain loads are altered, many of the same loads enter the crack conditions $BS = 0$.

Now f_{Δ} and g_{Δ} conform with one another and with b_m etc. which in turn conform with a set of loads not altered by the transformation B^* . This is indicated above by the partitioning.

In practice f_{Δ} will be found for all loads. We must then delete all rows and columns corresponding to those loads which we regard as transformed in order to obtain valid modifications. There is a choice about which loads to retain and the same cracking problem can be formulated by many different sets of equivalent equations.

This is a subject on which further work would be useful. To obtain a well conditioned transformation however it is plausible that loads not corresponding to the flexibility changes should be altered as little as possible by the transformation. As an example consider the cut boom shown below.



The original loads here are P_1 , P_2 and the transformed load is $(3P_1 + P_2)$. If we consider the alternative load systems

$$\begin{bmatrix} P_1 \\ 3P_1 + P_2 \end{bmatrix} = \begin{bmatrix} 1 & \\ 3 & 1 \end{bmatrix} \begin{bmatrix} P_1 \\ P_2 \end{bmatrix}$$

or

$$\begin{bmatrix} P_2 \\ 3P_1 + P_2 \end{bmatrix} = \begin{bmatrix} & 1 \\ 3 & 1 \end{bmatrix} \begin{bmatrix} P_1 \\ P_2 \end{bmatrix}$$

it can be seen that the latter is better conditioned. In the limit as the cut approaches P_1 the transformation becomes singular and this is the reason why the choice of load deletions does not present itself for simple cut-outs.

From the type of behaviour described above it is plausible to extract the rule of thumb;

"If there is a choice replace the loads which act nearest to the crack by the loads acting at the crack."

Finally (12) may be rearranged in the standard form

$$\left[\begin{bmatrix} 0 \\ f_{\Delta}^{-1} \end{bmatrix} + \begin{bmatrix} Bb_1 \\ b_{1m} \end{bmatrix} D^{-1} [b_1 B Db_{1m}] \right] \begin{bmatrix} H_{c^*} \\ H_m \end{bmatrix} = \begin{bmatrix} BS \\ S_m \end{bmatrix} \dots (13)$$

where S_m , S and H_m (H_{m^*}) refer to b , b_1 etc. while H_{c^*} refers to the transformed system, although this has no practical consequence. The brackets $\llbracket \quad \rrbracket$ will always denote a matrix of this type called a modification matrix.

From the modified stresses

$$T_* = cR - c_1 D^{-1} c_1^t H_*$$

of the transformed system premultiplication shows that

$$\begin{aligned} S_* &= bR - b_1 D^{-1} [b_1^t B^t b_{1m}^t] \llbracket \quad \rrbracket^{-1} \{ Bb \ b_m \} R \\ &= b_* R \text{ say.} \end{aligned}$$

The deflections are

$$\begin{aligned} w &= gT_* + H_* \\ v_* &= fS_* + IB^t H_* \end{aligned}$$

i.e.

$$\begin{aligned} &\dots (14) \\ &= fbR - \{ fb_1 D^{-1} [b_1^t B^t b_{1m}^t] - [I \ B^t] \} \llbracket \quad \rrbracket^{-1} \{ Bb \ b_m \} R \end{aligned}$$

The internal work is $b_*^t v_*$ and if we substitute for b_* and recall that

$$b_*^t f b_1 = 0,$$

by the theorem of virtual work, the modified flexibility will be displayed as

$$F_* = F + [b^t B^t b_m^t] \llbracket \quad \rrbracket^{-1} \{ Bb \ b_m \} \dots (15)$$

(where $F = b^t f b$) while

$$\begin{aligned} b_* &= b - b_1 D^{-1} [b_1^t B^t b_{1m}^t] \llbracket \quad \rrbracket^{-1} \{ Bb \ b_m \} \\ &\dots (15A) \end{aligned}$$

2.0 Inverse of Modification Matrix

When f_{Δ} is small the two inversions implied by $\llbracket \rrbracket^{-1}$ will be extremely inaccurate unless a more direct method can be found. One such method is described here based on the partitioning between cutouts and modifications. The main importance of this procedure is as a background to the proof of a more efficient method in the next section.

To establish our notation write the modification matrix of (13) in the form

$$\llbracket \rrbracket = \begin{bmatrix} 0 & \\ & f_{\Delta}^{-1} \end{bmatrix} + \begin{bmatrix} K_c & K_{cm} \\ K_{mc} & K_m \end{bmatrix}$$

where the bold type has been eschewed to give a milder appearance to the steps below. From the partitioned inverse

$$K^{-1} = \begin{bmatrix} K_c^{-1} & -K_c^{-1}K_{cm}K_m^{-1} \\ -K_m^{-1}K_{mc}K_c^{-1} & K_m^{-1} \end{bmatrix}$$

where $K_{c^*} = K_c - K_{cm}K_m^{-1}K_{mc}$ and $K_{m^*} = K_m - K_{mc}K_c^{-1}K_{cm}$.

It is now convenient to introduce the $-t$ notation for the inverse of a transpose. We also make use of the identity

$$\begin{aligned} A^{-1}(I+A)^{-1}A &= A^{-1}(I+A^{-1})^{-1} \\ &= (I+A)^{-1}. \end{aligned}$$

Thus

$$\llbracket \rrbracket^{-1} = \begin{bmatrix} I & -K_c^{-1}K_{cm}K_m^{-1}f_{\Delta}^{-1} \\ 0 & I + K_m^{-1}f_{\Delta}^{-1} \end{bmatrix}$$

and upon inverting and cancelling part of the upper right hand section

$$\begin{aligned}
 \left[\begin{array}{cc} & \\ & \end{array} \right]^{-1} &= \begin{bmatrix} \mathbf{I} & \mathbf{K}_c^{-1} \mathbf{K}_{cm} (\mathbf{I} + \mathbf{f}_\Delta \mathbf{K}_{m^*})^{-1} \\ \mathbf{0} & (\mathbf{I} + \mathbf{f}_\Delta \mathbf{K}_{m^*})^{-1} \mathbf{f}_\Delta \mathbf{K}_{m^*} \end{bmatrix} \begin{bmatrix} \mathbf{K}_c^{-1} & \mathbf{K}_c^{-1} \mathbf{K}_{cm} \mathbf{K}_{m^*}^{-1} \\ -\mathbf{K}_m^{-1} \mathbf{K}_{mc} \mathbf{K}_c^{-1} & \mathbf{K}_{m^*}^{-1} \end{bmatrix} \\
 &= \begin{bmatrix} \{ \mathbf{I} - \mathbf{K}_c^{-1} \mathbf{K}_{cm} (\)^{-1} \mathbf{K}_m^{-1} \mathbf{K}_{mc} \} \mathbf{K}_c^{-1} & \mathbf{K}_c^{-1} \mathbf{K}_{cm} \{ (\)^{-1} - \mathbf{I} \} \mathbf{K}_{m^*}^{-1} \\ - (\)^{-1} \mathbf{f}_\Delta \mathbf{K}_{m^*} \mathbf{K}_m^{-1} \mathbf{K}_{mc} \mathbf{K}_c^{-1} & (\)^{-1} \mathbf{f}_\Delta \end{bmatrix} \\
 &= \begin{bmatrix} \mathbf{K}_c^{-1} \{ \mathbf{K}_c - \mathbf{K}_{cm} (\)^{-1} \mathbf{K}_m^{-1} \mathbf{K}_{mc} \} \mathbf{K}_c^{-1} & \mathbf{K}_c^{-1} \mathbf{K}_{cm} \mathbf{K}_{m^*}^{-1} \{ (\)^{-t} - \mathbf{I} \} \\ - (\)^{-1} \mathbf{f}_\Delta \{ \mathbf{K}_{mc} - \mathbf{K}_{mc} \mathbf{K}_c^{-1} \mathbf{K}_{cm} \mathbf{K}_m^{-1} \mathbf{K}_{mc} \} \mathbf{K}_c^{-1} & (\)^{-1} \mathbf{f}_\Delta \end{bmatrix} \\
 &= \begin{bmatrix} \mathbf{K}_c^{-1} \{ \mathbf{K}_c - \mathbf{K}_{cm} \mathbf{K}_m^{-1} \mathbf{K}_{mc} - \mathbf{K}_{cm} [(\)^{-t} - \mathbf{I}] \mathbf{K}_m^{-1} \mathbf{K}_{mc} \} \mathbf{K}_c^{-1} & \\ & \mathbf{K}_c^{-1} \mathbf{K}_{cm} \mathbf{K}_{m^*}^{-1} [(\)^{-t} - \mathbf{I}] \\ - (\)^{-1} \mathbf{f}_\Delta \mathbf{K}_{mc} \mathbf{K}_c^{-1} (\mathbf{I}) & (\)^{-1} \mathbf{f}_\Delta \end{bmatrix}
 \end{aligned}$$

Now $(\mathbf{I} + \mathbf{K}_{m^*} \mathbf{f}_\Delta)(\mathbf{I} + \mathbf{K}_{m^*} \mathbf{f}_\Delta)^{-1} = \mathbf{I}$ and this also takes the form

$$(\)^{-1} - \mathbf{I} = -\mathbf{K}_{m^*} \mathbf{f}_\Delta (\)^{-1}$$

When this is substituted above the off-diagonal submatrices become transposes while the leading one reduces to

$$\mathbf{K}_c^{-1} \{ \mathbf{I} + \mathbf{K}_{cm} \mathbf{f}_\Delta \mathbf{K}_{m^*} (\)^{-1} \mathbf{K}_m \mathbf{K}_{mc} \mathbf{K}_c^{-1} \}.$$

From the identity the second term here can be written (ignoring some prefactors) as

$$\begin{aligned}
K_{m^*} ()^{-1} K_m^{-1} K_{mc} K_{c^*}^{-1} &= (K_{m^*+f_\Delta}^{-1})^{-1} K_m^{-1} K_{mc} K_{c^*}^{-1} \\
&= (K_{m^*}^{-1} (I + K_{m^*} f_\Delta))^{-1} K_m^{-1} K_{mc} K_{c^*}^{-1} \\
&= ()^{-t} (I - K_{mc} K_c^{-1} K_{cm} K_m^{-1}) K_{mc} K_{c^*}^{-1} \\
&= ()^{-t} K_{mc} K_c (K_c - K_{cm} K_m^{-1} K_{mc}) K_{c^*}^{-1} \\
&= ()^{-t} K_{mc} K_c^{-1} .
\end{aligned}$$

The whole submatrix is therefore

$$K_c^{-1} + K_c^{-1} K_{cm} f_\Delta (I + K_{m^*} f_\Delta)^{-1} K_{mc} K_c^{-1}$$

which does not require $K_{c^*}^{-1}$.

Finally we have the exact result

$$\left[\begin{array}{cc} \left[\right]^{-1} & = \left[\begin{array}{cc} K_c^{-1} + K_c^{-1} K_{cm} f_\Delta ()^{-t} K_{mc} K_c^{-1} & -K_c^{-1} K_{cm} f_\Delta ()^{-t} \\ - ()^{-1} f_\Delta K_{mc} K_c^{-1} & (I + f_\Delta K_{m^*})^{-1} f_\Delta \end{array} \right] \\ & \dots (20) \end{array} \right.$$

which may be factorised if desired. When the change in flexibility is sufficiently small this becomes

$$\left[\begin{array}{cc} \left[\right]^{-1} & = \left[\begin{array}{cc} K_c^{-1} + K_c^{-1} K_{cm} f_\Delta K_{mc} K_c^{-1} & -K_c^{-1} K_{cm} f_\Delta \\ -f_\Delta K_{mc} K_c^{-1} & f_\Delta \end{array} \right] \dots (20A) \end{array} \right.$$

and of course $K_{cm} = B b_1 D^{-1} b_{1m}^t$ etc. The inversion of (20) can be achieved with a knowledge of K_c^{-1} , $K_{mc} K_c^{-1}$ and $(I + f_\Delta K_{m^*})^{-1}$.

2.1 Solution by Elimination

It is well known that the refined variants of Gaussian elimination known as the Chio, Choleski,⁷⁶ Crout⁷⁷ or Doolittle⁷⁸ methods are equivalent to factorising the coefficient in the equation

$$Ax = y \quad \dots (21)$$

as $A = LU$

where L, U are lower and upper triangular matrices. The intermediate stage in the solution of (21) is

$$Ux = L^{-1}y, \text{ with } L \text{ in storage, which is}$$

followed by the back solution

$$x = U^{-1}L^{-1}y.$$

Now apply Crout's method to the partitioned matrix K and suppose that the elimination procedure has just passed the rows and columns of the cutout coefficients K_c . Then at this stage we have achieved the following factorisation

$$\begin{bmatrix} K_c & K_{cm} \\ K_{mc} & K_m \end{bmatrix} = \begin{bmatrix} L_c & \\ & K_{mc} U_c^{-1} L_* \end{bmatrix} \begin{bmatrix} U_c & L_c^{-1} K_{cm} \\ & U_* \end{bmatrix} \quad (K_c = L_c U_c) \quad \dots (22)$$

Here L_c and U_c are obvious. In addition we must have

$$L_c (L_c^{-1} K_{cm}) + 0 \cdot U_* = K_{cm} \quad \dots (23)$$

$$(K_{mc} U_c^{-1}) U_c + L_* \cdot 0 = K_{mc}$$

which establishes the off-diagonal factors. Finally

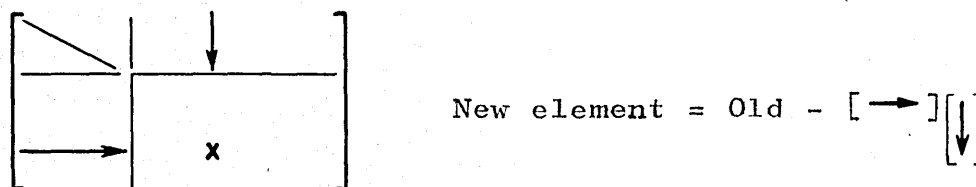
$$K_{mc} U_c^{-1} L_c^{-1} K_{cm} + L_* U_* = K_m \quad \dots (23A)$$

or

$$L_* U_* = K_m - K_{mc} K_c^{-1} K_{cm} \quad \dots (24)$$

$$= K_{m^*}$$

from the previous definition. Apart from this restriction L_* and U_* are arbitrary. At the stage envisaged in the computation we have factorised K_c and found the off-diagonal factors. From (23A) it can also be seen that the process of finding K_{m^*} is exactly the same as ordinary elimination except that the subtracted scalar products only contain terms numbering up to the order of K_c . Pictorially,



Having an algorithm for K_{m^*} , we can now outline the essential steps in the solution of a combined cutout and modification problem. In practice only one or at most two arrays are necessary, or in a computer the same storage space can be used, for the entire problem. To start with there is (13) in the form

$$\begin{bmatrix} L_c U_c & K_{cm} \\ K_{mc} & K_m \end{bmatrix} \begin{bmatrix} H_c^* \\ H_m \end{bmatrix} = \begin{bmatrix} B \ S \\ S_m \end{bmatrix}$$

After proceeding with the usual elimination as far as K_m we have the three arrays

$$\begin{bmatrix} U_c & L_c^{-1} K_{cm} & L_c^{-1} B \ S \\ L_c & & \\ K_{mc} U_c^{-1} & K_m & S_m \end{bmatrix} .$$

Acting as in (24) the coupling between cutouts and modification can be removed and we then have

$$\left[\begin{array}{c|c|c} U_c & L_c^{-1} K_{cm} & L_c^{-1} B S \\ \hline L_c & & \\ \hline K_{mc} U_c^{-1} & K_{m^*} & S_m - K_{mc} K_c^{-1} B S \end{array} \right] \dots (25)$$

Confining ourselves to the lower corner only we can now form the correct equation for the modification strains

$$(I + f K_{m^*}) H_m = f (S_m - K_{mc} K_c^{-1} B S). \dots (26)$$

This is still part of the array (or in the same storage block) and the elimination can proceed as before except that the operations are now confined to the elements of (26). When the whole elimination is completed then (22) has been completely factorised and the back solution can proceed without any special provisions.

2.2 Discussion

As the crack progresses in a fatigue problem there is a continuous change in the flexibility and an occasional cutout as various members are severed. At each crack step the array (25) becomes larger and in order not to waste previous computations it is desirable that the loads associated with the current flexibility changes should correspond to elements near the lower right hand corner especially since the type of change involved alters a large number of elements. When another cutout occurs there is no way of avoiding a recalculation of the lower corner but its effect can still be confined to this part by suitable ordering of elements in the array.

In themselves the modified loads found by calculations such as these have no interest and one needs only those required for estimating stress intensities. Since these are on the whole the loads corresponding to the currently changing flexibilities the economies above will also tend to reduce the time or labour of the back solutions.

However it is obvious that as the solution of the crack-damage equations progresses the amount of structural analysis for each crack step will increase. It is reasonable to expect this because, the cutout technique represents an alteration of an undisturbed structure and as the cracks extend this disturbance increases also. For this reason it may be worth considering updating the "undisturbed" structure at some interval to be determined. If this were done (and only an elegant means is worthwhile) the size of the structural problem would decrease with each step because of the decrease in redundancy.

3.0 The Representation of Cracking

To solve a fatigue problem one starts to integrate (4.35) or (4.36) and at each crack step the change in flexibility f_{Δ} is added to the previous changes followed by a check for the complete failure of any member, which must be indicated by another row in the set of load conditions. In the programming it was found that numerical methods were best for this purpose and the general principles are set out below. By a change of wording much of the discussion can be made applicable to the elements in displacement type analyses.

Apart from an overall constant the geometry of a given type of element determines its flexibility. Conversely if the type is defined closely enough this

flexibility represents the geometry. It follows that the number of independent elements in a flexibility matrix must at least equal the number of parameters defining its geometry. As an example consider the general flexibility

$$a_0 = a \begin{bmatrix} 1 & \frac{1}{2} \\ \frac{1}{2} & 1 \end{bmatrix}$$

for one-dimensional elements. This can represent uniform beams, booms or torsional members and if the leading element is unity there remain two independent elements. Symmetry is implied by the equality of diagonal elements while the $\frac{1}{2}$ reflects the uniformity of properties along the length since a linear variation of load is almost implicit. If a boom is now weakened by a crack whose effect is approximated as a concentrated flexibility f then it is easily shown that the flexibility becomes

$$f_0 = \frac{\ell}{AE} \begin{bmatrix} \frac{1}{3} & \frac{1}{6} \\ \frac{1}{6} & \frac{1}{3} \end{bmatrix} + f \begin{bmatrix} (1-\alpha)^2 & \alpha(1-\alpha) \\ \alpha(1-\alpha) & (1-\alpha)^2 \end{bmatrix} \dots (27)$$

where the crack divides the boom in the ratio $\alpha:(1-\alpha)$. Conversely, if we have such a flexibility then the form (27) can be used to solve for ℓ/AE , f and α . If only two elements of f_0 are taken to be independent then we can find fAE/ℓ , a non-dimensional crack length, and α which indicates its position. In the next chapter we consider cracks in rectangular skin panels. When these are partially cracked their non-dimensional description requires four parameters, for example,

Aspect ratio ; Tip position (2 coordinates); Orientation.

Thus if n is the order of the flexibility

$$\frac{1}{2}n(n+1) - 1 \geq 4$$

or $n > 2.7$. This may be realised by a shear panel which is also allowed to carry two uniform direct stresses.

By making one principal stress zero this system can also represent a completely cracked panel. However the uniform stresses would not allow the crack position to be localised so that this representation becomes no better than a simple cutout. In effect the flexibility has become singular so that the number of independent elements decreases to such an extent that the geometry cannot be fully described. A complete crack in a panel can be localised by a 5-th order flexibility, which allows linear variations in the direct stresses. In Chapter VII we derive 9-th order and 13-th order flexibilities from which those of lower order can be derived.

A uniformly stressed triangle has three natural modes of deformation and the corresponding stiffness matrix can describe a partial crack. As above however a complete crack cannot be localised in a uniform stress field for which six natural modes are required.

3.1 The Use of Moving Elements

Consider the section shown of an idealised structure with a crack which first extends from panel 5 in Fig. 22 (a) to A and then to B in the next step. It is plausible that the growth to A be represented by changing the flexibility (or stiffness) of panel 3a as well as that of 5 and any other panels. The failure of 5 is then described by imposing various conditions on its local stresses.

When the crack tip reaches B nothing is changed except that we now expect the effect of the tip singularity to be felt in the neighbouring panels. If the flexibility of 3a is suitably altered this will occur but not to its fullest extent because, until they are reached by

the crack, the panels 1a, 2a and 4a are essentially different from 3a. Another objection is that the nature of a stress pattern will change rather too suddenly when the crack enters a panel.

These difficulties can be partially overcome as in Fig. 22(b) by supposing the flexibilities of 1a, 2a and 4a to derive from the strain energies of a fictitious moving element M, containing the tip, and from the remaining parts 1b etc. of the actual elements. The stress pattern in M is appropriate to a crack tip while the stresses in 1b etc. belong to ordinary idealised systems. When a crack moves a short distance, as in Fig. 23 (a) the change in flexibility is given by the integral of strain energy over the shaded areas, namely

$$\left\{ \int_B - \int_A \right\} (dU_m - dU_a) + \int_C (dU_{m2} - dU_{m1})$$

the subscripts referring to the different types of panel.

Before it is overlapped by M the flexibility of a panel P is undisturbed. Consider the remaining effect after M has passed. At the start and finish P and M do not overlap and the first and last flexibilities cannot depend on M. Thus we need only consider the idealised stress systems whose energy is represented by U_a . The complete effect of a passage such as that shown in Fig. 23 (b) may be represented as

$$U^* = \sum_i \left\{ \int_{A_i P} - \int_{B_i P} \right\} dU_a \quad \dots \quad (28)$$

where the regions of integration $A_i P$, $B_i P$ are those common to P and to the particular region of type A or B in Fig. 23 (a).

Now consider a small element dP which must successively be outside, inside and again outside of M . If it is first covered by M_i then it must make a negative contribution in the integral over $B_i P$ and this is the only negative contribution. Similarly, if M_j leaves dP ($j > i$) there is a corresponding positive contribution from $A_j P$ and this also occurs once only.

Thus dP makes no contribution to U^* . This is true also if M never crosses it and if it is crossed more than once the sequence above is merely repeated. By considering all parts of P it is now obvious that $U^* = 0$ so that the final flexibility is the same as the original. (Not all of it can be used however for new cutout conditions will appear for which some of the corresponding loads must be deleted.) The proof here applies also to stiffnesses and elements of any shape.

The loads on M do not belong to S or BS but must be obtained from them by interpolation. In a computation the intrinsic flexibility of M is a known quantity not greatly affected by its translation. Thus the contribution of dU_m to the flexibility with respect to S arises from the change in this interpolation and only the idealised stress systems need to be considered for direct integration. This will become clearer with the detailed analysis below.

For rectangular panels the optimum positioning and intrinsic flexibility of M are treated in Chapter VII.

3.2 Fitting Generalised Stresses to Arbitrary Stress Systems

The loads acting on M can be approximated by MS_a where M is an interpolation matrix and S_a a submatrix

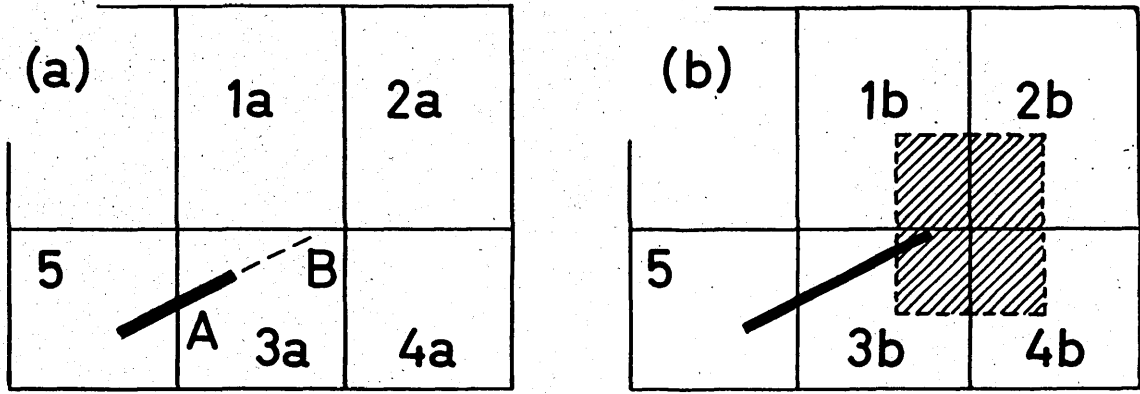


FIG. 22 MOVING ELEMENT

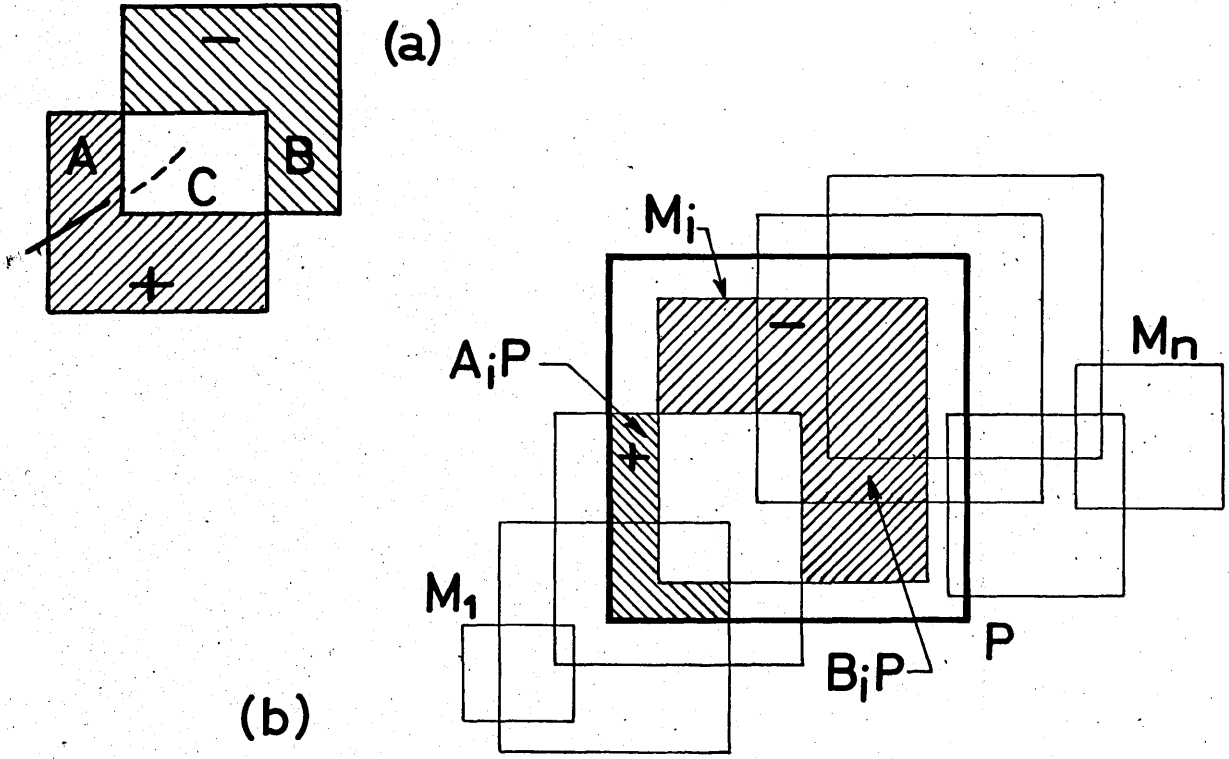


FIG. 23 FLEXIBILITY INTEGRALS WITH MOVING ELEMENT

of S containing those loads likely to be needed in the interpolation. Generally, the interpolated forces cannot be in complete equilibrium with the internal stresses $\sigma_m(r)$ assumed for M ($r =$ radius vector). However in the idealised elements there will be a set of stress patterns $\sigma_{Ni}(r)$ for each natural load and these will have corresponding modes of deformation $\rho_{Ni}(r)$ such that

$$\int \sigma_{Ni}^t \rho_{Nj} dV = \delta_{ij}$$

or with equilibrium

$$\int \sigma_{Ni}^t(s) \rho_{Nj}(s) dS = \delta_{ij}, \text{ where}$$

$s =$ boundary position,

$dS =$ element of boundary.

These systems can be postulated for M also in which we now suppose that

$$\sigma_m(s) \approx \sum_i a_i \sigma_{Ni}(s) \quad \dots (29)$$

For a good fit we now postulate that the virtual work done by each side of (28) over an arbitrary displacement $u(s)$ is the same. Since there is internal equilibrium this can be expressed as

$$\int_S \sigma_m^t(s) u(s) dS = \sum_i \int_S a_i \sigma_{Ni}^t(s) u(s) dS$$

integrating around the boundary. Since it is arbitrary each natural mode can be substituted for $u(s)$. Using the orthogonality enjoyed by these it is found that

$$a_i = \frac{\int \sigma_m^t(s) \rho_{Ni}(s) dS}{\int \sigma_{Ni}^t(s) \rho_{Ni}(s) dS} \quad \dots (30)$$

where the denominator is retained in order to indicate the formal resemblance to Fourier coefficients. Owing to the finiteness of the approximation, equality in (29) is restricted to the linear combinations

$$u(s) = \sum_i b_i \rho_{Ni}(s)$$

of the natural modes. The virtual work is then

$$\sum_i a_i b_i \int_S \sigma_{Ni}(s) \rho_{Ni}(s) ds$$

3.3 Modified Flexibilities

We can now calculate the modified flexibilities. It is assumed that the size and relative position of M have been determined and we also assume that we know the values of strain energy and the forces corresponding to MS_a for a standard element of type M with a fixed level of $\sigma_m(r)$. These forces are fitted by (30) and in our case the standard element is a rectangle of unit area and unit thickness under the plane stress system corresponding to a stress intensity of

$$K^2 = 2\pi.$$

In the standard elements, for which aspect ratio and crack orientation are variables, let

μ = Strain energy (by integration of $\sigma_m^t(r) \varphi \sigma_m(r)$)

Σ = Standard system of generalised forces, fitted beforehand by (30).

φ = Flexibility of element $dx dy$.

For the uncracked structure the flexibility is given by

$$\begin{aligned}
2U_o &= S_a^t r_a \\
&= S_a^t f S_a \\
&= S_a^t \int_V \sigma_a^t(r) \varphi \sigma_a(r) dV \quad \text{say.}
\end{aligned}$$

When M is removed, the reduced integral

$$\int_{V-M} \sigma_a^t \varphi \sigma_a dV$$

defines $f - f_m$ and the contribution f_m is replaced by a flexibility from U_m where

$$U_m = \frac{K^2}{2\pi} \mu t \ell,$$

obtainable from dimensional considerations, where

t = sheet thickness

K^2 = energy release rate, still to be related to S_a ,

and ℓ^2 = area of M.

Now the forces on M are

$$tK\sqrt{\ell} \Sigma$$

which must be related to the interpolated forces MS_a .

This is done by fitting K through the least squares model

$$\Sigma tK\sqrt{\ell} = MS_a + e,$$

e being an error vector. Minimising $e^t e$,

$$\hat{K} = \Sigma^t M S_a / t\sqrt{\ell} \Sigma^t \Sigma \quad \dots (32)$$

and substituting into (31),

$$2\pi U_m = S_a^t M^t \frac{\mu \Sigma \Sigma^t}{t(\Sigma \Sigma)^2} M S_a \quad \dots (33)$$

The form of this shows that

$$f_M = \mu \Sigma \Sigma^t / \pi t (\Sigma^t \Sigma)^2$$

may be regarded as the intrinsic flexibility of the fictitious moving element. Its rank of one could be expected from the fact that (for a given geometry) K uniquely determines the stress in M . The independence from ℓ follows basically from having a fixed stress intensity in the standard element.

Equation (33) also shows that $M^t f_M M$ is the contribution of M to the complete flexibility which can be written

$$f_1 = f - f_m + M^t f_M M \quad \dots \quad (34)$$

In application f_m is found by numerical integration and there is also a programme for using (30) to find the standard forces in the normalised form

$$\Sigma / \Sigma^t \Sigma$$

and another to form $\Sigma^t M$ from the values thus obtained, after the loads for the modified structure have been found.

In Chapter II we discussed the probability distribution of K and of local stresses. Now the forces S_a used in (32) come from an equation such as (15A) and if we suppose that the numerical values there are related to unit magnitude of the corresponding external load system R_i (belonging to R) then we have a factor of proportionality between K and R_i . If there are several systems and R is not a scalar one can in this way find the required elements of A^{-1} in (2.20).

The same argument applies to the local stresses responsible for damage but here there are no general rela-

tions such as (32) although a linear form will appear for each specific case.

Before leaving this chapter it is worth noting that the method described of modifying flexibilities need not be confined to fatigue cracks and can be generalised. Suppose a structure has a small discontinuity where the stress pattern differs from that elsewhere and consists of a superposition of basic patterns with the vector of magnitudes K and the intrinsic flexibility f_I . Then Σ becomes rectangular and (32) becomes

$$K = (\Sigma^t \Sigma)^{-1} \Sigma^t M S_a$$

while

$$f_M = \Sigma (\Sigma^t \Sigma)^{-1} f_I (\Sigma^t \Sigma)^{-1} \Sigma^t$$

with the rank of f_I .

If a displacement method were contemplated the theory for the modified stiffnesses would be exactly analogous to these two sections. The roles of forces and displacements would be interchanged⁷⁵ so that Σ would represent the modes of a standard element and M would interpolate between modes. Values of u and the optimisations of Chapter VII apply to both methods.

Chapter VII

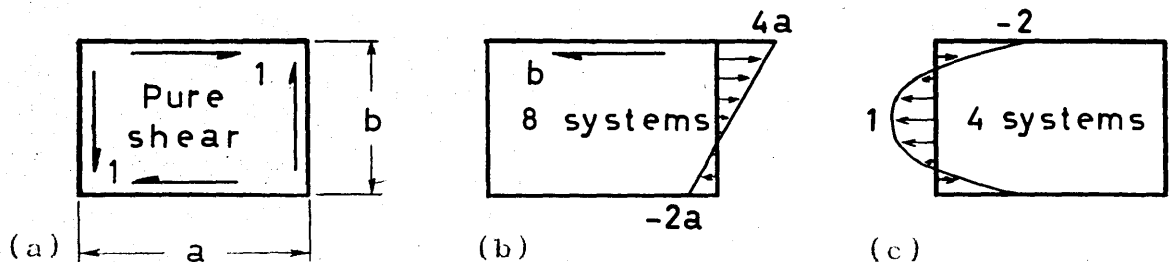
CRACKS IN RECTANGULAR PANELS

To demonstrate the feasibility of the direct analysis of crack growth a FORTRAN IV programme has been devised for flat rectangular reinforced sheet structures. The basic elements here are booms and shear panels which in our case require to carry direct stress also. Below we consider suitable generalised stresses and the corresponding flexibility for whole and cracked rectangular panels. We also discuss self-equilibrating systems and the load conditions to simulate a complete crack.

1. Generalised Stresses

For the boom we have used the normal model with two different loads at each end and a constant shear flow to maintain equilibrium. In the panels however there are mostly nine natural forces giving rise to membrane stresses.

These consist of the corner systems shown together with a uniform shear flow. For more refinement it is also possible to add the quadratic modes below and obtain a thirteenth order system. This would allow the stress to increase on both sides of a crack whereas a linear representation in a cracked element means that a tension on one end is matched by a compression on the other. This is not true in practice but the smaller set has been chosen because of limitations in computer storage.



To find general formulae for overall flexibility and to calculate changes in flexibility we require the internal stresses corresponding to these load systems. These can be found by assuming linear or quadratic decay of the direct stresses and considering the equilibrium at a general cross section. For the quadratic systems the differential equations of equilibrium are also needed. The results are shown below in terms of the non-dimensional coordinates ξ, η where the panel edges are $\xi = \pm 1$ and $\eta = \pm 1$. These stresses also satisfy the equations of compatibility so that they are exact.

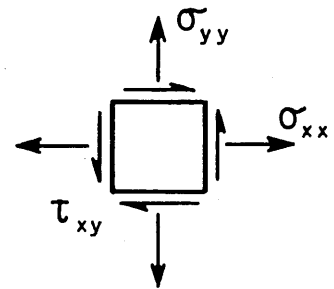
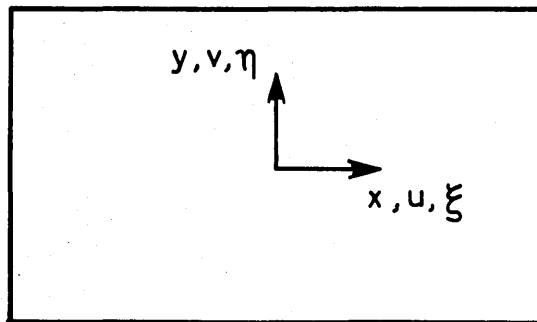


TABLE III

NATURAL LOADS AND DEFORMATIONS

(a) Pure Shear

$$\begin{aligned}\tau_{xy} &= 1 \\ (a+b)u &= \frac{1}{4} \eta(1+3\xi^2) \\ (a+b)v &= \frac{1}{4} \xi(1+3\eta^2)\end{aligned}$$

(b) Corner Load

$$\begin{aligned}\sigma_{xx} &= \frac{1}{2}a(1+\xi)(1+3\eta) \\ \sigma_{yy} &= 0 \\ \tau_{xy} &= \frac{1}{4}b(3\eta-1)(\eta+1) \\ 4ab u &= \frac{1}{2}(1+\eta) \left\{ 3\xi^2 \frac{2+\beta}{1+\beta} + 4\xi + \frac{\beta-2}{1+\beta} \right\} - \\ &\quad - \frac{1}{2} \frac{1}{1+\beta} \{ 3\xi^2 + 1 + 4\beta \} + 1 - \xi \\ 4ab v &= - \frac{3}{2(1+\beta)} (1-\eta^2)\end{aligned}$$

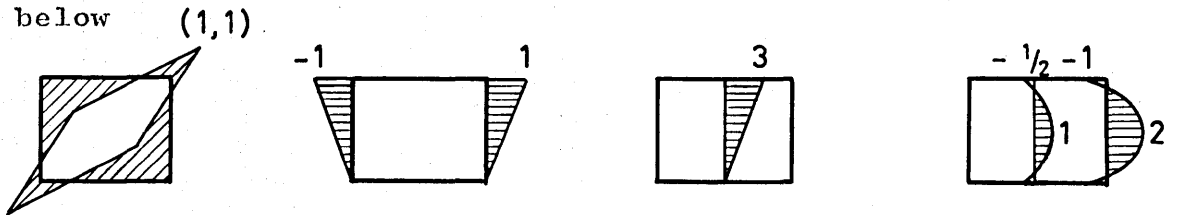
$$\text{where } \beta = b/a.$$

(c) Quadratic System

$$\begin{aligned}\sigma_{xx} &= \frac{1}{4}(1+\xi)^2(1-3\eta^2) \\ \sigma_{yy} &= \frac{1}{8} \beta^2(1-\eta^2)^2 \\ \tau_{xy} &= -\frac{1}{2}\beta\eta(1+\xi)(1-\eta^2) \\ 1.6bu &= (1+\xi)(1-3\eta^2+3(1-\xi)) \\ v &= 0\end{aligned}$$

Mirror images of the systems (b) and (c) are obtainable by putting $\xi, -\xi$ or $\eta, -\eta$ or both. Similarly rotations may be effected by interchanging σ_{xx}, ξ, a and u with σ_{yy}, η, b and v respectively. These variations lead to eight forms of (b) and four of (c), making up the total number of systems.

The natural modes were determined by the following standard method. They were first taken to be linear combinations of the four types of mode typified by those below



Algebraically

$$\rho_N = A \rho \quad (\rho \text{ given } \rho, \rho_N \text{ square}) \quad \dots (1)$$

and the problem becomes that of finding A . Consider the virtual work evaluated on the boundary

$$U = \int_S P \rho_*^t \, dS$$

where P, ρ_* are arbitrary forces and displacements which are respectively in equilibrium and compatible. However these are expressible as

$$\rho = C^t P_N \quad (P_N = \text{set of natural loads})$$

and

$$\rho_* = g^t \rho = g^t A^{-1} \rho_N$$

so that

$$\begin{aligned} U &= C^t \int_S P_N \rho_N^t \, dS \cdot A^{-t} g \\ &= C^t \int P_N \rho^t \, dS \cdot A^t \cdot A^{-t} g . \end{aligned}$$

In this expression $A^{-t}g$ may be regarded as the factor needed to obtain ρ_* from ρ_N . Since C and g are arbitrary

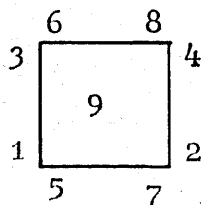
$$\int P_N \rho^t A^t dS = \int P_N \rho_N^t dS$$

and by definition the right hand side is diagonal. On the left this can be ensured by making

$$A^t = \left[\int_S P_N \rho^t dS \right]^{-1} \dots (2)$$

1.1 Flexibility

Because of the various symmetries the 9×9 flexibility matrix has elements falling into 10 categories and taking 14 separate values. For the 5×5 and 13×13 flexibilities the corresponding numbers are 5(8) and 15(22). The load systems for each of the ten categories are shown in Fig. 24. The calculation of each element of the flexibility is a tedious but simple task. It was shortened in the present instance by the use of a programme devised for checking the routine used to integrate the changes in flexibility caused by cracking. Three elements were calculated in detail from which it was apparent that every element consisted of terms in $a^3b/3Et$ and $ab^3/30Gt$ or similar ones with a and b exchanged. When the programme was working all the non-zero elements for a unit square were fitted with these quantities. The results for non-zero elements are shown in Table IV. If the natural loads are arranged in the order



$$\text{and } B = \begin{bmatrix} 1/3 & 1/6 \\ 1/6 & 1/3 \end{bmatrix}, \quad \theta = \begin{bmatrix} 1 & -1 \\ -1 & 1 \end{bmatrix}$$

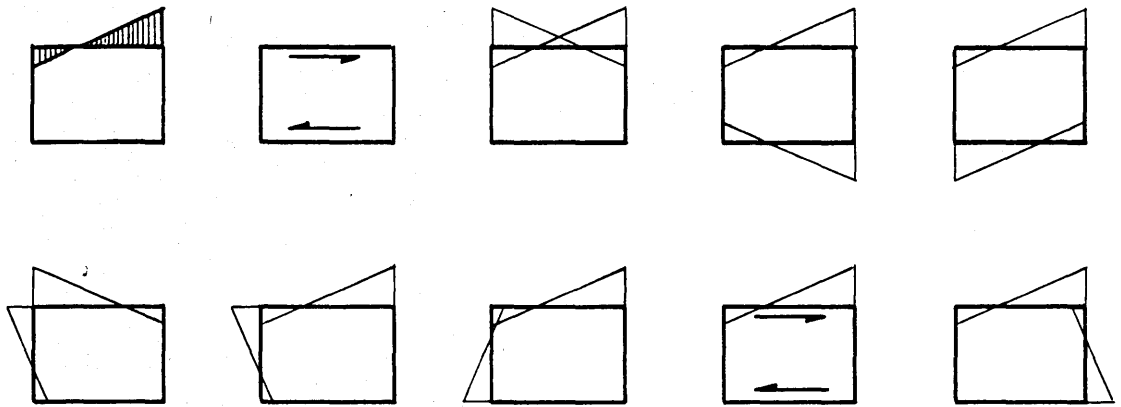


FIG. 24 TYPICAL FLEXIBILITY ELEMENTS

TABLE IV

NINTH ORDER FLEXIBILITY ELEMENTS

Natural Loads

Element of Flexibility



$$\frac{4a^3b}{3Et} + \frac{2}{15} \frac{ab^3}{Gt}$$



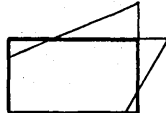
$$- \frac{2}{3} \frac{a^3b}{Et} + \frac{1}{30} \frac{ab^3}{Gt}$$



$$\frac{2}{3} \frac{a^3b}{Et} - \frac{2}{15} \frac{ab^3}{Gt}$$



$$- \frac{1}{3} \frac{a^3b}{Et} - \frac{1}{30} \frac{ab^3}{Gt}$$



$$- \nu \frac{a^2b^2}{Et}$$

Pure Shear

$$\frac{ab}{Gt}$$

then the complete flexibility takes the form

$$\begin{bmatrix} \frac{a^3 b}{Et} I_4 \\ \frac{ab^3}{Et} I_4 \\ 1 \end{bmatrix} + \begin{bmatrix} 4B & -2B & * & * \\ -2B & 4B & * & * \\ * & * & 4B & -2B \\ * & * & -2B & 4B \\ & & & 0 \end{bmatrix} + \begin{bmatrix} \frac{ab^3}{30Gt} I_4 \\ \frac{a^3 b}{30Gt} I_4 \\ ab/Gt \end{bmatrix} + \begin{bmatrix} 4\theta & \theta & & \\ \theta & 4\theta & & \\ & & 4\theta & \theta \\ & & \theta & 4\theta \\ & & & & 1 \end{bmatrix} \quad (3)$$

where the asterisks denote Poisson's ratio elements of $-\nu a^2 b^2 / Et$ and these 4×4 submatrices are filled out with zeros.

2.1 Crack Conditions

Let $\sigma_N(\xi, \eta)$ be the 9×3 matrix of the stresses listed in Table III while $P_N^{(9 \times 1)}$ refers to the magnitudes of the natural loads. Then the stresses across axes inclined at an angle ψ are

$$\begin{aligned} \sigma(\xi, \eta, \psi)^t &= \frac{1}{2} P_N^t \sigma_N \begin{bmatrix} 1 + \cos 2\psi & 1 - \cos 2\psi & -\sin 2\psi \\ 1 - \cos 2\psi & 1 + \cos 2\psi & \sin 2\psi \\ -2\sin 2\psi & 2 \sin 2\psi & 2 \cos 2\psi \end{bmatrix} \\ &= \frac{1}{2} P_N^t \sigma_N \psi(\psi)^t \quad \text{say,} \quad \dots (4) \end{aligned}$$

If we now have a crack at (ξ, η) , inclined at ψ then two of the total stresses on the left must vanish and after the coordinates (ξ, η) and ψ are substituted two columns of equation can be interpreted as conditions on P_N and identified with rows of B . Since σ consists of continuous functions (ξ, η) must lie on each of two curves along one of which the tangential shear vanishes while the other is a locus of zero transverse stress. These will be

called shear cracks and stress cracks and for a crack in the accepted sense they must coincide.

Suppose that the crack is defined by

$$\eta = \eta(\xi) \quad \dots \quad (5)$$

which also implies

$$\psi = \psi(\xi) \quad \dots \quad (5A)$$

Along the crack we can substitute (5), (5A) into (4) and when the result is expanded as a series in ξ the matrix of natural stresses becomes

$$\sigma_{\psi} = \sigma_0 + \xi \sigma_1 + \xi^2 \sigma_2 + \dots \quad \dots \quad (6)$$

where the notation indicates that the direction has been included. Each of these terms contributes two restrictions on P_N , arising like those at a single point.

For a straight crack ψ is constant and (6) contains just three terms so that six conditions can define the crack exactly. If quadratic systems are included the degree of (6) rises to 4, requiring 8 conditions. If (5) is quadratic and we use quadratic systems the degree of (6) is at least 8 so that even the thirteenth order systems cannot exactly represent curved cracks.

For straight cracks the coefficients in (6) can be found by finite difference techniques using stresses evaluated at each edge and at the centre. This is awkward however and in the programme we have chosen to use a maximum of six conditions. These are derived by a direct use of (4) which is evaluated at solution points of the crack-damage equations. Two of the points are near the edges and the third near the centre. If the crack is short compared with the panel width then only two points or four conditions are used as there is a possibility that conditions derived from nearby points

will resemble one another and lead to problems of ill-conditioning. At each point chosen the conditions are

$$\psi_c(\xi, \eta) \sigma_N^t(\xi, \eta) P_N = 0 \quad \dots \quad (7)$$

ψ_c being the relevant rows of ψ . This collocation method can be used for curved cracks as well and ensures that the shear cracks and stress cracks are tangential at two or three points which in practical terms makes them fairly close along the whole length. Since they can be exactly simulated all possible conditions for straight cracks must be equivalent and therefore the collocation method becomes exact.

2.2 Cut Corners and Averaged Conditions

It is possible that a crack following a diagonal course will have entered three panels during an integration step, cutting the corner of an intermediate panel. In the absence of other information the intermediate crack must be assumed to be a straight line, requiring six conditions.

However the contributions of some natural loads to the stresses originally across the crack may be small and the three collocation points unavoidably close, leading to ill-conditioning. Accordingly only three conditions are specified for these cases, nullifying the total loads transmitted in each direction and the total moment.

From (4) the average normal and shear stresses across the crack are

$$\frac{\cos \psi}{(\xi_2 - \xi_1)} \int_{\xi_1}^{\xi_2} \begin{bmatrix} \psi_2 \\ \psi_3 \end{bmatrix} \sigma_N^t P_N \frac{d\xi}{\cos \psi}$$

while the moment depends linearly on

$$\int_{\xi_1}^{\xi_2} \psi_2 \sigma_N^t P_N \xi d\xi$$

The three corresponding rows of B are

$$B' = \frac{1}{(\xi_2 - \xi_1)} \int \begin{bmatrix} \psi_2 \\ \psi_3 \\ (\xi - \bar{\xi})\psi_2 \end{bmatrix} \sigma_N^t d\xi$$

$\bar{\xi}$ being the position of the resultant load. The term in $\bar{\xi}$ is equivalent to the first row however and may therefore be ignored.

With the assumed straight crack the integrands here are respectively quadratic and cubic and exact integrals are obtainable by the 3/8 rule for numerical integration. When this applied

$$B' = \frac{1}{8} \left\{ \begin{bmatrix} \psi_2 \\ \psi_3 \\ -\frac{1}{2}\psi_2 \end{bmatrix} \sigma_N^t \Big|_{\xi_1} + 3 \begin{bmatrix} \psi_2 \\ \psi_3 \\ -\frac{1}{6}\psi_2 \end{bmatrix} \sigma_N^t \Big|_{\xi_2} + 3 \begin{bmatrix} \psi_2 \\ \psi_3 \\ \frac{1}{6}\psi_2 \end{bmatrix} \sigma_N^t \Big|_{\xi_3} + \begin{bmatrix} \psi_2 \\ \psi_3 \\ \frac{1}{2}\psi_2 \end{bmatrix} \sigma_N^t \Big|_{\xi_4} \right\} \dots (8)$$

where $\xi_i = \xi_1 + (i-1)(\xi_4 - \xi_1)/3$.

The deleted loads, replaced by $B' P_N$, are here the two systems on the relevant corner and one other. As the panel is likely to remain effective in shear for small cuts the best third deletion is probably one of the loads on an adjacent corner.

2.3 Choice of Deleted Loads

In (7) each column of $\psi_c \sigma_N^t$ represents the normal and shear stress at (ξ, η) arising from unit value of the relevant generalised load in the absence of a crack. Following the principle suggested in Chapter VI we delete from P_N and S those loads corresponding to the largest elements of $\psi_c \sigma_N^t$. In our formulation of the natural loads unit corner loads are proportional to the adjacent sides and unit shear is constant or non-dimensional. Thus for physical consistency "largest" must be interpreted in relation to the maximum value in the panel of unit natural stress.

The panel remains fully effective for carrying load (for our purpose here) until completely crossed by the crack at which time the conditions are found and the corresponding loads deleted. In the programme, as suggested above, each panel leads to three, four or six conditions and the last indicates that a crack joins two opposite sides. In these circumstances the panel is unlikely to bear a large amount of pure shear and this load is therefore included among the deletions.

3.0 Self-Equilibrating Systems

These fall into five different classes, for reinforced structures, which are shown in the next figure. To derive them we begin by finding the order of redundancy.

Consider the fully reinforced structure of Fig.32 with booms around the edge and between all panels. Then

$$\text{No. of booms} = \alpha(\beta+1) + \beta(\alpha+1)$$

$$\text{No. panels} = \alpha\beta$$

$$\text{No. joints} = (\alpha+1)(\beta+1), \text{ including external joints.}$$

Thus

$$\text{Total no. of forces} = 2(\alpha(\beta+1) + \beta(\alpha+1)) + 9\alpha\beta$$

For each boom there is one longitudinal equation of equilibrium and two transverse which may also be regarded as conditions between adjacent panels. With the two conditions for each joint

$$\text{No. conditions} = 3(\alpha(\beta+1) + \beta(\alpha+1)) - 2(\alpha+1)(\beta+1).$$

Having natural loads the panels are automatically in equilibrium and when overall equilibrium is allowed for

$$\begin{aligned} \text{Redundancy } r &= 5(\alpha-1)(\beta-1) + 2(\alpha+\beta-2) \\ &= 5 \text{ (Internal joints) + (External joints} \\ &\quad \text{not on corners)} \end{aligned}$$

When there is no reinforcement this becomes

$$r = 3(\text{Internal joints})$$

The smallest redundant reinforced structure has two bays and an appropriate system is shown in Fig.25(a). When there are four bays in a square there are eight such systems and it is also possible to form the standard cover redundancy based on pure shear in the panels. This completes the total and for reinforced structures these two types are sufficient.

The second type of redundancy in unreinforced structures must also involve pure shear but in this case there are no booms to "mop up" the shear flows which must therefore be reacted by corner loads. When this is done

the system of Fig. 25(e) is obtained, analogous to the standard cover system.

It is now possible to find the order of redundancy for any structure of this type by counting self-equilibrating systems at each joint. It was found expedient to use the pure shear system of Fig. 25(e) for all degrees of reinforcement in order to have a uniform procedure.

4.0 Natural loads for Moving Element

In Chapter VI it was shown that the effect of a crack tip on the overall flexibility could be accounted for by a knowledge of the strain energy and natural forces on a standardised moving element M within which the stress pattern is appropriate to a crack tip. We now consider M more closely, beginning with its specification.

4.1 Form of M

The form of M is arbitrary but if it is to best serve its purpose of allowing separate considerations of the crack tip there are several plausible conditions to be met.

The first is that M should cover the region where the idealised type of stress system becomes inadequate. In turn this implies that M should be roughly the same size as the panels containing it. We have also chosen to make it the same shape and of such a nature that it is possible for M to coincide with one of the ordinary panels. If the orientation of M is kept the same also this simplifies the interpolation matrix. For triangular elements these considerations become more difficult.

For rectangular elements we are thus led to the moving element which is rectangular and can contain a

crack in any direction, (Fig. (26)). The standard element has unit area and to optimise the tip position it is moved about the asymptotic stress field of Westergaard ($K=2\pi$) until the strain energy is a maximum (μ of Ch. VI Sec.3.3).

4.2 Strain Energy of Cracked Panel

The notation used is shown in Fig. 26 (a) and as the figures imply it is convenient to rotate the panel rather than the crack. We find the strain energy in each of the triangles subtended by the sides 12, 23, etc.

From the asymptotic stress field (Chapter III)

$$\begin{aligned}\sigma_{Ny} &= \frac{K}{\sqrt{2\pi r}} \left\{ \cos \frac{\theta}{2} + \frac{1}{2} \sin \theta \sin \left(\frac{3\theta}{2} - 2\psi \right) \right\} \\ \sigma_{Nx} &= \frac{K}{\sqrt{2\pi r}} \left\{ \cos \frac{\theta}{2} - \frac{1}{2} \sin \theta \sin \left(\frac{3\theta}{2} - 2\psi \right) \right\} \\ \tau_N &= \frac{K}{\sqrt{2\pi r}} \frac{1}{2} \sin \theta \cos \left(\frac{3\theta}{2} - 2\psi \right) \quad \dots (9)\end{aligned}$$

Putting $\psi = \theta$ we obtain the polar stresses and from these the element of strain energy appears as

$$E dU = \frac{K^2}{4\pi} dr d\theta \{ (1+\cos \theta)(3-\cos \theta) - (1+\cos \theta)^2 \} .$$

Now rotate the axes and put

$$\theta = \varphi + \psi .$$

After this we expand the energy integrals in terms of $\sin \varphi$ and $\cos \varphi$ and integrate over each triangular region

Thus

$$E U_{12} = \int_{\varphi_1}^{\varphi_2} \int_0^{h_+/\sin \varphi} (\dots) dr d\varphi$$

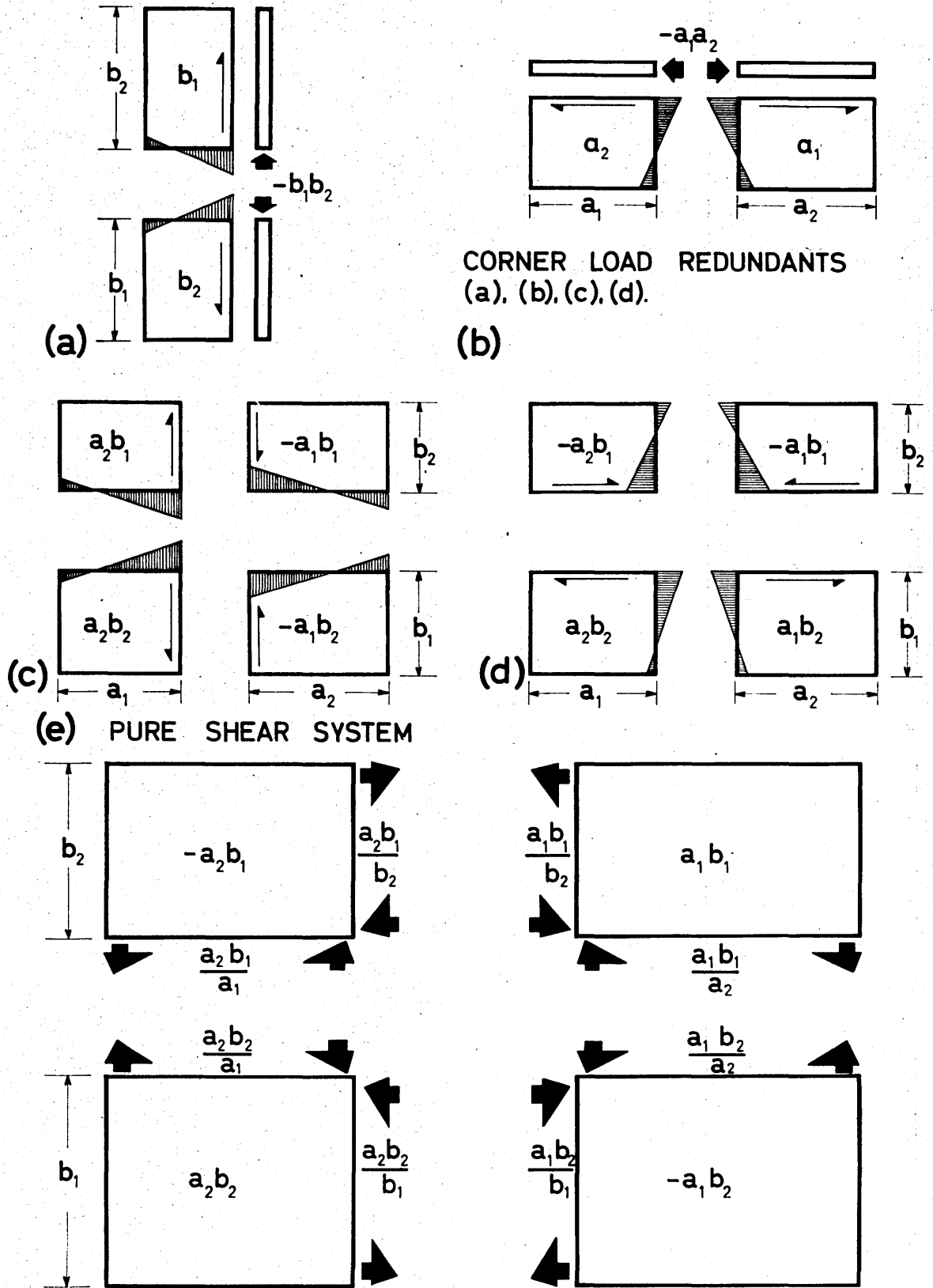


FIG. 25 REDUNDANT SYSTEMS FOR PANELS.

$$= \frac{K^2}{4\pi} \int_{\varphi_1}^{\varphi_2} \frac{h_+}{|\sin \varphi|} \{ \quad \} d\varphi \quad \dots (10)$$

after substituting for the energy and integrating. The only other type of integral is similar with the factor $1/|\cos \varphi|$.

The only unusual integrals arising from (10) or the other integrals are

$$\int \frac{d\varphi}{|\cos \varphi|} \quad \text{and} \quad \int \frac{d\varphi}{|\sin \varphi|}$$

which through the substitution $t = \tan \frac{1}{2}\varphi$ prove to be

$$s(\varphi) \log \tan \frac{1}{2}\varphi \quad \text{and} \quad c(\varphi) \log \frac{(1 + \tan \frac{1}{2}\varphi)}{(1 - \tan \frac{1}{2}\varphi)} \quad \text{respectively,}$$

$$\text{where} \quad s(\varphi) = |\sin \varphi| / \sin \varphi$$

$$\text{and} \quad c(\varphi) = |\sin \varphi| / \cos \varphi.$$

The energy of each type of triangle turns out to be typified by

$$\begin{aligned} h_+ H_{12} = & s(\varphi) \frac{K^2 h_+}{2\pi} \left| \left| \frac{1}{4} \log \frac{\tan \frac{1}{2}\varphi_2}{\tan \frac{1}{2}\varphi_1} \cdot [5 - 3\nu - (1 + \nu) \cos 2\psi] \right. \right. \\ & + (1 - \nu) \cos \psi \log \frac{\sin \varphi_2}{\sin \varphi_1} - (1 - \nu) \sin \psi (\varphi_2 - \varphi_1) \\ & - \frac{1}{2} (1 + \nu) \cos 2\psi (\cos \varphi_2 - \cos \varphi_1) \\ & \left. \left. + \frac{1}{2} (1 + \nu) \sin 2\psi (\sin \varphi_2 - \sin \varphi_1) \right| \right| , \quad \dots (11) \end{aligned}$$

for these beside the crack, and

$$\begin{aligned}
w_+ U_{41} = c(\varphi) \frac{K^2 w_+}{2\pi} & \left\| \left\| \frac{1}{4} \log \frac{(1 + \tan \frac{1}{2} \varphi_1)(1 - \tan \frac{1}{2} \varphi_4)}{(1 - \tan \frac{1}{2} \varphi_1)(1 + \tan \frac{1}{2} \varphi_4)} [5 - 3\nu + (1 - \nu) \cos 2\psi] \right. \right. \\
& + (1 - \nu \sin \psi \log \frac{\cos \varphi_1}{\cos \varphi_4} + (1 - \nu) \cos \psi (\varphi_1 - \varphi_4) \\
& - \frac{1}{2} (1 + \nu) \cos 2\psi (\sin \varphi_1 - \sin \varphi_4) \\
& \left. \left. - \frac{1}{2} (1 + \nu) \sin 2\psi (\cos \varphi_1 - \cos \varphi_4) \right\| \right\| \dots \quad (12)
\end{aligned}$$

for the triangles cut by the crack or by its extension. The total strain energy is therefore

$$U = (h_+ U_{12} + h_- U_{34}) + (w_+ H_{41} + w_- U_{23}) \dots \quad (13)$$

This procedure extends to any type of polygon if ψ is appropriately varied for the triangles subtended by each side. For triangles h_+ etc. are replaced by the homogeneous triangular coordinates of the tip position.

4.3 Computation of Generalised Stresses

Unfortunately, when the normal and tangential stresses represented by (9) are substituted into the scalar product of (4.30) the presence of factors $(\sin \varphi)^{-\frac{1}{2}}$ or $(\cos \varphi)^{-\frac{1}{2}}$ excludes the possibility of a closed form for Σ .

It is therefore necessary to integrate numerically and over each side a four point Gauss-Legendre⁷² formula is used. Unlike the strain energy μ , found in the programme by an empirical formula, Σ is calculated afresh for each crack step by a special subroutine. This incorporates the integration formula whose coefficients are premultiplied by values of the various natural modes. (Actually, before integration these modes are first de-

composed into various symmetric and antisymmetric components and reassembled afterwards.)

The components of Σ depend on the optimum tip position whose computation is now described.

4.4 Optimum Tip Position

Superficially the problem here is to maximise (13) with respect to h_+ and w_+ with

$$h_- = b - h_+ \quad \text{and} \quad w_- = a - w_+$$

but a straightforward application to (11) and (12) soon becomes intractable.

In Fig. 26 (b) we have considered directly the effect of small rigid body movements parallel to one side, denoted by dh in the figure. Now let

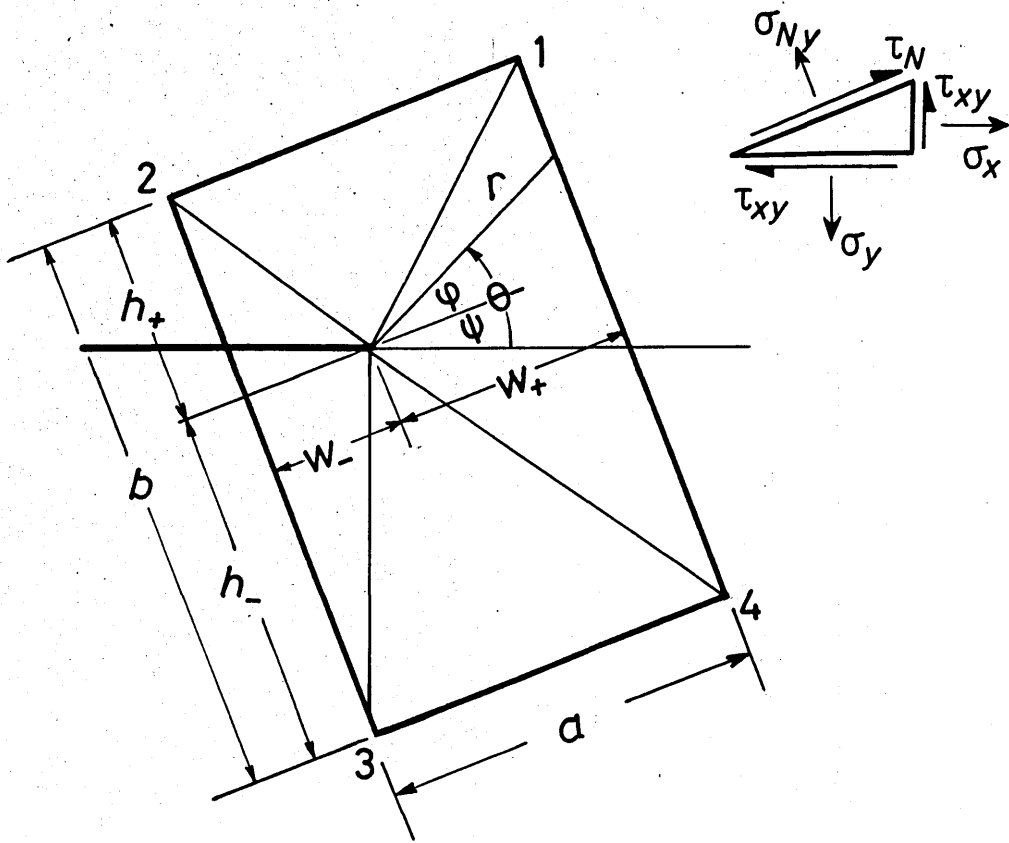
$$h_+ \rightarrow h_+ + dh \quad \text{and} \quad h_- \rightarrow h_- - dh$$

in (13). In the figure the angles determining U_{12} etc. are the same and therefore the new region of integration is represented by the lightly hatched triangles and by the two original triangles corresponding to w_+ and w_- . Compared with the shifted panel this region is excessive by the (signed) sum of the four heavily hatched triangles. But this area is of second order in dh so that from (13), to the first order,

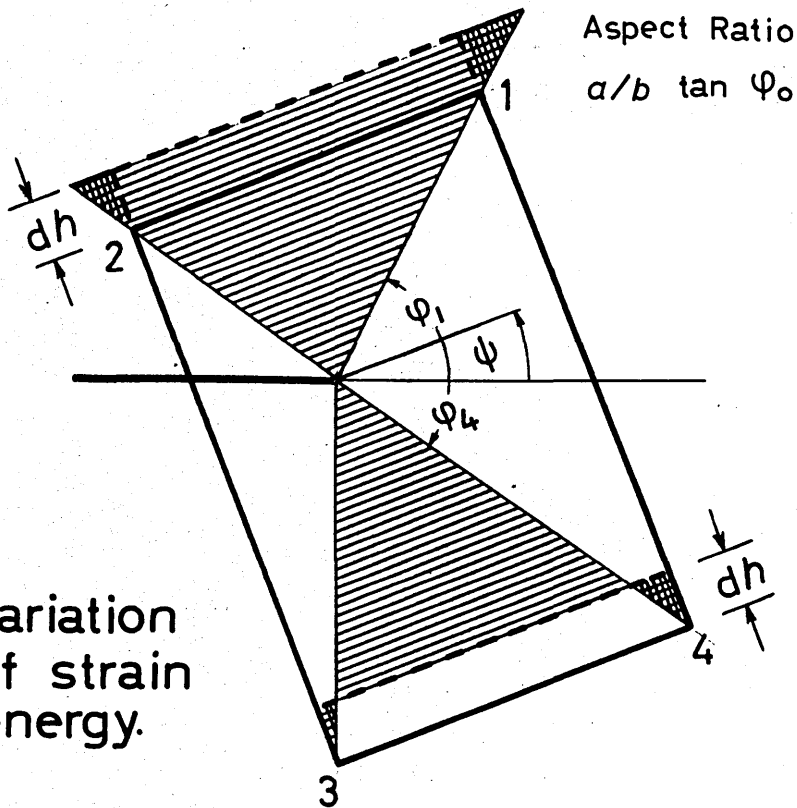
$$\frac{\partial U}{\partial h} = U_{12} - U_{34}$$

for rigid body movements. A similar equation holds for w and the maximum is given by

$$\begin{aligned} U_{12} &= U_{34} \\ U_{23} &= U_{41} \end{aligned} \quad \dots (14)$$



(a) Notation



(b) Variation of strain energy.

FIG. 26 GEOMETRY OF MOVING ELEMENT

while $U_{\max} = aU_{12} + bU_{23}$.

The unknowns here are $\varphi_1, \dots, \varphi_4$ and the other equations required define the aspect ratio and express the fact that the panel is rectangular. The equations (14) were solved numerically by a FORTRAN IV programme whose flow diagram is shown in Fig. 27. The algorithm used was essentially Newton's method in two dimensions but the gradients were replaced by finite differences calculated from a grid of fixed size, placed at the current estimate. At each iteration the angles φ_i for the three points are recalculated, maintaining the aspect ratio and right-angled corners (Appendix B).

Fig. 26(b) is easily generalised and for a k-sided polygon (14) becomes

$$\sum_{i=1}^k U_{i \ i+1} \frac{\sin \psi_{i \ i+1}}{\cos \psi_{i \ i+1}} = 0 \quad (k+1 = 1)$$

where $\psi_{i \ i+1}$ is the angle between the crack and side (i, i+1).

4.41 Results

For eleven aspect ratios (or 21 if the inverses are counted) the loci of optimum tip positions have been plotted in Fig. 28. For reasonable panels these resemble ellipses slightly flattened at the "corners".

In the notation of Fig. 30, if they are parametrically represented as

$$\begin{aligned} \xi - \frac{1}{2} &= a \cos \theta \\ \eta - \frac{1}{2} &= b \sin \theta \end{aligned}$$

then $\psi \approx \theta \dots (15)$

The axes depend on the aspect ratio expressed in the form

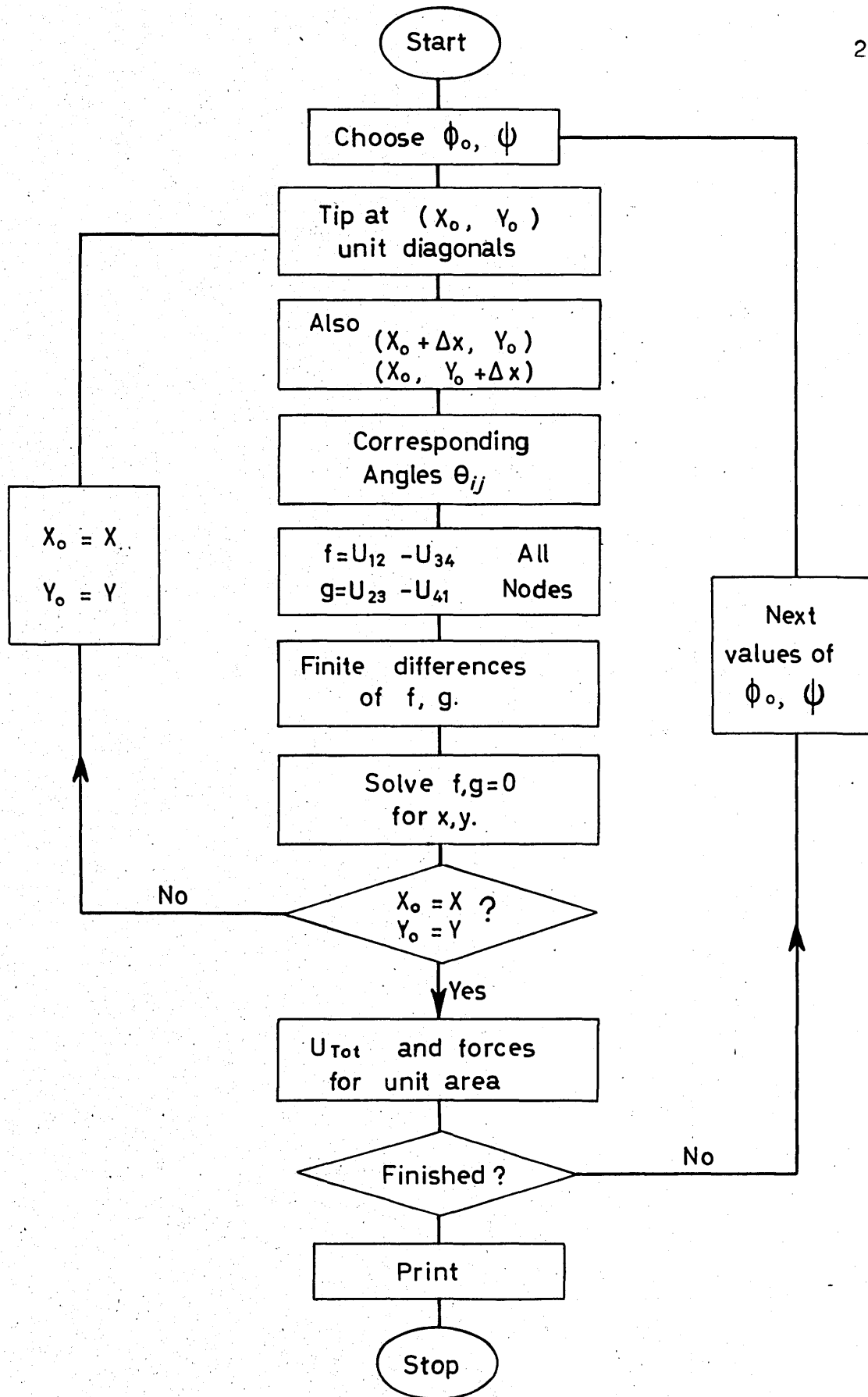


FIG. 27 MAXIMISATION OF PANEL STRAIN ENERGIES.

PANELS OF
UNIT AREA

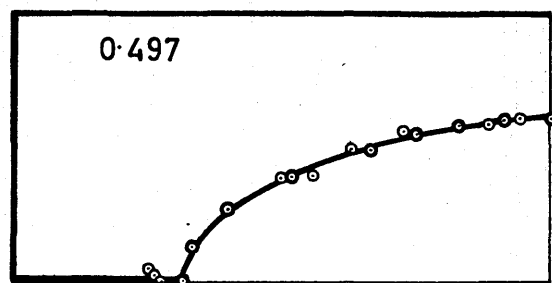
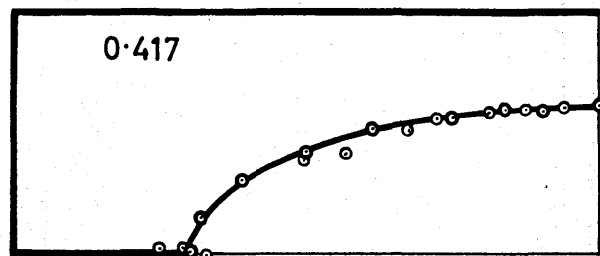
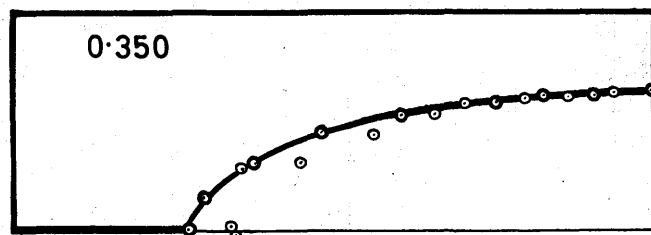
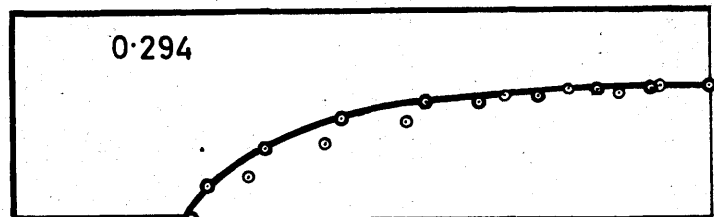
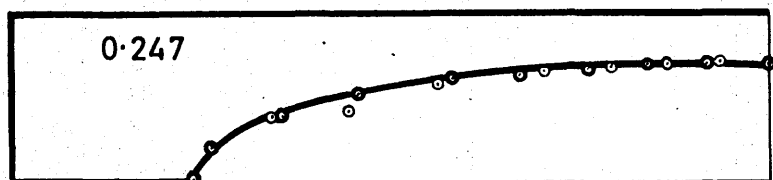
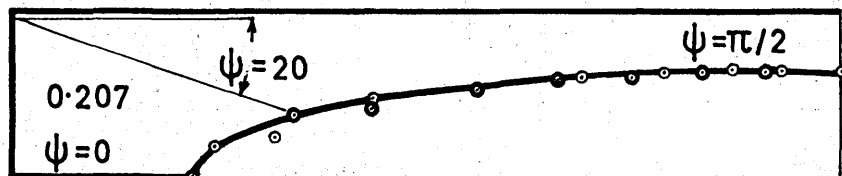
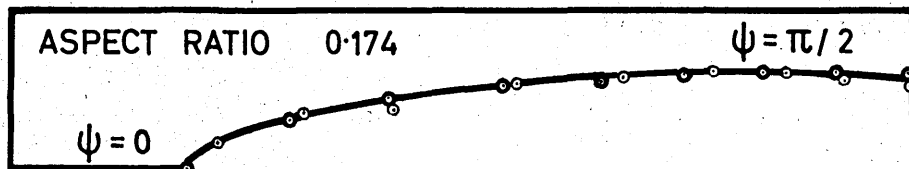
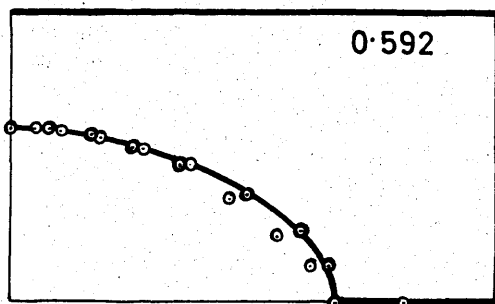
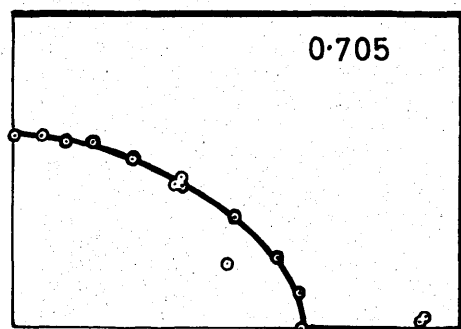
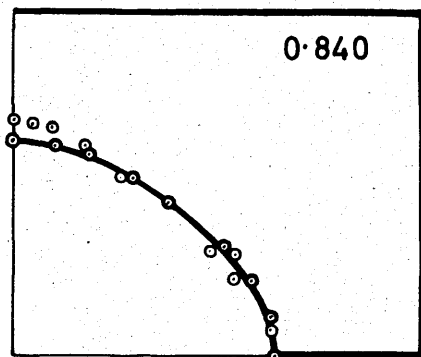
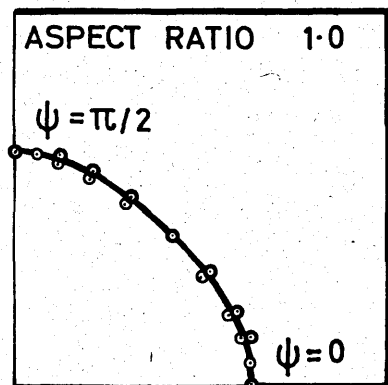


FIG.28 LOCI OF OPTIMUM TIP POSITIONS

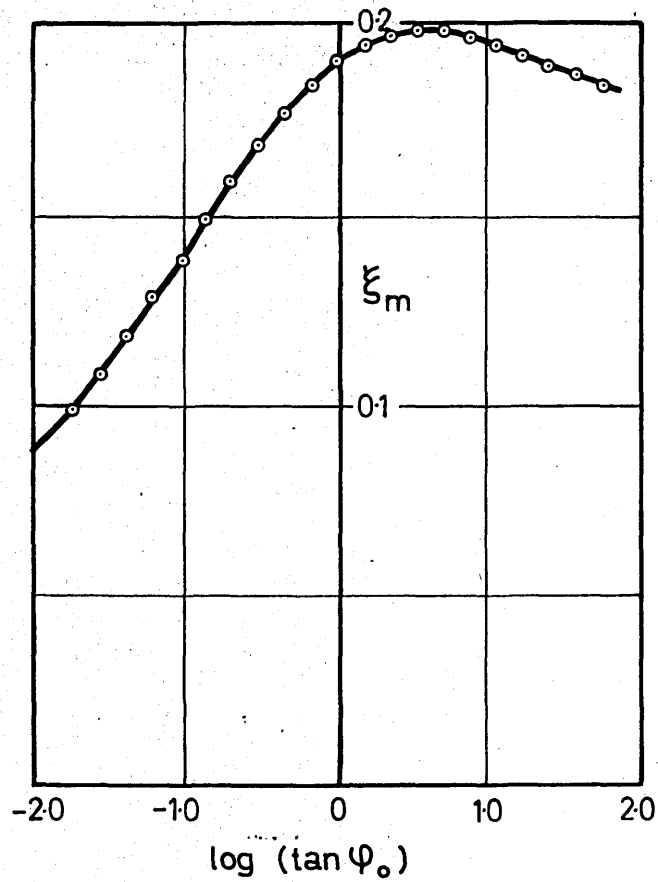


FIG. 29 POSITION OF MAJOR AXES MEASURED FROM EDGE OF PLATE

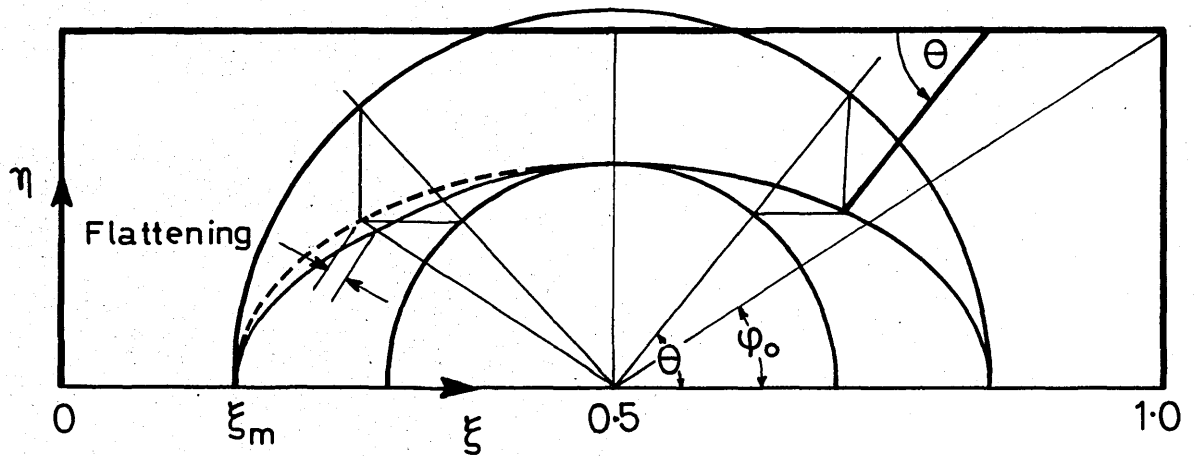


FIG. 30 GEOMETRY OF OPTIMUM TIP POSITION AND CALCULATION OF FLATTENING

$$x = \log \tan \varphi_0$$

and empirical formulae for a and b are

$$a = 0.5 - P(x)$$

$$b = 0.5 - P(-x)$$

where

$$P(x) = 0.189\ 953 + 0.028\ 583 x - 0.023\ 407 x^2 - 0.001\ 491 x^3 + 0.002\ 391 x^4 \dots \quad (16)$$

For the flattening, let us suppose that it arises by a reduction of the semi-axes;

$$a \rightarrow a F(\theta), \quad b \rightarrow b F(\theta)$$

where $F(\theta)$ has a period $\pi/2$. From the construction shown in the figure we have the approximate result

$$F(\theta) = 0.96 + 0.04 \cos 4\theta.$$

To summarise, the locus of optimum positions for the standardised panel can be approximated as

$$\begin{aligned} \xi - \frac{1}{2} &= -(0.96 + 0.04 \cos 4\psi) \cdot \left(\frac{1}{2} - P(x)\right) \cos \psi \\ \eta - \frac{1}{2} &= (0.96 + 0.04 \cos 4\psi) \cdot \left(\frac{1}{2} - P(-x)\right) \sin \psi, \end{aligned} \quad (17)$$

$P(x)$ being given by (16). The negative sign in the first equation agrees with a standard crack extending in the direction of positive ξ . For a square panel and the four nearest aspect ratios the average corresponding to $(0.96 - 0.04)$ is actually 0.9228.

4.5 Maximum Strain Energies

The values of μ corresponding to the optimum positions above have been plotted in Fig. 31 in terms of aspect ratio for crack angles of 0, 20 and 40 degrees

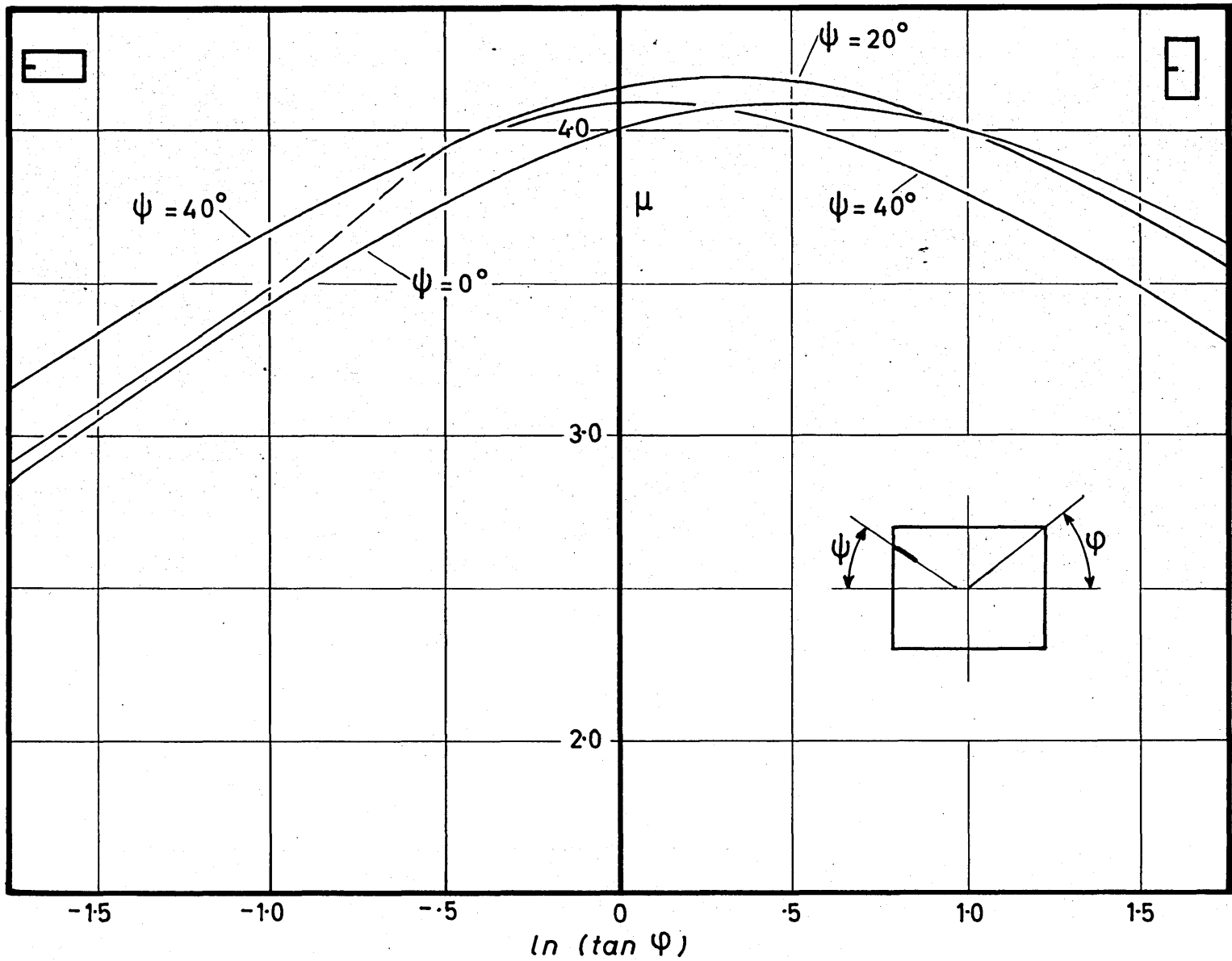


FIG. 31 VALUES OF MAXIMUM STRAIN ENERGY
(panel of unit area and thickness)

which are enough to allow estimates for the whole range of practical values.

For cracks parallel to one side ($\psi = 0^\circ$ or 90°) the empirical form is

$$\mu = Q(x) \quad (x = \log \tan \varphi_0)$$

where

$$Q(x) = 3.993\ 907 + 0.317\ 543\ x - 0.291\ 603\ x^2 \\ - 0.033\ 219\ x^3 + 0.013\ 965\ x^4 \quad \dots \quad (18)$$

but for other crack angles the accuracy of a polynomial form of this degree cannot be maintained. If μ is assumed to vary sinusoidally with ψ then within the range $-1.75 \leq x \leq 1.75$ the resultant expression

$$\mu = Q(x) \cos^2 \psi + Q(-x) \sin^2 \psi \quad \dots \quad (19)$$

is accurate within 4%. By Paris' fourth power law the error in crack rate would be about twice this if (19) were used.

The kink in the curve for $\psi = 20^\circ$ is probably associated with the corner of the panel crossing the region of high strain energy radiating from the crack tip, along which yielding first occurs. Owing to problems of convergence reliable values could not be found for this region and the curve is shown dotted.

By cross plotting Fig. 31 with numerical aid two correction terms were found for (19) which reduce the error beyond 0.02. These terms are

$$\mu_\Delta = 0.077\ 563 \sin^2 2\psi \exp(-1.25816\ x^2) \\ + 0.106\ 809 \sin^2 4\psi \exp(-0.97536\ x^2), \dots \quad (19A)$$

to be added to (19).

Chapter VIII

INTERPOLATION AND PROGRAMME STRATEGY

So far we have described the general two-stage fatigue problem and outlined one application to reinforced structures by means of matrix force methods. In applications there remains a large amount of detailed description of crack movements and the calculation of the interpolation matrix. In addition there are the standard operations involved in the primary stressing, integration of the crack damage equations and the calculation of crack rates, damage rates and the modified loads. This has been programmed in FORTRAN IV for the IBM 7090 at Imperial College and some of the methods particular to our type of force analysis have been described in general terms. The relevant sections are asterisked and may be omitted without loss of continuity.

It was found convenient to use two overall systems of coordinates and two local systems. The overall systems and the structure are shown in Fig. 32. The normal axes (x,y) are used for following cracks, finding boom lengths etc. in floating point numbers while the second set, called lattice coordinates, are essentially a two-way listing of each joint, beginning with $(1,1)$. The loads are listed in cells of 13, each in the standard order

$$\left\{ \begin{array}{l} 2 \text{ x-boom} \\ \text{loads} \end{array} \right. ; \begin{array}{l} 9 \text{ panel loads in standard order} \\ \end{array} ; \begin{array}{l} 2 \text{ y-boom} \\ \text{loads} \end{array} \left. \right\}$$

As shown each cell is related to lattice coordinates (i_x, i_y) which are integral or fixed point numbers.

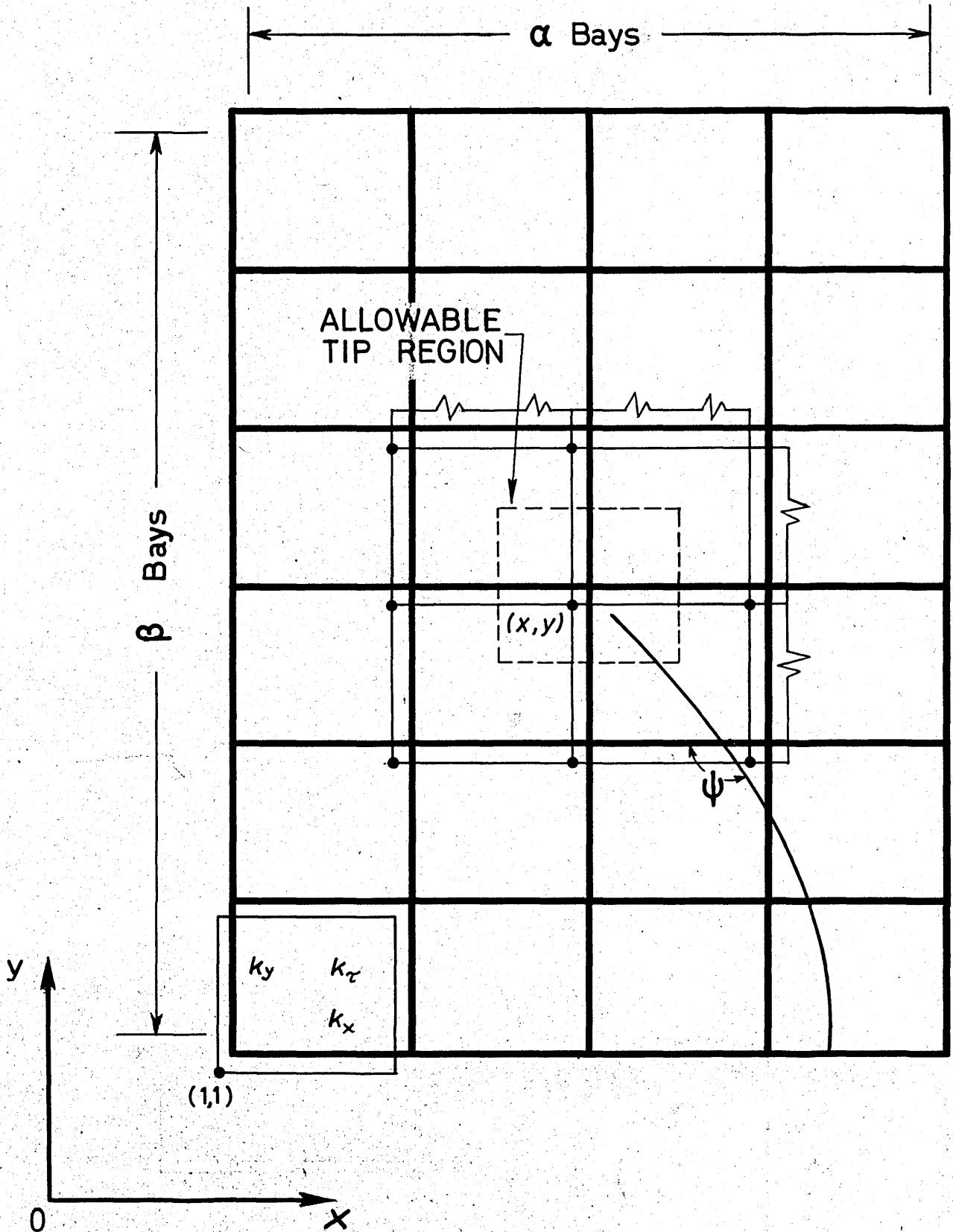
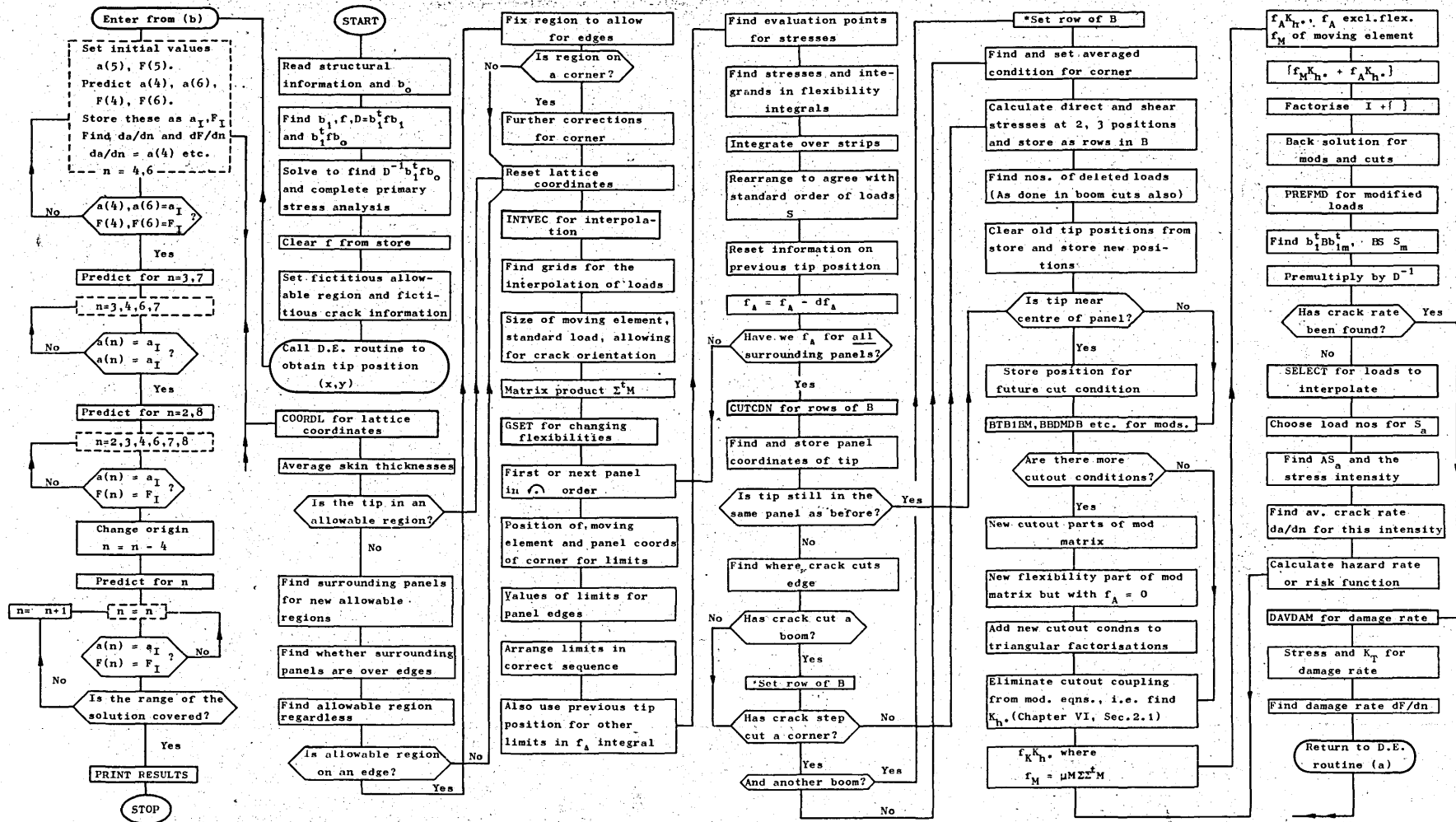


FIG. 32 LATTICE COORDINATES AND LOAD CELLS



(a) Predictor-corrector integration of d.e.s

(b) Primary structural analysis, modifications, stress intensities, and damage rates.

FIG. 33 SOLUTION OF CRACK-DAMAGE EQUATIONS

1.0 Main Programme

Fig. 33 shows flow diagrams for the main operations in solving a fatigue problem for our rectangular structure. In the small diagram the block CORRECT, normally relating to evaluation of a function, now contains instructions to modify the loads and the structure, calculate average rates and damages and then to use these for the correction in the routine for the differential equation. The predictions are made in the normal manner by finite difference methods but for a crack a two-dimensional method is needed.

2.1 General Crack Step

The immediate output of the crack-damage equations is an increment of crack length without direct indication of the new tip position which is now considered. In the course of computation one stores values of a, x, y at each step and each of these can be individually predicted. In the correction we must now make sure that a or (x, y) remain consistent while the crack follows the principal stress trajectory. (We follow the results of Cox and Field⁸⁰ and assume that a crack follows one of the trajectories present before its extension.)

Suppose that small segments of the crack path are parabolic and consider the locus of a fixed length l of the curve

$$y = a x^2; \quad dy/dx = 2ax = 2y/x.$$

It can be shown that

$$l = \frac{x^3}{4y} \left[u + \frac{1}{2} \sinh 2u \right] \quad (\sinh u = 2y/x)$$

when a is eliminated. When l is fixed this is an implicit form of the required locus which can be further reduced to the form

$$l = \frac{1}{2}x \left(\frac{u}{\sinh u} + \cosh u \right).$$

In terms of $t = \sinh u$ this can be expanded as

$$l = x \left(1 + \frac{1}{6} t^2 + \frac{3}{20} t^4 + \frac{30}{7(64)} t^6 + \dots \right) \dots \quad (1)$$

Now t is also the gradient which can be estimated from the principal stress trajectories at the current and previous tip positions. If l is known then x can be found from (1), $y = \frac{1}{2}xt$, and the trajectory at the improved tip position (x,y) then furnishes t for another iteration. In practice if (x,y) is also predicted convergence is rapid.

2.2 *Quadrature with Mixed Quantities

In the calculation of covariance the derivatives are not stored. From the correction stage of the differential equation routine however we do obtain a derivative y'_i say.

We must now integrate y' over the interval $((i-1)h, ih)$ to find y_i , h being the size of the equal intervals of time or cycles. Choosing more convenient subscripts, suppose we are given y_{-1}, y_0 and y'_1 and assume that

$$\begin{aligned} y &= ax^2 + bx + c \\ y' &= 2ax + b. \end{aligned} \quad \dots \quad (2)$$

From the two values and the derivative one obtains the equations

$$\begin{bmatrix} 1 & -1 \\ 2 & 1 \end{bmatrix} \begin{bmatrix} h^2 a \\ hb \end{bmatrix} = \begin{bmatrix} y_{-1} & -y_0 \\ & hy'_1 \end{bmatrix}$$

leading to

$$y_1 = y(h)$$

$$= \frac{1}{3} [-y_{-1} + 4y_0 + 2hy'_1]$$

when the solution is substituted into (2). The same procedure can be used to find a four point formula expressible in the form

$$y_3 = \frac{1}{11} [2y_0 - 9y_1 + 18y_2 + 6hy'_3].$$

3.1 Interpolation of Loads

The interpolation routines were made applicable to any structure which could be regarded as a set of quadrilateral panels through the use of lattice coordinates. In these non-dimensional terms the moving element is also a unit square contained in four surrounding panels as in Fig. 32. In local lattice coordinates let these squares lie between the limits

$$-1 \leq \xi, \quad \eta \leq 1.$$

In one dimension if the load $S(\xi)$ varies quadratically then

$$S(\xi) = S_0 + \frac{1}{2}(\Delta^2 \xi^2 + \Delta \xi) \quad \dots (3)$$

where

$$\Delta = -S_{-1} + S_1$$

$$\Delta^2 = S_{-1} - 2S_0 + S_1$$

in an obvious notation. In matrix form this expression may be regarded as a scalar product

$$\frac{1}{2}(\Delta^2 \xi^2 + \Delta \xi + \Delta^0)^t \{S_{-1} S_0 S_1\} \quad \dots (4)$$

where

$$\begin{aligned} \Delta^2 &= \{1 \ -2 \ 1\} \\ \Delta &= \{-1 \ 0 \ 1\} \\ \Delta^0 &= \{0 \ 2 \ 0\}. \end{aligned}$$

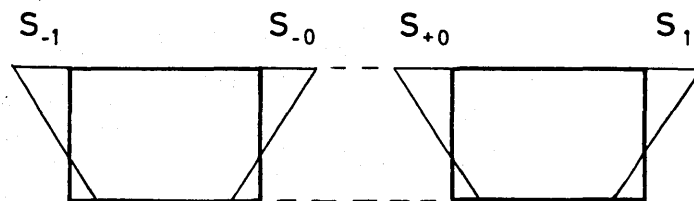
The vector of differences in (4) is a particular case of the interpolation matrix M described previously and with appropriate zeros it can be expanded to formally conform with the complete load matrix S .

In two dimensions⁸¹, with $S(\xi, \eta)$, one can first interpolate with respect to ξ for $\eta = -1, 0$ and 1 in succession. These three values can then be interpolated with respect to η . Now suppose the loads $S(-1, -1) \dots, S(1, 1)$ to be arranged on a 3×3 grid, as they appear in the structure. Then the corresponding elements in the row of the interpolation matrix can be arranged in a similar way (like the stencils used in relaxation methods) and when this is done for the two-way interpolation above it will be found that the grid elements have the form,

$$\frac{1}{4}(\Delta^2 \eta^2 + \Delta \eta + \Delta^0)(\Delta^2 \xi^2 + \Delta \xi + \Delta^0)^t, \quad \dots (5)$$

forming the non-zero elements for one row of M . The proof follows from a comparison of the two-way interpolation with (4), regarding the interpolation matrix there as a 3×1 grid.

The generalised stresses are conceivably discontinuous and the interpolation of (4) is actually over four stresses such as



for which the difference matrices are expanded to

$$\begin{aligned} \Delta^2 &= \{ 1 \quad -1 \quad -1 \quad 1 \} \\ \Delta &= \{ -1 \quad 0 \quad 0 \quad 1 \} \\ \Delta^0 &= \{ 0 \quad 1 \quad 1 \quad 0 \} , \end{aligned}$$

again used as in (5). This equation is used for each load corresponding to an element of Σ (Chapter VI) the standard loads on the moving element. The problem of choosing the interpolation points (ξ, η) is now considered.

3.2 Imbedding of Moving Element

We have previously stated that a moving element M which can coincide with actual panels is advantageous. Consider the four panels containing M. For a given crack orientation ψ , each of them contains a point which would be the optimum tip position if M were the panel in question. The four points define a quadrilateral, called the allowable tip region, and it can be seen that if the tip is outside ABCD (Fig. 34) then M is partially outside the four panels shown or in other words (i_x, i_y) is not the appropriate centre.

We now set up non-dimensional coordinates for the position of P within ABCD. Briefly

$$\xi_o = \Delta CDP / (\Delta CDP + \Delta PAB)$$

$$\eta_o = \Delta CPB / (\Delta CPB + \Delta PDA)$$

and $0 < \xi_o, \eta_o < 1$. We note that the area of a typical triangle is

$$\begin{aligned} \Delta CPB &= \begin{vmatrix} x_C & x_P & x_B \\ y_C & y_P & y_B \\ 1 & 1 & 1 \end{vmatrix} = (x_B - x_P)(y_C - y_P) - (x_C - x_P)(y_B - y_P), \\ & \dots \quad (6) \end{aligned}$$

with C, P and B in anticlockwise order. If p_1 and p_2 are perpendiculars from P to BC and AD then from the definition

$$\begin{aligned} \xi_o &= p_1 CB / (p_1 CB + p_2 AD) \\ &= \frac{CB}{CB + AD \cdot p_2 / p_1} \end{aligned}$$

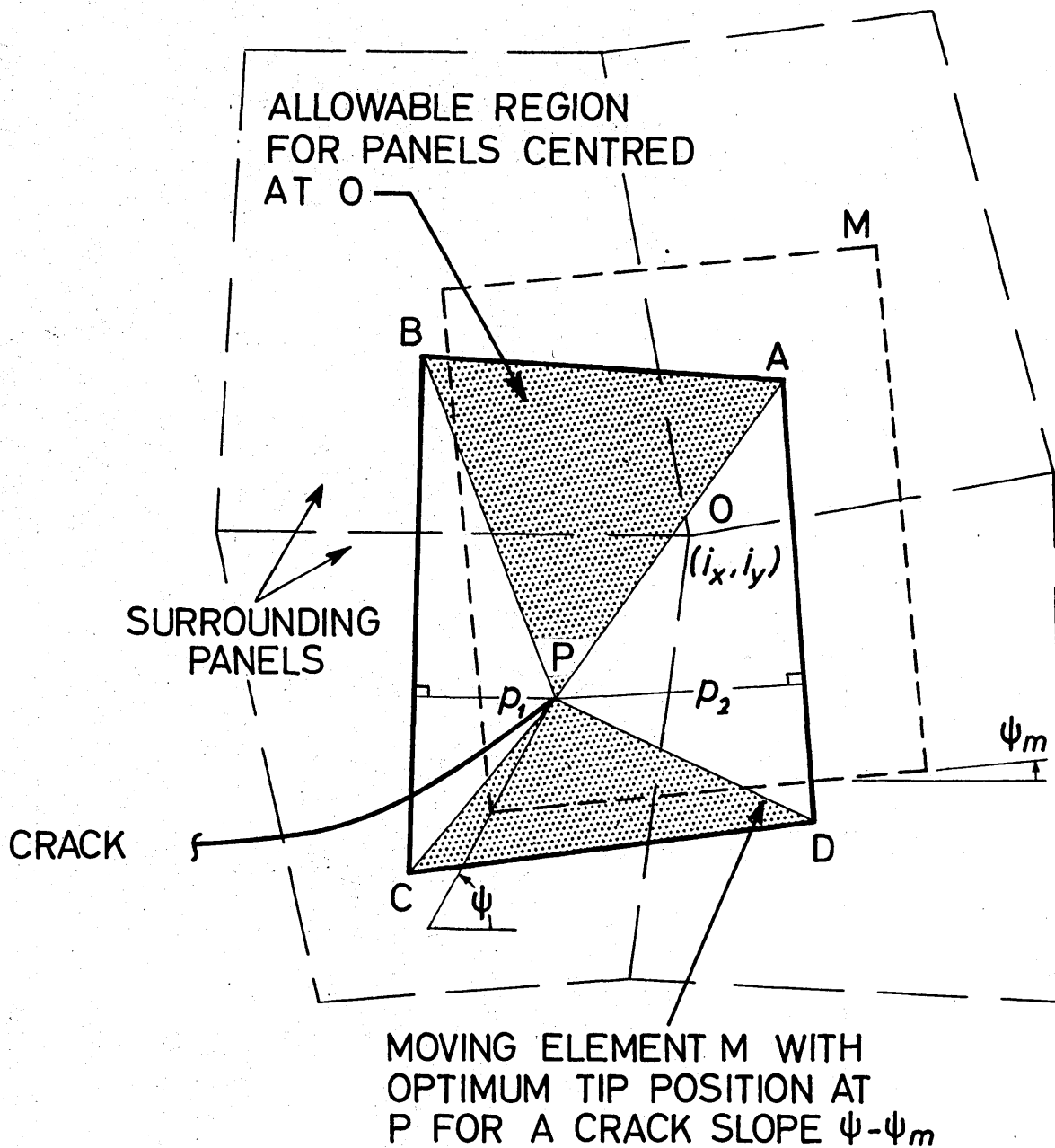
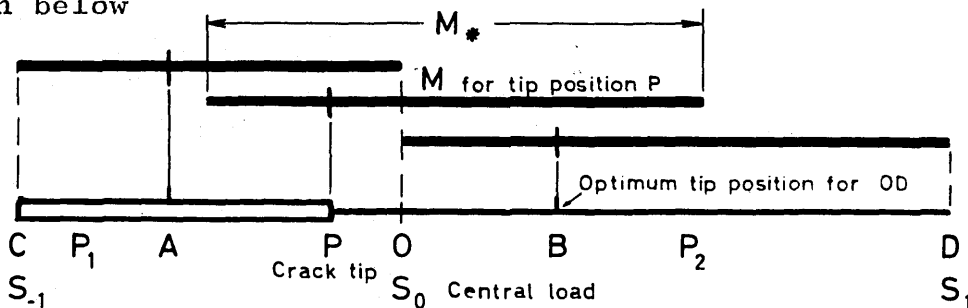


FIG. 34 LOCAL LATTICE COORDINATES FOR ALMOST RECTANGULAR PANELS.

and it follows from geometric similarity that $\xi_0 = \text{constant}$ defines a straight line through the intersection of AD and BC. A similar result holds for η_0 .

3.21 Local Lattice Coordinates

With the origin at O, M is between the lattice bounds $-1 < \xi, \eta < 1$ and in this system it is also a unit square. It is helpful to begin with the one-dimensional analogue shown below



where CO and OD replace the four panels and AB is the allowable region containing the tip P, now constrained to CD. Three successive positions of M are shown, as ξ_0 increases from 0 to 1. In the local lattice coordinates, if $\xi_0 = 0$ then

$\{M : -1 < \xi < 0\}$, as shown, while if $\xi_0 = 1$ $\{M : 0 < \xi < 1\}$

so that for the intermediate values of ξ_0 it is natural to place M between $\xi = \xi_0 - 1$ and $\xi = \xi_0$ or in the present notation $\{M : \xi_0 - 1 < \xi < \xi_0\}$. These are then the two values of ξ to be used in (4) if such an interpolation were required. The actual size of M may here be taken as

$$M_* = (1 - \xi_0)CO + \xi_0 OD, \quad \dots (7)$$

a linear interpolation similar to (3) or (4). From a knowledge of M_* and the optimum tip position it is now possible to place the actual moving element in correct relation to the "tip" P and the two "panels" CO, OD.

This procedure carries over to two (and three) dimensions with little change. The corners of M then have the local lattice coordinates

$$(\xi_0, \eta_0), (\xi_0 - 1, \eta_0), (\xi_0 - 1, \eta_0 - 1), \text{ and } (\xi_0, \eta_0 - 1),$$

in the standard order, and these values are used in (5) for vertical and horizontal corner loads. The interpolation (7) has a two-dimensional form similar to (5) and it is applied to pure shear forces and the fitted widths, heights and slopes of the four panels.

3.22 Edges

Suppose that some of the four panels are on the edge of the structure and the crack tip is between the allowable region and this edge, at which we suppose the crack to start. In our one-dimensional analogue this corresponds to a crack tip in CA. Since the crack is smaller now, M is also reduced in scale and it is possible to use a different approach altogether and treat the crack as an edge crack with the stress intensity

$$K^2 = g(\psi) \sigma \sqrt{\pi l}.$$

However to be consistent let us retain the moving element but now make CA the allowable region for edge cracks. As the tip moves from C to A, M grows from zero to CO and we may take

$$M_* = \xi_0 CO,$$

where now

$$\xi_0 = CP_1/CA \quad (< 1 \text{ for edge cracks}).$$

In lattice coordinates

$$\{M: -1 < \xi < \xi_0 - 1\} \quad \dots (8)$$

adjoining the internal interval

$$\{M : \xi_0 - 1 < \xi < \xi_0\}. \quad \dots (9)$$

If the crack starts from D the allowable region is BD and

$$\xi_0 = BP_2/BD \quad (>0 \text{ for right hand edge cracks}),$$

and the positive direction of ξ is retained. In addition

$$M_* = (1 - \xi_0)OD$$

$$\text{and} \quad \{M : \xi_0 < \xi < 1\}, \quad \dots (10)$$

adjoining the internal interval. One can now situate the actual moving element, just as above. In two dimensions the lattice corners are obtainable by appropriate combinations of extreme values of ξ and η from any of the regions (8), (9) or (10). The eight cases thus obtainable allow for M touching any side or containing any of the four corners of the structure. The interpolations and placement of M proceed exactly as before.

3.23 * Note

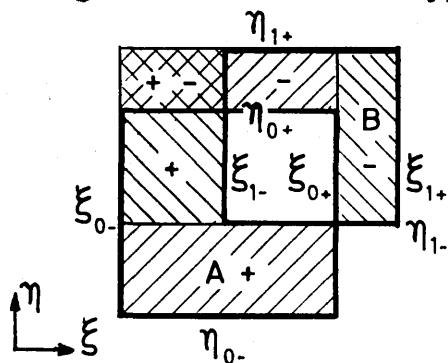
The allowable regions and hence (ξ, η) depend on the angle between the crack and the general direction of the surrounding panels and this may change as it extends. In the programme the allowable region is set up as soon as the set of surrounding panels changes and it is retained until a new set is needed. The error thus occasioned is of the same order as that involved in the linear approximation to M_* .

4.1 *Changes of Flexibility

These involve a second system of local coordinates in which each of the surrounding panels in the region $-1 \leq \xi, \eta \leq 1$, these coordinates being those used in the

natural stress systems of Chapter VII. Equation (6) is again used in their calculation where (x_p, y_p) now refers to a corner of M and an actual panel replaces the allowable region.

The regions of integration in Fig. 23 (Chapter VII) are generally split into four by the boundaries of the surrounding panels but each of these can be regarded as a figure of the same type and this specification also covers the exceptional cases when the crack is near the edge. Let us redraw Fig. 23 (a) with the limits of integration shown. It can then be verified that with the appropriate integrand the four integrals



$$\int_{\eta_{0+}}^{\eta_{0-}} \int_{\xi_{0+}}^{\xi_{0-}} + \int_{\eta_{0+}}^{\eta_{0-}} \int_{\xi_{1+}}^{\xi_{1-}} + \int_{\eta_{1+}}^{\eta_{1-}} \int_{\xi_{0+}}^{\xi_{0-}} + \int_{\eta_{1+}}^{\eta_{1-}} \int_{\xi_{1+}}^{\xi_{1-}}$$

cover A and B with the correct allowance for sign. If the eight limits are now written in two sets in the orders

$$\xi_{0-} \quad \eta_{1+} \quad \xi_{0+} \quad \eta_{1-} \quad \text{and} \quad \eta_{0+} \quad \xi_{1+} \quad \eta_{0-} \quad \xi_{1-}$$

then the group of cyclic permutations of each of these has four members, corresponding to each integral, and a particular limit always corresponds to the same element of the appropriate group member.

In the subroutine for flexibility changes this permutation is effected by renaming these variables and in the loop for these four integrals the first essential instructions are

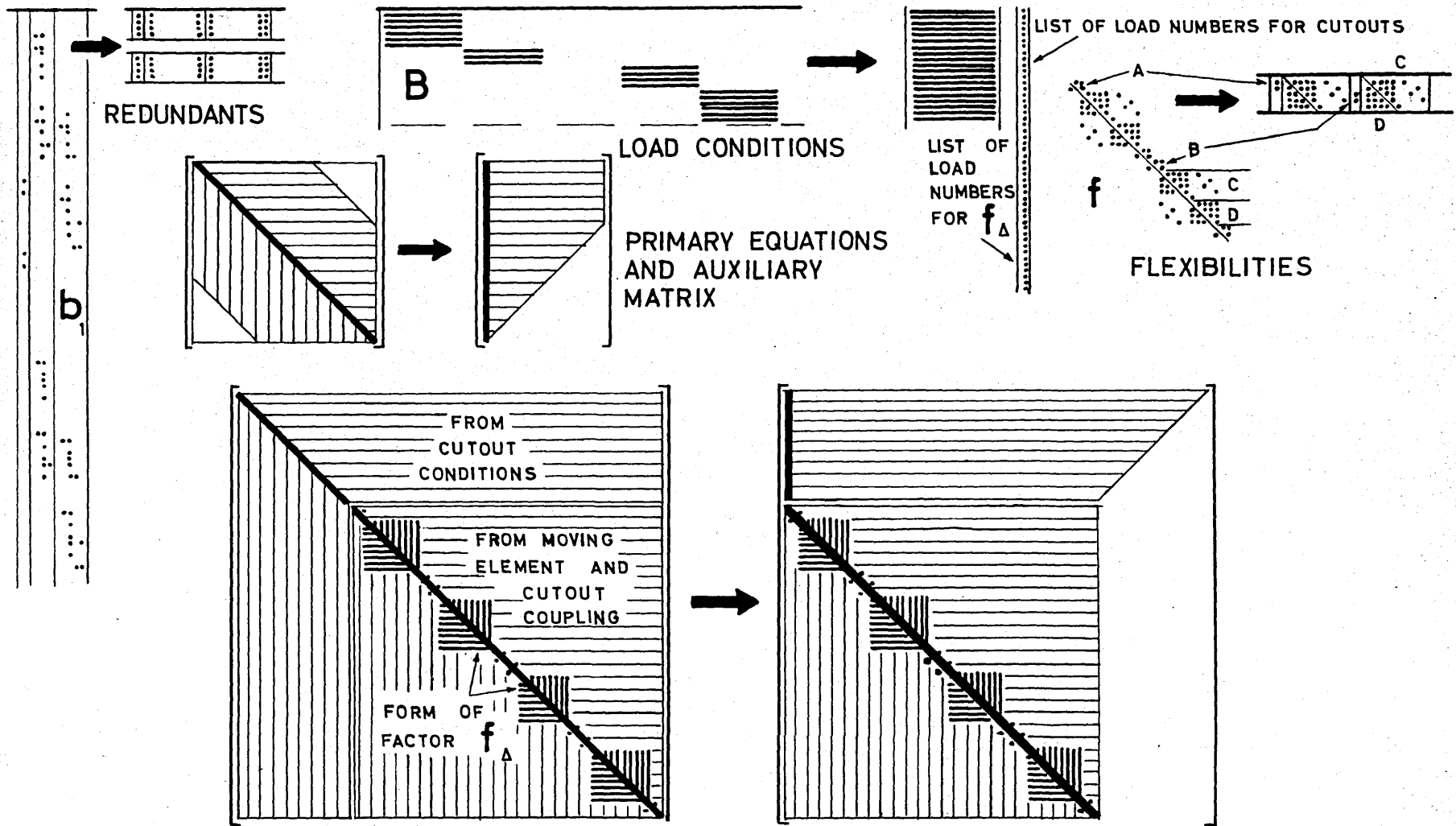


FIG. 35

COMPUTER STORAGE OF MATRICES

$$\begin{aligned}
 A &= \xi_{0-} && \text{(There are similar instructions} \\
 \xi_{0-} &= \eta_{1+} && \text{for the second set of limits)} \\
 \eta_{1+} &= \xi_{0+} \\
 \xi_{0+} &= \eta_{1-} \\
 \eta_{1-} &= A = \text{Previous value of } \xi_{0-}.
 \end{aligned}$$

Thus this loop is essentially subscripted according to these permutations. This renaming procedure is also useful for computing natural stresses or for geometric operations along each axis. In all applications it is possible to discern a group operation.

4.2* Computer Storage of Matrices

To save space the matrices f , b_1 , $b_1^t f b_1$ and the modification matrix were placed in smaller, effectively rectangular, blocks in the core storage of the computer. This ordinary economy was effected by eliminating those elements most obviously zero and by not duplicating the elements of symmetric matrices. The figure indicates the transformation from the mathematical form of our matrices to their effective shapes in core storage. Each panel has 9 load systems and there is also room for 4 boom loads. In the b_1 matrix, as shown, only eight rows are needed and the columns corresponding to the redundants are listed in the order of the joints. For each system with pure shear five columns are needed and therefore the column number i_q exceeds the corresponding column i_p of b_1 .

Without complex housekeeping the efficient storage of triangular arrays is not possible. The flexibility was therefore stored in the 10x5 cells shown. After the

primary stress analysis these were cleared and used for the changes in flexibility.

The matrix $b_1^t f b_1$ is also symmetric but in this case advantage was taken of its banded form and the upper diagonals were started as columns. It is not difficult to use standard elimination techniques on this form and adjoin it to the various right-hand sides. Furthermore, the Crout auxiliary matrix may be stored in the same locations as elimination proceeds and the back solution may be similarly treated. For a banded matrix this is the most economical way to store the inverse.

The band width is obviously an important parameter. We show below that this is

$$n_b = 5\alpha + 6$$

for fully reinforced structures while if there are no booms

$$n_b = 3(\alpha + 1),$$

other cases lying between these extremes but favouring the first.

4.3 * Matrix Operations

In rectangular structures

$$1 \leq i_x \leq \alpha+1 \quad \text{and} \quad 1 \leq i_y \leq \beta+1$$

and this knowledge enabled an alphabetical listing,

$$j_p = (i_y - 1)(\alpha + 1) + i_x,$$

of each cell. The loads were numbered in a similar manner with

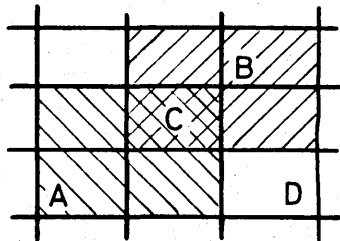
$$j = (i_y - 1)(13\alpha + 2) + 13(i_x - 1) + \text{Number of load in cell.}$$

regardless of their actual existence. Flexibilities were similarly numbered and the disposition of reinforcement

was decided by data known as J_{panel} , depending on j_p , which determined how many booms passed through a joint and their directions.

In the programme the primary analysis was begun by listing and finding the redundants, in order of increasing j_p . This was done by a double loop (DO statements) in i_x and i_y in which the redundant was numbered i_p and the corresponding column subscript in storage i_q was also found (see above). These were not stored and in any operations with b_1 the logic of the double loop was repeated, possibly with skipping rules to save time.

Now consider the band width n_b mentioned above. For finite interaction between different redundants the greatest difference in j_p must correspond to points such as A and B shown here. This spans $\alpha+1$ other joints each of which (say) can correspond to five redundants.



Thus the difference in i_p or the band width is roughly $5(\alpha+1)$ and more detailed counting leads to the result given. The band width for unreinforced and partially reinforced structures follows in the same way.

Because of the large order of $f, b_1^t f b_1$ was calculated in the form

$$b_1^t f b_1 = b_1^t \sum_{j_p} f_{j_p} b_1$$

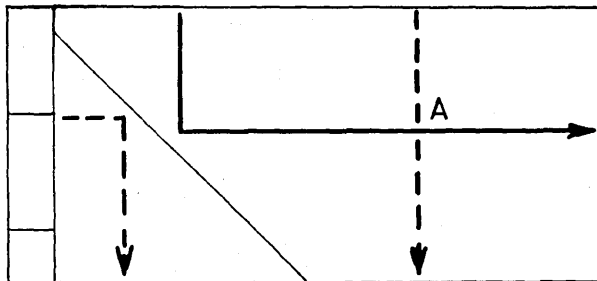
where the subscripts indicate that only flexibilities from cell j_p are used, with a corresponding reduction in the size of row-into-column products. In forming $f b_1$ and similar quantities coupling considerations arise, similar to those in the sketch for n_b . If products from disjoint cells are not computed the time taken by these routines is reduced by about 90%. The criterion in the case of $f b_1$ is that the distance (in lattice co-

ordinates) between the centre C of the panel concerned with f and D, say, where the redundant is located, exceeds $1/\sqrt{2}$. In integers, if (i_x, i_y) is the cell and (j_x, j_y) refers to the redundant, then for no contribution to fb_1

$$(2(i_x - j_x) + 1)^2 + (2(i_y - j_y) + 1)^2 > 2$$

illustrating the usefulness of the lattice coordinates. Whenever possible, decisions in the programme were based on the values of integral functions to avoid equivocation caused by rounding off errors.

In the virtual storage for each cell of f a single loop for a scalar product or the display of elements defines a path like one of those shown below.



Thus in the programme such loops appear as two or three successive loops within which the basic subscripts are calculated. The same logic is used for storing f_{Δ} also but in this case the double entries associated with points such as A must be avoided.

CONCLUSIONS

We have described a general method for the solution of problems in structural fatigue. This incorporates the now generally accepted view that fatigue proceeds essentially in two stages, here called damage and crack growth. The damage or microcrack stage, which may be defined in a way appropriate to the structure, is ended by initial failure whose probability distribution in the most general case is available from Bastenaire damage theory. Since the method fundamentally belongs to probability theory the assumptions about crack growth can be quite arbitrary but for practical application we have chosen to elaborate the fracture mechanics approach of Paris.

The improvement over previous methods is that one may consider the stress redistribution caused by one or several cracks and their interaction with damage or initial failure. In addition, the direction of cracking may also be made an unknown and one obtains in principle the complete probability distribution of initial failure times and of all crack lengths at any given time. There is also an important theorem that the distributions of initial failure times are independent, a result stemming from the independence of the physical processes at each damage site. The distribution of lives to final failure follows from an essentially separate reliability analysis based on the solutions of the crack-damage equations, preferably with a Griffith-Irwin criterion for final static fracture.

In order to create a more practical theory it was found necessary to apply Bastenaire damage theory to the log-normally distributed fatigue lives assumed in practice and the effect of endurance limits was also considered. This lead to a reasonably simple damage law

which made complete use of the usual data obtained for constructing S-N curves. Moreover, although this is an exact statistical theory for normal lives and one-parameter damage, no other information about the material is required. For those cases requiring more than one damage measure we have examined some statistical aspects of the analysis of programme test results and proposed a tentative theory of corrosion fatigue to illustrate a way in which other damage parameters may be identified and included.

For use in the crack-damage equations the crack propagation results were presented in a non-dimensional form based on the fracture mechanics viewpoint. By a proper choice of parameters it was found possible to correlate the effects of mean load on the crack rate. This is an advance and the same parameters also allow the fourth power law of Paris to be written in a more suggestive physical form where the crack rate is proportional to both the maximum size of the plastic zone and the driving force based on alternating load. A tentative theory for random load cracking has also been advanced on this basis.

However, the new presentation has emphasised the fact that the fourth power law does not account for all the effects present in fatigue cracking. In particular there is a range of stress intensities over which the crack rate changes less rapidly and, since this range corresponds to maximum plastic regions within the interval 0.006 to 0.02 inches, it is suggested that the effect may be related to the grain size of the material.

To make the general theory applicable to reinforced structures we have also discussed the representation of cracks in an idealised structure. In terms of the matrix force method which we use (and for displacement methods

also) this turns out to be a combined cutout and modification problem amenable to well known methods once the required data are available. However to solve the equations for initial strains a modified Crout method is described which is based on the partitioning between cutouts and modifications. This avoids the necessity of inverting the changes in the element flexibility matrix. The new method is also fully efficient in terms of computer storage and time and allows the same cutouts to be considered with different flexibility changes by a minimum amount of reworking.

This leaves the problem of actually specifying the crack conditions and the changes in flexibility. Basically, the first has been done by performing the analysis in terms of a transformed set of generalised stresses which of course include the loads to be nullified by crack growth. There may be a danger here of obtaining ill-conditioned transformations which needs further investigation. The changes in flexibility are obtained by supposing some of the idealised stress systems in the structure to be partially replaced by the asymptotic stress field appropriate to a crack tip. It is convenient to imagine the latter as the stress system in a moving element. This is then a finite element extension of fracture mechanics and the actual stress intensity is easily obtainable in terms of the surrounding loads. The method in fact can be applied to any type of discrepancy in otherwise standard idealised stress systems.

Future Work

At a basic level the crack-damage equations here do not allow for intrinsic randomness in crack propagation itself. We have suggested additional terms in the equa-

tions for higher cumulants but their nature needs elucidation. The method is likely to be most useful for analysing small segments of a structure and a test programme could be supplemented by studying sets of cracks in idealised structures (in a fatigue sense).

We have said that the orientation of a crack can be included as an unknown in the crack-damage equations but this supposes that the phenomenological behaviour is known in this respect. Changes in the principal stress trajectories here expose a large gap in knowledge however. The use of moving elements would also need to be generalised if such changes occur.

The matrix procedures outlined here can be extended to include other idealisations and displacement methods. Among the latter, triangular elements should be useful, because these idealisations will tend to be such that crack growth, in terms of elements crossed, is fairly constant.

Finally, experiments such as those suggested in Chapter III Sec.9.9 are required, supported by statistical analysis and thorough metallurgical examination. It may also be worthwhile to devise an experimental check of the strong possibility (Ch.III Sec.9.6) that increments of crack growth are the same as regions of reversed yielding at the tip.

Appendix A

JOINT DENSITY $f(a|n)$ AND NUMERICAL EXPECTATIONS

The advantage of the moment formulae for calculating expectations in Chapter V is their direct relation to the basic solution of (4.35) or (4.36) and (4.45), in particular their independence of the initial density. However it may be useful to indicate the procedure with numerical integration formulae.

First consider the joint density function. Starting with a bivariate distribution $F(x,y)$ say let us assume that the conditional densities have the same functional form as the marginal densities $f(x)$, $f(y)$, typified by (5.1A) and that m , n are also constant. For all conditional distributions $F(x|y)$ the probability of having no crack must be constant since the initial failures are independent. Since m, n and now F_x are constant any correlation must be effected by a variation $a(y)$ of the initial density. As the shape parameters m, n are constant and $a(y)$ is a scale parameter in $T(a(y)x)$ and in the exponential term of $F(x|y)$ we have geometric similarity in any part of $f(x|y)$ relating to $x > 0$. Therefore

$$u(x|y) \propto 1/a(y).$$

To agree with the marginal distribution $f(x)$ it is also necessary that

$$\begin{aligned} \int u(x|y) dF(y) &= F_x u_x / a_x \\ &= F_x u_x \int dF(y) / a(y) \end{aligned}$$

and for the initial densities

$$\int a(y)dF(y) = a_x \quad \dots \quad (A1)$$

where $\mu_x = \int xdT(x)$, the mean of the standard transition distribution. In addition there is the known second moment

$$\begin{aligned} \mu_{xy} &= \iint xyf(x|y)f(y)dx dy \\ &= \int y\mu(x|y)dF(y) \quad \dots \quad (A2) \end{aligned}$$

If we can now find a form of $a(y)$ satisfying (A1) then particular cases can then be chosen to satisfy (A2). Here it is convenient to redefine $T(x)$ as

$$F(x|y) = (1-F_x) + F_x T(a(y)x) \quad , \quad \dots \quad (A3)$$

the first term being the constant probability of zero length while the second combines the initial density and transition components. The two equations in (A1) can then be combined as

$$\left\{ \int \frac{dF(y)}{a(y)} \right\} \left\{ \int a(y)dF(y) \right\} = 1$$

which from (A3) becomes

$$\left\{ \frac{1-F_y}{a(0)} + F_y \int \frac{dT(a_y y)}{a(y)} \right\} \left\{ (1-F_y)a(0) + F_y \int a(y)dT(a_y y) \right\} = 1$$

reducing to

$$\begin{aligned} (1-F_y)^2 + F_y(1-F_y) \int \left\{ \frac{a(\xi/a_y)}{a(0)} + \frac{a(0)}{a(\xi/a_y)} \right\} dT(\xi) \\ + F_y^2 \iint \frac{a(\eta/a_y)}{a(\xi/a_y)} dT(\xi)dT(\eta) = 1 \quad \dots \quad (A4) \end{aligned}$$

If $a(\)$ is constant we have the trivial case of independence. Ignoring this let

$$a = a_y$$

$$A(\xi) = a(\xi)/a(0).$$

To satisfy both the equations (A1) $A(\xi)$ needs at least two parameters and we put

$$A(\xi) = 1 + \alpha\xi + \beta\xi^2$$

and for moderate correlations

$$A^{-1}(\xi) = 1 - \alpha\xi + (\alpha^2 - \beta)\xi^2 + \dots$$

When this is substituted and the integrals are evaluated (A4) becomes

$$(1-F_y)^2 + F_y(1-F_y)[2 + \alpha^2\mu_{2T}] + F_y^2[1 - (\alpha\mu_T + \beta\mu_{2T})^2 + \alpha^2(\beta+1)\mu_{2T} + \alpha^3\mu_T] \dots \quad (A5)$$

$$= 1$$

where

$$\mu_T = m/(n-1) ; \quad \mu_{2T} = m(m+1)/(n-1)(n-2)$$

are the moments of $T(\xi)$. This may be solved as a quadratic equation in β , in terms of α which remains as a disposable parameter to give the appropriate correlation in (A2).

Integration Formulae

We now consider some essentially Gaussian integration formulae⁷². These are the most efficient particularly in higher dimensions⁷³ although we do not discuss fully effective formulae for higher spaces.

A typical one-dimensional integral is

$$E = F(n) \int_0^{\infty} e^{-ax} \left[\frac{dT(ax)}{dx} - a(T(ax)-1) \right] R(x) dx \quad \dots (A6)$$

using (5.1A) and assuming that $R(0) = 0$. In our case

$$\frac{dT(ax)}{dx} = \frac{1}{B(m,n)} \frac{a^m x^{m-1}}{(1+ax)^{m+n}}$$

and with a change of variable

$$E = F(n) \int_0^{\infty} e^{-u} (T'(u) - T(u)+1) R(u/a) du \quad \dots (A7)$$

There is also the standard substitution

$$v = u/(1+u)$$

which reduces the range of (A7) to $(0,1)$ and changes $T'(u)$ to the standard density

$$\frac{dT}{dv} = \frac{1}{B(m,n)} v^{m-1} (1-v)^{n-1}$$

while E becomes

$$E = F(n) \int_0^1 e^{-v/(1-v)} \left\{ T'(v) - \frac{T(v)-1}{(1-v)^2} \right\} R\left(\frac{v}{a(1-v)}\right) dv \quad \dots (A8)$$

This is probably the best form for computation since the same Gauss-Legendre subroutine can be used for the main integral here and also for the incomplete B-function $T(v)$ and $B(m,n)$. It must also be remembered that the Gauss-Laguerre formula appropriate to (A7) is most accurate when the integrand, apart from e^{-u} , is largest in the neighbourhood of $u=1$ whereas we hope that it is largest near the mean $m/(n-1)$.

The Gauss-Legendre form of (A8) is, with the integrand abbreviated,

$$E = F(n) \sum_{j=1}^k H_j G(v_j)$$

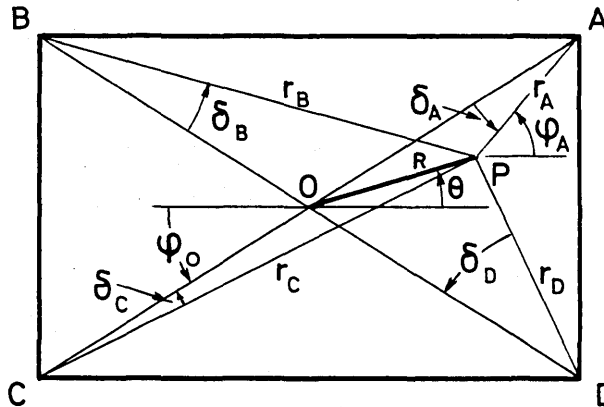
where the $H_j(k)$ and $v_j(k)$ are tabulated.⁷² This is exact for any polynomial integrand up to the degree $2k-1$. It has been shown by Hammer and Wymore⁷⁴ that Cartesian products of summations such as that here are exact for polynomials in the appropriate number of variables with the highest term

$$u^{2k-1} v^{2k-1} \dots$$

Other multidimensional formulae are described in the last reference which contains other recent references also. These remarks also hold for Gauss-Laguerre and other formulae for weighted integrands.

Appendix B

CALCULATION OF SUBTENDED ANGLES AT CRACK TIP



We take the origin at the centre of the panel which we now suppose to be vertical. Using vectors in complex form we first derive relations between the different angles. Let A, B, C, D be points in the complex plane, with the origin P, represented by

$$r_A = a e^{i\phi_A}$$

$$r_B = b e^{i\phi_B} \quad \text{etc.}$$

Then the two diagonals are

$$CA = r_A - r_C$$

$$BD = r_D - r_B$$

and these are complex conjugates. By equating two forms of the width BA one also obtains

$$r_A - r_B = r_D - r_C.$$

Separation of real and imaginary parts leads to the equations

$$\begin{bmatrix} \cos \varphi_A & & & \cos \varphi_D \\ \sin \varphi_A - \sin \varphi_B & & & \\ & \cos \varphi_B - \cos \varphi_C & & \\ & & \sin \varphi_C & \sin \varphi_D \end{bmatrix} \begin{bmatrix} a \\ b \\ c \\ d \end{bmatrix} = 0$$

For a nontrivial solution

$$\cos \varphi_A \sin \varphi_B \cos \varphi_C \sin \varphi_D - \sin \varphi_A \cos \varphi_B \sin \varphi_C \cos \varphi_D = 0$$

which ensures that a vertical rectangle can exist with corners on the four rays through A, B, C and D. In this case

$$a = \sin \varphi_B \cos \varphi_C \sin \varphi_D$$

$$b = \sin \varphi_A \cos \varphi_C \sin \varphi_D$$

$$c = \sin \varphi_A \cos \varphi_B \sin \varphi_D$$

$$d = \sin \varphi_A \cos \varphi_B \sin \varphi_C,$$

apart from a scale factor, and the aspect ratio reduces to

$$\tan \varphi_0 = \frac{\sin \varphi_A \sin(\varphi_B - \varphi_C)}{\cos \varphi_C \sin(\varphi_B - \varphi_A)}.$$

In the maximisation it is most convenient to solve for the angles φ_A , φ_B etc. when P is placed at $\text{Re}^{i\theta}$ with respect to the centre O. From the figure

$$\varphi_A = \varphi_0 + \delta_A \text{ etc.}$$

with due regard for sign. Making OA unit length, let us find δ_A . We know that

$$PA^2 = 1 + R^2 - 2R \cos(\varphi_A - \theta)$$

and by the sine rule

$$R/\sin \delta_A = PA/\sin(\varphi_A - \theta) .$$

The most convenient form of the solution is

$$\tan \delta_A = \pm \frac{R \sin(\varphi_A - \theta)}{1 - R \cos(\varphi_A - \theta)} ,$$

taking positive roots for A, B and negative for C and D.

REFERENCES

1. F. Bastenaire A critical discussion of the nature of cumulative damage in fatigue. trans. by F.H.Hooke Report, Department of Mechanical Engineering, University of Nottingham 1959.
2. I. Torbe A new framework for the calculation of cumulative damage in fatigue. Part II Historical theory. University of Southampton, U.S.A.A. Report 111 July 1959.
3. S.R.Swanson An investigation of the fatigue of aluminium alloy due to random loading. U.T.I.A. Report 84, Univ. of Toronto, Feb. 1963.
4. J.Y. Mann Unpublished tech. memo. Aeronautical Research Laboratories, Melbourne 1963.
5. M.A. Miner Cumulative damage in fatigue. p.153 Journal of Applied Mechanics, Series A. July 1945.
6. A. Palmgren Die Lebensdauer von Kugellagern. Zeitschrift des Vereines Deutscher Ingenieure 68 No.14 (April 1924).
7. B.F. Langer Fatigue failure from stress cycles of varying amplitude. Journal of Applied Mechanics p.A-160 4 1937.
8. A.M. Freudenthal, On stress interaction in fatigue and R.A.Heller a cumulative damage rule. Jnl. of Aero/Space Sciences 26 1959.
9. D.G. Ford The probability distribution of linear cumulative damage in fatigue. Australian Aeronautical Research Committee ACA-64 November 1962.
10. J. Schijve Fatigue life and crack propagation Current Aeronautical Fatigue Problems Pergamon 1965.
11. M.A. Melcon, Simulation of random aircraft service A.J.McCulloch loadings in fatigue tests. Current Aeronautical Fatigue Problems. Pergamon 1965.
12. A.M. Mood Introduction to the Theory of Statistics McGraw-Hill, 1950.

13. O.A. Kempthorne The Design and Analysis of Experiments.
Wiley, 1952.
14. W.T.Kirkby Constant amplitude or variable ampli-
P.R.Edwards tude tests as a basis for design
 studies. I.C.A.F. Symposium Munich
 June 1965. Pergamon Press.
 Also RAE Tech.Report 66023 January 1966.
15. Igor Bazovsky Reliability: Theory and Practice
 Prentice-Hall 1961.
16. Lennart von Appendix A: A statistical method for
Sydow fail-safe design with respect to
 aircraft fatigue. Bo K.O. Lundberg,
 Sigge Eggwertz. 2nd Intl. Congress
 ICAS Zurich September 1960. Pergamon.
 Also as FFA report.
17. W. Feller An Introduction to Probability Theory
 and its Applications. Volume I.
 Wiley 1950.
18. M.G. Kendall The Advanced Theory of Statistics.
 Griffin 1946.
19. H.W. Liu Fatigue crack propagation in thin
 metal sheet under repeated loading.
 Jnl. of Basic Engineering. Trans.
 A.S.M.E. Series D. 83 March 1961.
20. P.J.E.Forsyth, Fatigue fracture: some results
D.A. Ryder derived from the microscopic examination
 of crack surfaces. Aircraft
 Engineering April 1960.
21. P.J.E. Forsyth A two stage process of fatigue crack
 growth. Cranfield Symposium 1961.
22. C.E. Inglis Stresses in a plate due to the presence
 of cracks and sharp corners.
 Trans. Inst. Naval Architects 55
 March 1913.
23. H.M.Westergaard Bearing pressures and cracks.
 J. Applied Mechanics Series E June 1939.
24. G.R.Irwin Fracture: Handbuch der Physik VI
 Springer 1958.
25. J. Schijve Analysis of the fatigue phenomenon
 in aluminium alloys. M.2122 N.L.R.
 Report Trans. XXIX July 1964.
26. A.E.Green The distribution of stress in the neigh-
I.N. Sneddon bourhood of a flat elliptical crack in
 an elastic solid. Proc. Cam. Phil.Soc.
 46 1950.

27. G.R. Irwin
J.E. Srawley Progress in fracture toughness tests.
Material Prufung 4-1 Jan. 1962.
28. A.E. Green
W. Zerna Theoretical Elasticity. Oxford. 1954.
29. J. Lyell-Sanders, Jr. On the Griffith-Irwin fracture theory.
Jnl. Applied Mechanics Series E 27
1960.
30. J.E. Srawley
et al. Experimental determination of the
dependence of crack extension force on
crack length for a single-edge-notch
tension specimen.
NASA TN 2396 1964.
31. B. Gross et al. Stress intensity factors for a single
edge-notch tension specimen by boundary
collocation of a stress function.
NASA TN 2395 August 1964.
32. J.R. Dixon Stress distribution around a central
crack in a plate loaded in tension.
Jnl. Royal Aeronautical Society
LXIV March 1960.
33. P.C. Paris,
G.C. Sih Stress analysis of cracks.
Department of Mechanics Lehigh Univ.
June 1964. ASTM paper Chicago, June
21-26 1964.
34. R. Hill The Mathematical Theory of Plasticity.
Oxford 1950.
35. J.A.H. Hult,
F.A. McClintock Elastic-plastic stress and strain dis-
tributions around sharp notches under
repeated shear.
Journal Applied Mechanics ASME
E.24 1957
36. N.L. Williams Some observations regarding the stress
field near the point of a crack.
Cranfield Symposium 1961.
37. N.L. Williams The bending stress distributions at
the base of a stationary crack.
Journal Applied Mechanics ASMEE March 1961.
38. F. Erdogan et al. An experimental investigation of the
crack tip stress intensity factors in
plates under cylindrical bending.
Jnl. of Basic Engineering ASME D December
1962.
39. D.P. Rooke et al. Crack propagation in fatigue. Some
experiments with DTD 5070A aluminium
alloy sheet. R.A.E. Technical Rep.
64025 October 1964.

40. W.T. Koiter An infinite row of collinear cracks
in an infinite elastic sheet.
Ingenieur-Archiv 28 1959.
41. R.W. Peters Bursting strength of unstiffened
P.Kuhn pressure cylinders with slits.
N.A.C.A. Tech. Note 3993 April 1957.
42. D. Williams Crack propagation in thin sheet
materials - a Semi-empirical approach.
Cranfield Symposium 1961.
43. S.T. Rolfe Fatigue crack propagation in notched
W.H. Munse mild steel plates.
Welding Journal Research Supplement
June 1963.
44. D.S. Dugdale Yielding of thin sheets containing
slits. Journal of the Mechanics and
Physics of Solids 8 2 1960.
45. H.W. Liu Discussion. Cranfield Symposium 1961.
46. H.W. Liu Fatigue crack propagation and applied
stress range - an energy approach.
Jnl. Applied Mechanics ASME E. 30
March 1963.
47. B.A. Bilby The spread of plastic yielding from a
A.H. Cottrell notch.
K.H. Swindon Proc. Roy. Soc. A. 272 May 1964.
48. S.S. Manson Fatigue behaviour in strain cycling in
M.H. Hirschberg the low and intermediate cycle range.
Fatigue - An Interdisciplinary Approach:
Syracuse 1964.
49. P.C. Paris The growth of cracks due to variations
in load. Thesis.
Lehigh University, September 1962.
50. G.R. Irwin Fracture testing of high strength
materials under conditions appropriate
for stress analysis.
U.S. Naval Research Laboratory Report
5486 July 1960.
51. A.A. Griffith The phenomena of rupture and flow in
solids.
Phil. Trans. Roy. Soc. (London) Series A
221 1920.
52. D.K. Roberts The velocity of brittle fracture.
A.A. Wells Engineering pp.820-821 178 1954.

53. J.M. Kraft Effect of dimensions on fast fracture
A.M. Sullivan instability of notched sheets.
R.W. Boyle Cranfield Symposium 1961.
54. P.C. Paris et al. A rational analytic theory of fatigue.
The Trend in Engineering 13 1
January 1961.
55. G.P. Jones Fatigue crack propagation in Mustang
wings. Unpubl. A.R.L. Tech. Memo
Melbourne 1962.
56. Walter Illg The rate of fatigue crack propagation
A.J. McEvily, Jr. for two aluminium alloys under
completely reversed loading.
NASA TN D52 October 1959.
57. W.E. Anderson Crack propagation behaviour of some
D.R. Donaldson airframe materials.
Cranfield Symposium 1961.
58. T.D.J. Moag Fatigue crack propagation and hardness.
P.P. Benham p.760 The Engineer April 30 1965.
59. J. Schijve The effect of frequency of alternating
D. Broek load on the crack rate in a light alloy
P. de Rijk sheet. NLR Report M 2092 September 1961.
60. N.F. Harpur I.C.A.F. Symposium 1962, Pergamon.
61. P.C. Paris The fracture mechanics approach to
fatigue. Fatigue - An Interdisciplinary
Approach: Syracuse 1964.
62. Stimson and ARL-TR24, Wright Patterson Air Force
Eaton Base Jan. 1961.
63. H.F. Hardrath Engineering aspects of fatigue crack
A.J. McEvily, Jr. propagation. Cranfield Symposium 1961.
Also see NACA TN D960 September 1961.
64. J.A. Barnard Unpublished A.R.L. Internal Report 1963.
65. E. Orowan Notch brittleness and the strength of
metals. Trans. Inst. of Engineers and
Shipbuilders Scotland 89 1945.
66. N.E. Frost Alternating stress required to propagate
edge cracks in copper and nickel-
chromium alloy steel plates.
Jnl. Mechanical Engng Science 5 1 1963.
67. L.F. Coffin Jr. A mechanism for nonpropagating fatigue
cracks. p.570 Proc. ASTM 58 1958.
68. J. Schijve Fatigue crack propagation in unnotched
F.A. Jacobs and notched aluminium alloy specimens.
NLR Report M.2128 May 1964.

69. R.E. Bellman Stability Theory of Differential Equations. McGraw-Hill 1953.
70. D.G. Ford Fitting families of polynomial S-N curves to fatigue data.
Jeanette A. Lewis A.R.L. Report SM 296 Melbourne April 1964.
71. W.E. Milne Numerical Solution of Differential Equations. Wiley 1953.
72. Z. Kopal Numerical Analysis. Chapman and Hall 1955.
73. P.C. Hammer Numerical evaluation of multiple integrals. II. Mathematical Tables and Other Aids to Computation; XII 1958.
A.H. Stroud
74. P.C. Hammer Numerical evaluation of multiple integrals, I. Mathematical Tables and Other Aids to Computation. XI 1957.
A.W. Wymore
75. J.H. Argyris Energy Theorems and Structural Analysis. S. Kelsy Butterworth 1960.
76. L. Fox Practical solution of linear equations and inversion of matrices. Applied Maths Series US Bureau of Standards 39 1954.
77. P.D. Crout A short method of evaluating determinants and solving sets of linear equations with real or complex coefficients. Trans. Amer. Inst. Elect. Eng. 60 1941.
78. A.C. Atkins Analysis of Straight Line Data. Wiley 1962.
79. G.C. Sih Stress distribution near internal crack tips for longitudinal shear problems. Jnl. of Applied Mechanics ASME E32 March 1965.
80. H.L. Cox The initiation and propagation of fatigue cracks in mild steel pieces of square section. J.E. Field Aeronautical Quarterly IV August 1952.
81. J.B. Scarborough Numerical Mathematical Analysis. Johns Hopkins Press 1930.
82. B. Cotterell An interpretation of the mechanism of crack growth by fatigue. Trans. A.S.M.E. B Jnl. of Basic Engineering 31 1965.

General and supplementary references

- F.J. Plantema
J. Schijve eds. Full Scale Fatigue Testing of Aircraft Structures.
Proc. of ICAF Symposium Amsterdam 1959.
Pergamon Press 1961.
- W. Barrois
E.C. Ripley eds. Fatigue of Aircraft Structures.
Proc. of ICAF Symposium Paris 1961.
Pergamon Press 1963.
- J.Schijve et al. eds. Current Aeronautical Fatigue Problems.
Proc. of ICAF Symposium Rome 1963.
Pergamon Press 1965.
- John J. Burke
Norman L. Reed eds. Fatigue - An Interdisciplinary Approach.
Proc. of the 10th Sagamore Army
Materials Research Conference
August 1963.
Syracuse University Press 1964.
- Proc. of the Crack Propagation
Symposium, Cranfield September 1961
(Published by Cranfield College of
Aeronautics).
- Progress in measuring fracture tough-
ness and using fracture mechanics.
Fifth report of a special ASTM
Committee.
Materials Research and Standards
ASTM March 1964.
- A.J. Brothers
S. Yukawa Fatigue crack propagation in low-alloy
steels ASME Preprint 66-MET-2
To be published in Jnl. Basic
Engineering ASME D.
- Miss H.F. Borduas
L.E. Culver
D.J. Burns Fracture mechanics analysis of fatigue
crack propagation in polymethylmeth-
acrylate.
23rd Annual Technical Conference
Soc. Plastics Expts. Detroit May 1967.